TERRESTRIAL LASER SCANNING TO CHARACTERISE THREE-DIMENSIONAL FOLIAGE AND WOODY MATERIAL DISTRIBUTIONS IN TREES

FADAL FARAG K. SASSE

Ecosystems and Environment Research Centre

School of Environment and Life Sciences

University of Salford

Salford, M5 4WT, UK

Submitted in Partial Fulfilment of the Requirements of the Degree of Doctor of Philosophy, 05 May 2019

Contents

List of tables

List of figures

DEDICATION

I would like to dedicate this thesis to my mother, wife, and my children.

Acknowledgements

The long journey of finishing this research has been demanding in many respects. Since I came from the medical field, the stressful times I have experienced during the last four years had made me feel unsure about when this journey was going to come to an end. Nevertheless, it has been one of the most encouraging experiences of my entire life, that now has come to an end. I would like to extend my gratitude and thanks to a group of wonderful people who helped me to complete my journey.

I would like to start by expressing my deep gratitude to my beloved wife, who has suffered from a disease for so long, but she supported me with her unconditional love and believed in me from the first moment I planned to come to the UK to study for my PhD; to my mother, who I have not seen for almost five years, who has been sending her blessing and prayers all the time; and to the soul of my dad in his grave, whom I miss so much.

I would like to acknowledge Dr. Jon Murry from Lancaster University for helping me to access the Silverdale field location and for assistance with the data acquisition. I am deeply grateful to my supervisors, Professor Mark Danson and Dr. Richard Armitage. Without their help, encouragement, and patience, this work could not have been completed. Their trust, flexibility and generosity have made this journey more exciting. I would also like to thank Dr. Lucy Schofield, who helped me in many ways with great kindness. Finally, I would like to thank the University of Salford for the supportive and appropriate work environment that they offer to all students that enables them to complete their studies.

Declaration

I declare that the work presented in this thesis has not previously been submitted for a degree or similar award at Salford University or any other institution. To the best of my knowledge and belief, no material in this thesis has been previously published or written by another person, except where due reference is made. I further agree to give permission for fair use copying of this thesis for scholarly purposes

Signed: ……..

Date: …….

List of Acronyms

AGB	Above-ground biomass
ALS	Airborne laser scanning
AR	Apparent reflectance
ASD	Analytical spectral device
CANUPO	CAractérisation de NUage de Points
DBH	Diameter at breast height
DN	Digital number
DWEL	Dual Wavelength Echidna LiDAR
EWT	Equivalent Water Thickness
GCC	Global Carbon Cycle
GMM	Gaussian Mixture Model
HSL	HyperSpectral LiDAR
IPCC	Intergovernmental Panel on Climate Change
LAI	Leaf Area Index
LiDAR	Light detection and ranging
NB	Naïve Bayes
NDI	Normalised difference index
NIR	Near Infrared
PCA	Principle Components Analysis
ppm	Parts per million
QSM	Quantitative structure models
RF	Random Forest
RS	Remote Sensing
SALCA	Salford Advanced Laser Canopy Analyser
SRBL	Spectral Ratio Biospheric Lidar
SVM	Support Vector Machine
SWIR	Short Wave Infrared
TLS	Terrestrial laser scanning

Abstract

Three-dimensional characterisation of foliage and wood distribution within forests is essential for understanding, managing and monitoring forest ecosystems. The recent advances in terrestrial laser scanning (TLS) technologies have provided new opportunities to measure the 3D structure of forest canopies, which in turn can be correlated to tree attributes. In addition to estimation of variables such as stem density and the diameter at breast height and tree height, dual- and multi-wavelength systems are now being tested to distinguish foliage and wood based on their reflectance properties. Previous studies have suggested that using spectral information to distinguish foliage from wood materials is unlikely to provide an accurate classification on its own. In this thesis, a spectral approach was designed based on the frequency distribution of the reflectance and spectral ratios to distinguish between the foliage and woody materials. Additionally, a spatial classifier (CANUPO) approach was applied to describe the geometric relationships between the points of the TLS point clouds and characterise the local dimensionality at a given location and scale. TLS point cloud data of small broadleaf and needle-leaf trees in the laboratory, three single isolated oak trees with different structure and appearance and a full forest stand plot were used for foliage/wood classification in this research. The spectral and spatial classifications were compared to investigate the compatibility between them for all data sets. The results showed a clear separation of foliage and wood using 1063 nm and NDI data for the broadleaf tree and 1545 nm data for the needle-leaf tree. In contrast, the 1545 nm for the broadleaf and 1063 nm and NDI of the needle-leaf tree produced classification errors. A large number of foliage points were classified as wood for both trees using the spatial approach, with comparative errors of 67.35% and 73.18% for the broadleaf and needle-leaf tree respectively. For the three single trees, the 1545 nm data provide a clear separation for all trees while there was a variation in the classification using 1063 and NDI data for every tree. In general, the spatial classifier showed a clear separation for all of the trees with a few apparent errors in the canopy and on the stems with different results according to their structure and appearance. It was unlikely to be possible to separate foliage and wood using spectral data and ratios for the full forest data at ranges greater than 17m from the scanner. CANUPO classified 15% of the points as foliage and 85% as wood at a range of less than 15m. The classification showed a compatibility of 55.63% for the full stand data. Overall, the results highlight the potential of a dual-wavelength laser scanners for providing a wide range of data for forest ecology.

CHAPTER 1: INTRODUCTION

1.1 Research context

The global cover of forests in 2015 was estimated to be approximately 3.9 billion ha, or nearly 31% of Earth's land surface (Keenan et al., 2015). This global cover gives forests a critical role in many ecological services on Earth, which includes, for example, the global carbon cycle (GCC) (Keenan et al., 2015). As such, improving the accuracy of forest measurements would be beneficial for a wide variety of forest applications, such as ecological assessment, climate change studies and land management (Solberg et al., 2009). Forests provide a fundamental biological service for all species on Earth, including humans. For instance, forests are considered as one of the most important sources of freshwater, natural fuel, provide a habitat for wildlife and allow recreational opportunities for people (Costanza et al., 2017). In order to keep these services balanced, robust and fundamental data for forest management is essential in order to understand forest ecology and to allow a fast response to such as drought. Recently, terrestrial laser scanning (TLS) technology, a light detection and ranging (LiDAR) system, has provided new techniques for measuring forests in order to address the crucial needs related to forest mapping and monitoring. (Danson, Disney, Gaulton, Schaaf, & Strahler, 2018; Malhi et al., 2018). TLS systems will be further discussed in this thesis regarding its application to measure forests accurately.

Forests play a critical role in terms of climate change through the GCC, in which large amounts of carbon travel between the atmosphere and Earth's surface (Andrew & Ustin, 2008). The GCC represents the total amount of carbon that flows into and out of the Earth's atmosphere, oceans and land surface (Figure 1.1) (Ballantyne et al., 2015; Change, 2014). Carbon is an indispensable factor for life and can be found in the atmosphere as the greenhouse gas carbon dioxide (CO_2) (Pachauri & Meyer, 2015). In 2017, the average amount of CO_2 in the atmosphere was estimated at 405.0 parts per million (ppm). The assessment report of the Intergovernmental Panel on Climate Change (IPCC), stated that the CO_2 level in the atmosphere is now signifantly higher than it was 800,000 years ago (IPCC, 2018). While carbon fluxes and storage in forests vary over time (per year or decade) and space (local or global), both are highly influenced by climate change and human activities such as deforestation. For example, due to tropical forest deforestation, more than 1.5 gigaton of CO_2 is released into the atmosphere each year (Chen et al., 2014).

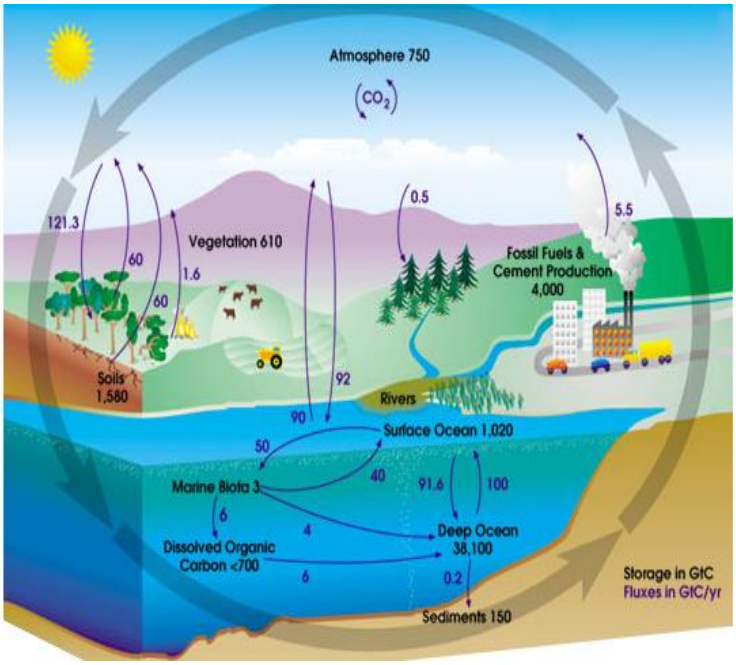

Figure 1.1: The global carbon cycle. Source: (Gonçalves-Araujo, 2016).

Forests are a key component in the GCC; they absorb CO_2 from the atmosphere and convert it into carbohydrate through photosynthesis. The carbohydrates become part of the tree's tissue and are partly released again into the atmosphere. In other words, at night time trees use oxygen respiration, which generates the CO_2 (Patenaude et al., 2004). More than 80% of the above-ground and about 40% of the below-ground carbon are stored in global forests; although the stored amounts depend on the type of vegetation (Kurz, Apps, Banfield, & Stinson, 2002). Vegetation structure in forests is an important element that controls the level of CO_2 exchange between the forest and Earth's atmosphere (Wallner et al., 2018).

According to research conducted by Drake et al. (2003), approximately 50% of the biological raw material or dry biomass of a tree is carbon. Several studies have revealed that tree biomass on a forest level is distributed in a complex three-dimensional structure (Gamon, Kovalchuck, Wong, Harris, & Garrity, 2015; Newnham et al., 2015). However, at the individual tree level, the leaves represent the dynamic photosynthetic factor in the forest ecosystem, influencing moisture levels, gas exchange and radiation interception (Ung, Bernier, & Guo, 2008). Forests are considered a key indicator of climate change. Indeed, the growth of foliage is influenced by the climate and phenological cycle, which strongly responds to the temperature and seasonal change over time. The biological response of foliage to climate change can, therefore, be used as useful information to understand the role of forest

ecosystems and future climatic change (Morin et al., 2009). The term ‘forest structure’ refers to the forest size, and includes tree volume and mass. In addition, it also refers to the physical arrangement of tree attributes that comprise the foliage, main and finer branches, and trunks and roots (McIntyre et al., 2015). Furthermore, the forest structure can be divided into two categories: above-ground (e.g. the tree trunk and canopy) and below-ground (e.g. the roots) (Calders et al., 2015). The work in this thesis is concerned with the aboveground part of the tree only.

Tree canopies control the interface between vegetation and the atmosphere; the spatial distribution of tree canopies, therefore, determines the nature of the exchange surface, including how much light can penetrate the gaps in the canopy (Pretzsch & Kahn, 1995). Forest structure, composition, and functional attributes are environmentally critical, and forest canopies provide habitat for almost 50% of the world’s plant and animales species (Huang et al., 2003). Moreover, the canopy structure is considered a key element in determining habitat stability and the structure of communities (Tews et al., 2004).

Measuring the spatial structure of trees is therefore important in order to study the function of forest ecosystems for both commercial and scientific purposes. In addition, understanding tree composition and its attributes is considered basic information in the forest research domain, such as forest meteorology, ecology, botany, climatology and forest mapping (Naidoo, Cho, Mathieu, & Asner, 2012). For instance, in the case of climatology, the change in temperature increases the length of the growing season, and measuring the spatial structure can be used as an indicator of forest growth (USGCRP, 2014). Moreover, quantifying the spatial distribution of forests is critical for land managers and researchers for accurate forest inventory and ecological monitoring (Naidoo et al., 2012).

The techniques that have been used to measure forests vary with both the needs of a specific application, and the costs and the availability of the measurements (Martin, Newman, Aber, & Congalton, 1998). Thus, forest inventories have traditionally been based on plot-scale terrestrial-based methods, which are labour intensive, and consume time but simple techniques (Liang et al., 2016; Shugart, Saatchi, & Hall, 2010). In addition, field parameters are limited due to the measurement techniques available and the exactness of these measurements. However, measuring tree attributes separately, such as the location, tree height, branches, and canopy for every tree, is both labour-intensive and error-prone. Due to

this, data tend to be collected at a limited number of sites and sampling times to prevent a rapid reaction to ecosystem disturbances (Bauwens, Bartholomeus, Calders, & Lejeune, 2016; Newnham et al., 2015).

More recently, new terrestrial laser scanner (TLS) technologies have been widely explored in many applications in different sectors, such as mining, archaeology, and building and infrastructure surveys (Portillo-Quintero, Sanchez-Azofeifa, & Culvenor, 2014; Wei et al., 2012). In the forest research sector, a new generation of single and multi-wavelength laser scanners have proved their potential by gathering robust data to quantify a wide range of forest parameters, such as stem volume and biomass components, with high accuracy (Disney et al., 2018; Saarinen et al., 2017). These technologies are able to support forest data collection without disturbing the surrounding environment (Schofield, 2016).

In the case of tree canopy classification, separate structural measurements of green foliage and woody materials may support the monitoring and modelling of a forest ecosystem. TLS scans consist of points that represent the surface properties of any desired target. It is possible to separate these points in order to understand the composition of those targets. Foliage/wood separation is critical for many tree measurements. For instance, woody points are a key to quantifying the number of branches, the measurements of every single branch, and the total wood volume of the desired tree (Li., et al., 2018; Zhu et al., 2018). Moreover, foliage points are fundamental in estimating quantities like leaf area index and leaf density which helps to understand forest ecology (Béland, Baldocchi, Widlowski, Fournier, & Verstraete, 2014). In order to generate three-dimensional visualisations based on the properties of forests canopies, the foliage and wood components may be separated according to their spectral reflectance (Béland et al., 2014; Tao et al., 2015). Visualisations are fundamental in generating interpretations regarding the extracted data to classify it into foliage or wood, based on their reflectance properties.

The work in this thesis investigates the potential of the first dual-wavelength TLS, the Salford Advanced Laser Canopy Analyser (SALCA), to characterise the spatial distribution of foliage and wood in tree canopies at the individual tree level and then assesses the approach for full forest stand environments. The instrument uses 1063 nm and 1545 nm wavelength lasers, which provides the potential to separate foliage from the wood points based on their different spectral response to the moisture content of the targets.

1. 2 Research aims and objectives

The main aim of this work is to investigate the spectral and spatial information recorded by the SALCA instrument to develop and test an approach to foliage and wood separation within forest targets.

According to previous studies such as Danson, Sasse, and Schofield (2018), Douglas et al. (2015) and Tao et al. (2015) using only spectral information to map the attributes of the target is unlikely to be successful. TLS instruments record x, y, and z coordinates, and new studies have started to explore the relationship between the points (spatial information) and use it to distinguish foliage points from wood points (Li, 2015). This research aims to compare spectral and spatial information to improve foliage and wood separation. This is achieved using: i) laboratory experiments, ii) field sampling activities, and iii) existing SALCA datasets of full forest stands. The aim of this project is split into the following three specific objectives:

1.2.1 Objective 1: To assess the potential of SALCA for foliage/wood separation in the laboratory at near-ranges using spectral and spatial information.

This step is important in order to develop a better understanding of the SALCA data, its potential and best practice for data collection and processing, before taking the instrument out into the complex environment of a forest. SALCA was designed to scan targets within a maximum range of a 105 m in an outdoor environment. In order to fulfil Objective 1, a series of measurements in a laboratory environment were performed to scan leaf-on and leaf-off conditions for a broadleaf and needle-leaf tree at four different short ranges (1, 3, 5, and 8 m). Two different species of tree in the laboratory were scanned using the SALCA instrument to test its potential for measuring the response of different tree species in the laboratory. A full description of the laboratory data is provided in Chapter 4. This objective leads to the first research question:

Can spectral and spatial information at short range from SALCA be used to develop a successful classification of tree components?

1.2.2 Objective 2: To assess whether the SALCA instrument can be used for foliage and wood separation at the level of the individual tree in the field environment.

Developing an effective technique to distinguish foliage from wood points would increase the accuracy of the forest structural measurements, which is known to be a limitation of current terrestrial laser scanners (Hosoi & Omasa, 2012). In order to satisfy this objective, three isolated single oak trees in Silverdale, Lancashire, UK, were targeted and scanned. The extracted information was used to map the tree attributes. A full description of the fieldwork and data is outlined in Chapter 5. This objective leads to the second research question:

Can spectral information and 3D point cloud patterns be used to classify tree components of individual trees in the field environment?

1.2.3 Objective 3: To assess whether the three-dimensional point cloud patterns can be used to separate foliage points from wood at the level of a full forest stand.

Trees are large, complex objects and it is challenging to use conventional methods to measure their physical features, including their size, shape and canopy structure. However, the spatial and spectral information on forest stands may provide critical elements in ecological studies, and forest resources management (Kelbe, Romanczyk, van Aardt, & Cawse-Nicholson, 2013). However, there have been no published studies on testing the spectral and spatial information at the level of a complete forest stand. The third objective of this research will be achieved by comparing the spectral and spatial information in order to perform a leaf-on scan of full stand data. A leaf-off scan will be used in order to validate the classification of the leaf-on scan. The data that will be used to satisfy this objective are detailed in Chapter 6. This leads to a specific research question:

Can spectral and the spatial information from SALCA be used to separate foliage from wood points at the stand forest level?

The general aim and objectives of this project, research questions, desired datasets, and thesis chapters, related to each objective, are summarised in Figure 1.2.

1.3 Structure of thesis

The work in this research was designed to use terrestrial laser scanning data extracted from a dual-wavelength instrument in order to develop a physically-based classification of foliage and wood at single and full forest stand scales. This thesis contains seven chapters. Chapter 1

has highlighted the context of the research and provided the main aim and objectives. Chapter 2 presents a review of the relevant literature and addresses the specific research areas that are related to this research. This is followed by Chapter 3, which contains a full description of the SALCA scanner, spectral data, CANUPO software, and spatial data analysis. The laboratory measurements designed to fulfil Objective 1 are outlined in Chapter 4. This chapter assesses both the spectral and spatial classifications in the laboratory including visualisation, and data analysis for the tree samples. Chapter 5 covers the experimental design and fieldwork measurements in order to address Objective 2 of this research. The chapter contains a full description of the fieldwork samples and experimental design. This is followed by a series of spectral and spatial classifications, visualisations, and analysis of single tree TLS data. Chapter 6 assesses the spectral and spatial classifications, visualisations, and analysis of a full forest stand. The measurements in Chapter 6 are designed to fulfil Objective 3. The final chapter (Chapter 7) provides a discussion of the main findings of this research, makes comparison with previous research and draws a range of conclusions including pointers for future research priorities.

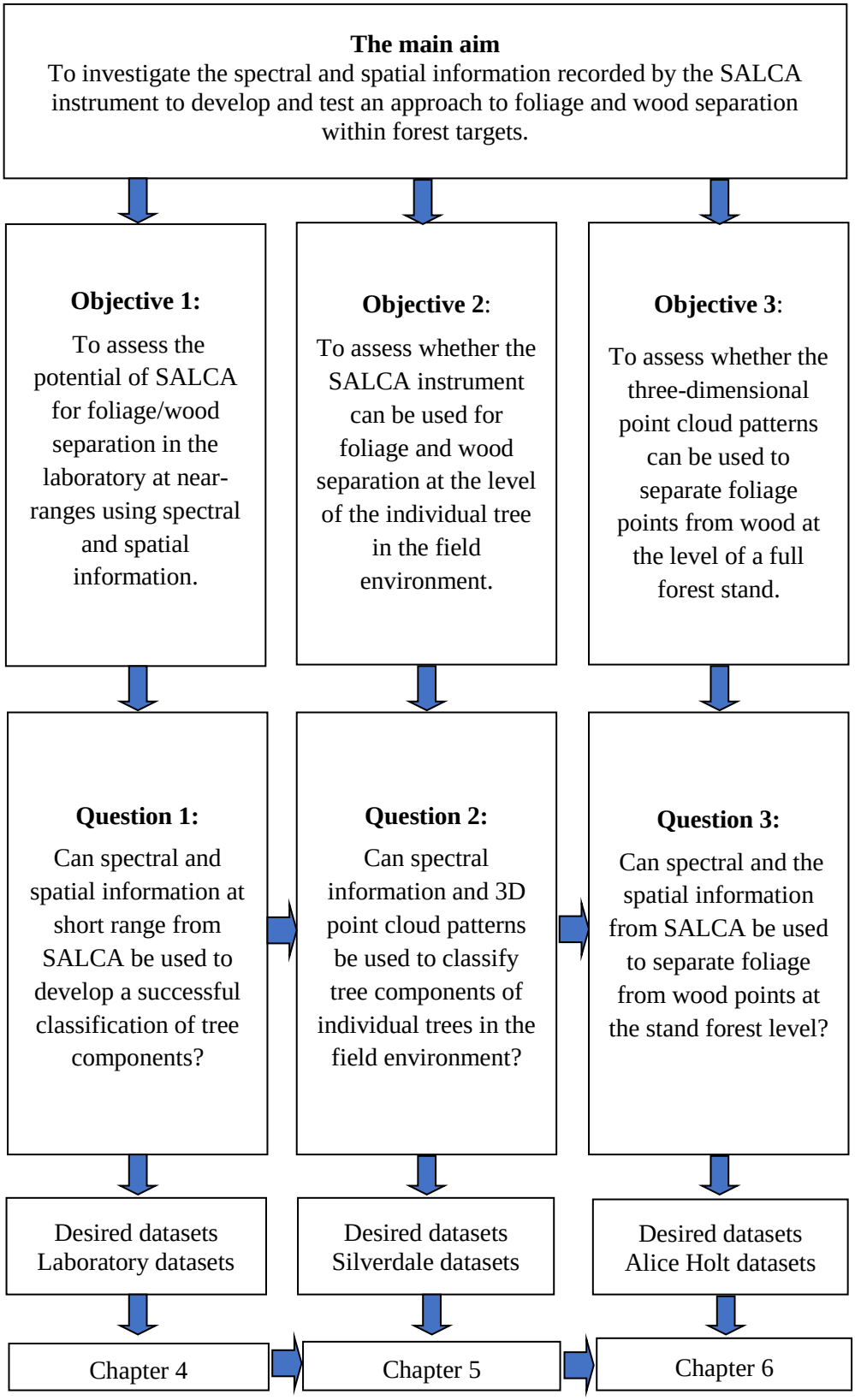

Figure 1.2: The general aim and objectives of this project, research questions, desired datasets, and thesis chapters related to each objective.

CHAPTER 2: LITERATURE REVIEW

Summary

This chapter reviews previous studies that have demonstrated the potential of LiDAR systems and terrestrial laser scanning (TLS) technologies in the forest measurement domain. The review provides a general overview of some of the laser scanners currently available. The chapter concludes with a discussion on the challenges existing within this field of study and some of the key research questions.

2.1 Introduction

Tree data are fundamental for forest ecosystem service management at the global to local scales, such as measuring biomass, stem volume, timber harvesting, and the changes in these characteristics (Bravo, LeMay, Jandl, & von Gadow, 2017). Due to forests' three-dimensional architecture, many tree characteristics are not directly measurable in traditional forest inventories, and various easy-to-measure variables are used to describe forest structure (Newnham et al., 2015). For instance, rapid semi-automatic measurements including density, height, biomass, and growth will be discussed, which are all relevant in the context of this project (Newnham et al., 2015). New technologies in the field of remote sensing have demonstrated the potential of terrestrial laser scanners to provide robust quantitative measurements, which are comparable to those gained using allometric approaches and may be derived in a semi-automatic way (Danson et al., 2018; Liang, Kankare, Yu, Hyyppa, & Holopainen, 2014; Malhi et al., 2018). In the case of forest ecology, TLS technology has been used widely to obtain accurate estimates of leaf area index and gap fraction as well as to attempt to distinguish the returns from foliage and woody materials (Ferrara et al., 2018).

2.2 Forest measurements

Forest inventories are generally based on plot-scale terrestrial-based methods using relatively simple techniques (Olofsson, Holmgren, & Olsson, 2014). Tree data are continually acquired in forest inventories as tree-by-tree measurements on which forestry policies are based (Murphy, Acuna, & Dumbrell, 2010). Decisions such as harvesting schedules, thinning, and regeneration are based on these tree measurements. The main data consist of tree characteristics, such as tree species, diameter at breast height (DBH) and tree height (Liang et al., 2016). The DBH can be defined as a standard technique for measuring the trunk or bole

diameter for the desired tree sample (Mackie & Matthews, 2008). This measurable parameter has been used in order to estimate the total tree volume, where DBH is measured in centimetres, based on which the forest timber volumes may be estimated (Garber & Maguire, 2003). These measurements are generated from stable research plots and produced for a range of tree species and location conditions (Newnham et al., 2015). Foresters frequently employ tree heights to estimate tree growth, productivity and tree stand volumes. Abundance parameters, such as density and frequency, are also important measurable parameters that are frequently used to describe forest structure (Blanc, Maury-Lechon, & Pascal, 2000).

The absolute stem density of an area comprises the number of individuals per unit area or per volume, while the frequency is the number of individuals that occur of a given species (Richards, 1952). The other common parameter determined in forest surveys is the basal area, which is used to determine the number of trees per hectare or the volume per hectare for timber inventories (Humphreys, 2014). The determination of the basal area per hectare of a forested area is a useful summary statistic for foresters because it incorporates both the average size and the density of the trees. The basal area is defined as the cross-sectional area of a tree at breast height and is normally expressed per hectare (Henning & Mercker, 2009).

In order to investigate the physiological drivers of tree growth in a desired forest, it is fundamental to obtain measurements of the leaf area index (LAI) (Qu, Zhu, Han, Wang, & Ma, 2014). LAI is defined as the total one-sided area of green foliage per unit of ground surface (Breda, 2003; Chen & Black, 1992). This parameter is key to understanding the gas exchange between the green parts of tree canopy and atmosphere, where most of the energy exchanges occur (Piayda et al., 2015). Previous studies have applied both direct and indirect approaches to quantify this parameter. However, they show that LAI is one of the most difficult parameters to measure and time consuming (Chen & Cihlar, 1995; Cutini, Matteucci, & Mugnozza, 1998; Schofield, 2016).

Due to the physical architecture of forests, tree measurements are difficult to obtain. To date, forest data have been measured using simple tools, such as callipers and clinometers, which has caused slow progress in the enhancement of forest field measurements. These methods are highly labour-intensive (Dassot, Colin, Santenoise, Fournier, & Constant, 2012) and so recent developments in remote sensing have started to assess the potential to provide rapid, affordable and accurate data at the level of a single tree or a full forest stand.

2.3 Remote sensing

Remote sensing (RS) technology acquires data on a target using instruments located on aircraft, satellites, or other platforms, that are not in contact with the target (Lillesand, Kiefer, & Chipman, 2014). Thanks to the increasing number of platforms and sensors that are being developed, and the evolution of Multilateral Environmental Agreements, numerous advances in the field have been made, helping to regulate the collection, monitoring, reporting, and evaluation of data pertaining to environmental change (Toth & Jóźków, 2016).

In the forest domain, RS technologies have been reviewed recently in many studies (Barrett, McRoberts, Tomppo, Cienciala, & Waser, 2016; Kirchhoefer, Schumacher, Adler, & Kändler, 2017; Wallner et al., 2018). In terms of data collection, passive optical sensors make it possible to collect data on the two-dimensional characteristics of above-ground vegetation, while LiDAR systems provide information about the vertical distribution of the canopy elements (Lim, Treitz, Wulder, St-Onge, & Flood, 2003; van Leeuwen & Disney, 2018).

RS techniques can be divided into active and passive methods. Active methods are where sensors are able to emit their own source of electromagnetic energy and measure the backscattered energy from the desired target. In contrast, passive sensors measure the natural solar energy or emitted radiation (Campbell & Wynne, 2011). The recent advances in RS methods allow us to use the spectral properties of vegetation in order to understand the spatial distribution of a desired target. In a forest, the basic idea of the RS measurements depends on measuring the reflectance and relating it to the vegetation surface's properties. Plants in forests have different water contents, organic materials, pigments, and structural distribution. However, every plant has its own spectral response to the radiation that allows us to distinguish it from its surrounding environment (Weber, 2015). Figure 2.1 shows the spectral reflectance signature of foliage in the optical spectrum. As the figure shows, there is strong absorption in the visible area (400-700 nm) caused by the chlorophyll pigment. This means that the reflectance at this range is low. There is high reflectance of foliage in the near infrared region (700-1400 nm) because of the internal scattering of light within the foliage. This strong absorption allows us to detect any biological changes that are occurring in the foliage such as stress or drought (Jensen, 2006). In addition, low reflection occurs in the shortwave infrared caused by the water content. These features responding to the spectral wavelength, are the key property used to map vegetation based on its spectral response.

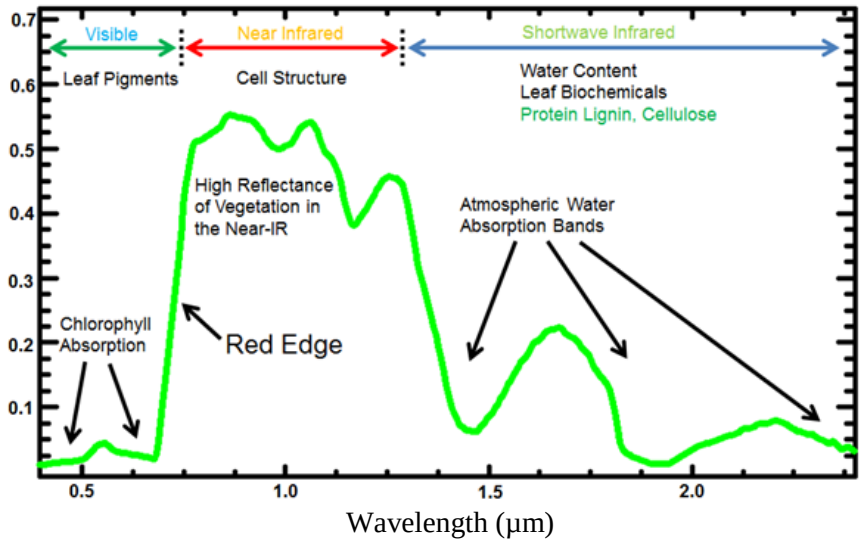

Figure 2.1: Spectral distribution of foliage across the electromagnetic spectrum. Source: (Elowitz, 2013).

Forest inventories are conducted in order to measure tree biomass and volume, and also to calculate yield production. Nowadays, the use of Airborne Laser Scanning (ALS) has expanded, especially in environmental fields, such as wildlife, recreation, watershed management and many other important areas (Guo, 2017). Although many studies have focused on the domain of Airborne Laser Scanning, others show that TLS has the potential to improve our capability to remotely sense the three dimensional physical features of vegetation (Li, Schaefer, Strahler, Schaaf, & Jupp, 2018; Malhi et al., 2018; Roşca, Suomalainen, Bartholomeus, & Herold, 2018).

2.4 Terrestrial Laser Scanning (TLS)

Terrestrial laser scanners are an active remote sensing ground-based technology designed to measure their surrounding environment in order to extract 3D point observations for the desired target (Li, 2015; Liang et al., 2016). Due to their efficiency, different industrial sectors have used terrestrial laser technologies to capture 3D models covering a wide range of applications, such as topography, mining, and engineering (Owers, Rogers, & Woodroffe, 2018). Recently, in the forestry sector, terrestrial laser scanners have been used to provide high-quality information for forest inventories, characterising woodland and forest areas (Moskal & Zheng, 2011; Yaman & Yılmaz, 2017). Moreover, it is recognised that terrestrial laser instruments can measure and record data as multiple returns from a single laser pulse, which is critical in terms of 3D model construction for forest applications (Hopkinson et al., 2013). Forest structural information may be needed at a small areas than data that can be

measured using ALS technologies to acquire forest data with millimetre level accuracy and resolution (Jupp et al., 2009).

From a ground-based viewpoint, TLS is able to obtain accurate information on vertical structure, leaf distribution and understorey vegetation properties (Lovell, Jupp, Culvenor, & Coops, 2003). There is also a positive environmental aspect associated with using these technologies, which is that they provide an opportunity to acquire physical measurements automatically without disturbing the environment, and also demand less time and effort for data acquisition at this level of detail (Ahlberg, Söderman, Elmqvist, & Persson, 2004; Douglas et al., 2015).

2.4.1 TLS principles

TLS is based on the transmission and the reception of a single or multi-spectral wavelength laser pulse which hits a target with low spatial diffusion and high accuracy in terms of time (Fröhlich & Mettenleiter, 2004). The 'time-of-flight' of the fired beam provides ranges of objects up to several hundred metres, with a centimetre-level or better accuracy (Pfeifer & Briese, 2007). As illustrated in Figure 2.2, when a ground-based scanner fires a laser beam, it will hit any target within the maximum measurement range of the device.

Most of the currently available TLS rotate horizontally and vertically during the scan in order to provide full coverage of the desired surrounding environment within a given time. Part of the fired laser energy is scattered back to the source and captured as digitized intensity, recorded in digital counts as a digital number (DN). The amount of backscattered energy is based on many variables; the surface reflectance properties of the target, the distance between the sensor and the target (range), the proportion of the object in the footprint, and the scattering properties of the targets (Danson et al., 2014). Through accurate 3D measurement of the backscattered energy and range, TLS generates 3D observations that may lead to a better understanding of tree structure and forest ecosystem function.

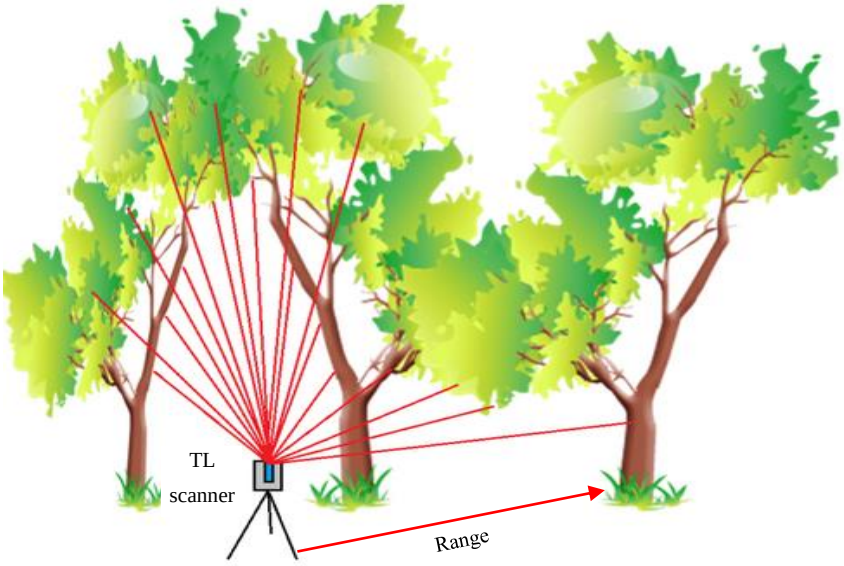

Figure 2.2: TL scanner fires a laser beams to hit collection of trees within a certain range. Source: (Nölke et al., 2015).

2.4.2 TLS applications in forest ecology

Forest information is traditionally represented as one-dimensional (e.g. the mean tree height) or two dimensional (e.g. tree location) in order to characterise the forest structure and composition (Trochta, Krůček, Vrška, & Král, 2017). However, the physical structure of a forest in reality is three-dimensional so 1D or 2D information may not adequately represent the forest's characteristics (Trochta et al., 2017).

2.4.2.1 Plot-based measurements

Forest plots are usually small areas designed as squares or circles to provide forest information by taking measurements tree by tree (Liang et al., 2016). For the last two centuries, plot-scale manual measurements have been key to forest surveys. However, over the last two decades, TLS technologies have been used to provide robust measurements at the plot-scale (Newnham et al., 2015). TLS has been widely used to build useful 3D models to facilitate research and the monitoring of forest ecosystems and to understand forest functions by describing their 3D structure (Wulder et al., 2013). TLS data may be used to calculate the tree abundance and basal area and the results are comparable with other results, obtained by classical plot sampling. In some cases, the results have shown that the TLS data provide more valid information compared to that produced via classical plot sampling (Corona, Di Biase, Fattorini, & D'Amati, 2018). The Echidna scanner was used at a plot scale level over several

years to measure the DBH, stem density, basal area and woody biomass of the trees in Harvard Forest, USA (Orwig et al., 2018; Strahler et al., 2011). These measurements were used to create three-dimensional models of the trees and the datasets were recently used in conjunction with airborne images in order to understand the effect of ice storms on the forest and characterize the forest dynamics over time

2.4.2.2 Above-ground biomass (AGB) measurements

AGB is estimated based on allometric equations and using indirect relationships between the samples and the constructed variables. TLS provides detailed 3D information without the need for allometry (Calders, 2015; Malhi et al., 2018). For example, a TLS scan was used to acquire high-resolution point clouds for mangrove vegetation in Southeast Australia, in order to estimate the ABG from the TLS points (Owers et al., 2018). These points were used to build a volumetric model and then compared with the result of a biomass estimation model using a traditional allometric equation. The results of both approaches were possible to estimate the ABG for the desired data accurately using TLS information. In addition, allometric and volumetric models were evaluated separately by comparing the regression to a 1:1 line.

Quantitative structure models (QSM) offer a new approach for quickly building and automatically modelling tree stems and main branches extracted from TLS or mobile laser scanner data (Raumonen et al., 2013). Tree points are constructed using a local tool to represent every point in the scan as a small patch connected to the tree surface. These points are then modelled as cylindrical shapes, based on their size, into the main stems and branches. The results provide a quick approach that allows us to extract and build tree structures and, in conjunction with wood density estimates, measure single trees' woody biomass (Raumonen et al., 2013).

2.4.2.3 Gap fraction and Leaf Area Index measurements

Until recently, researchers have rarely investigated the application of TLS data in the domain of forest ecology. However, TLS data have now been tested for the estimation of LAI and gap fraction (Li et al., 2017; Wu et al., 2018). A study attempted to measure LAI in a forest environment in the Swiss National Park, located in eastern Switzerland, by deriving the canopy directional gap fraction distribution measured using TLS (Danson, Hetherington, Morsdorf, Koetz, & Allgower, 2007). The output was compared with distributions obtained

from digital hemispherical photographs recorded at the same location. The results showed that the directional gap fraction distributions were similar in both recorded datasets. In a more recent study, LAI was estimated using TLS data at the level of a plot of conifers and deciduous trees in the Bavarian Forest National Park, Germany (Wallner et al., 2017). The study corrected the effects of foliage clumping and woody materials and showed that the leaf angle distribution and LAI can be estimated using TLS.

2.4.2.4 Leaf water content estimation

Foliage Equivalent Water Thickness (EWT) refers to the water content in vegetation or within a given foliage area. It is recognised as a good indicator of any vegetation stress or drought condition (Yilmaz et al., 2008). Elsherif et al. (2018) used the NDI of the 808 nm near-infrared wavelength and the 1550 nm shortwave infrared wavelength, used in the commercially-available Leica P20 and Leica P40 TLS instruments, respectively, to generate 3D estimates of the leaf Equivalent Water Thickness (EWT) of two broadleaf and needle-leaf canopies. The 3D EWT estimates, which revealed a significant difference in terms of water content between foliage and woody materials, were used for foliage/wood separation by choosing an EWT threshold by trial and error. It was reported that, in the case of the broadleaf canopies, the visual assessment showed that this foliage/wood separation approach was successful, as only very few points corresponding to foliage were misclassified as wood. However, in the case of the needle-leaf canopies, the dry needles were wrongly classified as wood, showing that this method has limitations. Manual refinements were needed to improve the classification. In addition, the method was only tested indoors, and further experiments are still needed to test its applicability in real forest environments, where challenges such as the wind effect and the partial hits must be addressed (Elsherif et al., 2018).

Gaulton, Danson, Ramirez, & Gunawan, (2013) used the SALCA instrument to estimate the biochemical contents of foliage. In the laboratory, five sets of foliage from three different tree species were scanned. The foliage reflectance of both laser wavelengths was extracted using simulated datasets, and then the NDI and the EWT were calculated. A strong relationship was found between the NDI and the foliage EWT, which were highly correlated (R^2=0.80).

2.4.2.5 Voxel-based approaches

Several studies have extracted TLS information and attempted to represent it in voxel-based models in order to understand a range of biophysical processes within a forest ecosystem

(Béland et al., 2014; Hess, Härdtle, Kunz, Fichtner, & von Oheimb, 2018; Li, Guo, Tao, & Su, 2018). Voxels are small cubic spaces that are used to visualize the structure of targets and represent it in three-dimensions (Durrieu, Allouis, Fournier, Véga, & Albrech, 2008). The intensity of a single spectral channel (1550 nm) was used to map the foliage area distribution using volume elements to process the TLS data. An ILRIS-3D scanner was used to measure the intensity return from six small trees. The intensity of a first return was extracted, and a threshold adopted and applied in order to distinguish foliage points from woody materials, after which the foliage and wood components were visualized and represented as voxels grids. These visualizations showed that parts of the trees' crowns (finer branches and leaves) were inaccurately represented as voxels due to their small size (Béland, Widlowski, Fournier, Côté, & Verstraete, 2011). Béland et al. (2014) used the same approach to test multiple returns from a blue oak tree using the Riegl VZ-400 instrument (1550 nm) in California, USA. The output showed that the data from multiple return scans have the potential to represent the desired data in more detail, including the finer branches. The output of this study was more accurate compared to the technique employed in Béland et al. (2011) but partial hits were an issue.

2.4.3 Foliage/wood separation

Foliage and wood separation is important for deriving spatial information on tree attributes. In the case of forest ecology, accurate foliage and wood separation is a condition for LAI estimation, while the quantification of the wood materials is important for monitoring the carbon stock within forest ecosystems (Wang, Hollaus, & Pfeifer, 2017). Foliage plays a critical role in energy cycling through photosynthesis and evapotranspiration. Therefore, it is fundamental to obtain accurate quantification for foliage spatial distribution to help to drive research in the domain of forest ecology and climatology (Levick, Hessenmöller, & Schulze, 2016). In order to distinguish foliage from wood points, the majority of previous studies employed single-wavelength scanners, such as the ILRIS-3D scanner and Riegl VZ-400, to acquire data (Béland et al., 2014; Béland et al., 2011). A study was conducted in a northern Idaho Forest, USA, to distinguish foliage from woody points based on the number of returns of each laser pulse (Clawges, Vierling, Calhoon, & Toomey, 2007). TLS used to measure three deciduous conifer trees in multiple locations in order to scan their leaf-on (with foliage) and leaf-off (without foliage) conditions. A group of leaves was harvested from the three trees at a height of 1 meter from the ground in order to calculate the leaf points area manually. For the TLS data, the leaf areas were estimated by subtracting the leaf-off from the leaf-on

returns. The output was then compared to the manual approach and the two sets of results were found to be strongly correlated ($R^2 = 0.822$). However, this approach is only useful for measuring deciduous trees (leaf-on and leaf-off scanning) and is inapplicable to coniferous trees. Moreover, it is difficult to represent true foliage returns using this technique due to the random distribution of woody material compared to the foliage position (Piayda et al., 2015). Perhaps the most serious disadvantage of this method is that successful intensity-based wood-leaf segmentation using one LiDAR system does not guarantee accurate segmentation nor provide a straightforward interpretation of the desired data (Tao et al., 2015). In other words, different species of trees respond differently to the LiDAR wavelength, which means that the intensity approach cannot be used to classify tree species without additional information (Piayda et al., 2015).

Recent studies have started to use spatial classifiers to classify foliage and wood data based on the geometric features of the point-cloud data (Disney et al., 2018; Tao et al., 2015; Wang et al., 2017). For example, Tao et al. (2015) attempted to separate foliage points from wood materials based on the x, y, and z coordinates' distribution of each point. The Riegl VZ-400 instrument was used to scan camphor and magnolia trees in order to compare them with a virtual tree model, created using 'Maya' software to simulate the point clouds. The point clouds were sliced into circles and circle-like shapes and then the x, y and z-axis were featured to represent foliage and woody materials as layers connected to each other by line nodes. The results showed that the foliage/wood separation for the simulated points of the virtual model was more accurate than that for the camphor and magnolia trees. The results revealed misclassifications errors of 10.7% in the virtual model, while 16.9% and 13.4% of the errors were recorded on the camphor and magnolia trees respectively.

From the previous studies, the ability to use single-wavelength scanners for foliage/wood separation is limited because the majority of the currently available single-wavelength scanners acquire the target's coordinates of the backscattered energy returns as uncalibrated intensity. This makes it very difficult to generate outputs related to the target reflectance properties. In order to extract useful, detailed information from TLS scanners, the scanned data need to be calibrated in order to compare the targets' reflectance, which can be achieved only by deriving the calibration equation that accounts for the scanner's characteristics and range-dependence. For the single-wavelength TLS, the target reflectance and area of the scatterer together control the intensity. This means that it is hard to determine the reflectance

of a target without first determining the area from which it arises. As a consequence, the apparent reflectance produced by single-wavelength TLS may not represent the real values concerning the target reflectance (Danson et al., 2018).

2.4.4 Recent advances in TLS technology

New prototype multi-spectral laser instruments have been developed recently in order to address the limitations of single-spectral scanners and improve the accuracy of collected data across a wide range of forest applications. A multi-spectral scanner such as the HyperSpectral LiDAR (HSL) was designed to measure the chlorophyll content of foliage, which makes it possible to distinguish between the photosynthetic and woody areas of vegetation (Eitel, Vierling, & Long, 2010; Hakala, Nevalainen, Kaasalainen, & Mäkipää, 2015). Some of these prototypes are being used to assess different applications of vegetation. For instance, Rall & Knox, (2004) scanned a deciduous tree canopy using the multi-spectral Spectral Ratio Biospheric Lidar (SRBL). The scanner used 660 and 780 nm wavelengths and the trees were scanned at a different location beside a wall to distinguish the reflectance of trees from non-living targets. The results showed a significant difference between foliage reflectance and the wall reflectance.

A laboratory multi-spectral prototype with four laser wavelengths has been developed by Wei et al. (2012) to measure the reflectance, nitrogen and chlorophyll contents of six samples of broadleaves and one sample of a needle. A sample of black soil and cement were scanned beside the vegetation in order to test the discrimination ability and feasibility of the multi-spectral scanner. The outputs of all of the samples were then visualised based on their geometric properties. The final discrimination accuracy was then assessed using the Support Vector Machine (SVM) method described in Milgram, Cheriet, & Sabourin, (2005). The results showed that the total discrimination accuracy was 83%, which means that the scanner with four laser wavelengths has the potential to distinguish foliage reflectance from other targets, such as soil and cement (Wei et al., 2012).

Another prototype was designed by Vauhkonen et al. (2013) to scan spruce and pine trees in a laboratory in order to classify their components. The analysis in this research focused only on the pulses that penetrate the foliage areas in order to improve the accuracy of the classification of the desired data. In the laboratory, leaf samples were scanned at a distance of seven meters from the instrument, before being harvested, and the leaf samples along being scanned again.

Then the reflectance of the leaf-on scan and leaf-off were calculated and compared. The classification of the leaf-on scan showed similar values of reflectance produced by the leaf-off scan.

More recently, two new scanners have been developed and tested to work in a field environment, the Dual Wavelength Echidna LiDAR (DWEL) (Douglas et al. 2012) and the Salford Advanced Laser Canopy Analyser or (SALCA) developed by the University of Salford, UK (Danson et al., 2014). SALCA is a dual-wavelength, full-waveform laser scanner, designed by the University of Salford, UK, and built by Halo Photonics Ltd in order to measure tree canopies. SALCA records the backscattered energy at 1063 and 1545 nm wavelengths. This feature gives the device the potential to distinguish between tree foliage and woody components. A full description of the SALCA system's specifications is presented in Chapter 3.

An approach related to intensity calibration to apparent reflectance was tested using neural networks for each laser wavelength (Schofield, Danson, Entwistle, Gaulton, & Hancock, 2016). In a recent study, Schofield (2016) used spectral information from dual-wavelength scanning data to classify the foliage and wood materials of three oak trees from Alice Holt Forest, south of Farnham in Hampshire, Surrey, UK. Foliage and wood were separated using a specific threshold at AR for a signal channel (1545 nm). The scans were tested for single and multiple returns, then the AR was visualised, and a threshold of AR 0.3 at 1545 nm was applied to classify the tree components into two categories, with less than 0.3 being foliage and higher than 0.3 being wood. The outputs showed that the foliage classes recorded higher values of AR, and some of the multiple returns were represented by low values. A group of partial hits on the stems were incorrectly classified as foliage. In addition, some of the fine branches and edges were represented as foliage materials, as expected for leaf-off conditions. These errors in the leaf-off scan classification encouraged the investigation of the use of the NDI to distinguish woody partial hits from foliage returns. A threshold of 0.1 on NDI was applied in the above study. The results showed that the woody partial hits were classified as foliage returns and that it was impossible to classify them as wood.

More recent research tested the sensitivity of NDI to the incidence angle between the laser and leaf orientation (Hancock, Gaulton, & Danson, 2017). The SALCA instrument was used to acquire data for a range of (dry, green) leaves in the laboratory. The reflectance and NDI

for the desired data were obtained. The angular dependence of the reflectance was measured and the effect of the angle of incidence on the NDI was then obtained. The results showed a small change in the NDI compared to the difference measured in the NDI between the green and the dry leaves.

2.4.5 Spatial classification approach

It is clear from the work reviewed above, that using the spectral information to map tree attributes is unlikely to be successful using spectral information alone. However, it may be useful to combine spatial classification based on x, y, z positions extracted using spatial classifier (SC) with the spectral classification from multispectral scanners. Using spatial classifiers allows the processing of the point clouds to map 3D patterns on the scan based on the x, y and z coordinates alone. The classifier is generally designed to map a group of points as 1D, 2D, or 3D. These patterns may then be related to tree canopy features like foliage, branches or stems.

In order to understand how the spatial classifiers influence the classification process, four machine classifiers (Support Vector Machine (SVM), Naïve Bayes (NB), Random Forest (RF), and Gaussian Mixture Model (GMM)) were tested using TLS data on *Erytrophleum fordii and Betula pendula* trees. The same scales were chosen to train the same number of points in all classifiers. The results showed that RF was the most accurate classifier in representing the local distribution of points related to the tree features (Wang et al., 2017).

Li (2015) combined spectral data collected by the DWEL and spatial data produced by extracting the geometric features of foliage and wood hits, and then coloured them using colour-composite figures. The spatial outputs were created using a multi-scale dimensionality algorithm using the K-means classifier. The scans were performed at Harvard Forest, Massachusetts, USA, presenting leaf-on and leaf-off conditions. All of the points were divided into 100 clusters based on three variables: apparent reflectance at two wavelengths and the NDI, after which each cluster was visualised as a three-dimensional model and classified as foliage, wood, or mixed class. The outputs showed that accurate values were extracted from the classifier to illustrate the degree of accuracy of the discrimination. The discrimination accuracy of the foliage-wood components for the leaf-off and leaf-on conditions was 79% and 75%, respectively. However, the investigations concluded that the fine branches and edges at far ranges showed errors in terms of classification.

The spatial classifier used in this research project was the CAractérisation de NUage de Points or CANUPO classifier. The classifier was developed by Brodu & Lague (2012) to provide methods for point cloud separation based on geometric features. The classifier works by identifying the best combination of homogeneous points in a trained sample and classifying them, according to their position, into two classes within a given location. The spatial classifier was used to separate vegetation from ground materials, including rock, soil, and water. The authors used a multi-scale approach and the spatial classifier efficiently separated the vegetation points from the rest of the points representing soil, rock, and water. In a more recent study, forest carbon storage was estimated using publicly-available datasets. The data were classified, using CANUPO, into foliage and wood and then voxelized for volume quantification. The results showed that DBH and biomass were very easy to estimate after spatial separation, and strongly correlated (Stovall, Vorster, Anderson, Evangelista, & Shugart, 2017).

2.5 Research challenges

Previous studies Clawges et al. (2007); Tao et al. (2015) employed single-wavelength TLS, which rarely provides information related to the surface properties of the target due to the absence of reliable calibration. In terms of classification, using the spectral data of the single-wavelength scanners has produced errors, mainly related to partial laser hits. The new generation of multi-wavelengths scanners, such as SALCA, has the potential to provide additional information that will allow us to extract more valuable information, which has not yet been widely investigated, such as beam width and the number of returns. There exists a range of challenges related to the accurate reflectance calibration and analysis of data produced by SALCA. It is clear that the classification approach that combines spectral and spatial information offers a new area of interest in terms of tree component classification. However, there is a lack of published studies that investigate the application of spectral and spatial classification for foliage /wood classification. Therefore, this is one of the biggest challenges for this research.

2.6 Research questions

Based on the literature review, a group of research questions has been developed in order to address the main objectives outlined in Section 1.2. In order to satisfy Objective 1, a series of laboratory scans were acquired at short-range to assess the potential of SALCA regarding

foliage and wood separation using spectral and spatial information. The spectral classifier required reliable calibration in the laboratory in order to produce reflectance related to the properties of the sample. Produce reflectance related to the target properties allowed the data to be used for spectral classification. The research questions related to Objective 1 are, therefore:

Question 1.1 Can SALCA spectral data be used to separate foliage and wood in short-range scans in the laboratory?

Question 1.2 Can SALCA spatial data be used to separate foliage and wood in short-range scans in the laboratory?

Question 1.3 What is the relationship between the outputs of these two classification approaches?

Objective 2 aims to test whether SALCA instrument can be used to classify the returns from foliage and wood at the level of the individual tree in an open environment. To address this objective, high-resolution multi scans were acquired for three isolated oak trees in Silverdale, Lancashire. Based on the literature review, TLS data have opened up a new area of research on the use of both spectral and spatial data for foliage/wood classification of individual trees. In order to understand the TLS data in more detail, a combination of spectral and spatial information was used to map individual tree components and the outputs were then compared in order to clarify the relationship between the spectral and spatial information in an outdoor environment. The research questions related to Objective 2 in this research are, therefore:

Question 2.1 Is it possible to separate foliage/wood at the individual tree level in an open environment using spectral information?
Question 2.2 Is it possible to use spatial information to improve foliage/wood classification at the individual tree level?

Question 2.3 Is there a relationship between the spectral and spatial approaches at the individual tree level?

Objective 3 aims to investigate whether SALCA three-dimensional point cloud patterns can be used to separate foliage form wood at the level of a full stand. To satisfy this objective, datasets from Alice Holt Forest were used to apply the spectral and spatial approach to foliage and wood separation. The interference between the components of the tree (foliage, small and

main branches) at long distances can impede the determination of an accurate threshold for spectral classification. The same issue may limit spatial classification, where the physical architecture of the full stand is complex. This might limit the ability of the spatial classifier to remap the foliage and woody materials based on their geometric properties according to these scales. The research questions related to Objective 3 are, therefore:

Question 3.1 Is it possible to separate foliage/wood using spectral information at the full stand plot level?

Question 3.2 Is it possible to obtain accurate classifications at the full stand level using spatial classification?

Question 3.3 Is there a relationship between the spectral and spatial approaches at the full stand plot level?

CHAPTER 3: RESEARCH METHODOLOGIES

Summary

Chapter 3 reviews the methodologies adopted to fulfil the main aim of this research and its objectives. This includes a full description of the SALCA instrument, the protocols used to collect the data, processing procedures, calibration, and spectral information extraction. In addition, a full description of the spatial classification software (CANUPO) that was employed to extract the spatial information is included. Both spectral and spatial information are required in order to map the point clouds of the desired datasets in this research.

3.1 Introduction

In this research, two approaches were used to fulfil the main aim of this research, as mentioned in Section 1.2. Spectral measurements were acquired using a dual-wavelength terrestrial laser instrument (SALCA) in order to obtain point clouds for the desired samples both in the laboratory and outdoor environments. The acquired datasets were then processed to produce apparent reflectance (AR). This was done in order to separate the foliage and wood materials based on their reflectance properties. In addition, a spatial classifier known as CAractérisation de NUages de POints (CANUPO), developed by Brodu & Lague (2012), was used to distinguish foliage from wood points based on their x, y, z coordinates. A full description of the data preparation and processing is presented in this chapter.

3.2 Research methodologies

In order to generate a spectral approach, the SALCA point clouds were classified into foliage and wood classes by applying specific thresholds to the frequency distribution of AR at both laser wavelengths and NDI. In order to do this, the AR 1063 and 1545 nm and NDI data were visualised using Cloud Compare software as a 3D figure. The AR and NDI frequencies were then plotted in order to apply a threshold at a specific change in the histogram (Figure 3.1). The thresholds were selected based on a visual assessments to distinguish clearly between foliage and wood, which often required testing more than one threshold for each sample. Every group of points was allocated a different colour (green for foliage and red for wood). The points were then recombined into a single figure to test the distribution of the points and

the effectiveness of the threshed. This approach was applied for the single samples and the full forest stand.

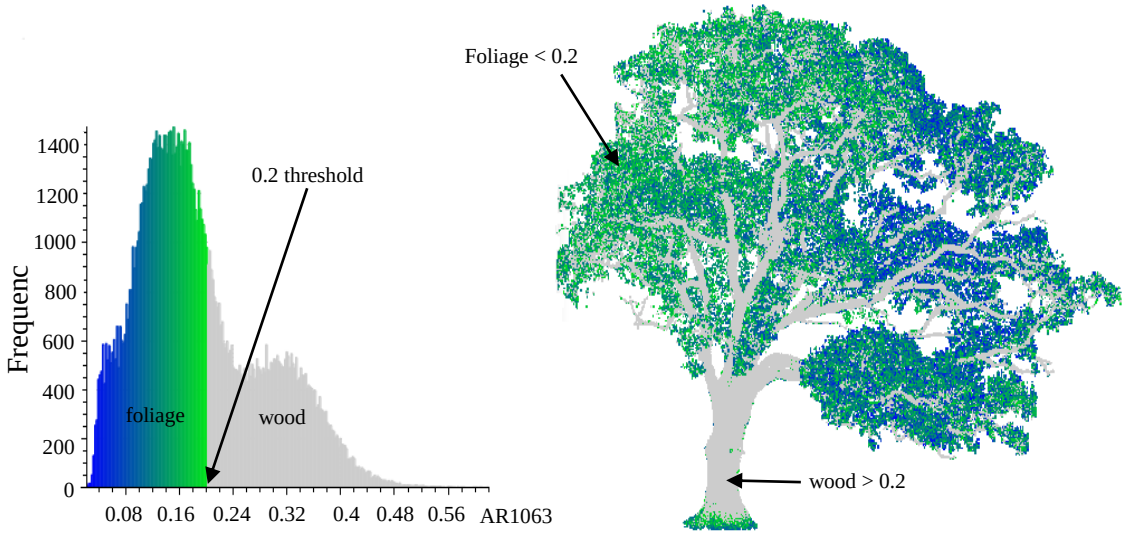

Figure 3.1: Using a visual assessment to apply a threshold on the AR histogram using 1063 nm.

The points were then classified in CANUPO software based on the geometrical properties of the points to produce a spatial approach for foliage and wood classification as described in Section 3.7. To compare the outputs of the two approaches of the classifications, all of the outputs were placed in a matrix to represent four classes: spectral classifier foliage (SF), spectral classifier wood (SW), CANUPO classifier foliage (CF), and CANUPO classifier wood (CW). This step allows the generation of agreement or disagreement between CANUPO and the spectral classification. It is expected that this approach will help to determine which kind of classification is more effective for foliage and wood separation. The full process of the classification is shown in Figure 3.2

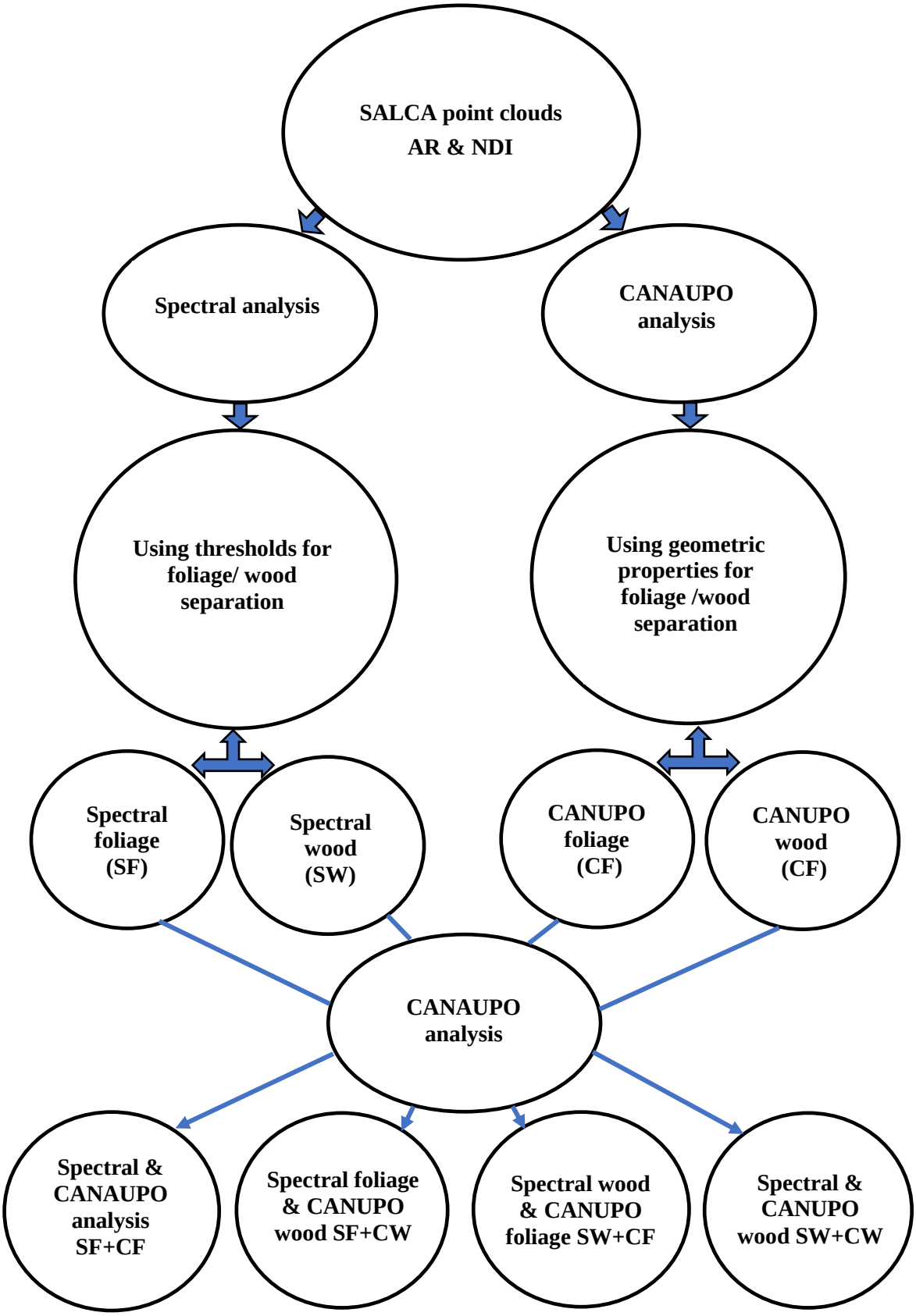

Figure 3.2: Classification of the spectral and spatial information.

3.3 Salford Advanced Lased Canopy Analyser (SALCA)

The Salford Advanced Laser Canopy Analyser is a dual-wavelength laser instrument designed to measure and quantify the structure of forest canopies (Danson et al., 2014). The scanner has the potential to measure full-waveform information by acquiring the energy returned at a 1 GHz sampling rate with a range resolution of 15 cm. As shown in Figure 3.3, the instrument upper unit is a movable chamber from which the two laser wavelengths are fired. The laser chamber rotates slowly to record more than nine million points in around two hours and at a fixed azimuth step angle of 0.06º for a high-resolution scan. The instrument is designed to pulse co-aligned laser beams in order to scan the desired targets at 1063 and 1545 nm at a maximum range of 105 m (Schofield, 2016). Due to its power, the 1545 nm laser hits the target first and is then followed by the 1063 nm. In order to reduce the 1545 nm power, filters are fixed in the scanner. The lower chamber consists of a computer that is used to store the acquired data. The instrument is a 15 kg portable device that is equipped with a battery as a power source (Danson et al., 2014; Gaulton et al., 2013).

Figure 3.3: Salford Advanced Laser Canopy Analyser (SALCA) instrument

3.4 Information content of SALCA

SALCA offers a wide range of information that can be used to classify tree components. This information can be summarised into three groups based on their physical features. The first kind of information is spatial information, which comprises x, y, and z coordinates (Cartesian), azimuth, zenith, and range (spherical), and the spatial relationships between the

points. The second kind of information is spectral information, which contains the backscattered energy or intensity, calibrated intensity or apparent reflectance, and apparent reflectance ratio or normalised difference index. The third type of SALCA information is the waveform information, which includes the number and order of the returns in addition to the pulse width and shape. In this research, spectral and spatial information was mainly used in order to separate the foliage points from the wood points. However, foliage and wood separation based on the number of returns is also considered.

3.5 SALCA data extraction

SALCA fires the1063 nm and 1545 nm laser to hit the desired target in their path. Therefore, a countable value of backscattered energy is recorded and then stored on a 150 Gb hard drive as a set of binary files. The raw datasets are then transferred from SALCA and processed in Matlab© using algorithms in order to extract physical units to use for the target components' classification. The algorithms are described in detail in Schofield (2016). The raw datasets in the binary file are processed in order to separate it into two different files according to the wavelengths 1063 nm and 1545 nm. This step is fundamental for extracting the number of returns for each wavelength. The output file contains six columns, listed in Table 3.1.

Table 3.1: The output from the first step of the SALCA data processing.

Column number	Description
1	Number of returns (1=first return, 2=second, etc.)
2	Intensity (digitised signal returned for each return)
3	Width (number of range bins for each return)
4	Range (distance between the instrument and the target)
5	Azimuth index (to calculate geometry)
6	Zenith index (to calculate geometry)

The second step is to add the geometric coordinates for each return of the 1063 nm and 1545nm using the azimuth and zenith indices and the range. The x, y, and z-axes are created along with azimuth and zenith in degrees or radians. The returns can then be visualised as three-dimensional figures using the x, y, and z or in two-dimensions using the azimuth and zenith angle or indices. The output contains 13 columns as; x, y, z coordinates as column 1, 2, and 3 respectively, while columns 4 to 9 comprise the same variables in Table 3.1. In addition, columns 10 and 11 present the azimuth and zenith angles in radians, while 12 and 13 represent the azimuth and zenith angles in degrees, respectively (Table 3.2). The third step is to remove or clean the noise or returns produced by the SALCA 'ringing'. Ringing is

information recorded from hard targets such as tree trunks and this kind of information causes false returns (Hakala et al., 2012). The noise is removed by choosing all of the returns above a certain noise threshold in order to separate the intensity returns from the ringing returns. Table 3.2 shows columns of all of the variables extracted from the SALCA raw data.

Table 3.2: Columns showing all extracted information from the SALCA data.

Column number	Description
1	x coordinate
2	y coordinate
3	z coordinate
4	Number of returns
5	Intensity
6	Width
7	Range
8	Azimuth index
9	Zenith index
10	Azimuth elevation (angles in radians)
11	Zenith elevation (angles in radians)
12	Azimuth angle (degrees)
13	Zenith angle (degrees)

3.5.1. SALCA intensity

The backscattered energy from a target is recorded and quantified as a digital number (DN), which provides information related to the reflectance of the surface (Koma, Rutzinger, & Bremer, 2018; Vain, Yu, Kaasalainen, & Hyyppa, 2010). However, this depends on many factors, such as the target characteristics, atmospheric conditions, and scan geometry (Mallet & Bretar, 2009). The amount of backscattered energy is controlled by the reflectance properties of a target, range, the proportion of the target in the footprint, and the scattering properties of a target (Danson et al., 2014; Danson et al., 2018).

3.5.2 Effect of temperature

Due to the operating system in SALCA, the temperature inside the instrument tends to be higher than that of the surrounding environment, which reduces the amount of outgoing energy over time (Danson et al., 2014: Schofield, 2016). In order to understand the effect of temperature on SALCA intensity, data from one white calibrated panel were used to generate a relationship between the intensity and case temperature of both 1063 nm and 1545 nm wavelengths. More details about the panel calibration may be found in Section 4.2. The scan was performed at an 8m range and the case temperatures for both wavelengths were recorded

every five minutes during the scanning period using a digital thermistor tool with a screen. Figure 3.4 shows that a strong negative linear relationship was observed for both laser wavelengths.

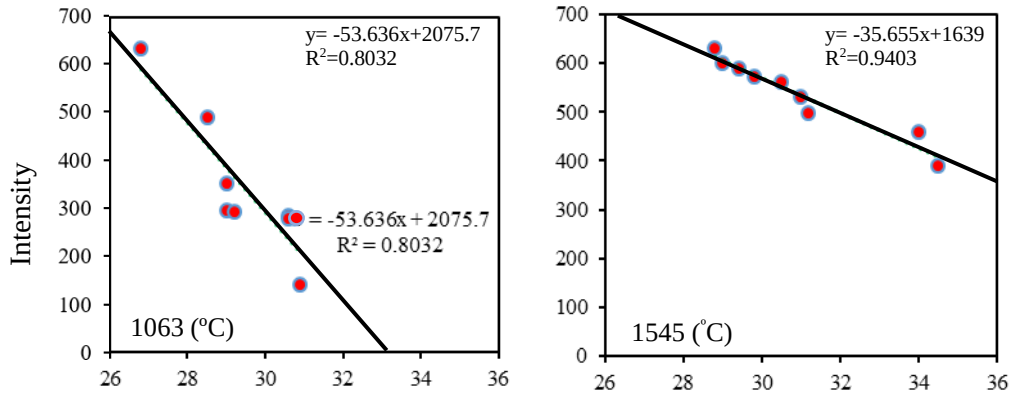

Figure 3.4: The relationship between SALCA laser temperatures and the intensity for one white panel at a range of 8 m for 1063 nm 1545nm laser wavelengths.

3.5.3 Number of returns

For each laser pulse, multiple returns may be recorded. Where there is only one return, this is referred to as a 'single return'. Multiple returns are referred to as first, second, and third. Up to ten returns are observed for a single laser pulse (Danson et al., 2018). Figure 3.5 shows the components of a single broadleaf tree scanned at 1 meter are classified based on the number of returns. The single returns are green colour and the multiple returns red for the 1063 nm and 1545 nm wavelengths. The figure comprises the main trunks, branches, and most of the tree canopy come from the single returns. The multiple returns are mostly in areas of foliage.

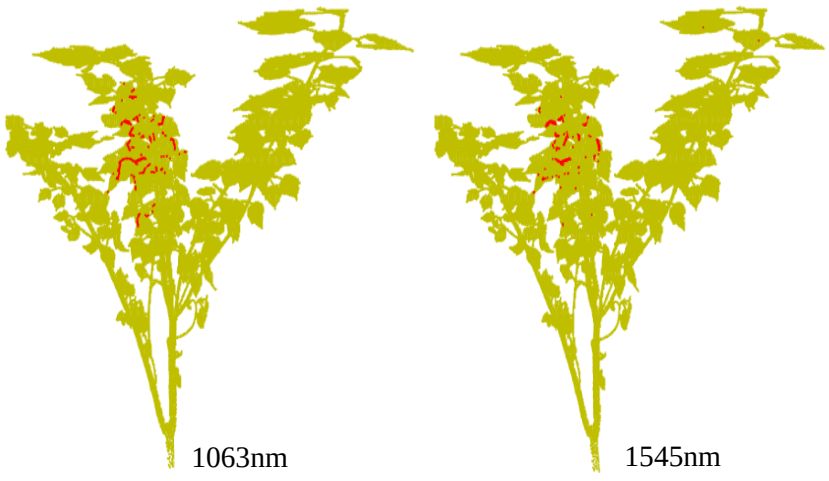

Figure 3.5: Separation of the components of a small broadleaf tree based on single and multiple returns. Green refers to single returns and red multiple ones.

3.5.4 Pulse width

The number of range bins in the returns produced by both wavelengths can provide more information on the return related to the target features; for instance, roughness (Wagner, Roncat, Melzer, & Ullrich, 2007). The frequency distribution of the width of the tree shown above was investigated in order to understand the information in the pulse width data. The histogram of width is visualised in Figure 3.6 for both laser wavelengths. Returns with a width of 1 show a very low frequency for both channels. The highest values for both the 1063 nm and 1545 nm laser wavelengths were recorded at 5 and 6, with low frequency respectively. Both of the laser wavelengths show a high frequency at width 3.

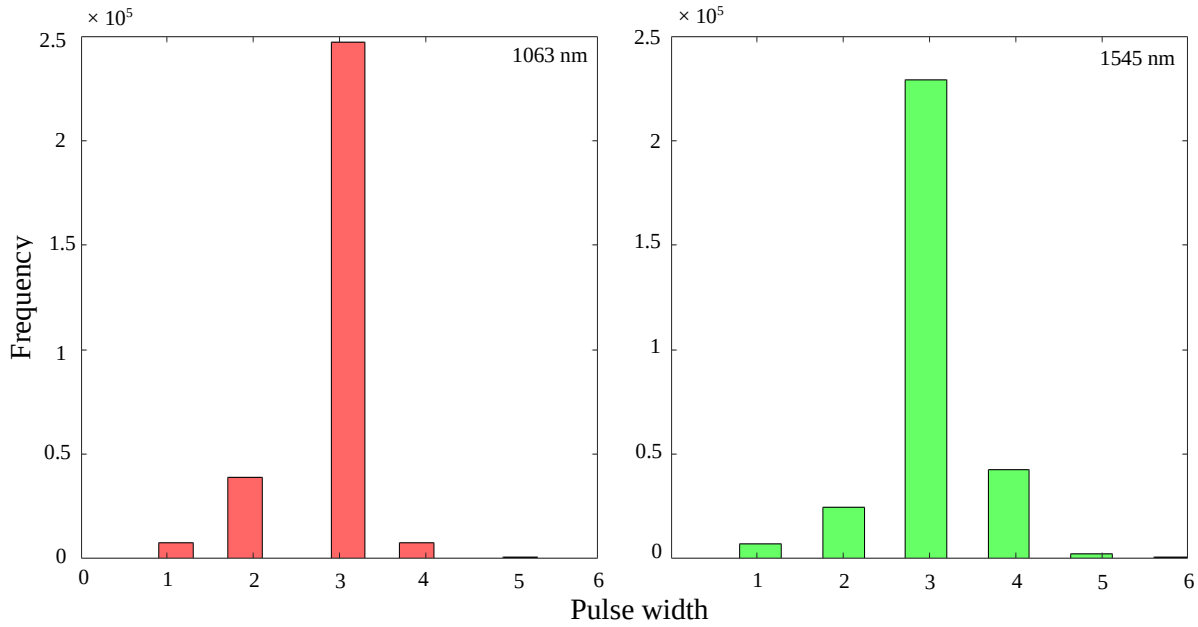

Figure 3.6: Histogram of width distribution of 1063 (red) nm and 1545 nm (green).

3.5.5 Range

Range represents the distance between the SALCA and the desired target where the amount of intensity is governed by the range. There is a drop in the intensity value as the range increases following the relationship $1/R^2$. SALCA has the potential to capture targets with a maximum range of 105 m and the range of each return is generated using the information on range and intensity combined (Hancock et al., 2015). Moreover, in order to add geometry to the SALCA data, a range needs to be computed with zenith and azimuth indices allowing 3D visualisation. In addition, SALCA calibration is performed by intensity over a certain range with recorded temperatures (Danson et al., 2014).

3.5.6 Reflectance

The reflectance properties of the desired samples are a key factor influencing the amount of returned backscattered energy (Wagner, Ullrich, Ducic, Melzer, & Studnicka, 2006). In order to extract information from the SALCA raw intensity related to the target properties, it is fundamental to apply a series of corrections to the raw intensity in order to convert it into the target reflectance using neural networks (Kaasalainen et al., 2008). The calibrated intensity or AR was used in order to separate the TLS point clouds into foliage or wood points. However, this approach did not account for the partial hits on the edges and classified these as foliage (Schofield, 2016). In order to address this issue, Gaulton et al. (2013) and Danson et al. (2014) suggested using the ratio of the apparent reflectance (NDI) of both laser wavelengths. As the water content in foliage is higher than in wood (stem, branches), taking the ratio of both laser wavelengths should be sensitive to the moisture content in the foliage, which allows the threshold to distinguish between the foliage and wood points.

3.5.7 Normalised Difference Index NDI

NDI is sensitive to the water content in foliage. This feature might help to address the misclassification caused by the partial hits. The parameter can be calculated by taking the spectral ratios of both laser wavelengths as:

$$NDI = \frac{(AR1063 - AR1545)}{(AR1063 + AR1545)} \tag{3.1}$$

The normal range of this parameter is restricted to between -1 and +1, where the positive values indicate that the 1545 nm reflectance is smaller than the 1063 nm reflectance and negative values mean that the 1545 nm is greater than the 1063 nm reflectance.

3.6 SALCA calibration

In order to perform SALCA calibration and measure the intensity response to the range, reflectance and SALCA case temperature, neural network sets for both laser wavelengths were used to calibrate the data in this research. The networks were produced using SALCA scans for six different calibrated panels at multiple ranges. The data processing and network generation are detailed in Schofield et al,. (2016). The laboratory measurements, detailed in Chapter 4, were conducted indoors with high laser temperatures caused by the high ambient air temperatures. In addition, the field-based calibration did not include many measurements

at the short-ranges used. Therefore, in order to produce apparent reflectance for the laboratory datasets for this research, five calibrated panels of 5%, 20%, 50%, 90%, and 95% reflectance were scanned by SALCA in the laboratory at 8 m range. The panels were scanned throughout the data acquisition in order to gain temperatures close to those recorded for the scan temperatures of the laboratory samples. The data were then processed, and the extracted information was used to generate equations to calibrate the intensity of the laboratory datasets for the 1063 nm and 1545 nm within a range of temperatures close to the measurements. These equations are shown below, where **(**x**)** represents the intensity and **(**y**)** the reflectance:

AR 1063 nm $y=5E\text{-}14x^{5.283}$ (3.2)

AR1545 nm $y=0.0058x^{1.0527}$ (3.3)

The relationship between the intensity and panels' reflectance for the 1063 nm and 1545 nm is visualised in Figure 3.7 respectively, from which the equations are derived. For each wavelength, the intensity for each panel was extracted at the same azimuth position and plotted with the panel reflectance. As shown in the figures, 1063 nm is represented by a curved line with a range of intensity that is relatively wide compared to the 1545 nm, which is represented by a linear trend.

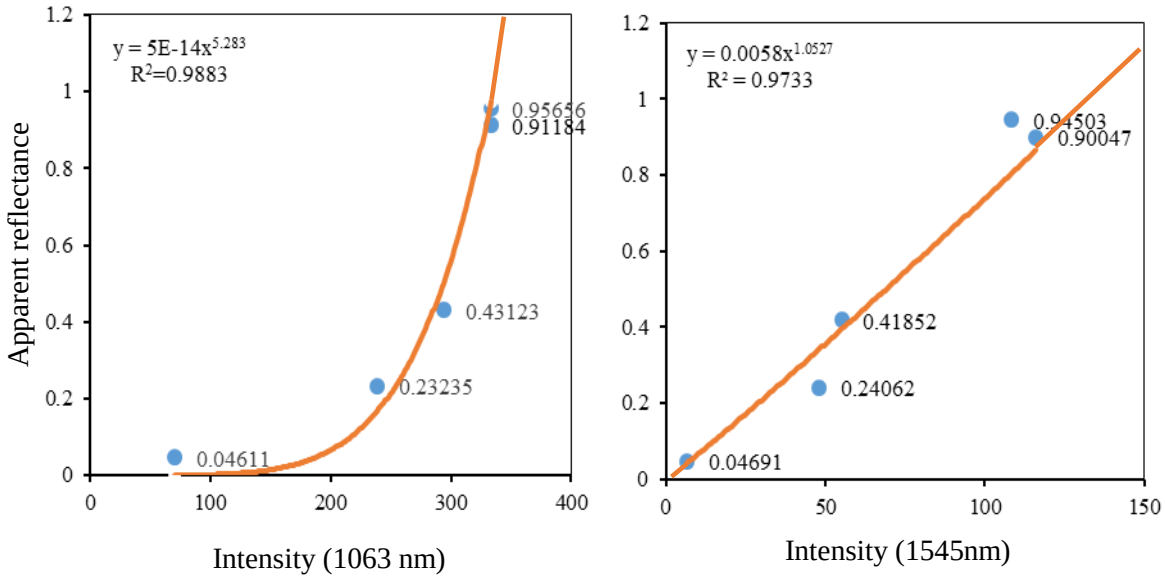

Figure 3.7: The relationship between intensity and apparent reflectance extracted from five subpanels at a range of 8m for 1063 nm and 1545 nm laser wavelengths respectively. Each sub-panel is represented by one point.

3.7 Spatial classifier (CANUPO)

CAractérisation de NUages de POints (CANUPO) is a spatial classifier designed to classify the features in LiDAR point clouds. It is a simple yet efficient method for automatically classifying TLS data. In addition, it has the potential to produce confidence values for each point in the scene to show how certain the classification is (Brodu & Lague, 2012). The classifier is designed to process and analyse TLS point clouds and assess the coordinates between the points or the relations between them in the cloud, and then classify them based on their local dimensionality features or geometric properties (Brodu & Lague, 2012; Danson et al., 2018). The local dimensionality refers to how the points in the scene appear at a given location and on a measured scale. The spatial classifier works by mapping the distribution of the points within a desired scale or sphere of variable diameter around desired points and then classifying them as 1D, 2D, 3D.

Figure 3.8 shows how tree components may appear at a scale of 100 cm. The branch appears as 1d, where the desired points are in greater alignment along a line. If the desired points in the scene make a plane, the trunk then appears as 2D. Leaves or the canopy where the points fill the space in the sphere appear as 3D. The basic idea behind the CANUPO classification is to find the best combination of scales at a given location, which allows the maximum separability of two or more categories. This grants a maximum separability between the desired points. Knowledge of the scene is required in order to choose the proper scale. Thus, choosing the relevant set of scales depends on how the target appears in reality, which means that every target needs to be trained with a different scale. Small trees must be trained with scales that cannot be used for larger targets such as mature trees.

The classifier is designed to classify each point using Principal Components Analysis (PCA). The desired points in the scene are computed at each a given scale of interest and PCA is performed to map the coordinates in the sphere centre to assess the eigenvalues for each point in the scene. The points are distributed in a 1D around the scene points if only a single eigenvalue accounts for the total spatial variance in the sphere at a given location and a given scales. That means the points will appear as a branch. The points appear mostly as 2D if two eigenvalues account for the variance in the sphere and the points are visualised as a stem or trunk. Similarly, three eigenvalues are necessary to account for the variance in order to build a 3D shape and the final outputs are classified as foliage.

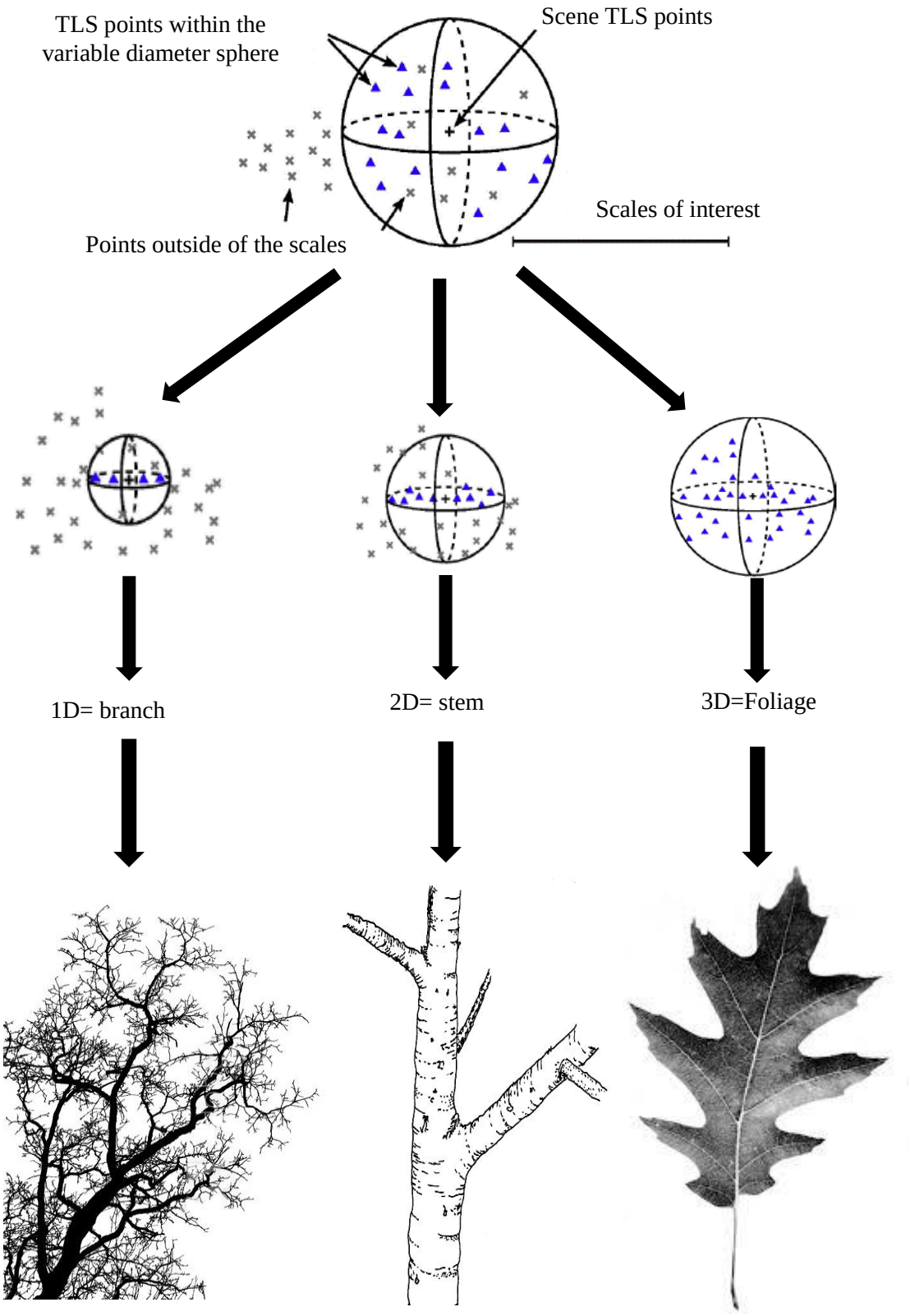

Figure 3.8: Neighbouring point at a given location and scale [The scales here are presented as the diameter of a circle centred on a point of interest] Source: (Brodu & Lague, 2012).

3.7.1. Spatial data preparation and analysis

The general steps of the data analyses in CANUPO are classified under four main steps to identify foliage and wood classes, as summarised in Figure 3.9. First, two clouds of points are segmented from the NDI output of SALCA point clouds. CANUPO provides a scissor tool that makes it possible to segment groups of points from different areas of the scan, even the small areas of the scan such as finer branches and small foliage. In the case of a single mature tree, as visualised in Figure 3.9, it is easier to separate wood points from the stem and foliage from the canopy, as most of the points are clear in the image. However, it is a challenge to segment the foliage group of points in the case of the small trees in the laboratory as one of them is a needle-leaf tree. This lead to errors in the classification as some points on the finer branches which be classified as foliage.

However, one clear group of separated foliage and a group of wood set extracted from a single tree can be used to classify any other single tree sample and so may minimise the errors in the classification. In the case of the full stand scale, applying segmented points extracted from a single tree does not provide a clear separation due to the complexity of the tree distribution and the effect of the range on the size of the points. This means that some trees located at far ranges from the device will be classified incorrectly and some of the wood points appear as foliage to the classifier. Therefore, the errors in classification for this scan can be minimised by segmenting foliage and wood points from different ranges in the scan and recombining the foliage points as one set, and the same for the wood points. The imported data must contain x, y, and z coordinates in order to make it possible to compare the final output of the spectral and spatial classifications.

Second, appropriate scales are applied for both of the segmented points in order to train them and define polygons that distinguish foliage from wood classes. Third, once the training classifier has validated the two samples (foliage and wood samples), multi-scale separate files are produced in order to define two groups of points. Finally, the cloud is classified into two final classes based on the geometrical properties of the points in the data. The spatial classes can be split into a foliage class (green) and wood class (black) automatically.

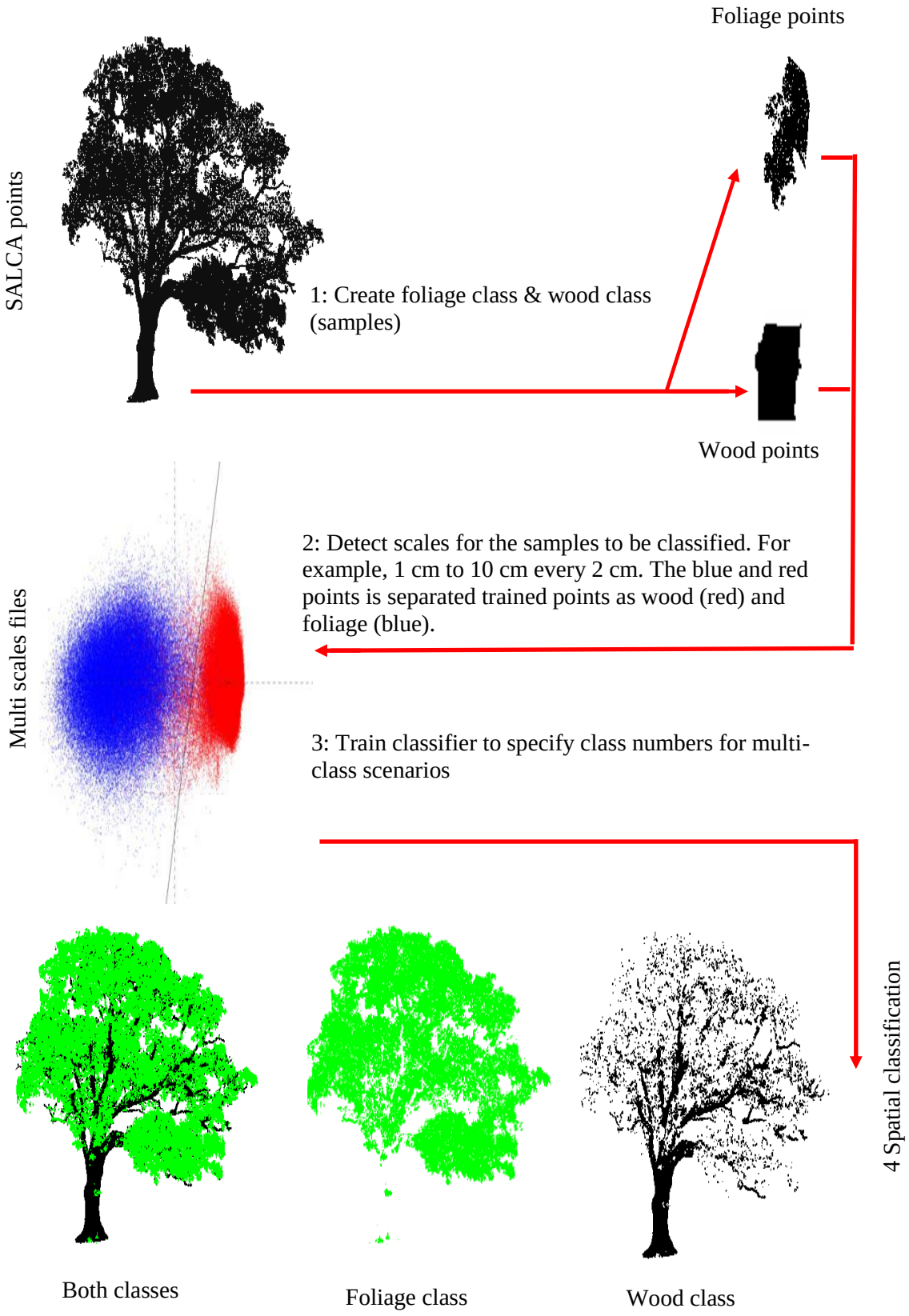

Figure 3.9: The four main steps of data processing in CANUPO.

3.7.2 CANUPO confidence

The spatial classifier has the potential to provide a statistical output as a percentage called the Confidence Value. For every spatial class that is produced from the TLS point cloud spatial classification, there is a confidence value that indictes the statistical confidence of the separation of classes in the training data. This allows the classifier to remove the points for which the classification is uncertain and to minimise the errors. However, this does not mean that the classifier is 100% reliable regarding the output; it means that the classification was performed accurately for a given scale and location. The values can be calculated based on the position of the point within the classification space. The classification output for the spatial classifier outputs a matrix of five columns as; x, y, z, spatial class, and confidence value (%). The spatial classification confidence can be visualised by choosing all values greater than 80% confidence and separating them as a new set of data. This set contains both classes of spatial foliage and wood. The new class set then can be visualised as foliage or wood, with a given level of confidence.

3.8 Conclusion

In order to address the main aims and objectives of this research, spectral and spatial information was used to provide approaches to foliage and wood separation using SALCA data. This chapter presented a description of the SALCA instrument and a range of extracted data including spectral information such as raw intensity, calibrated intensity, and reflectance ratios. Additional information, such as pulse width and the number of returns, range, and zenith and azimuth indices and the effect of temperature, was also considered. In order to produce reflectance related to the desired samples, a brief description of SALCA calibration was presented. The spatial approach was adopted for foliage/wood separation. The classifier was described, and the data processing is shown in Figure 3.8, with a clear description of the final outputs. The following chapter investigates the potential of SALCA for foliage and wood separation in an indoor environment at short-ranges before the instrument is transferred into an outdoor environment.

CHAPTER 4: LABORATORY MEASUREMENTS ON SINGLE TREES

Summary

In this Chapter, SALCA was used to measure a broadleaf and a needle-leaf tree in a laboratory environment at 1, 3, 5, and 8 meters range. The work aimed to investigate the potential of SALCA for mapping the three-dimensional distribution of foliage and woody materials. The raw data were processed to extract information including range and spectral information such as intensity, AR, and NDI. The point cloud data were then used to compute spatial attributes and visualized as three-dimensional images to distinguish foliage points from wood. Two main approaches were adopted in this research in order to distinguish foliage points from wood. The first was applying specific thresholds on the AR of 1063 nm, 1545 nm, and NDI. The second approach was a spatial classifier used to produce spatial classification based on tree geometric features. In order to investigate the correspondence between the classifications, the spectral and the spatial classifications were represneted as one matrix and visualized as three-dimensional point-clouds.

4.1 Introduction

Chapter 4 contributes to Objective 1 of this research. The Chapter contains a full description of the experimental samples, followed by the experimental design and set-up. Spectral and spatial analysis of SALCA data is described and a series of spectral and spatial classifications used to test discrimination of foliage and wood materials. The data analysed in this chapter were acquired for leaf-on and leaf-off conditions for two tree species. In order to distinguish foliage points from wood materials, two approaches were adopted in this research. The first approach used specific thresholds on the spectral information. The thresholds were adopted based on a visual interpretation and comparison with the images of the experimental samples. The spectral classification was designed to produce two groups of classified points referred to as: ‘spectral foliage’ and ‘spectral wood’. The second approach was to introduce a geometric technique for the spatial analysis of foliage and wood points. This was done by analysing the spatial relationships between the x, y, and z coordinates of all points in each scan. The output of the spatial classification was designed to represent ‘spatial foliage’ and ‘spatial wood’. In order to compare the spectral and spatial classifications for the laboratory trees, all the outputs

were represented as a matrix to represent four classes: Spectral classifier foliage (SF), Spectral classifier wood (SW), CANUPO spatial classifier foliage (CF), and CANUPO spatial classifier wood (CW). A key aim of the work was to develop a better understanding of the SALCA data characteristics and develop best practice methods for data acquisition and processing, before taking the scanner out into the complex environment of a forest. As described above, two classification approaches were applied at the level of the individual tree. Therefore, testing these approaches in a laboratory environment was expected to give a general understanding of these methods and test their effectiveness.

4.2 Experimental design, data collection and data pre-processing

Laser scanning measurements were conducted in an indoor environment at the School of Environment and Life Sciences, Salford University, Salford, in July 2017 to scan leaf-on, and in October 2017 to scan leaf-off conditions, using two trees from the same orientation. The SALCA was used to scan a broadleaf Snake-bark Maple (*Acer Davidii*) and a needle-leaf Corsican Pine (*Pinus nigra*) (Figure 4.1). The trees samples were obtained from a garden centre. The broadleaf tree height was 170 cm and the crown width was 100 cm with a medium amount of healthy green leaves. The average dimension of the leaves in this tree was 5 cm in length and 3 cm width. The needle-leaf tree was 130 cm in height, and the canopy width was 70 cm, with healthy dense needles. The needles in this tree were narrow in shape with lengths of 3 to 5 cm. The datasets from the laboratory experiment with the file names, ranges, start azimuth, azimuth steps, and the elevation angles are shown in Table 4.1.

Figure 4.1: Tree laboratory samples (a) leaf-on and (b) leaf-off conditions.

Table 4.1: Description of SALCA datasets acquired in laboratory.

Date 27/07/17				Leaf-on condition		
No	File name	Start/End time	Range	Start azimuth index	Stop azimuth index	Zenith angle range 0-190º
1	1m_3732	12:08/12:38	1 m	0	2249	0-190º
2	3m_3733	14:00/14:40	3 m	0	1082	0-190º
3	5m_3734	14:51/15:28	5 m	0	999	0-190º
4	8m_3735	15:40/16:05	8 m	0	1500	0-190º
Date 28/10/17				Leaf-off condition		
1	off1m_3796	10:30/11:15	1 m	0	1916	0-190º
2	off3m_3797	12:15/12:40	3 m	0	999	0-190º
3	off5m_3746	12:46/13:08	5 m	0	500	0-190º
4	off8m_3798	13:35/13:50	8 m	0	416	0-190º

The SALCA instrument was set up on a table 1m from the ground with the targets set on a second table at the same height (Figure 4.2). In order to cool the scanner, a fan was fixed close to the instrument for every scan for the leaf-on condition. A calibrated white panel target was included in every scan to check the intensity response with range and the reflectance calibration. Data collection acquired scans with the main stem of the sample trees at 1, 3, 5, and 8 metres range.

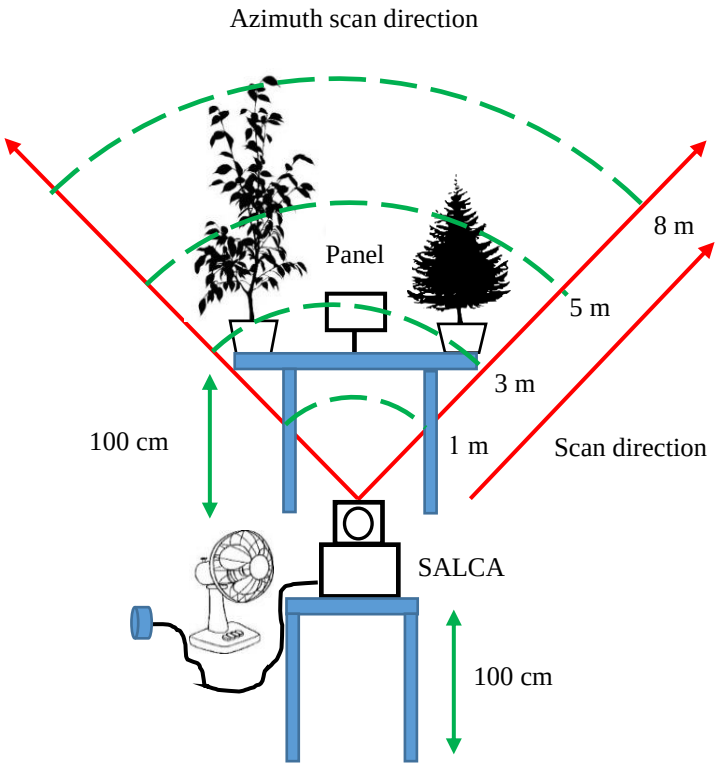

Figure 4.2: The experimental design in the laboratory, where the broadleaf tree, calibrated white panel, and needle-leaf tree are scanned at 1, 3, 5, and 8 m. Green dashed lines show the azimuth scan range.

Data were acquired for the leaf-off conditions by first removing the foliage or needles from both trees manually and then following the same experimental design as outlined for leaf-on. The room temperature was cooler for these scans and a fan was not used to cool the instrument. SALCA datasets were pre-processed as described in Section 3.4. For each laboratory scan, the waveforms were processed in order to extract returns for 1063 nm and 1545 nm. The x, y, z coordinates were then added based on range, azimuth and zenith indices. The range of each return and intensity values were obtained and recorded for both wavelengths. The apparent reflectance was then produced using equations (3.2) for 1063 nm data and (3.3) for 1545 nm as detailed in Chapter 3. Finally, the NDI was computed and quantified for both scans for leaf-off and leaf-on conditions.

4.3 Point-cloud data characteristics by range

This section comprises an initial analysis of the effects of range on the appearance of the point clouds. Figure 4.3 shows SALCA points of leaf-on and leaf-off conditions coloured by range with blue at the nominal target range, light blue closer, and green more distant. The range scales are displayed on the right of the tree visualisations. All scans were visualized using azimuth and zenith indices and all scans were plotted using the same relative point size (0.12) in Matlab to investigate the range impact on the point cloud visualisations. Closer inspection of the figure shows that the range has a clear effect on the visualisation. There is a clarity issue generated due to the distance between the targets and the instruments especially at 5 and 8 m respectively. This issue of clarity (points not clear to be seen) is noticed in both conditions of scanning for both trees.

To provide evidence for the range effect on the point visualizations, collections of SALCA points from main branches were segmented from the tree samples for the leaf-on condition. These points are visualized as 3D images using the same point size and then compared with the branch photographs as outlined in Figure 4.4. The figure shows that, as expected, the further away the branch is from the scanner the lower the point density. For the broadleaf branch in (Figure 4.4a), the points visualisation is clear at 1m, 3 m and 5 m. However, it is clear that there is a clarity issue related to the lower point density at 8 m range. The point-cloud for the needle-leaf branch (Figure 4.4b) demonstrates that the visualisations at 1 and 3 m range are clear, whilst the point density decreases at 5 m and 8 m range making visualisation less clear. Overall, it is still possible to distinguish the foliage of the broadleaf

branch, whilst for the needle-leaf sample it hard to distinguish individual needles, especially 5 and 8 m due to their narrow width.

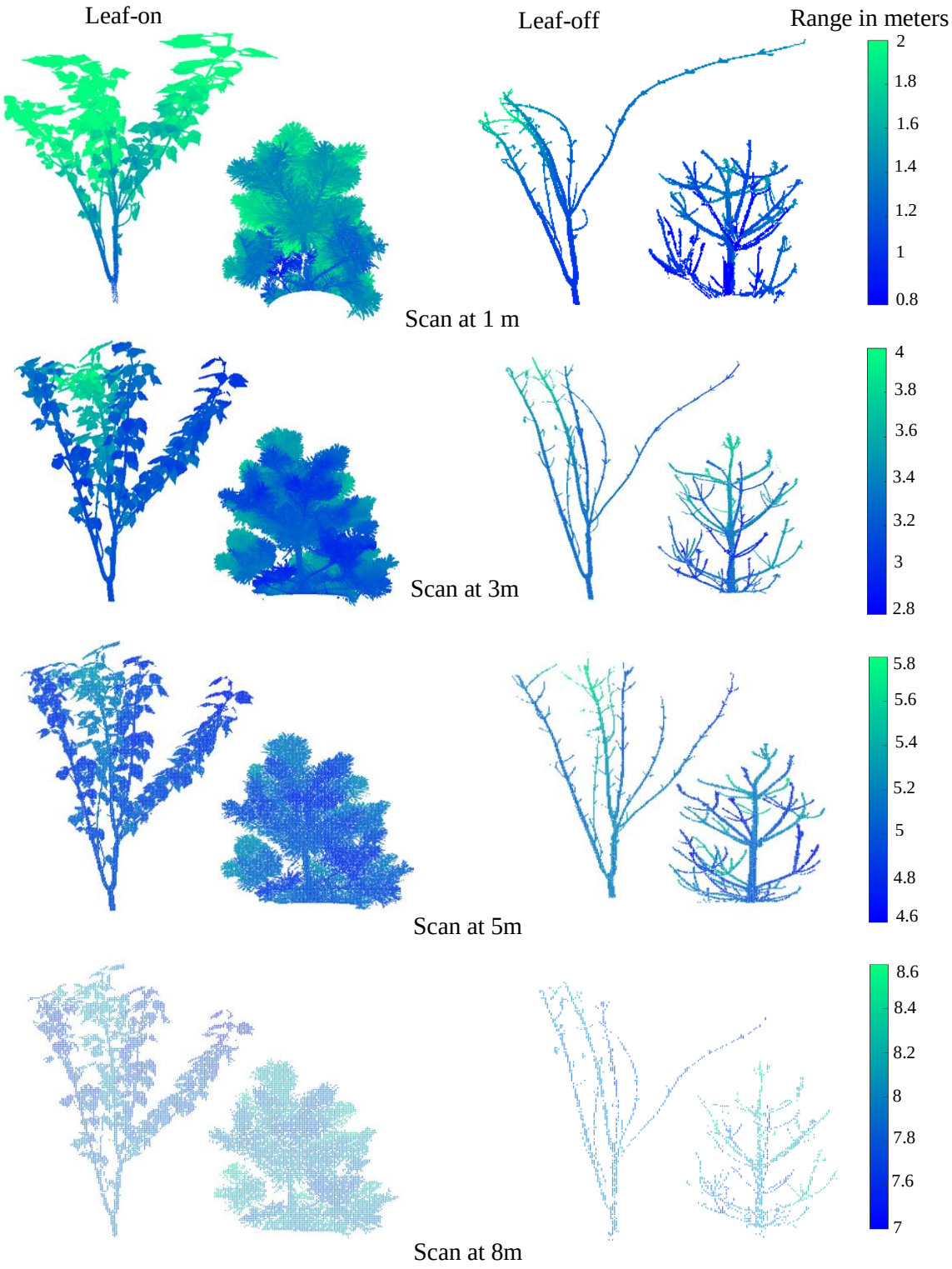

Figure 4.3: SALCA range visualisation effect for broadleaf and needle-leaf trees leaf-on and leaf-off conditions. Blue at the nominal target range, light blue closer, and green more distant.

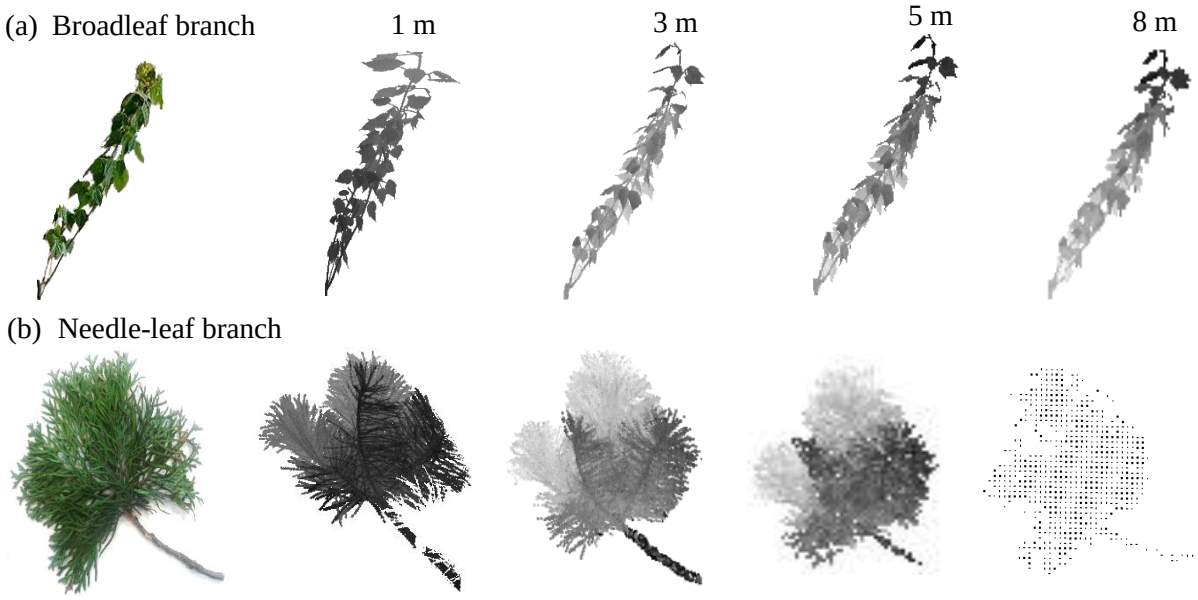

Figure 4.4: Photo sample of (a) broadleaf branch and SALCA points at four near ranges, and (b) needle-leaf branch compared with its SALCA points. The points for both branches scaled as 1524 x 942 pixels but they are not at the same absolute scale.

4.4 Spectral characteristics of leaf-on scan

This section describes the spectral analysis of the targets, where intensity, AR, and NDI variables were extracted for broadleaf and needle-leaf trees leaf-on scans using the calibrated panel and the reflectance of them was 0.988 for 1063 nm and 0.986 for 1545 nm. The outputs were visualized in order to test thresholds on the variables that classify the target points as foliage or woody material. Although the laboratory tree samples were scanned at 1 m, 3 m, 5 m, and 8 m, the scans at 8 m were adopted in this chapter to assess the spectral information in laboratory work. The 8 m range data was chosen due to the accurate AR values extracted for both trees when compared with the calibrated panel as shown in Figure (4.5b). Trees at 1, 3, & 5 m provided AR values outside the normal range compared to the panel and were not used as samples in this research. The visualisations of other ranges are available in Appendix I.

4.4.1 Spectral characteristics of broadleaf tree leaf-on

Figure 4.5 shows the point-clouds visualized by zenith and azimuth indices on the left of the figure and the corresponding frequency histogram is shown on the right of the figure. It is clear that the 1063 nm data have a higher intensity overall, compared to the 1545 nm data, and a wider spread of values (Figure 4.5a). The maximum intensity for the 1063 nm data is 325

and the highest frequency peak is recorded at 240 DN. For the 1545 nm, the maximum intensity is 280 with a frequency peak at 30 DN. This difference is primarily caused by a difference in object reflectance and the instrument sensitivity in each wavelength. The AR data (Figure 4.5b) should be related only to object reflectance and whether the laser hits are 'full' or 'partial'. The results suggest the distribution of reflectance values for the 1063 nm data came with a maximum value of 0.75 whereas this was 0.71 for the 1545 nm. The average values of panel reflectance for both wavelengths are shown in (Figure 4.5b).

Figure 4.5c highlights that the NDI data shows the expected range (between -1 and 1) with a high peak of NDI between -0.1 and -0.2. It is clear from the figure that the woody points on the main stem and the main branches show a higher NDI with values greater than 0.3 (orange and red colour), whereas most of the tree canopy including the finer branches and foliage are coloured by values smaller than 0.3 (yellow-green). There are a group of scattered blue points on the edges of the foliage areas and the stem showing an NDI smaller than 0.

4.4.2 Spectral characteristics of needle-leaf tree leaf-on

Figure 4.6 provides visualisations for intensity, AR, and NDI for the needle-leaf tree leaf-on condition with their frequency distribution on the right of the figure. For Figure 4.6a, the 1063 nm data comprises a wider range for intensity with a maximum of 325 and the most frequent peak recorded at 220 intensity. Most of the tree stem and main branches show a high intensity of more than 250. A large amount of the foliage points comprises average values (green-yellow), while minimum values are recorded on the edge of the tree canopy. The 1545 nm wavelength shows a narrower distribution with a very high peak at 50 intensity.

Most of the main stem for the needle-leaf tree shows values of > 250 for the 1063 nm > 110 for the 1545 nm data, whilst the rest of the tree components show lower values for both laser wavelengths. The AR for both laser wavelengths is visualized in Figure 4.6b where the values are within the normal range (0 to 1). The maximum AR 1063 nm is 0.65 nm and the wood parts comprise higher values of AR (red) for both laser wavelengths compared to other tree components and the maximum AR value of 1545 nm is 0.60. Figure 4.6c shows the NDI data within the normal values of range with a high-frequency peak at -1.0 NDI value. Most of the tree components are coloured (yellow-green) which means their values are less than 0.3. A few random points show very high NDI values or more than 0.5 as can be seen on the colour scale in the figure.

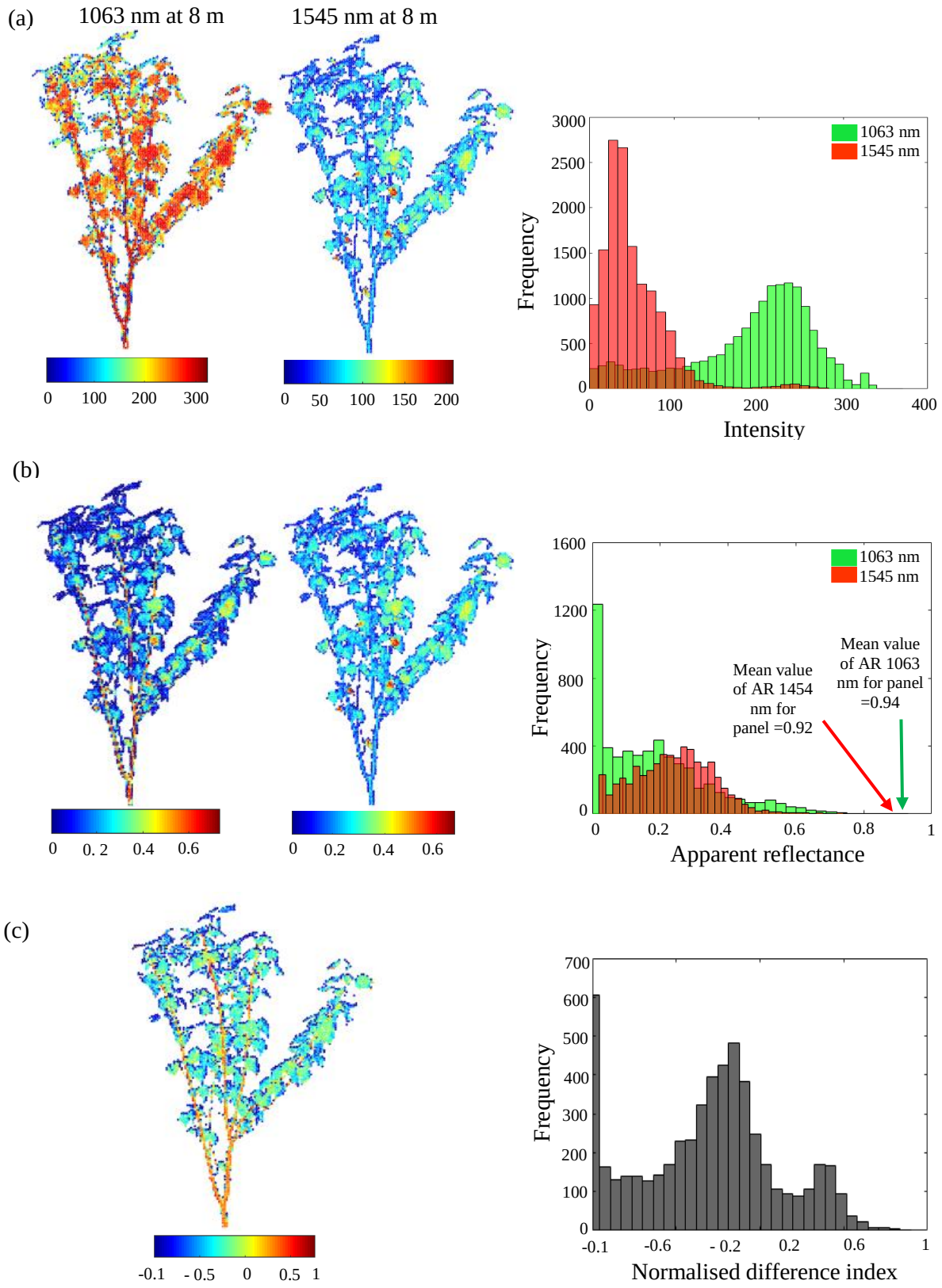

Figure 4.5: SALCA point clouds for (a) intensity, (b) apparent reflectance, and (c) normalised difference index with their histograms for broadleaf tree leaf-on scan respectively. Blue on the scales refers to minimum values, green to average values, and the high values are coloured red. Average values of panel reflectance are included for both laser wavelengths.

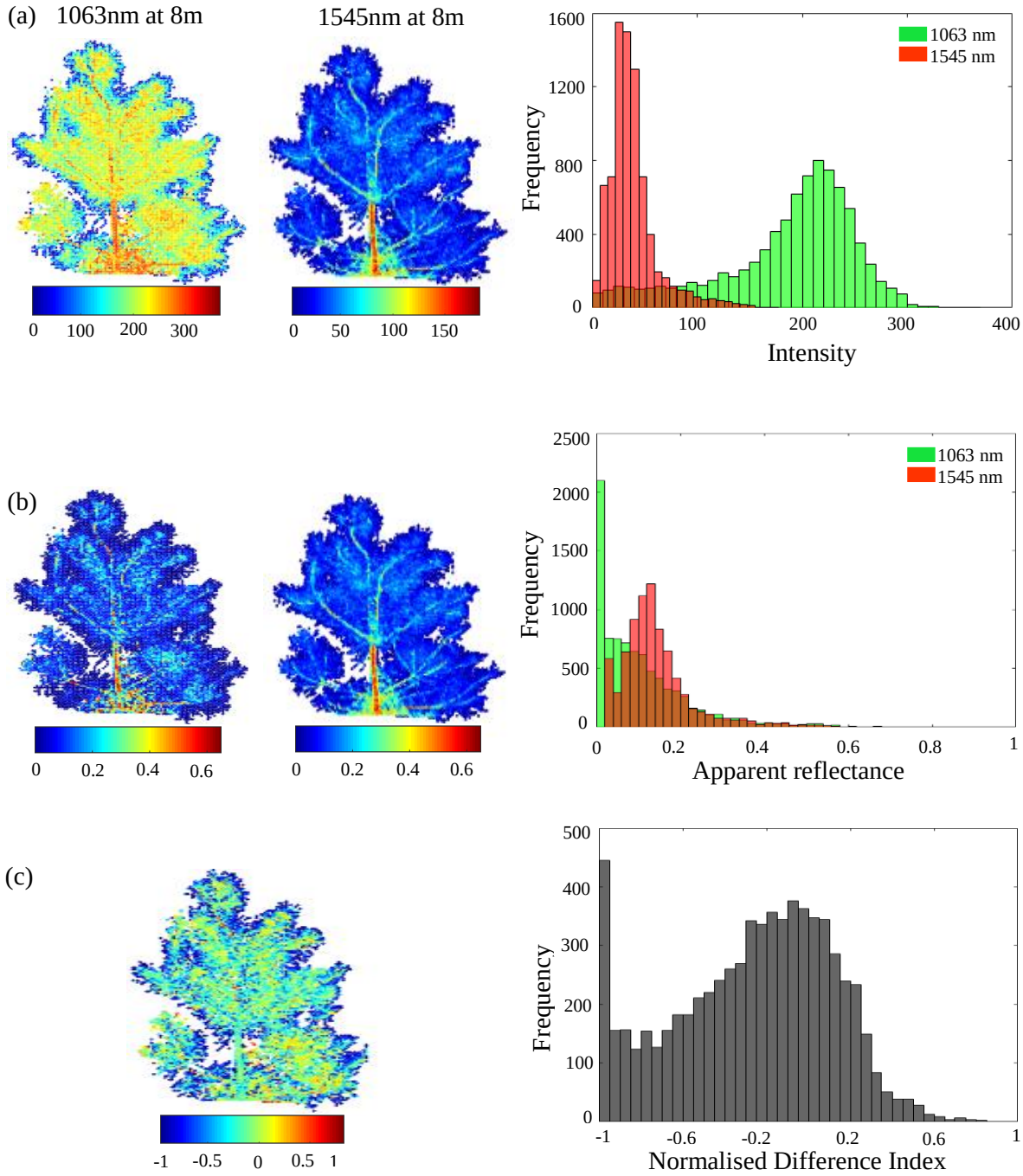

Figure 4.6: SALCA point clouds for (a) intensity, (b) apparent reflectance, and (c) normalised difference index with the histograms for the needle-leaf tree leaf-on condition. Blue refers to low values, green to average values, and the high values are coloured green.

4.5 Spectral characteristics of leaf-off scan

This section discusses the visualisations of the spectral analysis of laboratory datasets of broadleaf and needle-leaf trees for the leaf-off data. The leaf-off scans in this chapter are used

to validate the applied thresholds in order to distinguish the foliage points from woody materials. All the scans in this section are visualized using azimuth and zenith indices.

4.5.1 Spectral characteristics of broadleaf tree leaf-off

Figure 4.7 provides 3D visualisations for intensity, AR, and NDI extracted from SALCA points for a broadleaf leaf-off scan on the left and their frequency distributions on the right. Figure 4.7a confirms as mentioned before in Section 4.4.2 that the 1063 nm has a much wider distribution of intensity with a maximum value of 325. Most of the tree components are coloured orange and red showing an intensity greater than 270. In contrast, 1545 nm shows a narrower intensity distribution of smaller than 82 where most of the tree is coloured green or blue with intensity between 25 and 50. Figure 4.7b shows the distribution of the AR for both laser wavelengths where the 1063 nm comprises a maximum range of 0.60 with a high peak frequency at 0.1 AR. Most of the high values (red, or > 0.5) are restricted to the stem and the main branches. The 1545 nm shows a small AR range with a maximum value of 0.45 and a high frequency peak at 0.1. Most of the tree components are coloured blue (<0.2) with a few high values on the branches visualised as red. Figure 4.7c shows the distribution of NDI within the normal range. The figure significantly supports the NDI distribution for the leaf-on condition scan where the woody materials have much greater values of NDI compared to the foliage areas. There are multiple high peaks between 0.3 and 0.4 on the NDI scale distribution on the figure.

4.5.2 Spectral characteristics of needle-leaf tree leaf-off

Figure 4.8 highlights the visualisations for extracted intensity, AR, and NDI for the needle-leaf tree leaf-off condition. A general view of Figure 4.8a shows the difference of the instrument sensitivity in each wavelength where 1063 nm comprises a wide range of intensity with a maximum of 330, while 1545 nm shows a maximum of 80. For Figure 4.8b, the 1063 nm AR shows a maximum of 0.60, where most of the high values are restricted to the main stem. A maximum AR of 0.5 is recorded for the 1545 nm with a few large values (red) visualized randomly on the main branches. The NDI is visualized in Figure 4.8c where the woody materials are represented by values more than 0.3 or (orange and red) and the scan shows NDI values within the normal range.

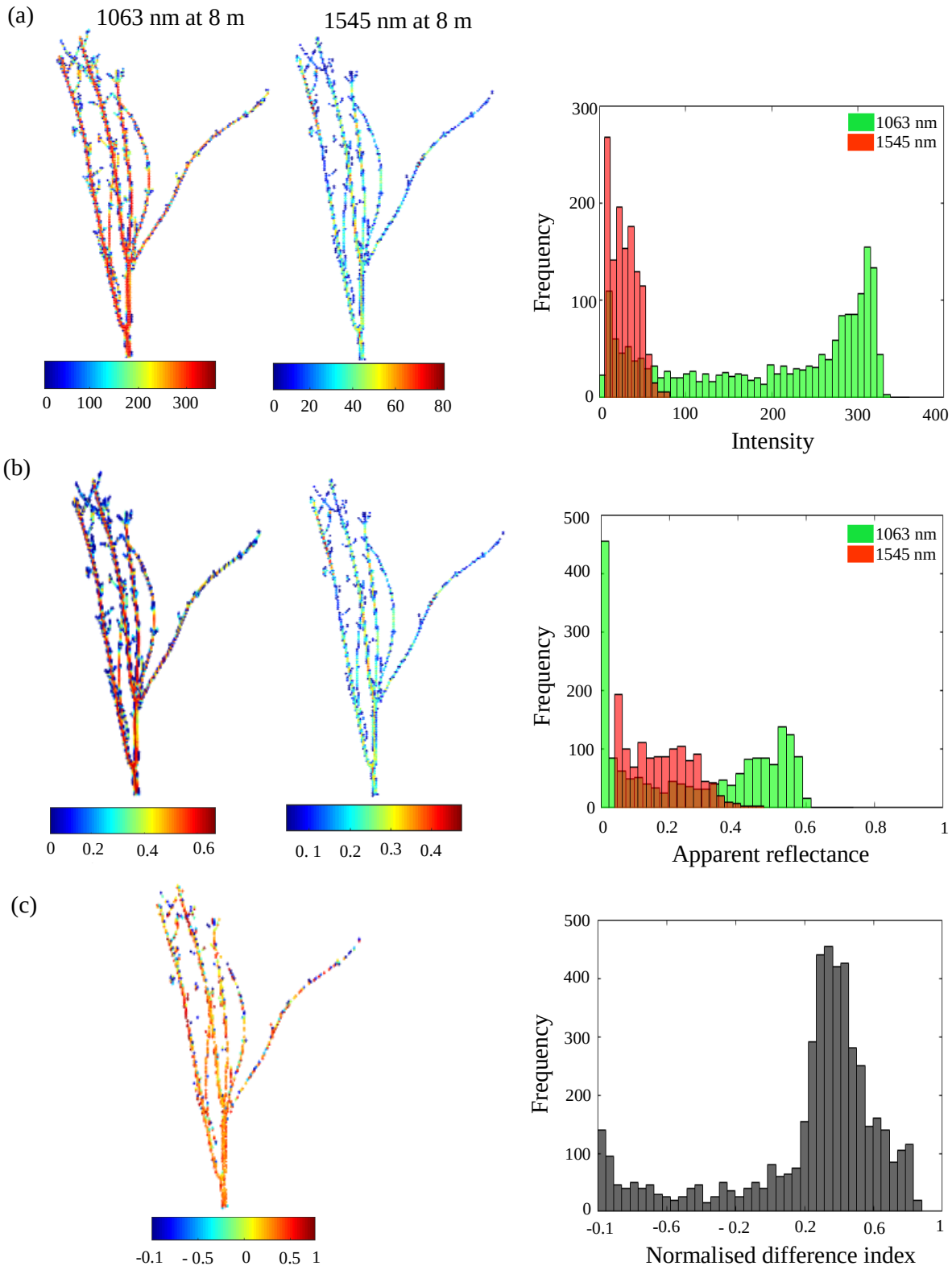

Figure 4.7: SALCA point clouds for (a) intensity, (b) apparent reflectance, and (c) normalised difference index with their histograms for the broadleaf tree leaf-off condition respectively. Blue on the scales refers to minimum values, green to average values, and the high values are coloured red.

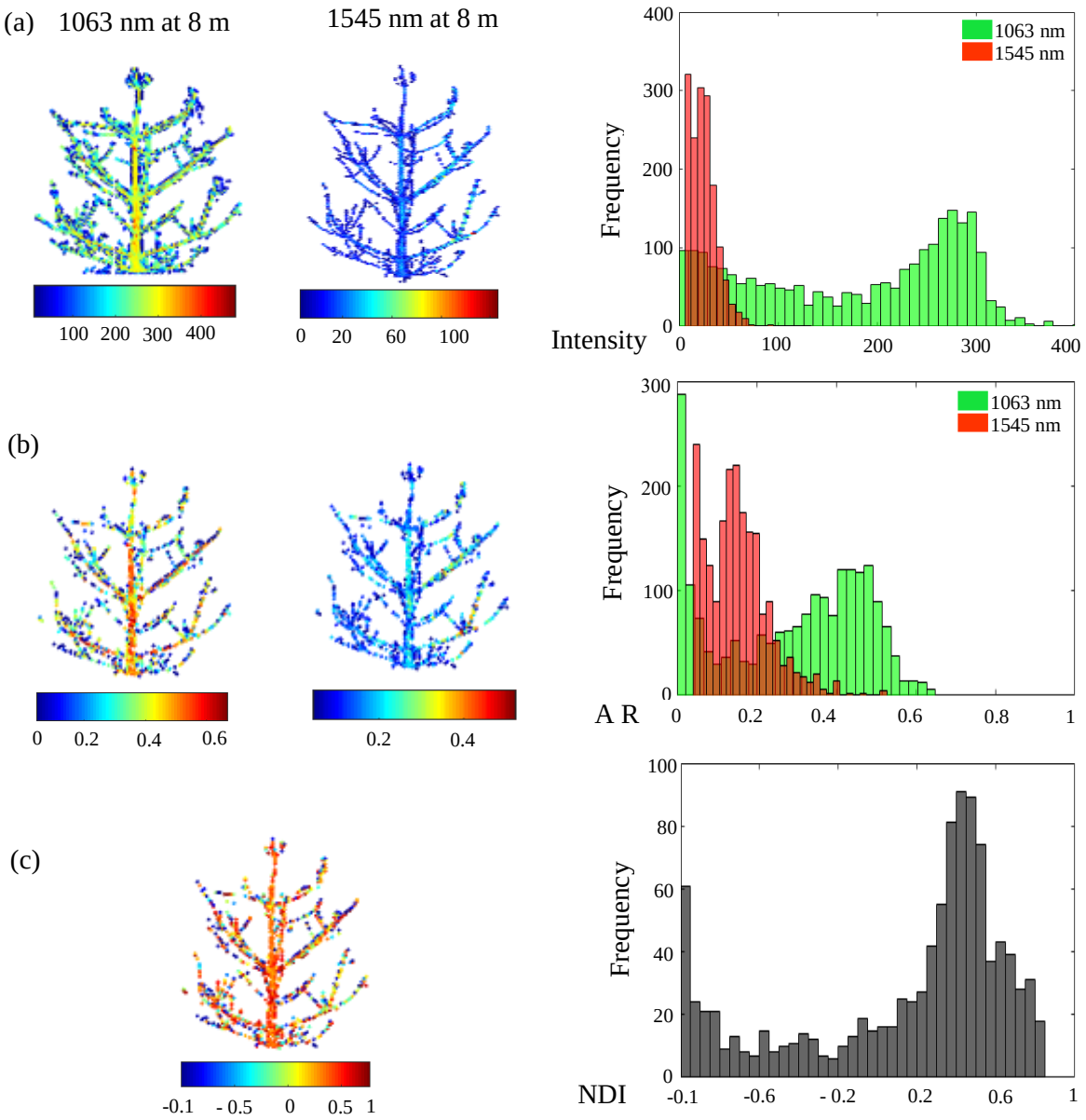

Figure 4.8: SALCA point clouds for (a) intensity, (b) apparent reflectance, and (c) normalised difference index with their histograms for the needle-leaf tree leaf-off scan respectively. Blue on the scales refers to minimum values, green to average values, and the high values are coloured red.

4.6 Spectral classifications

This section presents the first test of the application of the spectral classifications for foliage and woody points extracted from the laboratory samples for 1063 nm and 1545 nm data.

4.6.1 Leaf-on scan

SALCA 1063 nm AR, 1545 nm AR, and NDI data were classified into foliage or wood using thresholds based on visual interpretation. No assumptions were made in terms of whether the trees will respond to the same threshold or whether every tree needed a different threshold.

4.6.1.1 Thresholding 1063 nm apparent reflectance

Figure 4.9 shows foliage and wood separation based on 0.3 and 0.1 thresholds for broadleaf and needle-leaf tree respectively. For the figure, the contrast of 1063 nm on the stems is greater than the foliage areas for both trees. Due to this, it is expected that foliage (green) is represented by small values and wood (red) by large values of AR. Despite some misclassified points on the stem caused by partial hits, the classification for the broadleaf tree suggests that it is possible to distinguish foliage points (≤0.3) from woody (>0.3) clearly (Figure 4.9a). For the needle-leaf tree in Figure 4.9b, the foliage points are represented by AR values ≤ 0.1 and woody by > 0.1 based on the applied threshold. For this tree, foliage elements are misclassified as woody materials as is clear when the points are combined in one figure. Some of the partial hits on the stem are also classified incorrectly as foliage.

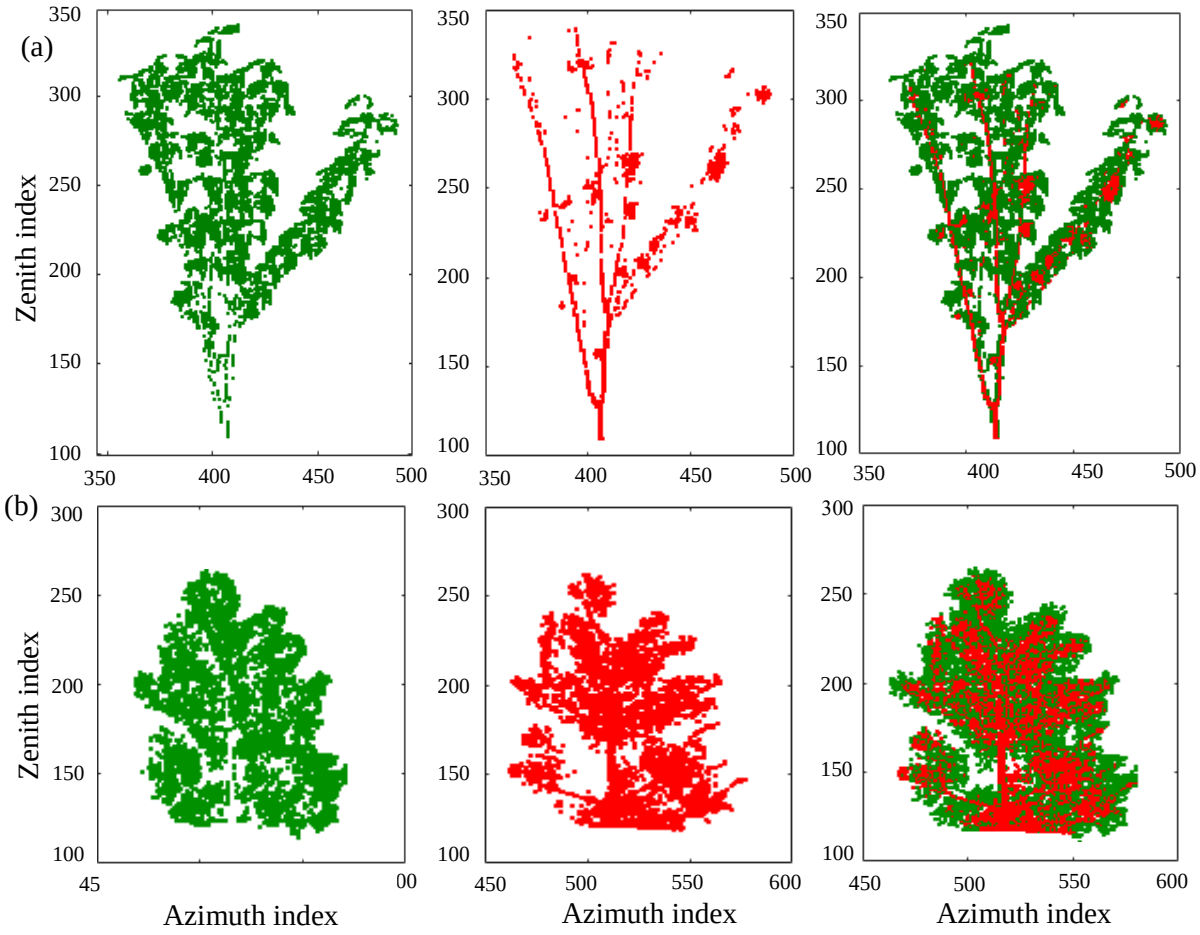

Figure 4.9: 1063 apparent reflectance for (a) broadleaf and (b) needle-leaf tree leaf-on scan separated into foliage or wood materials based on 0.3 and 0.1 thresholds respectively. Green points are allocated to foliage and red points to wood. The points are combined in one image.

4.6.1.2 Thresholding 1545 nm apparent reflectance

Figure 4.10 shows the results of the foliage and wood separation based on 0.2 threshold at 1545 nm for both trees. Due to the spectral contrast between NIR (1063) and SWIR (1545), it is expected that 1545 nm would present a successful separation. However, Figure 4.10a shows that most of the main stem and branches were incorrectly classified as foliage. Most of the misclassified woody materials are caused mainly by partial hits on the stem and the branches. In addition, some of the foliage returns are misclassified as wood for this tree. In contrast, Figure 4.10b shows successful separation for the needle-leaf tree between the foliage and woody where foliage is represented by low AR values of ≤0.2 and woody by values of >0.2. The output of the needle-leaf tree supports the hypothesis that the reflectance properties of the foliage material are different in the two laser wavelengths. However, it is likely there are few misclassifications on the stem as foliage due to their low contrast.

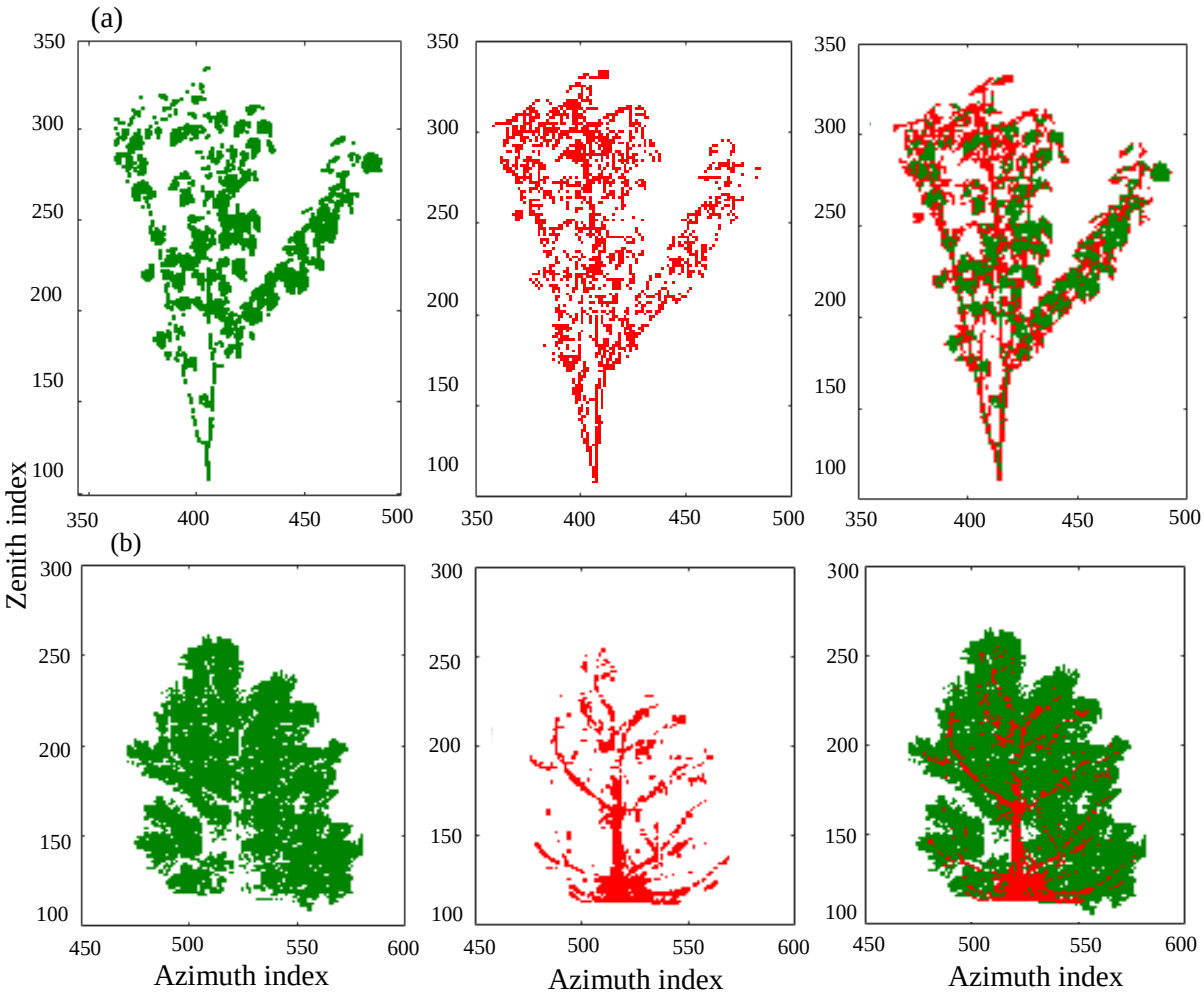

Figure 4.10: 1545 apparent reflectance for (a) broadleaf & (b) needle-leaf tree leaf-on condition classified into foliage or wood using 0.2 threshold. Green points are allocated to foliage materials and red points allocated to wood. The two groups of the points are combined in one image.

4.6.1.3 Thresholding Normalised Difference Index

Figure 4.11 presents the results for the broadleaf and needle-leaf tree where thresholds of 0.2 and -0.1 were applied to the NDI respectively. It is expected that foliage returns are represented by large values and woody materials by smaller values of NDI. However, the contrast of NDI wood for the broadleaf tree is higher than the foliage. Figure 4.11a shows a successful separation for the broadleaf tree with a few misclassified points on the edge of the stem, which were classified as foliage. A few hits on the foliage are allocated to red points or woody materials. Figure 4.11b shows the outputs of applying -0.1 threshold to the NDI for the needle-leaf tree. The points classified as foliage suggest misclassification errors in the main stem and the branches. Many foliage points are classified as woody and this can be seen when the points are combined in the figure on the bottom right.

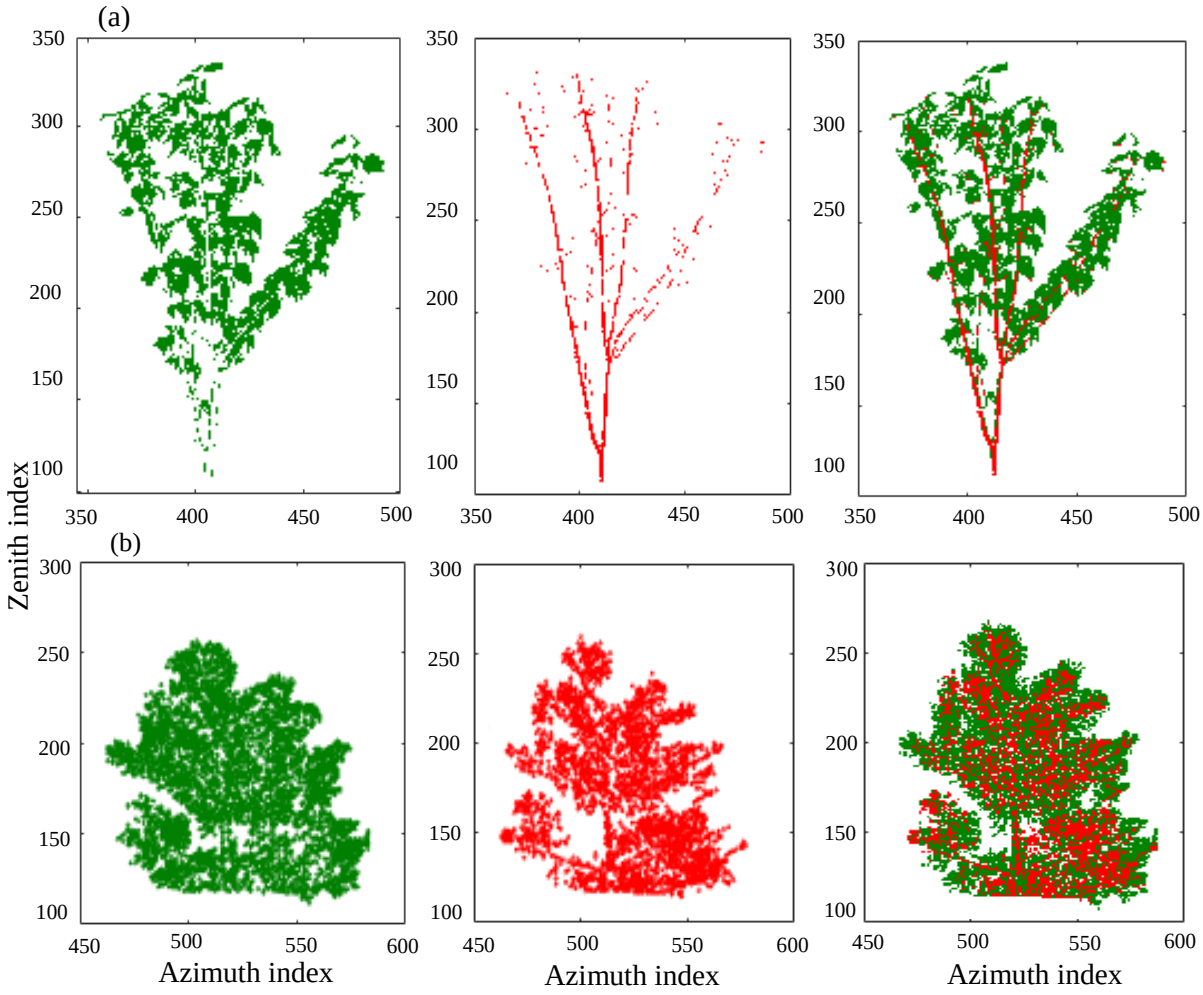

Figure 4.11**:** NDI for (a) broadleaf & (b) needle-leaf tree leaf-on condition classified into foliage or wood using 0.2 & -0.1 thresholds respectively. Green points are allocated to foliage materials and red points allocated to wood. The two groups of the points are combined in one image.

4.6.2 Leaf-off scan

This section discusses the visualizations for the leaf-off scans extracted from the laboratory data. The same thresholds that were applied for the leaf-on scan of both trees were applied for the leaf-off scan. The two sample scans consist of wood materials only, and it is therefore expected that the points will be classified as wood based on the applied threshold. This was done in order to validate whether the applied threshold for the leaf-on scan was successful or not. Points misclassified as foliage are allocated to the green and true woody points to the red.

4.6.2.1 Thresholding 1063 nm apparent reflectance

Figure 4.12 shows the outputs of applying 0.3 and 0.1 thresholds at AR 1063 nm to the leaf-off scan for both trees respectively. The figure shows that 67% of the broadleaf points are classified correctly as wood and there are misclassification errors of 33% points represented by ≤0.3. For the needle-leaf tree, 75% of the points are validated as wood, while 25% points are recorded as misclassification errors with ≤0.1 values of AR 1063 nm.

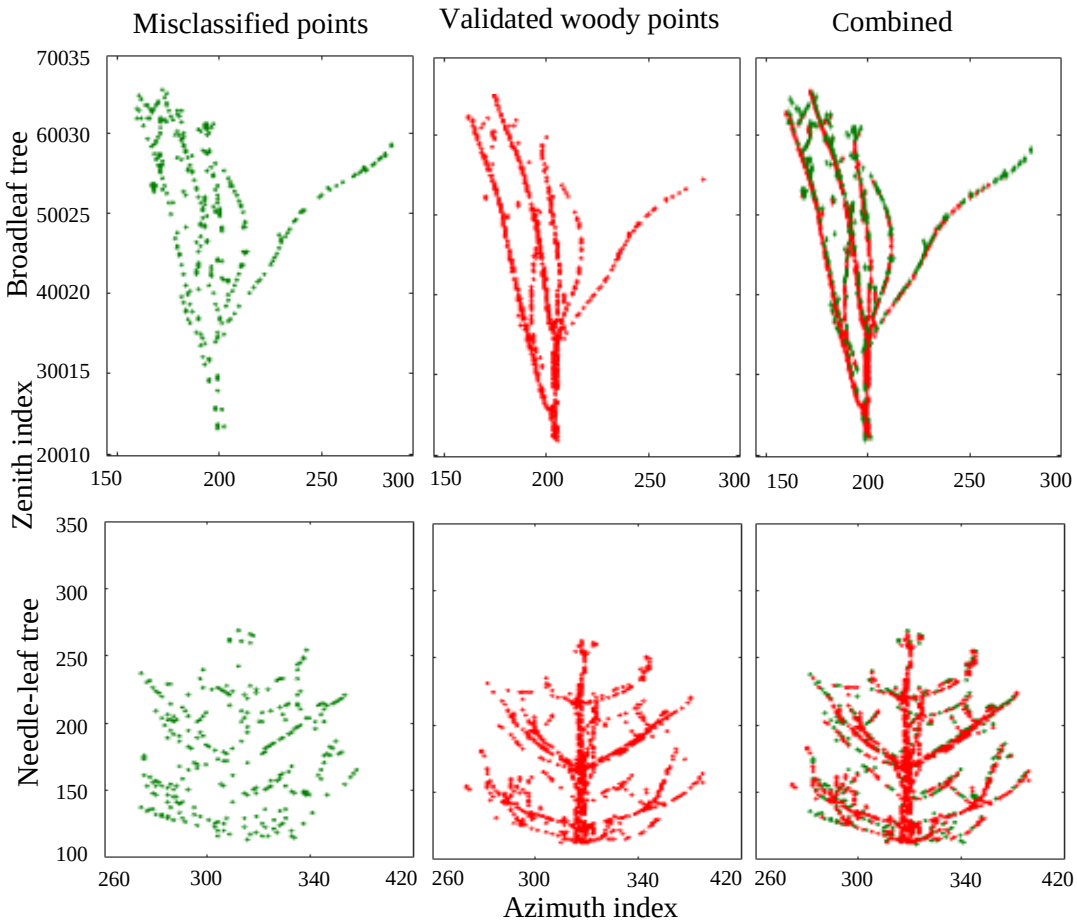

Figure 4.12: The misclassification errors produced by applying 0.3 and 0.1 thresholds on the 1063 nm data for the broadleaf and needle-leaf tree leaf-off condition.

4.6.2.2 Thresholding 1545 nm apparent reflectance

Figure 4.13 highlights the outputs of applying 0.2 threshold at 1545 nm for both trees in leaf-off condition. Visual examination of the outputs suggests that this approach was not very successful for both trees with 59% of the broadleaf points misclassified as foliage (green), and 77% of points for the needle-leaf tree points were recorded as errors.

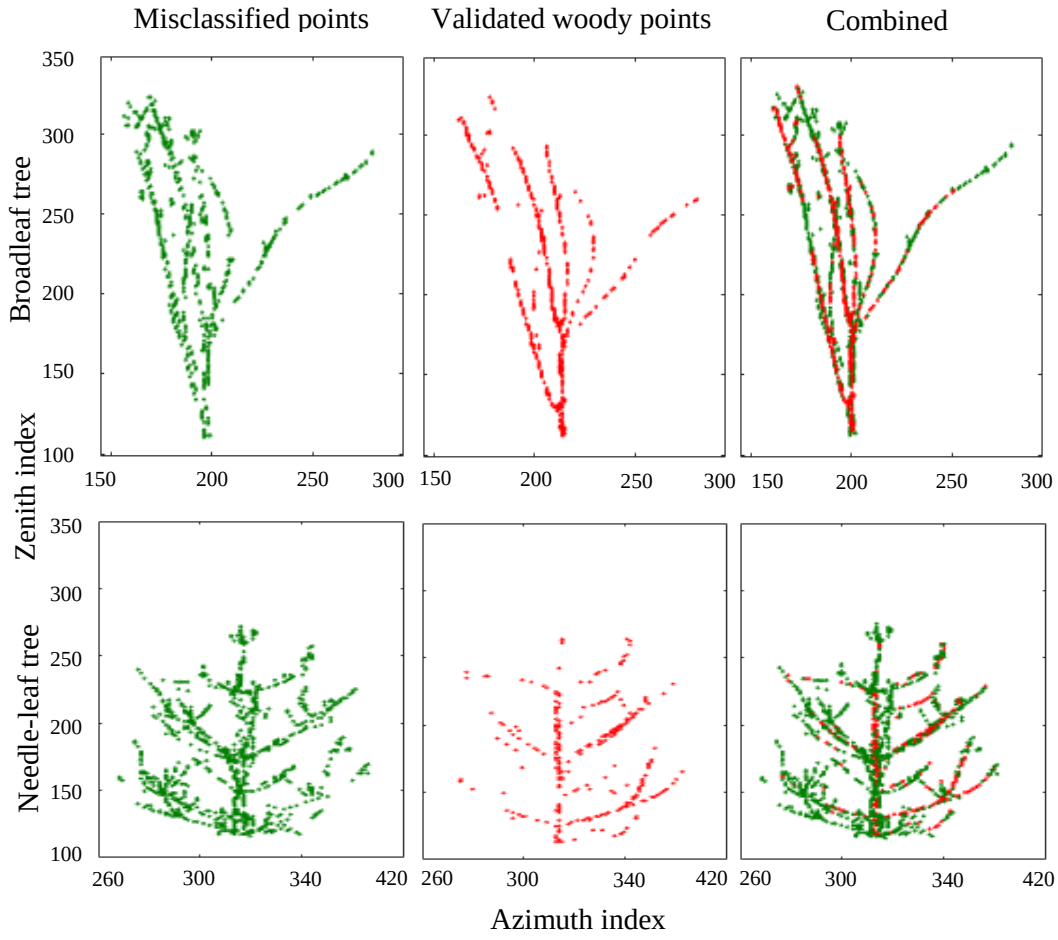

Figure 4.13: The misclassification errors produced by applying 0.2 threshold on the 1545 data nm for the broadleaf and needle-leaf tree leaf-off condition.

4.6.2.3 Thresholding Normalised Difference Index

The final spectral classification for the leaf-off scan is visualised in Figure 4.14. NDI thresholds of 0.2 and -0.1 were applied for the broadleaf and needle-leaf respectively. For the broadleaf tree, 27% of the total points were classified incorrectly as foliage, while 73% were validated as woody materials. For the needle-leaf tree, 26% of the points were classified incorrectly to the green points as foliage and 74% were correctly allocated to the woody materials (red).

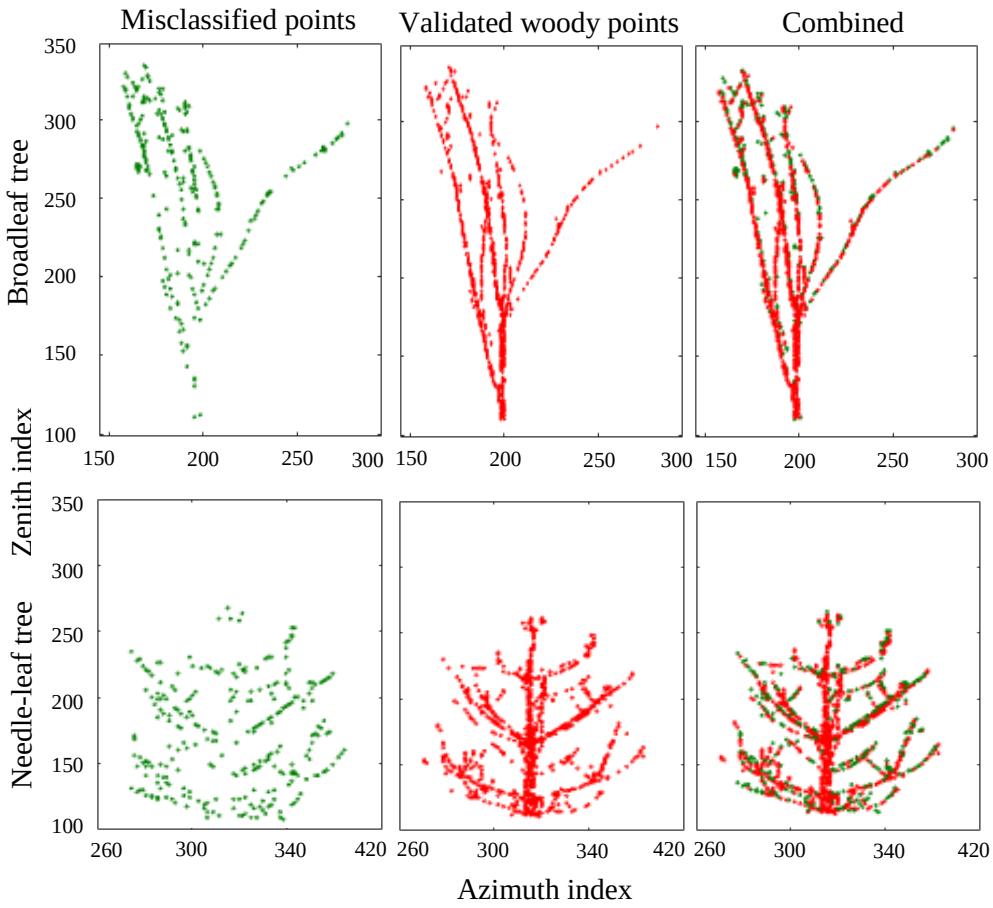

Figure 4.14: The misclassification errors produced by applying 0.2 and -0.1 thresholds on the NDI for the broadleaf and needle-leaf tree leaf-off condition respectively.

4.7 Spatial classification

This section provides an assessment of the spatial classification of the dual-wavelength data sets acquired by the SALCA scanner using the same data as described in Section 4.6. The x, y, and z of the NDI variable from this were computed and processed in CANUPO software as detailed in Section 3.3.4 in order to characterise the points in the scan based on their arrangement in space. The classified woods are allocated to black, whilst foliage to green.

4.7.1 Leaf-on

The NDI with x, y, and z coordinates of the broadleaf and the needle-leaf tree were imported into CANUPO. Two groups of points were separated manually using the scissor tool in the software to create training points for the foliage and wood classification. Based on the size of the tree, a range of 0.05, 0.1, 0.2, 0.3, 0.4, 0.5 m scales was used to train the points in CANUPO. It is possible to use this set of scales to process different point clouds obtained

from different tree species. Figure 4.15 highlights the outputs of the CANUPO classifications for both trees. The spatial classification of the broadleaf tree suggests that most of the main branches are misclassified as foliage points. In addition, a large number of foliage points are incorrectly classified as woody classes. For the needle-leaf tree, most of the points are classified as foliage returns except a few returns on the main stem and random points in the tree canopy, which were classified as wood. In order to improve the classification of the needle-leaf tree, smaller scales of 0.25 m were applied in CANUPO. However, the spatial classification for this tree gave similar outputs and misclassifications errors.

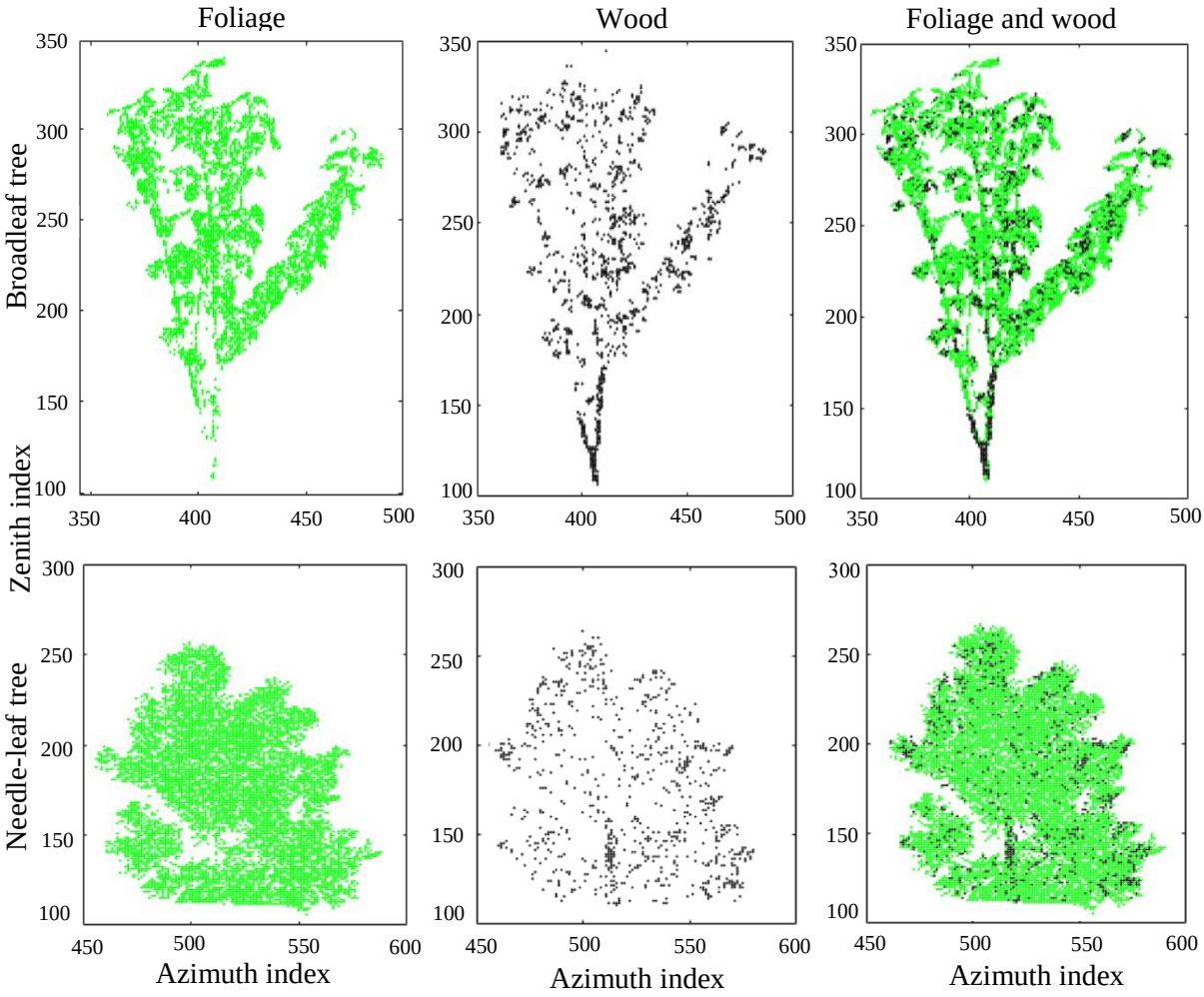

Figure 4.15: The spatial classification for the broadleaf & needle leaf tree leaf-on condition classified into foliage or wood based on their geometrical properties respectively. The green points are allocated to foliage class and black points to the wood class.

4.7.2 Leaf-off

In the case of a 'leaf-off' condition, a scale of 0.5 m was used to process the data for both trees as shown in Figure 4.16. It was expected that all the returns would be classified as a

wood class. However, the classification showed errors as a large number of woody points were incorrectly separated as foliage as shown in the figure below.

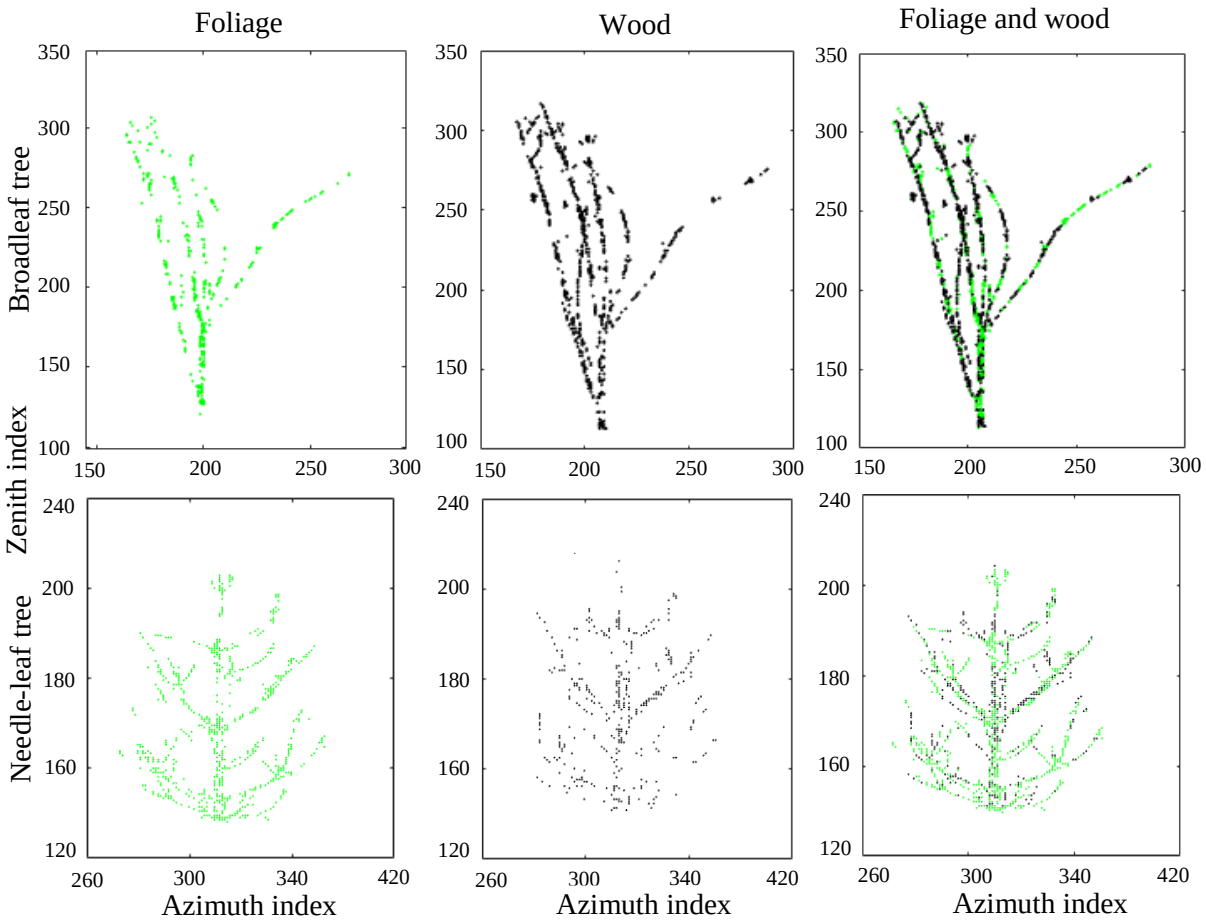

Figure 4.16: The spatial classification for the broadleaf & needle-leaf tree leaf-off condition classified into wood or foliage (errors) based on their geometrical properties respectively.The green points are allocated to foliage class and black points to the wood class.

To test the spatial classification, CANUPO has a statistical feature called 'Confidence' allowing us to determine the points for which CANUPO is uncertain. For each x, y, and z of a point in the scan, a confidence value is computed as a percentage in the final output of the classification.

Figure 4.17 presents the confidence percentage of the broadleaf tree where the confidence is divided into two groups of points; points with confidence greater than 80% and another group of points with confidence smaller than or equal to 80%. According to Brodu & Lague, (2012), the classification produced with confidence more than 80% is considered as accurate and a certain spatial classification. Figure 4.18 shows the confidence output for the broadleaf tree, where confidence > 80% is allocated to red points and confidence ≤ 80% to blue points. By

calculating the total percentage confidence for the foliage and woody separately, the calculations show that, for the spatial foliage class, the certainty of the spatial classification of CANUPO is 27.73% and the classifier shows that 72.26% has confidence of ≤80%. For the spatial wood class, the certainty of the spatial classification is 29.73% and CANUPO shows that 70.27% has a confidence ≤80%.

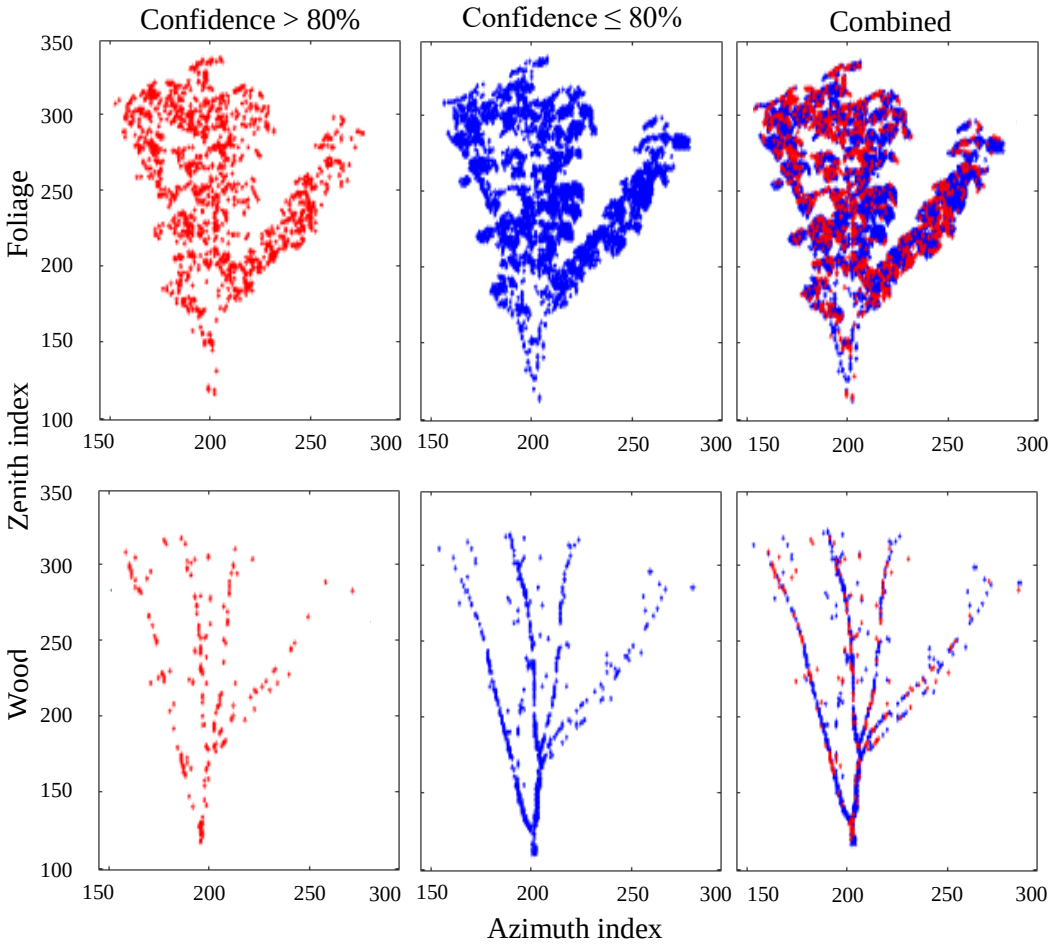

Figure 4.17: CANUPO confidence percentage for the spatial foliage and wood extracted from broadleaf tree point clouds. Red coloured for confidence > 80 % and blue for ≤ 80 %.

For the needle-leaf tree, Figure 4.18 shows that the spatial classifier is certain for 45.66 % of the total foliage points and uncertain for 54.33 % of the total foliage points. For the spatial wood classification, CANUPO is certain and confident for 7.02 % and uncertain for 92.97 % of the spatial classification of the wood points of the needle-leaf tree leaf-on condition. Overall, the results of the spatial classification for both trees show that CANUPO is uncertain for large numbers of the points.

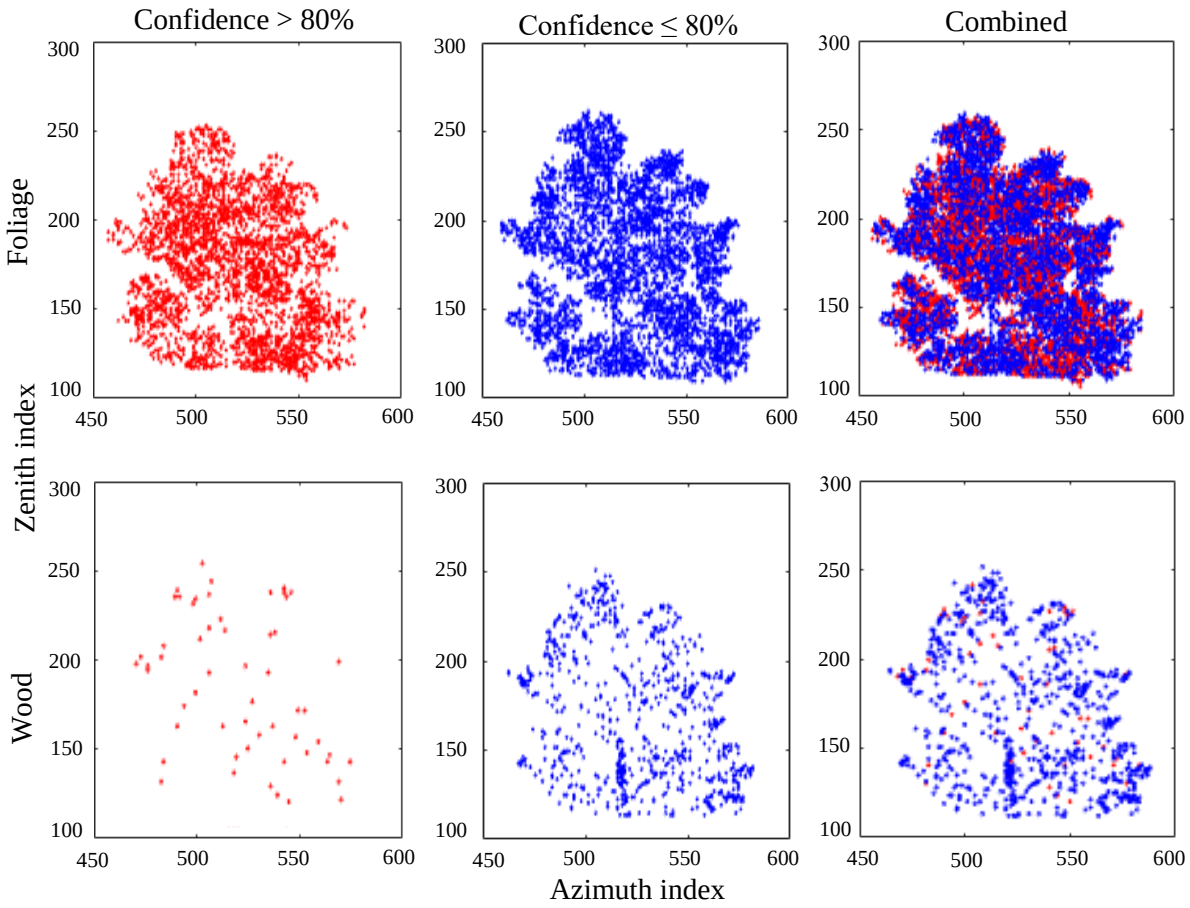

Figure 4.18: CANUPO confidence percentage for the spatial foliage and wood extracted from needle-leaf tree point clouds. Red coloured for confidence > 80% and blue for ≤ 80%.

4.7 Analysis of spectral and spatial information content

To compare the spectral and spatial classifications for leaf-on gained from the laboratory trees, both of the classifications were represented in one matrix. The classification matrix was built to comprise four classes with specific names as was detailed earlier in Section 3.2. The matrix shows whether there is agreement or disagreement between the spatial and spectral classes.

4.7.1 Broadleaf tree

A summary of the information in the matrix is illustrated in Table 4.2. This provides the total percentages for the agreement and disagreement between the spectral and spatial points in the matrix. The classification matrix for the broadleaf tree leaf-on sample was represented by 5423 returns in CANUPO. Class SFCF was represented by 3259 returns or 60.09% of the total CANUPO returns. On the other hand, class SWCW was represented by 394 returns or

7.26 % of the total returns. From the table, the results show that there was an agreement between the spectral and the spatial classification for 67.32% of the points.

Table 4.2: The spectral and spatial classes for broadleaf leaf-on tree sample.

Four classes 5423 returns	CANUPO foliage	CANUPO wood
Spectral foliage	3259 (SFCF), agreement of 60.09%	952 (SFCW), disagreement of 17.55%
Spectral wood	818 (SWCF), disagreement of 15.08%	394 (SWCW), agreement of 7.26%
The total percentage of agreement between the spatial and spatial points was 67.35%		

Figure 4.19 shows the red points allocated to class SFCF, the black points for class SFCW, the green to represent a class CWSF, and the blue points for class SWCW. For the broadleaf tree, the classifications showed a scattered distribution of the four colours or classes in the tree crown. However, the spectral and CANUPO foliage class SFCF (red) dominated most of the tree canopy and a few points on the trunk. This was expected due to the high number of returns that were recorded for this class.

Most of the main branches, foliage edges, and a few points on the trunk were represented by class SFCW (black) or 17.55% of the points. For the class CWSF (green), the returns were distributed on the edges of the foliage areas and few parts of the main stem and branches. A large number of the trunk points were defined by the class SWCW (blue) or spectral and CANUPO wood. However, these returns comprised only 7.26% of the total CANUPO classification. The four CANUPO classes with their colours were recombined in one two-.dimensional figure to map the class distribution (Figure 4.20).

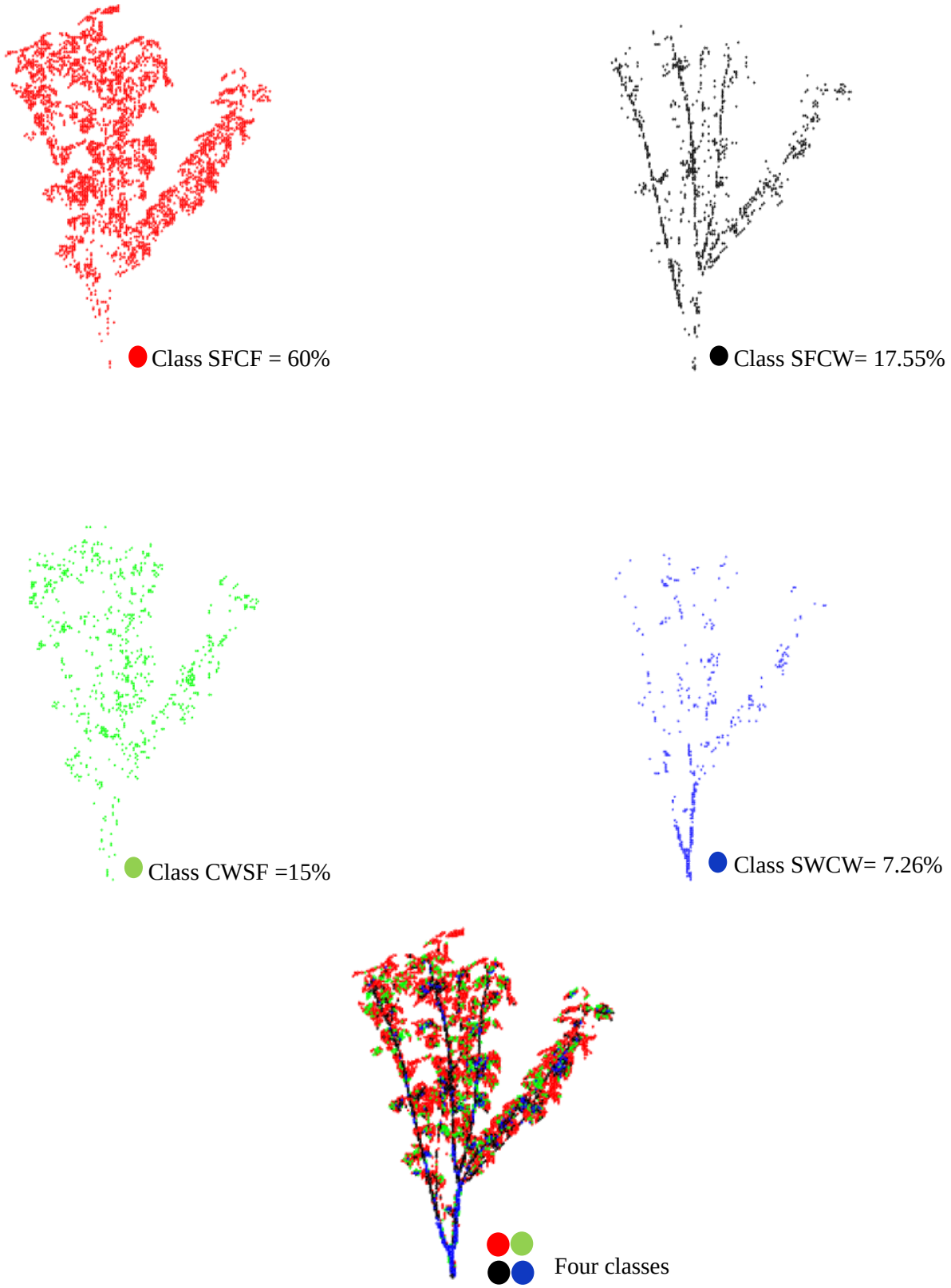

Figure 4.19: The spectral and spatial classes of broadleaf tree leaf-on scan. The red points allocated to class SFCF, black points to class SFCW, green to class SWCF, and the blue points to class SWCW. The four classes are recombined into one image.

4.7.2 Needle-leaf tree

The final CANUPO classification for the needle-leaf tree leaf-on condition is detailed in Table 4.3. As the table shows, the spatial classification in CANUPO was represented by 6922 spatial returns. Class SFCF recorded the highest number with 4861 spatial returns in the matrix and comprised a total agreement of 70.22% between the spectral and spatial points of foliage. The total agreement between the points for the needle-leaf classification was 73.18%. However, there was a disagreement of 26.8%, which means that these points were a mixture of foliage and wood points.

Table 4.3: The spectral and spatial classes for needle-leaf leaf-on tree sample.

Four classes 6922 returns	CANUPO foliage	CANUPO wood
Spectral foliage	4861 (SFCF), agreement 70.22%	1238 (SFCW), disagreement 17.88%
Spectral wood	618 (SWCF), disagreement 8.92%	205 (SWCW), agreement 2.96%
The total percentage of agreement between the spatial and spatial points was 73.18%		

The spatial classes were mapped in Figure 4.20 in order to visualise the spatial classes of the needle-leaf tree leaf-on scan sample from Table 4.3. Most of the tree canopy or the foliage materials were allocated to class SFCF (red) in this Figure which represented 70.22% of the total returns in the table above. This class showed a large percentage of agreement between the spectral and spatial classification for the foliage areas for this tree.

The spectral foliage and CANUPO wood SFCW (black) were allocated to most of the main branch, wood materials, and some parts of the tree canopy. Class SWCF (green) was distributed randomly around the foliage parts. Class SWCW (blue) was represented by only 2.96% of all returns and most of the points were displayed as a part of the tree trunk. However, some points of the wood class were randomly distributed around the tree canopy. To investigate whether the points were allocated in the right place, all the classes were visualised into one 2D image in Figure 4.21 where the tree was dominated by the class SFCF (red).

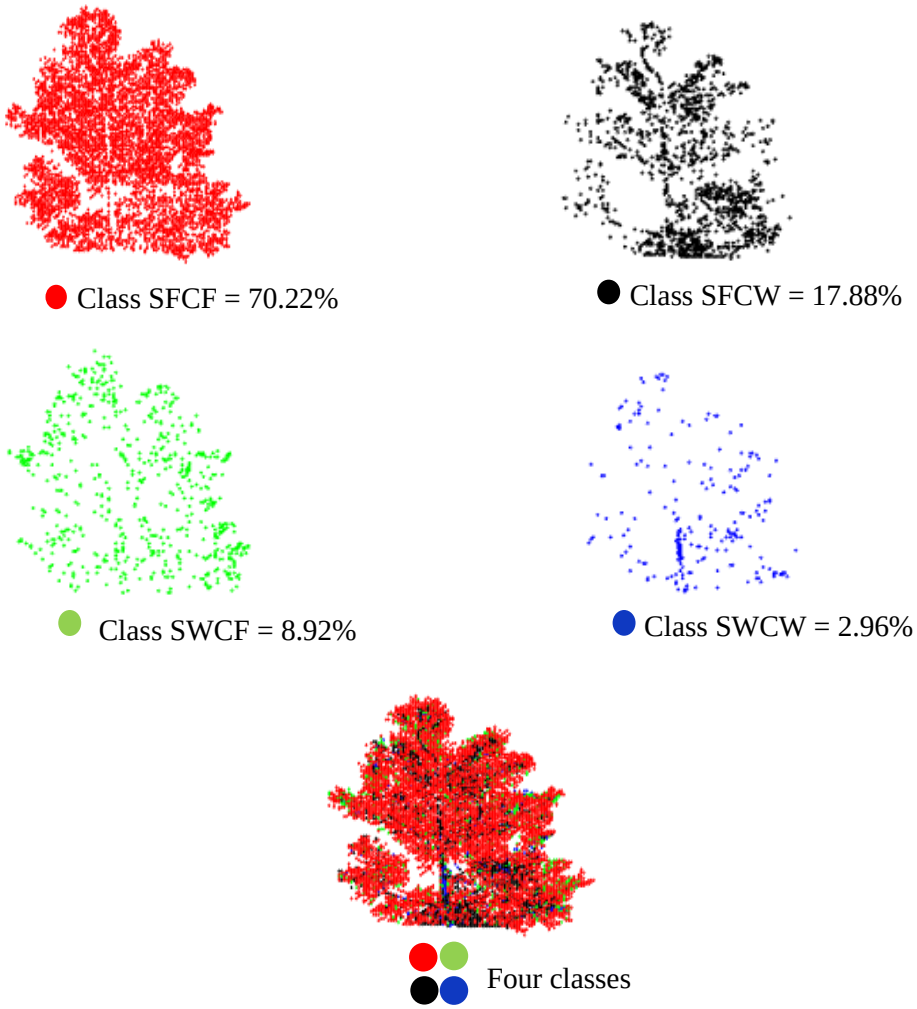

Figure 4.20: The spectral and spatial classes of needle leaf tree leaf-on scan. The red points allocated to class (SFCF), black points to class (SFCW), green to class (SWCF), and blue points to class (SWCW). The four classes are combined into one image.

4.8 Conclusion

The aim of this chapter was to examine the potential of a dual-wavelength (SALCA), that is used to distinguish foliage from wood points. This was done in a laboratory before taking SALCA to scan a complex forest environment. A series of scans were undertaken at short-ranges to characterise point clouds for broadleaf and needle-leaf trees in leaf-on and leaf-off conditions. The SALCA data were processed in order to extract information related to the research objectives. The data were classified into foliage or wood based on visual thresholds and the geometric relationships between the x, y, and z of the points. The initial visualisations of the data showed the effect of range on the visualisations, where the point clouds looked

clearer at 1, 3, and 5 m (Figure 4.4). The initial results for 8 m data show a normal range of apparent reflectance, and the NDI was within the normal range for both trees as well.

For the spectral classification, different thresholds were applied on the 1063 nm, 1545 nm and NDI for both trees. Unexpectedly, the separation of foliage and woody materials that was produced by applying a threshold on the 1063 nm for broadleaf trees was more successful than for the 1545 nm. On the contrary, for the needle-leaf tree, the separation that was generated by applying a threshold on the 1545 nm was more accurate than the one produced by the threshold on the 1063 nm. In addition, the classification of the NDI confirmed that it was possible to distinguish between the foliage and wood in the case of the broadleaf tree. However, in the case of the needle-leaf tree, there were a large number of misclassification errors and most of the tree components were classified incorrectly based on different thresholds. In terms of validation, the same thresholds were applied for the leaf-off scan variables of both trees. The outputs showed that 33% and 25% of the 1063nm data and 59% and 77% of the 1545nm data of the leaf-off points were misclassified as foliage for the broadleaf and needle leaf trees respectively. Overall, this part of the analysis has shown that foliage wood classification, when based on a threshold, is unlikely to provide accurate separation due to the differences in the spectral properties of sample components (e.g. stem, branches, and foliage). The NDI provided errors in the classification of 27% and 26% for the broadleaf and needle-leaf trees respectively.

For the spatial classification, the spatial classifier separated the tree samples based on the distribution of the points within spatial certain scales. The initial classification showed that it was possible to distinguish between the foliage points and woody materials in the case of the broadleaf tree. However, due to the foliage shape and size, it was hard to generate scales to distinguish between the needle-leaf components properly. The same scales were applied for leaf-off scans, which showed a large number of misclassified points as foliage. Representing the spectral and spatial classifications into one matrix has provided information about how far the classifications are in agreement. The visualisation of the cross-comparison of both trees showed the areas of which the foliage areas dominate most of the classifications. Overall, the findings of this chapter have demonstrated the potential of SALCA data to be used in order to identify basic information related to tree components. In the next chapter, the same approach of spectral and spatial classification was investigated for single trees in an open field environment.

CHAPTER 5: POINT CLOUD CLASSIFICATION ON SINGLE TREES IN A FIELD ENVIRONMENT

Summary

The aim of this chapter is to test a range of approaches for foliage and wood separation using SALCA datasets for three isolated oak trees from Silverdale, Lancashire, UK. A combination of spectral and spatial analysis of leaf-on and leaf-off scans was tested in order to classify the point clouds and improve the foliage and wood separation. A range of methods was used to assess the accuracy of the classification approaches.

5.1 Introduction

This chapter describes the experimental design and classification approaches used in order to satisfy Objective 2 of this research. The datasets used in this chapter were collected from a private farm near Silverdale, Lancashire, UK. The SALCA instrument was used to acquire 3D points cloud measurements of the leaf-on and leaf-off conditions of three isolated oak trees located in a single field. All of the datasets were pre-processed using the methods described in Chapter 3, to derive spectral information, including intensity, apparent reflectance, and NDI.

A series of spectral and spatial classifications were conducted in order to map the 3D spatial distribution of foliage and wood. For the spectral classification, different thresholds were applied to the 1063 nm, 1545 nm apparent reflectance product and NDI. The spatial classification was also applied to the point clouds using the CANUPO classifier based on scales of 0-50 cm. A general overview of the classifications applied is summarised in Figure 5.1.

In order to validate the classifications, the same spectral thresholds applied for the leaf-on scans, were subsequently applied to the leaf-off scans. In addition, CANUPO classifications were performed on each tree from the south, north, east, and west scan directions. The outputs of the spectral and spatial classification were compared in a matrix to investigate the comparability of the classifications.

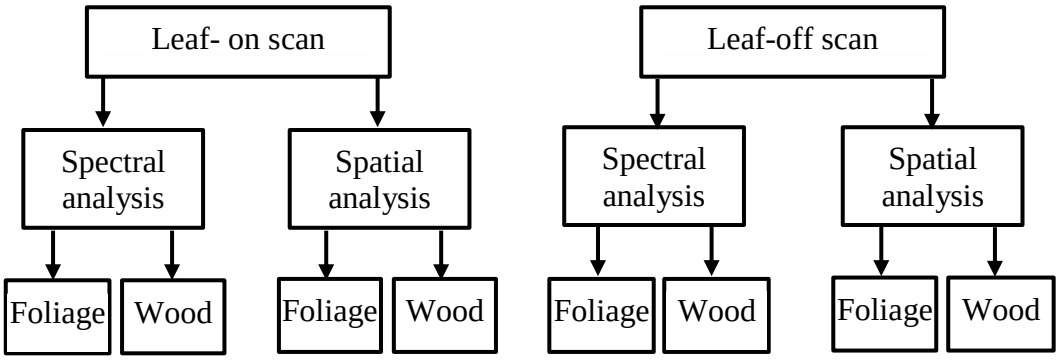

Figure 5.1: Overview of the spectral and spatial classifications in chapter 5

5.2 Field site and data collection

Silverdale village is located close to the city of Lancaster, UK. It lies on Morecambe Bay, near to the border with Cumbria, about 140 km north of Manchester (Silverdale Parish, 2011). The datasets were acquired from a private farm near Silverdale, Lancaster (54.1766° N, 2.8151° W), as shown in Figure 5.2. The ground on the farm is not flat due to the presence of small hills. The study area consists of undulating land and comprises several areas of open land and nature reserve areas.

Figure 5.2: Location of three isolated oak trees on a private farm near to Silverdale, Lancashire (54.1766° N, 2.8151° W). The scale of Silverdale in the figure is 1536 m and 86m for the fieldwork. (a) the Poor tree (b), the Moderate tree, and (c) the Good tree. Source: (Google Earth, 2019).

High-resolution SALCA scans were acquired in July and August 2015 for the leaf-on condition and in April 2018 for the leaf-off condition, as shown in Figure 5.3. The field sampling activities formed a part of a collaboration between Salford University and Lancaster University in order to study tree conditions. The trees are labelled as being in 'Poor', 'Moderate' and 'Good' condition, based on a visual survey of them.

The Poor tree (Figure 5.3 a) consists of woody materials mixed with a few leaves distributed randomly at the ends of the finer branches of the tree canopy. The tree height was estimated to be 9 m. For the Moderate tree (b), the tree height was 14 m, and it showed moderate leaf density in the tree canopy in the leaf-on condition. The Moderate tree was close to a small hill, which surrounds the tree from the east, west, and north, which impeded the scanning process from these directions. The Good tree (c) stands beside clumps of small trees, was almost 14 m in height and had a crown in full leaf with no visible signs of stress. The lower parts of the trees' trunks were covered in places by green material or lichen, which might affect the response of the lasers and so lead to misclassification in these parts of the trees. The datasets for the leaf-on scans were acquired from the north, south, east, and west in order to compare the classifications of each tree from different aspects. The first scans were performed on 23rd July 2015, and the second scans on 13th August 2015. In addition to each scan, temperature measurements were taken using the SALCA protocol to record the internal laser temperature separately at five minutes intervals. Due to the nature of the TLS data collection, weather conditions, such as rain, wind, and fog, can limit the data quality. For instance, the laser beam might be scattered by rain or suspended fog particles, thereby triggering a false return.

However, the first day of the leaf-on data collection was sunny, with a clear sky. In addition, low winds speeds were recorded for most of the scans, as mentioned in Appendix II. On the second day of the data collection, the wind speed was very low and there was no significant movement in the trees recorded. The SALCA instrument was fixed on a tripod 20 m away from the tree stem for each scan. One scan was incomplete due to the expiration of SALCA's battery charge; this scan was repeated to cover all parts of the desired trees. The leaf-off scans were acquired on 15th April 2018. The trees were scanned from the south only, at a distance of 20 meters from the stem. The datasets of all of the desired samples were processed in order to produce useful information for classification purposes. In order to obtain the point cloud that belongs to the trees only, each individual tree was segmented using the CloudCompare©

tools in order to remove undesired points from the scan output. CloudCompare© is open source software, available at (https://www.danielgm.net/cc/). Details of the data sites, with the tree names, scan directions, scan durations, file names, range, winds speed, zenith, azimuth, scan ranges and the elevation angles for the leaf-on and leaf-off scans are highlighted in Appindex II:

Figure 5.3: (a) Poor tree, (b) Moderate tree, and (c) Good tree leaf-on and leaf-off conditions at Silverdale, Lancashire, respectively; green moisture algae material covers the lower parts of the trunks (the red arrow). The tree figures have been taken from the south for both conditions.

5.2 Point-cloud description

This section discusses the outputs from the Silverdale scans for the Poor, Moderate, and Good tree in leaf-on and leaf-off conditions. The intensity, AR, and NDI were extracted for both conditions. The point clouds were then visualised using azimuth and zenith indices. In the visualisations, the minimum values were coloured blue, the average values green, and the maximum values were red on the scale bar.

5.2.1 Leaf-on scans

Figure 5.4 shows the point clouds for the Poor tree, coloured by intensity, AR and NDI respectively, with their frequency distributions. Figure 5.4a comprises a narrow range for the 1063 nm intensity with a maximum value of 45. Most of the high values are seen in the stem and a few parts of the main branches. The 1545 nm shows a wider range of intensity, with maximum values of 58 which appears in the tree canopy. Figure 5.4b suggests that the AR values lie within the normal range for both laser wavelengths. A maximum value of 0.43 is recorded for the 1063 nm AR, with a frequency peak at 0.2. The largest value recorded for the 1545 nm is 0.7, with a peak at 0.45, and it is clear from the figure that most of the stem and the main branches are showing values between 0.4-0.5. The NDI shows values within the normal range in the figure, with the highest value of 0.5, which is coloured as the foliage area on the finer branches, as shown in Figure 5.4c.

Figure 5.5 shows the data for the Moderate tree. From Figure 5.5a, it is clear that the 1063 data represent a narrow range compared to the 1545 nm. The maximum values for both wavelengths are visualised randomly in the tree canopy as red which are very hard to be seen due to the small number of these points. The distribution of the AR shows that the 1545 has a wide range, with a maximum value of 0.55, while the 1063 nm is represented by a narrower value, as visualised in Figure 5.5b. The NDI lies within the normal values, with a peak at zero, and most of the foliage shows values of zero or greater (yellow) (Figure 5.5c).

The Good tree data are visualised in Figure 5.6. The data of the 1545 nm shows a wider range. with a maximum value of 69, while 45 is recorded for the 1063 (Figure 5.6a). Figure 5.6b suggests that most of the high values of the AR are visualised on the stem and a few parts of the tree canopy for both laser wavelengths. The NDI appears to lie within the normal range, with a peak at zero. Most of the stem and main branches appear to have values smaller than -0.2 (Figure 5.6c).

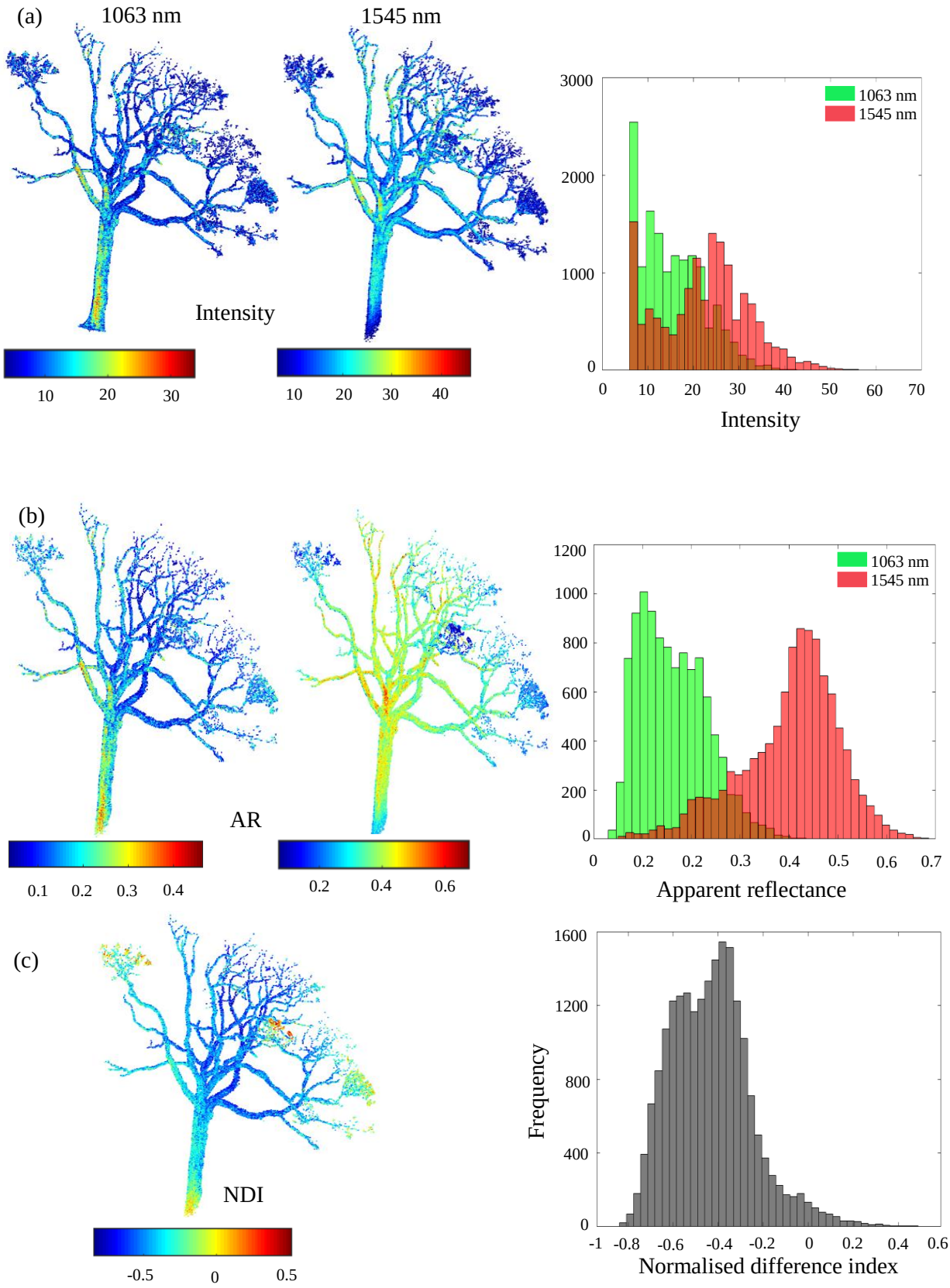

Figure 5.4: SALCA point clouds for the Poor tree leaf-on scan coloured by (a) intensity, (b) apparent reflectance, and (c) normalised difference index respectively, with their frequency distribution. Blue for minimum, green for average, and red for maximum values.

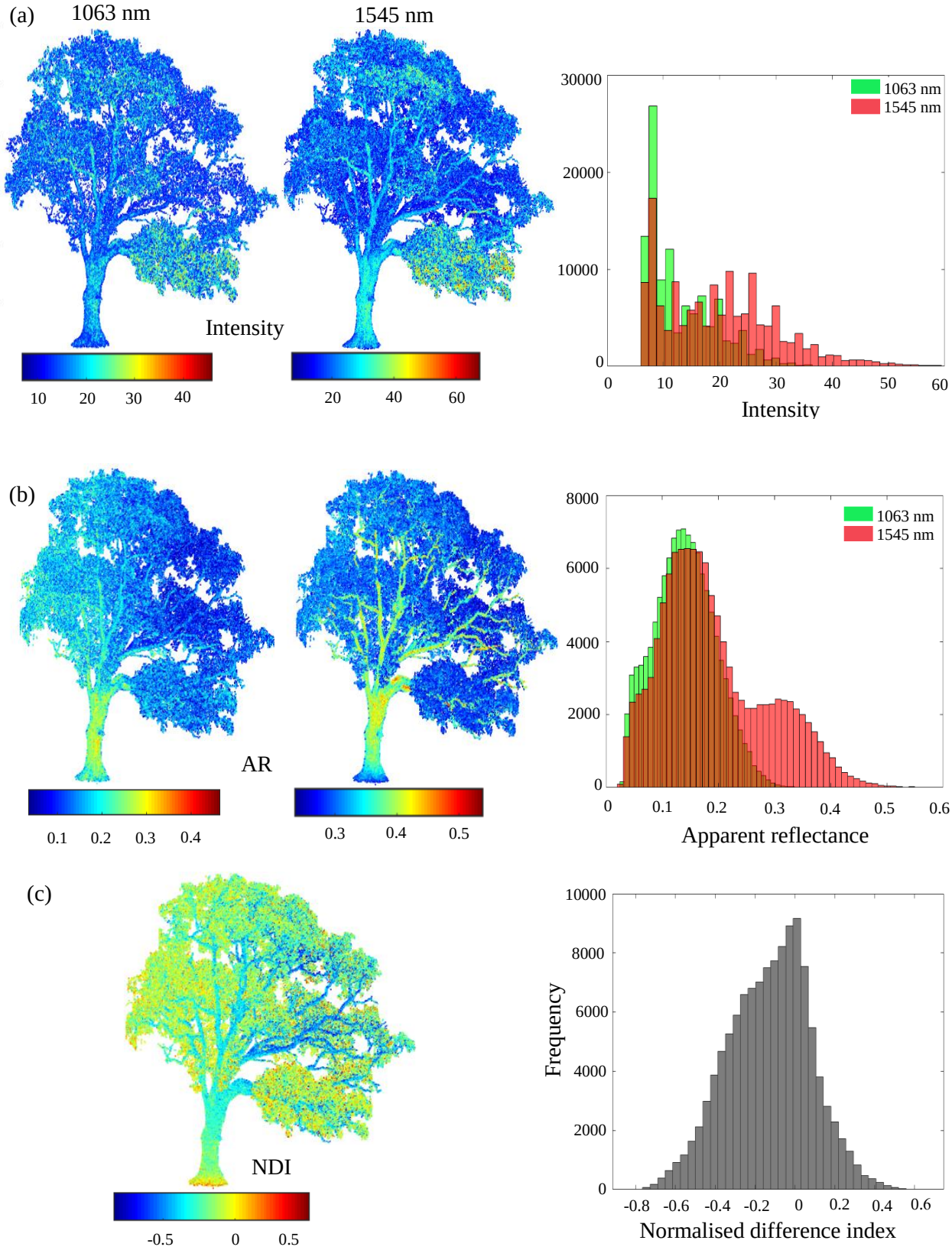

Figure 5.5: SALCA point clouds for the Moderate tree leaf-on scan coloured by (a) intensity, (b) apparent reflectance, and (c) normalised difference index respectively, with their frequency distribution. Blue for minimum, green for average, and red for maximum values.

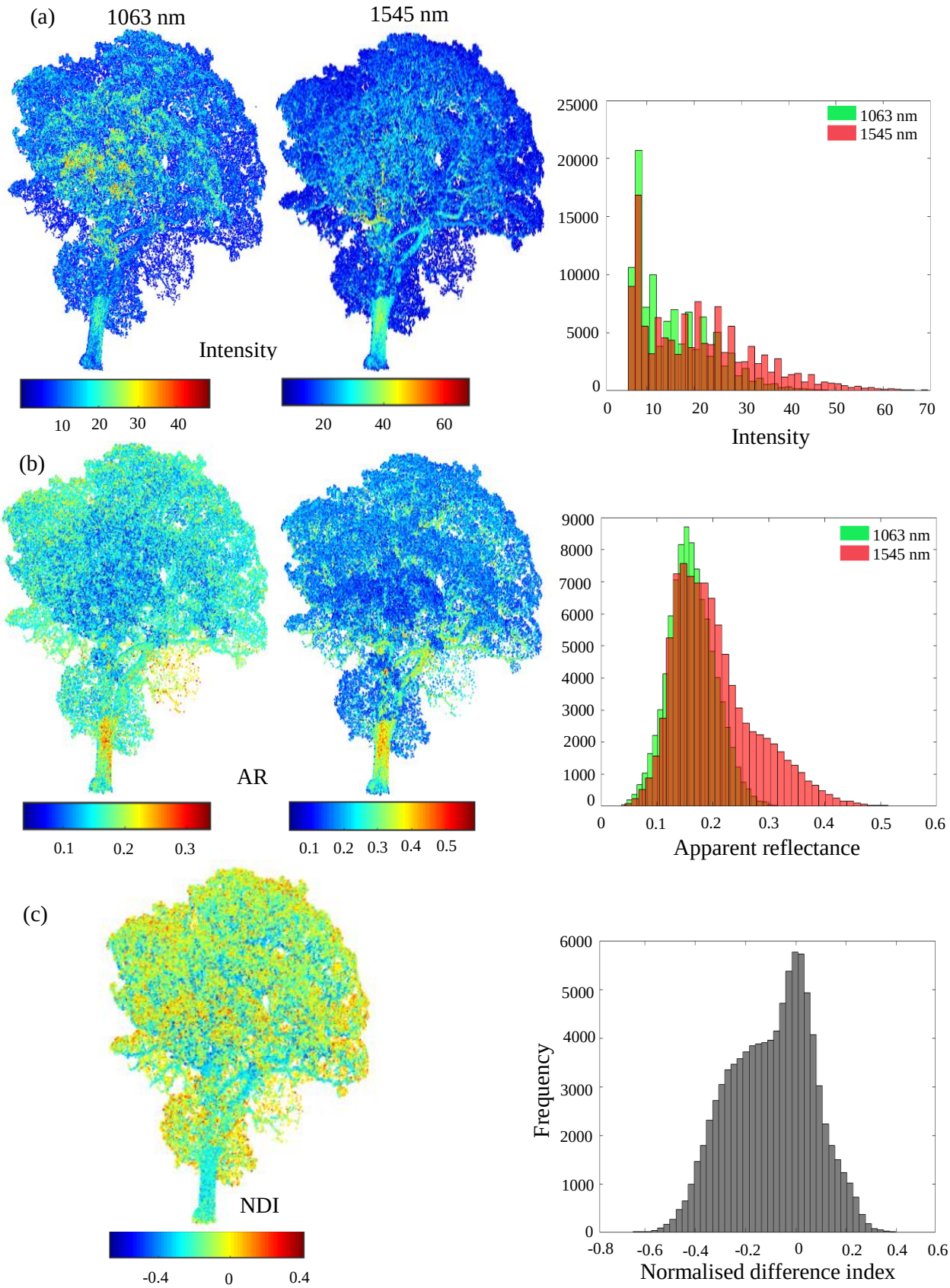

Figure 5.6: SALCA point clouds for the Good tree leaf-on scan coloured by (a) intensity, (b) apparent reflectance, and (c) normalised difference index respectively, with their frequency distribution. Blue for minimum, green for average, and red for maximum values.

5.2.2 Leaf-off scans

This section visualises the point clouds extracted from the leaf-off scans. The point clouds are visualised using azimuth and zenith indices on the left for the trees and their range distribution with the frequency on the right of the figures.

Figure 5.7 shows the point clouds for the Poor tree coloured by intensity, AR and NDI respectively, with their frequency distributions. Figure 5.7a shows that the intensity extracted from the 1063 nm data is greater than that from the 1545 nm, with a maximum value of 260 and a large peak at 180, while the 1545 nm shows a narrower range of 170, with a frequency peak at 90. This difference is caused by the sensitivity of SALCA and the reflectance of both wavelengths. The AR 1063 nm shows a very wide range within the normal range 0 -1, with a maximum peak at 0.63, and most of the tree components are coloured yellow and red or have values over 0.6. The largest value for the AR1545nm is 0.5, with a peak of 0.3. The NDI shows the normal values for this tree. However, the tree is mostly coloured by values greater than 0.4, with a few random points on the edges on the tree canopy represented by low values.

For the Moderate tree, Figure 5.8a presents the difference in the intensity for both wavelengths where the 1063 data comprises a maximum value of 288 with a frequency peak at 10. Most of the high values are distributed randomly in the tree canopy. The highest value of 1545 nm data is 140 and the peak is at 5. Figure 5.8b shows a big variation between the AR of both laser wavelengths, with 1063 data represented by a high of 0.85, while the 1545 nm comprises a maximum value of 0.43. The maximum values for both wavelengths are mainly visualized on the stem of the tree. Figure 5.8c illustrates a normal range of NDI with a high peak at zero, most of the tree components are coloured with red or orange with values more than 0.4.

Figure 5.9 visualizes the point clouds of the Good tree. For the intensity, the 1063 nm data show a wider distribution, with a maximum value of 245 and a frequency peak of 40. The 1545nm data comprise a narrower range, with a maximum value of 96 and a peak at 10 (Figure 5.9a). Figure 5.9b represents the frequency distribution of the AR for both laser wavelengths, with the 1063 nm showing a maximum value of 0.9 with a high peak frequency at 0.5, and the 1545 nm showing a small range with a maximum value of 0.36. Figure 5.9c shows a normal range (-1 to 1) of NDI with a unclear peak is at around NDI of 0.6. The tree trunk and branches are coloured red, orange or more than 0.4.

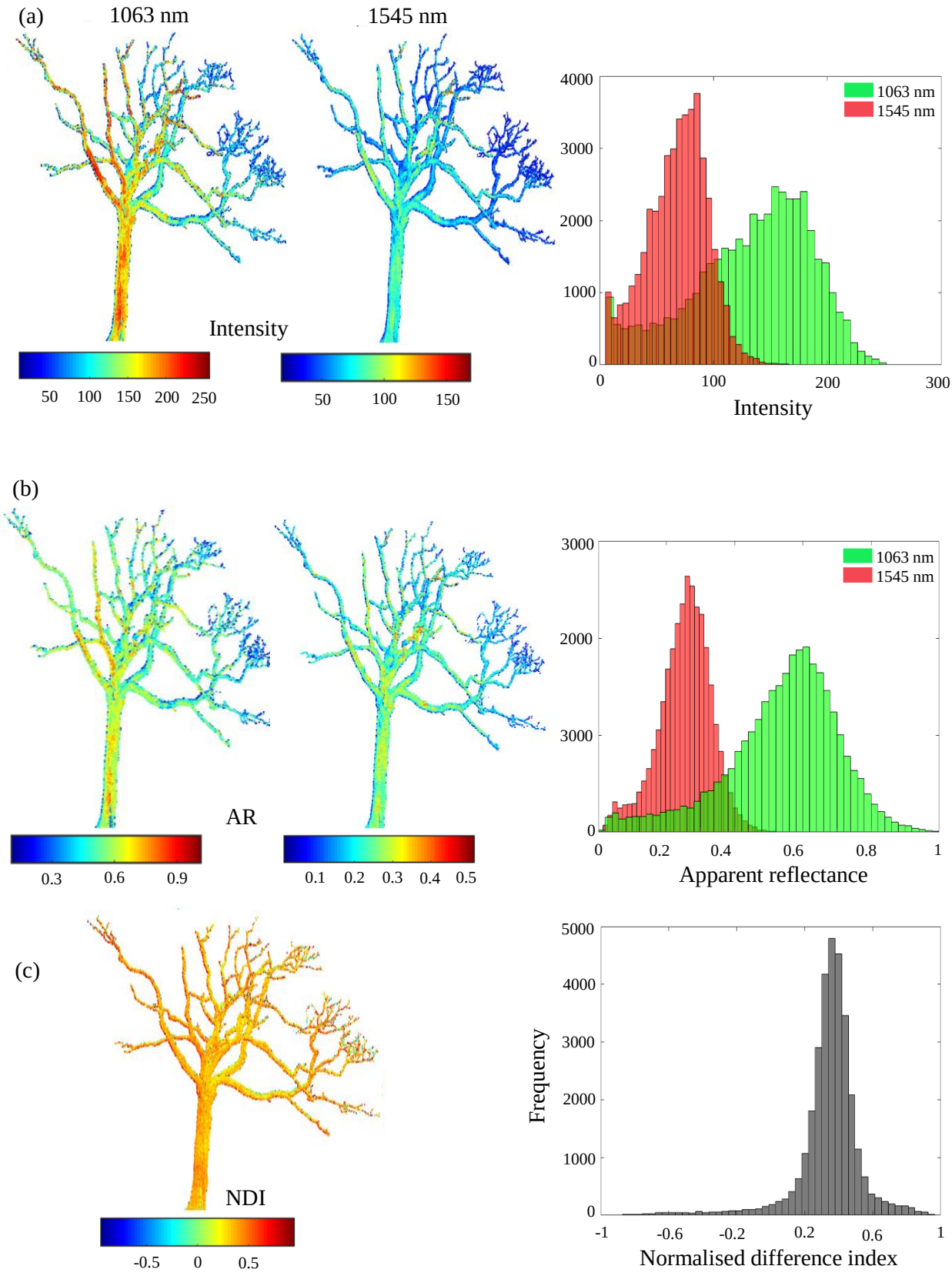

Figure 5.7: SALCA point clouds for the Poor tree leaf-off scan coloured by (a) intensity, (b) apparent reflectance, and (c) normalised difference index respectively, with their frequency distribution. Blue for minimum, green for average, and red for maximum values.

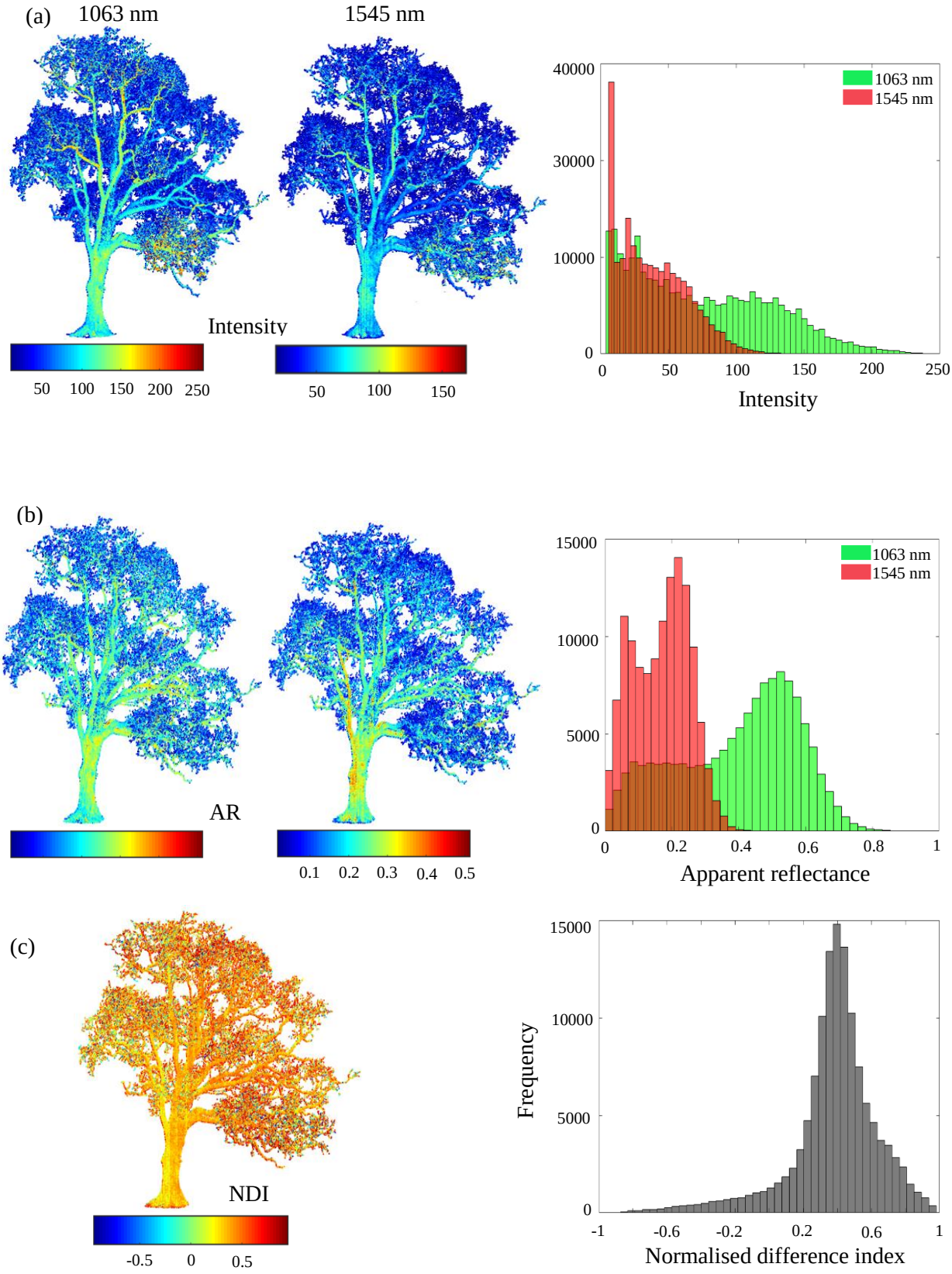

Figure 5.8: SALCA point clouds for the Moderate tree leaf-off scan coloured by (a) intensity, (b) apparent reflectance, and (c) normalised difference index respectively, with their frequency distribution. Blue for minimum, green for average, and red for maximum values.

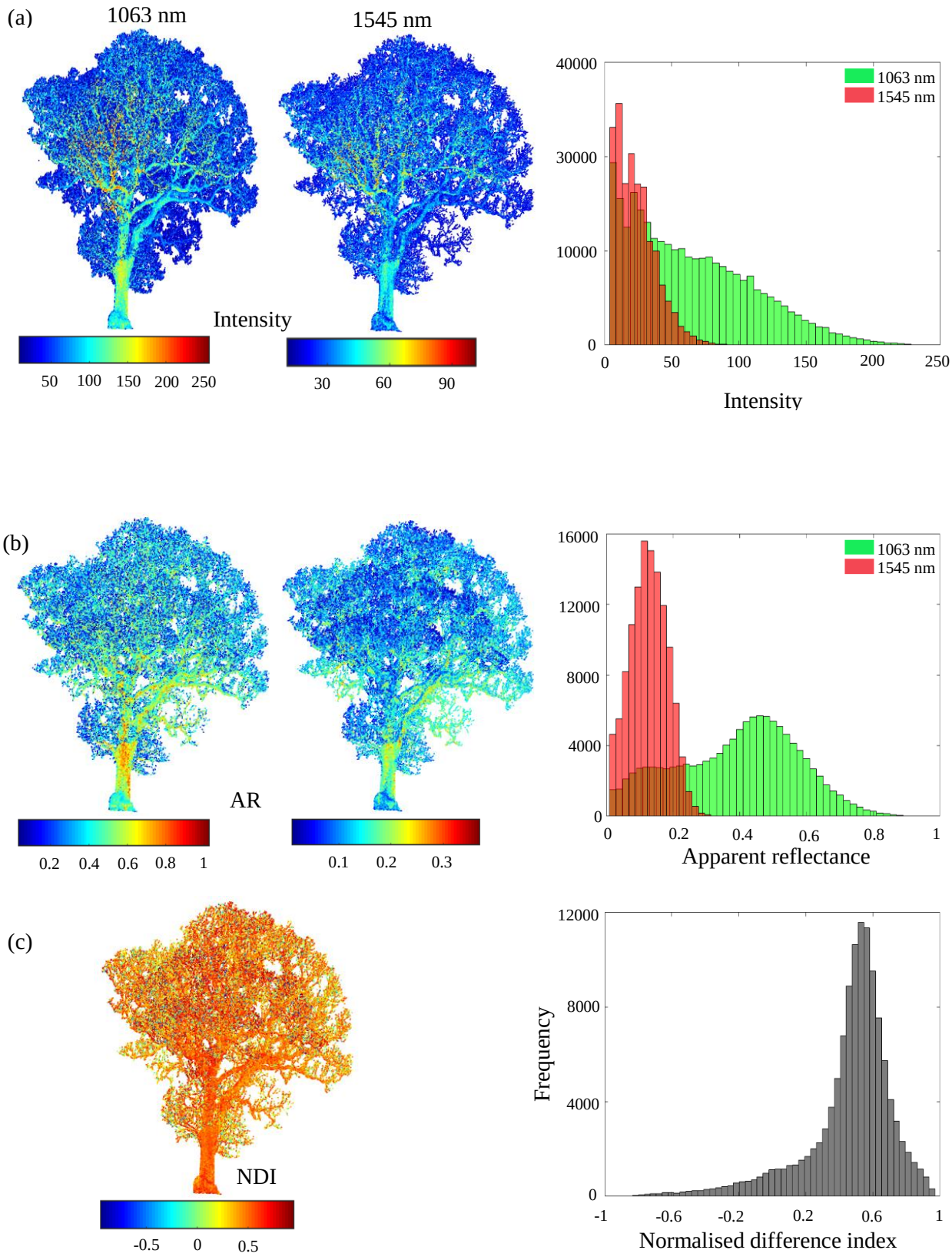

Figure 5.9: SALCA point clouds for the Good tree leaf-off scan coloured by (a) intensity, (b) apparent reflectance, and (c) normalised difference index respectively, with their frequency distribution. Blue for minimum, green for average, and red for maximum values.

5.3 Spectral analysis of leaf-on scans

SALCA AR and NDI were extracted for both the 1063 nm and 1545 nm wavelengths, as detailed in Section 3.3. Specific thresholds were applied on the AR and NDI histograms in order to separate the foliage from the wood points. The thresholds were generated based on a visual interpretation of the point clouds.

5.3.1 Thresholding 1063 nm apparent reflectance leaf-on scans

Figure 5.10 shows the initial separation produced by applying a 0.1 threshold on 1063 nm for the Poor, Moderate and Good trees in order to separate the SALCA point-clouds as either foliage or wood. All of the points were visualised using zenith and azimuth indices. The foliage points were highlighted in green and the wood in red, as visualised in the figure.

For the Poor tree, and based on the suggested threshold, a large number of the returns on the tree canopy, including the main and finer branches' returns, were incorrectly classified as foliage (≤0.1). These returns were mainly produced by full hits. A few partial hits on the main stem appeared as misclassification errors on this part of the tree. Most of the tree returns were represented by values greater than 0.1 and therefore classified as wood (red). However, there was a group of foliage points distributed in different parts at the edges on the finer branches which were classified as wood. This means that these foliage points have a large value of AR1063 nm that makes the threshold allocate them as wood. The points of both classes were visualised in a single figure to map their distribution, as shown in Figure 5.10.

The Moderate tree classification illustrates that using a 0.1 threshold was unsuccessful and that it was impossible to distinguish between the foliage and the wood of this tree by thresholding the 1063 nm AR. There was an overlap between the finer branches and the foliage, both of which have similar values (≤0.1), which caused the threshold fail to separate them accurately. In addition, a large number of the foliage hits show misclassification errors in the tree canopy, as these points were allocated to the wood points. The same phenomenon was observed for the Good tree, where most of the tree points were shown in red and classified incorrectly as wood due to the high values of AR for these points. Overall, it is not expected that the 1063 nm can present accurate classification due to the similar response of both foliage and wood in the NIR wavelength.

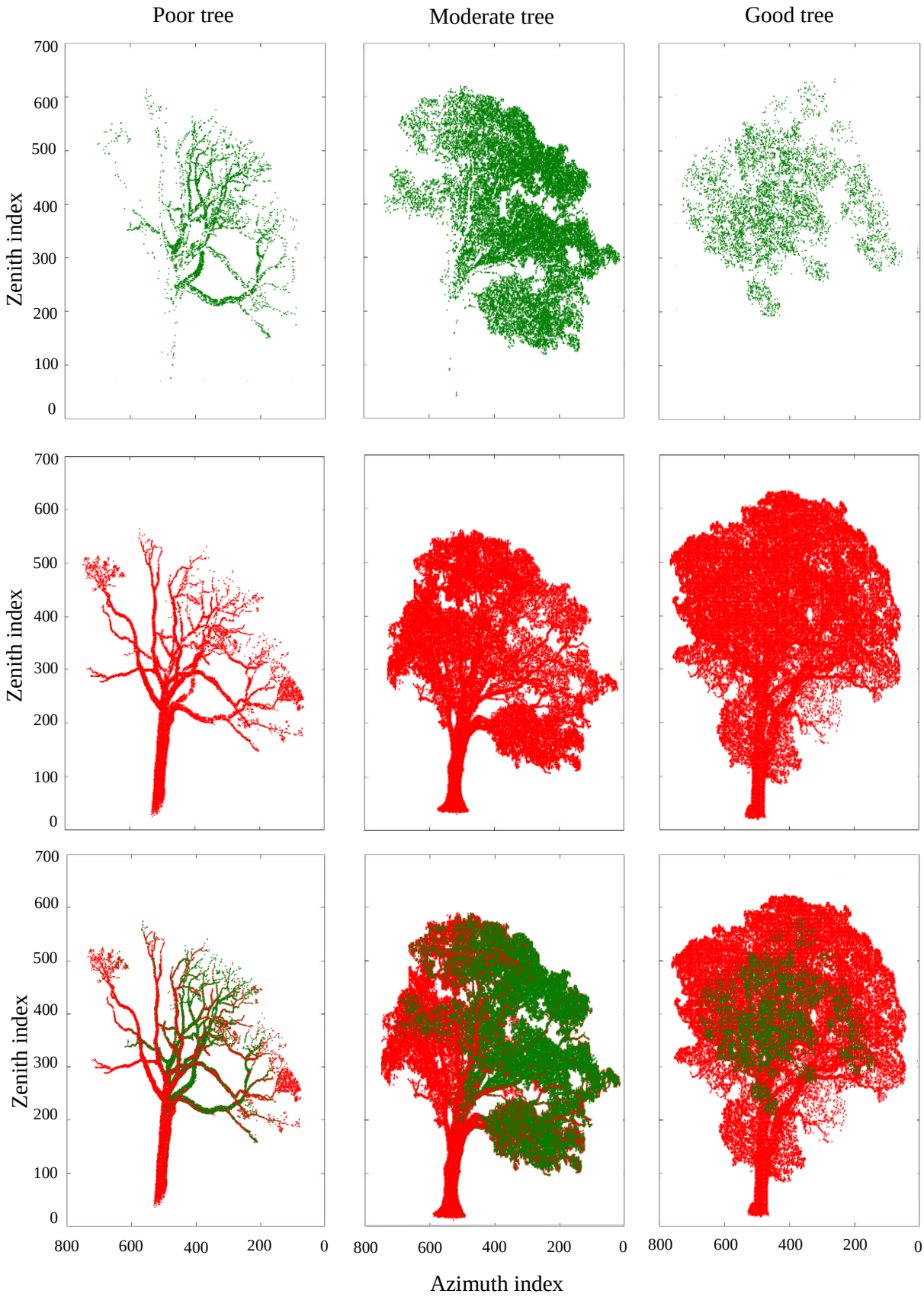

Figure 5.10: Point clouds of the Poor, Moderate, and Good tree leaf-on scans classified into foliage (green) or wood (red) using a 0.1 threshold for AR 1063 nm.

5.3.2 Thresholding 1545 nm apparent reflectance leaf-on scans

The foliage and wood of the Poor, Moderate and Good trees were separated by applying a 0.2 threshold to the AR 1545 nm, as shown in Figure 5.11. In general, the visual interpretation of the figure suggests that the foliage and wood separation was more accurate compared to that produced by the 0.1 threshold applied to the 1063 nm data previously. This supports the hypothesis that the foliage and wood have a different spectral response in the SWIR (1545 nm).

The classification of the Poor tree's components showed that it was easy to distinguish the few random groups of foliage points at the end of the finer branches or the edges of the branches. The majority of the tree points were correctly classified as wood as can be seen clearly, as the two groups of points were recombined (bottom of Figure 5.11). Overall, the separation for this tree was clear and successful.

For the Moderate tree, the classification showed the successful separation in the tree canopy area where most of the foliage returns were highlighted in green. Most of these points were produced by full hits, but there were some partial hits on the trunk of the tree that were classified as foliage. Moreover, the green patches on the lower part of the trunk were classified as foliage, possibly due to moisture or lichen on this part of the tree. There was a clear distribution of the woody materials on the tree canopy, including the main and the finer branches. The appearance of the foliage and wood (finer branches) separation at the top of the tree canopy is unclear due to some misclassified points, which may be attributed to partial hits. More details emerged once the two separated points were combined, as shown in the figure of the Moderate tree.

Based on a visual interpretation, the discrimination between foliage and wood for the Good tree was successful based on a 0.2 threshold. The foliage points were distributed accurately around the tree canopy and around the middle of the trunk where there was foliage on the branches. Moreover, the separation of the wood materials was distinguishable where most of the trunk and the main branches were illustrated in the figure. Due to the tree condition (Good), there was some confusion between the finer branches in the tree canopy, which make it harder to distinguish every branch separately based on visual interpretation. The lichen on the tree trunk may have caused misclassification in this part of the tree.

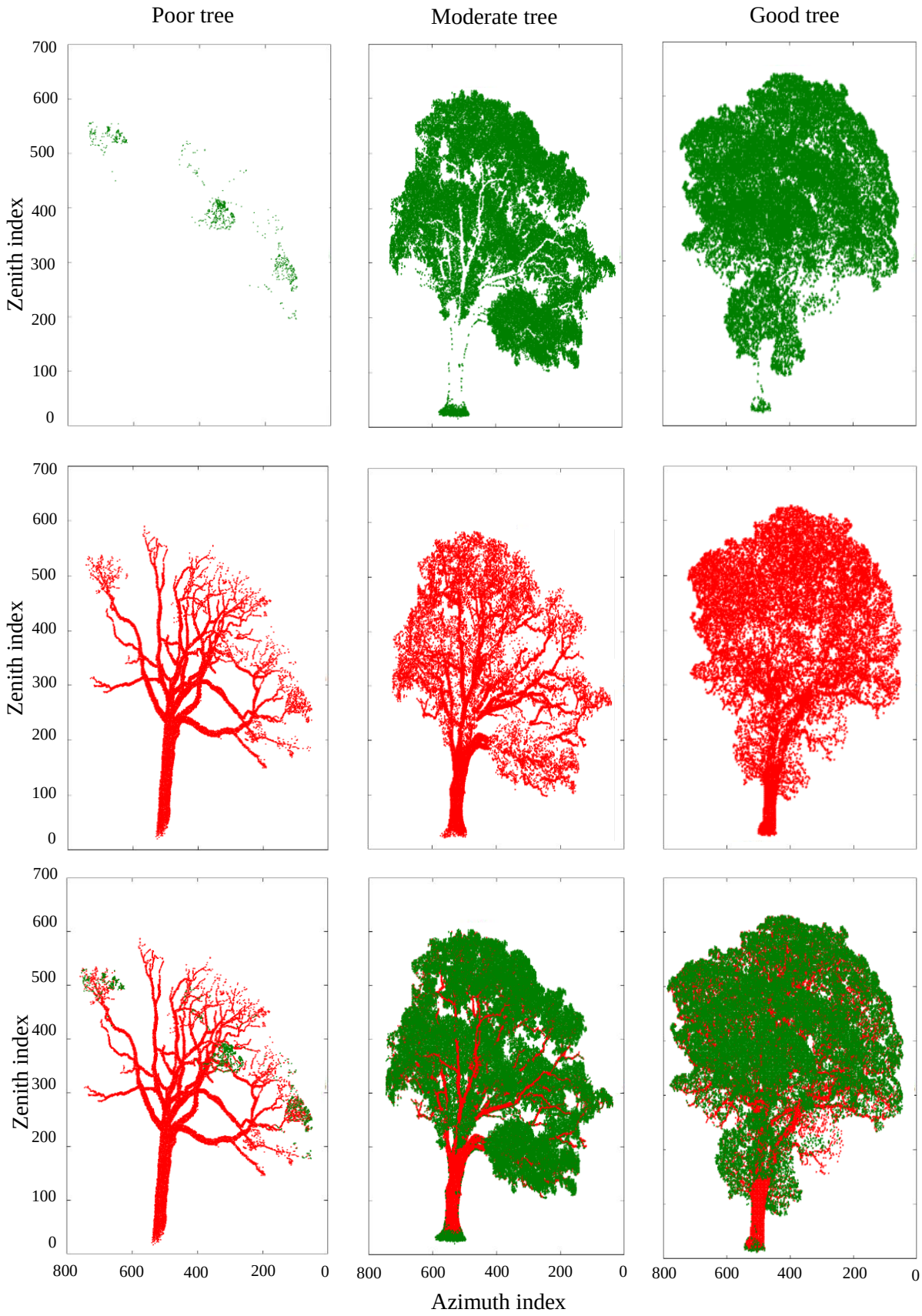

Figure 5.11: Point clouds for the Poor, Moderate, and Good tree leaf-on scans classified into foliage (green) or wood (red) using a 0.2 threshold for AR 1545 nm.

5.3.3 Thresholding of Normalised Difference Index leaf-on scans

The NDI of the Poor, Moderate, and Good trees was used in order to classify the trees' point clouds as either foliage or wood. A threshold of -0.1 was applied based on visual interpretation. Due to the sensitivity of the NDI to the moisture content of vegetation, it was expected that the foliage and wood separation would be accurate and that partial hits would be minimised in terms of classification. Based on the applied thresholds, it was expected that foliage will be represented by high and wood by low values of NDI.

A closer inspection of Figure 5.12 confirms that every tree provides a different response to the NDI threshold. The Poor tree classification shows that the tree points were successfully classified as foliage (>-0.1) and wood (≤-0.1). There is a group of green points that were classified incorrectly as leaves on the lower part of the trunk due to the presence of lichen. This further supports the hypothesis that NDI is sensitive to the moisture in foliage or the water content of vegetation. Most of the tree points are correctly classified as wood and highlighted in red.

For the Moderate tree, the initial spectral classification shows that it is possible to distinguish the foliage from the wood in the tree canopy, where most of the main branches do not appear in this area. Some of the low tree trunk points were classified incorrectly as foliage with values greater than -0.1, which means that these points comprise high values of the NDI. It was expected that the moisture content in this area of the tree exceeded that in the rest of the trunk or the trunk may have been moist. In addition, a large number of the tree foliage points were misclassified as wood in the tree canopy.

The spectral classification of the Good tree showed some misclassified returns for the tree trunk that were incorrectly allocated to the foliage class. In addition, most of the tree canopy points were classified as foliage and the most accurate part was the patch of foliage around the middle of the trunk. However, the separation of the wood was accurate as can be seen from the distribution of the tree in the figure. In general, there was a variation in the response of the trees to the same threshold which depended on the trees' condition since, the greater the density of foliage and finer branches, the more difficult the separation.

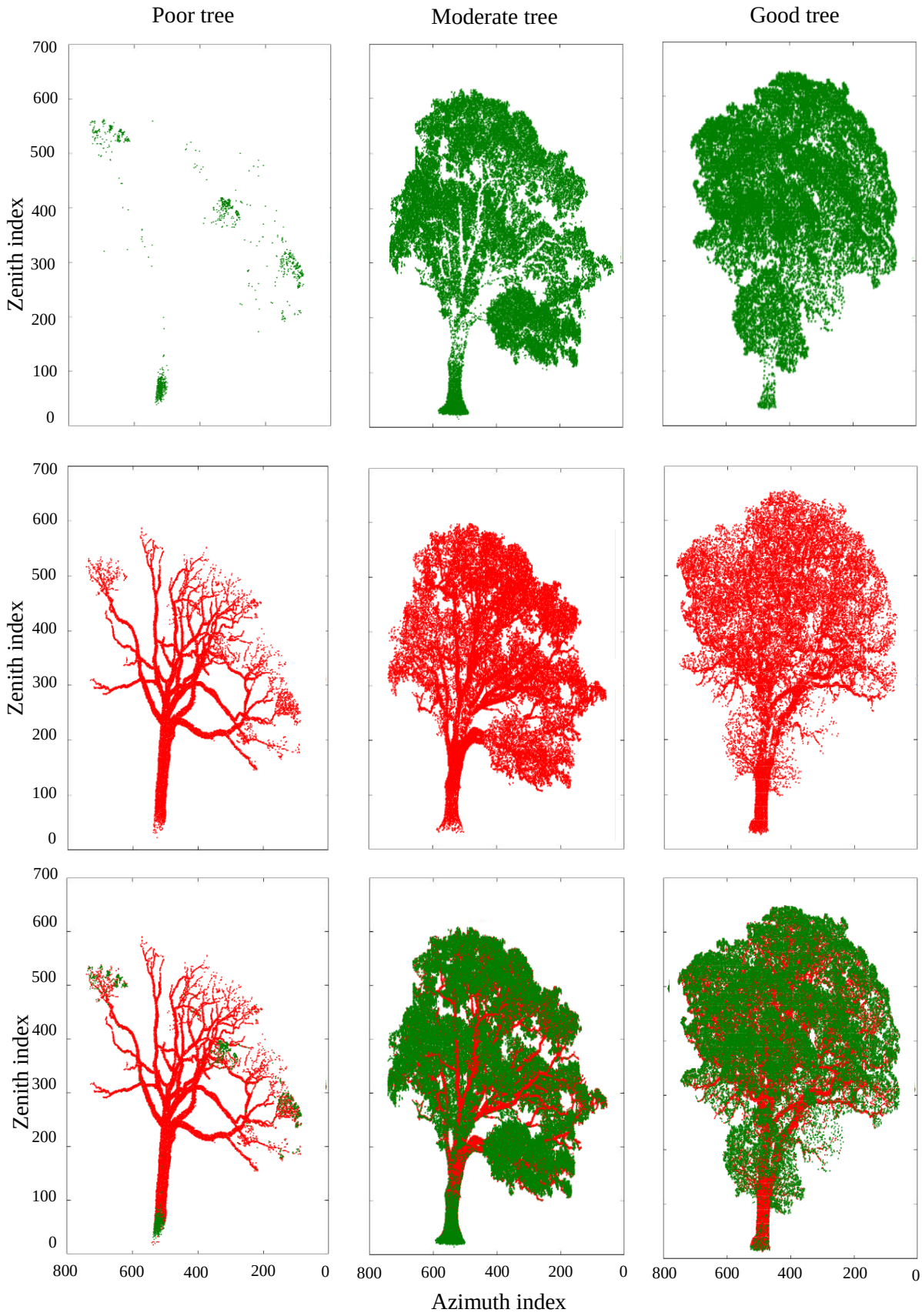

Figure 5.12: Point clouds for the Poor, Moderate, and Good tree leaf-on scans classified into foliage (green) or wood (red) using -0.1 threshold for the NDI.

5.4 Spectral analysis of leaf-off scans

In order to validate the classifications of the leaf-on scans, the same thresholds used for the leaf-on scans were applied during the leaf-off scans. In general, the initial observation of the adopted thresholds showed that these were successful for the 1063 nm data, but unsuccessful for the 1545 nm and NDI data.

5.4.1 Thresholding of 1063 nm leaf-off scans

Figure 5.13 presents the results of the leaf-off classification for the Poor, Moderate, and Good trees using a 0.1 threshold at the AR 1063 nm. The misclassified points were highlighted in green and the points classified as wood correctly in red. In general, most of the points were classified as wood, especially for the Poor tree, and some of the finer branches were highlighted in the green, with low values of ≤ 0.1.

5.4.2 Thresholding of 1545 nm leaf-off scans

Figure 5.14 visualises the point clouds for the leaf-off scans, classified into foliage or wood, using 0.2 apparent reflectance thresholds for the 1545 nm. The figure shows that a large number of SALCA points were incorrectly classified as foliage for the Poor tree, including the trunk and the main and finer branches. These misclassified points were produced by full and partial hits. The classification of the Moderate tree showed that most of the tree crown was green, including part of the main branches, a few points on the lower part of the tree trunk, and most of the finer branches. However, most of the point clouds of this scan were classified correctly as wood or red points. The same errors in classification occurred for the Good tree, where most of the tree was misclassified as foliage. These incorrect classifications might be caused by the presence of water in the tree.

5.4.3 Thresholding of NDI leaf-off scans

Figure 5.15 presents the classification using a -0.1 threshold at NDI for the three trees. An overview of the figure showed that the applied thresholds did not validate the leaf-off scan as wood materials for all trees. Most of the scans points were incorrectly classified as foliage, which means that the NDI of these points was represented by high values larger than the suggested threshold for the Poor, Moderate, and Good scans.

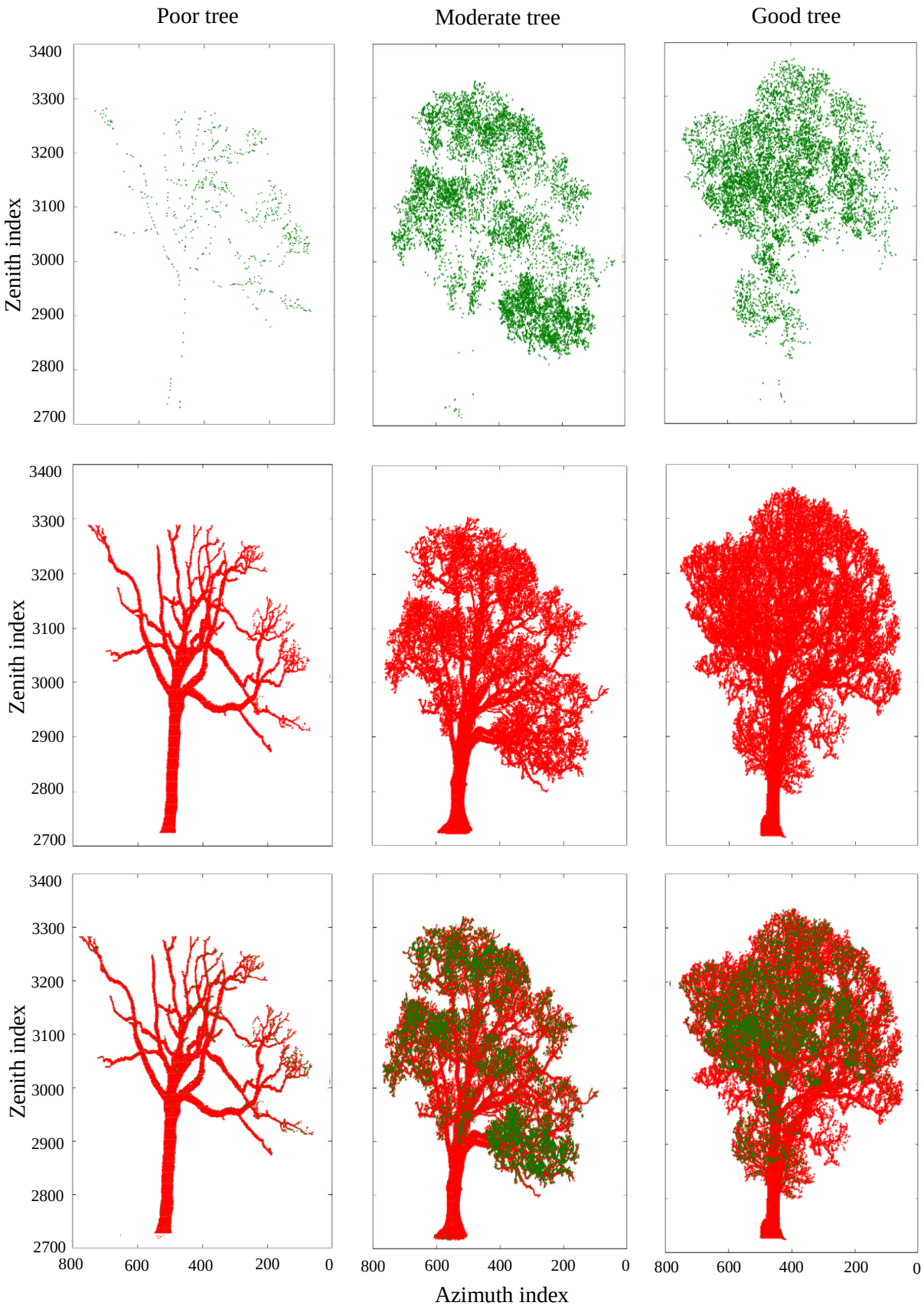

Figure 5.13: Point clouds for the Poor, Moderate, and Good tree leaf-off scans classified into foliage (green) or wood (red) using a 0.1 threshold for AR1063.

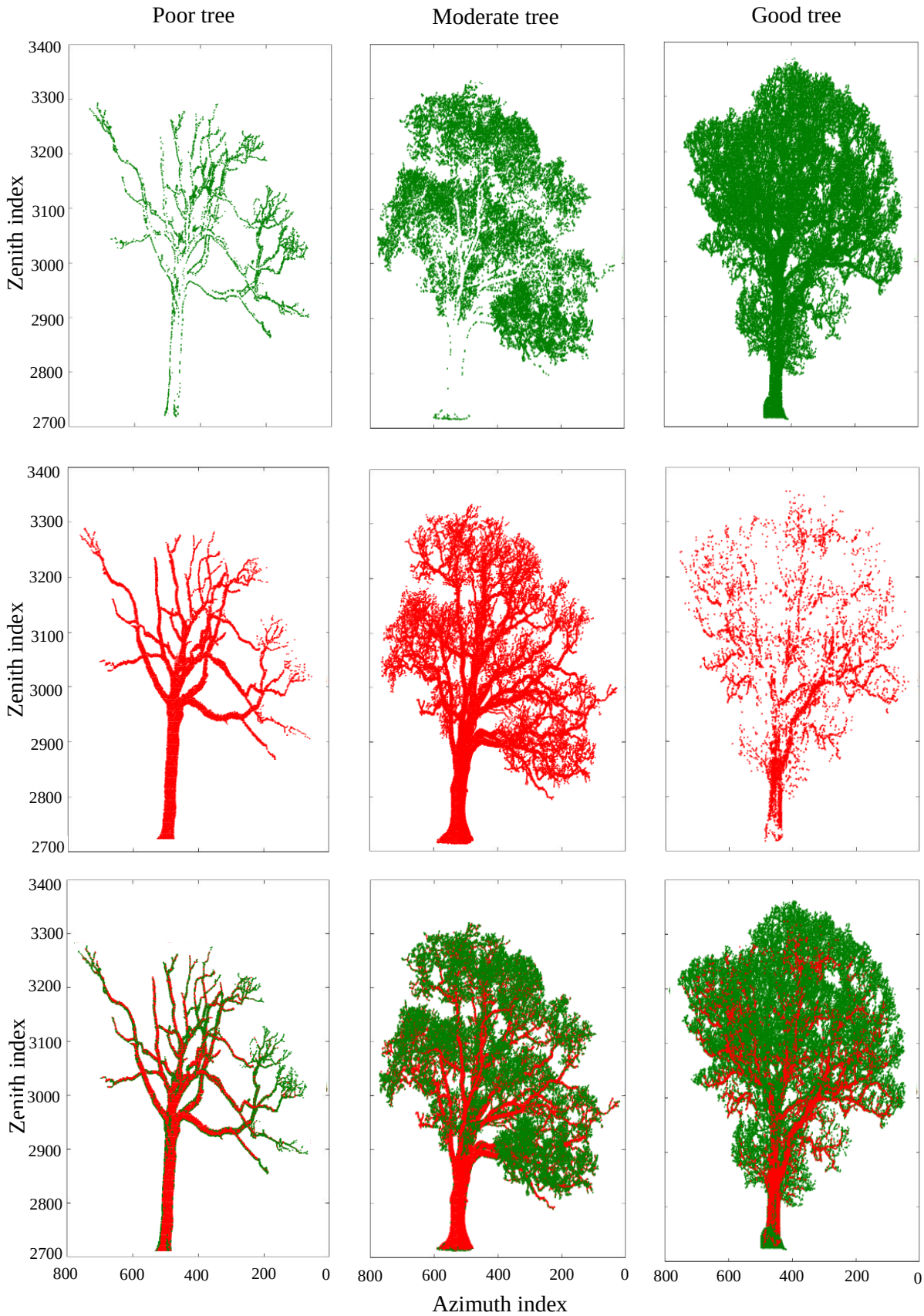

Figure 5.14: Point clouds for the Poor, Moderate, and Good tree leaf-off scans classified into foliage (green) or wood (red) using 0.2 threshold for AR 1545.

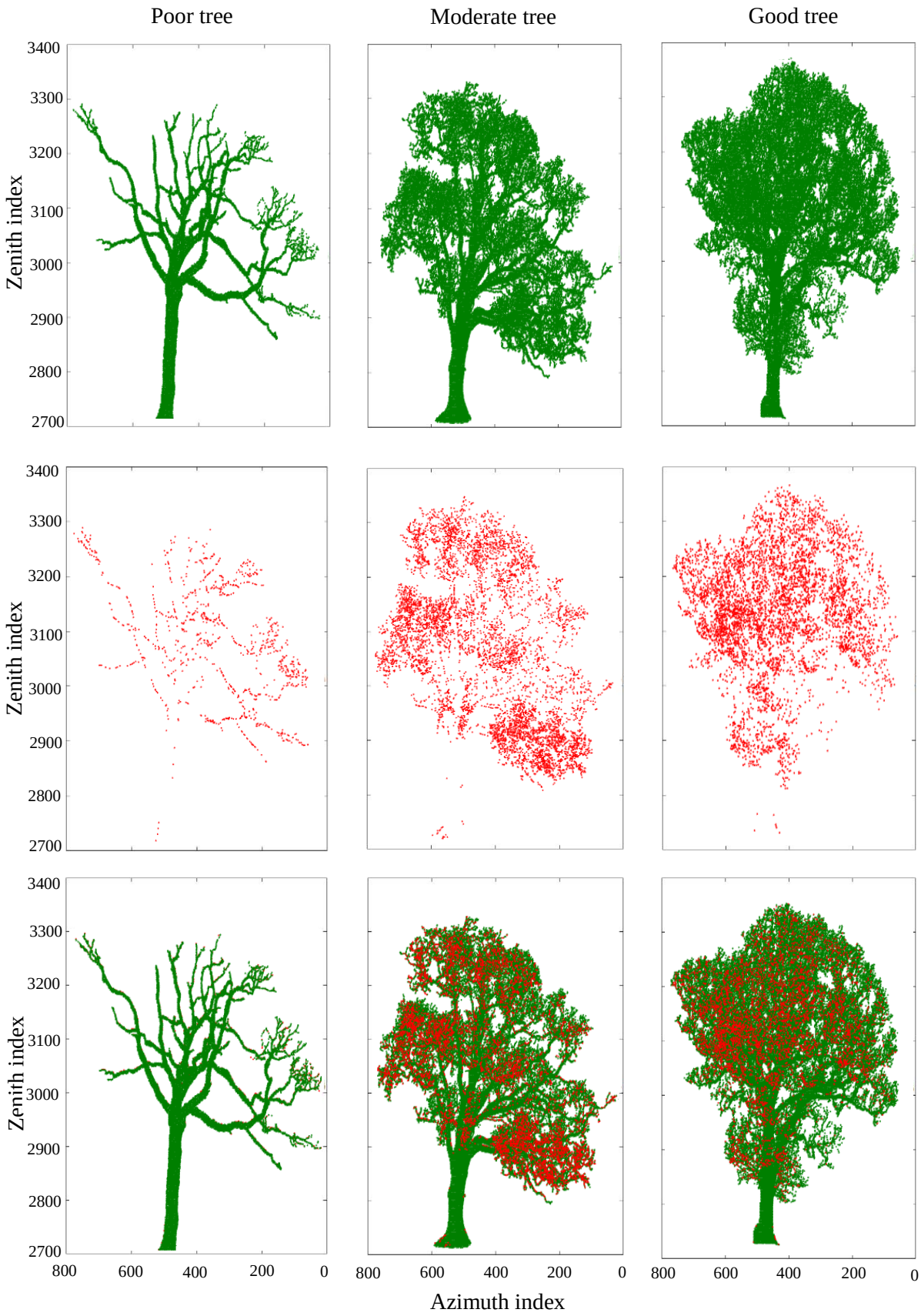

Figure 5.15: Point clouds for the Poor, Moderate, and Good tree leaf-off scans classified into foliage (green) or wood (red) using -0.1 threshold for NDI.

5.5 Spatial analysis for the Poor, Moderate, and Good trees

The NDI of the three oak trees was classified in CANUPO at scales of 0.5 m to classify the points into foliage or wood based on their 3D spatial properties. This section discusses the spatial classification for the tree samples form the south for leaf-on and leaf-off scans.

5.5.1 Leaf-on condition

Figure 5.16 illustrates the results of the CANUPO classification for the Poor, Moderate, and Good trees respectively, where the spatial foliage is highlighted in green and the wood in black. For the Poor tree scan, the classifier incorrectly classified the finer branches as foliage in the tree canopy and shows errors on the main branches and the tree stem. However, most of the tree points are classified correctly as wood. For the Moderate tree, the classifier distinguished the foliage points from the wood accurately, with most of the points in the tree canopy being classified as foliage and finer branches. There are a few groups of misclassified points in the middle and lower parts of the tree stem which belong to the woody class. Despite some errors in the finer branches, the distribution of the black points provides an accurate separation of the woody materials, which means that the chosen scales are accurate for this tree. The spatial classification for the Good tree shows that a large number of woody points are misclassified as foliage in the tree crown, including the main branches and the lower part of the tree stem. In addition, most of the finer branches are highlighted in green, based on their local dimensionality. The only explanation for this is that the points in this part of the scan appear to the spatial classifier as 3D. Due to this, these points in the canopy were classified as foliage which considers an error in the classification.

5.5.2 Leaf-off condition

Figure 5.17 shows the findings of the spatial classification for a leaf-off scan using a scale of 50 cm and the same training output that was used to classify the leaf-on scan. The visualisations show that the classifier has classified large amounts of the points as foliage. There are a large number of errors with regard to the Poor tree canopy and the stem. For the Moderate and Good trees, most of the main branches and the trunk are correctly classified as wood. It seems unlikely that the finer branches will be classified accurately as woody using 50 cm and using smaller scales might then produce errors in the main branch area.

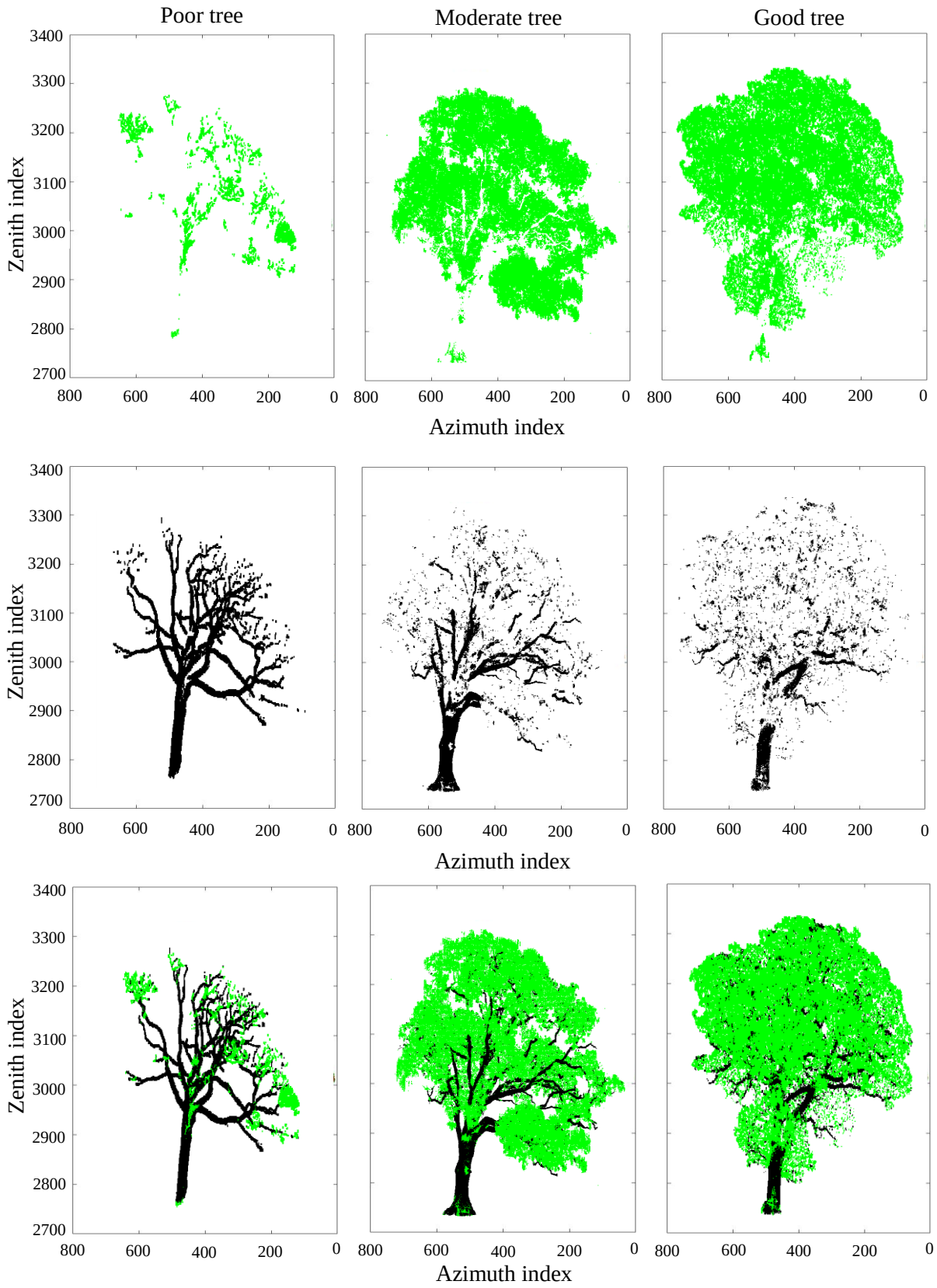

Figure 5.16: CANUPO spatial classification for the Poor, Moderate, and Good trees leaf-on scans classified into spatial foliage (green points) or spatial wood (black points).

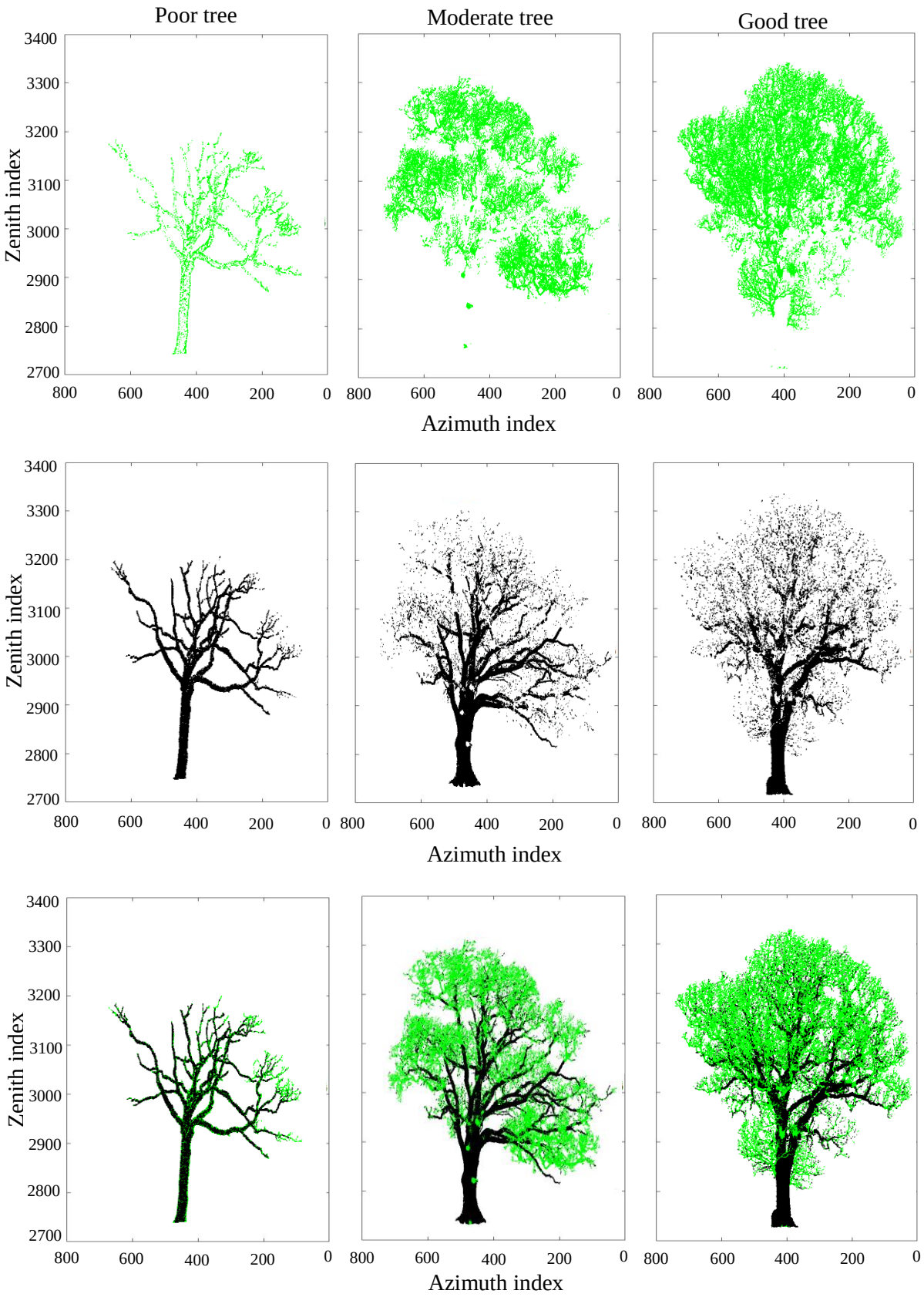

Figure 5.17: CANUPO spatial classification for the Poor, Moderate, and Good trees leaf-off scans classified into spatial foliage (green points/errors) or spatial wood (black points).

In terms of comparison, the Poor, Moderate and Good trees were classified using CANUPO and compared separately from four orientations; the south, north, east and west. Two groups of points are segmented from the south scan to trained the spatial classifier: one from the stem for wood and one from the foliage area of the canopy. The confidence of these points is greater than 80. Therefore, they are used to classify the scan from all directions. A scale of 50 cm was used to train the points for every scan and then the outputs were visualized as foliage (green) and woody (black). The points were then visualized in one figure in order to map the distribution of the spatial classification for every tree. The trees visualised in Figures 5.18, 5.19, and 5.20.

Figure 5.18 shows the CANUPO classification for the Poor tree from four directions. For the tree canopy, the tree classification shows the same amount of foliage on the edges of the branches for all directions. In contrast to the other direction, the north scans show that a large number of the branch returns are allocated to foliage. There is compatibility in terms of the stem spatial classification between the scans from the south, north and east but the scan from the west comprises spatial misclassification errors in most of the stem returns.

The classification of the Moderate tree is visualized in Figure 5.19. Part of the scans from the north and east were missed due to the presence of a small hill between the scanner and the target. Moreover, parts of the main branches were missed during the scanning time. A visualisation of the figure shows that it is possible to distinguish the spatial wood from the foliage from the south, east and west directions, but most of the stem returns from the north are classified incorrectly as foliage.

Figure 5.20 represents the point spatial classification for the Good tree. The figure shows the accurate classification for all of the scans from the north, where most of the stem is classified as foliage. The separation between the branches and the foliage was successful and accurate for all the scans except for that from the north. Overall, CANUPO provided an accurate approach to distinguishing foliage points from wood based on their location within a given scale. The classifier is more effective in separating the foliage compared to the wood, no matter how much foliage there is on the tree, and the Poor tree is a good example. One scan from every tree did not show a successful separation and produced misclassification errors, possibly because the scales are unsuitable for this side of the tree.

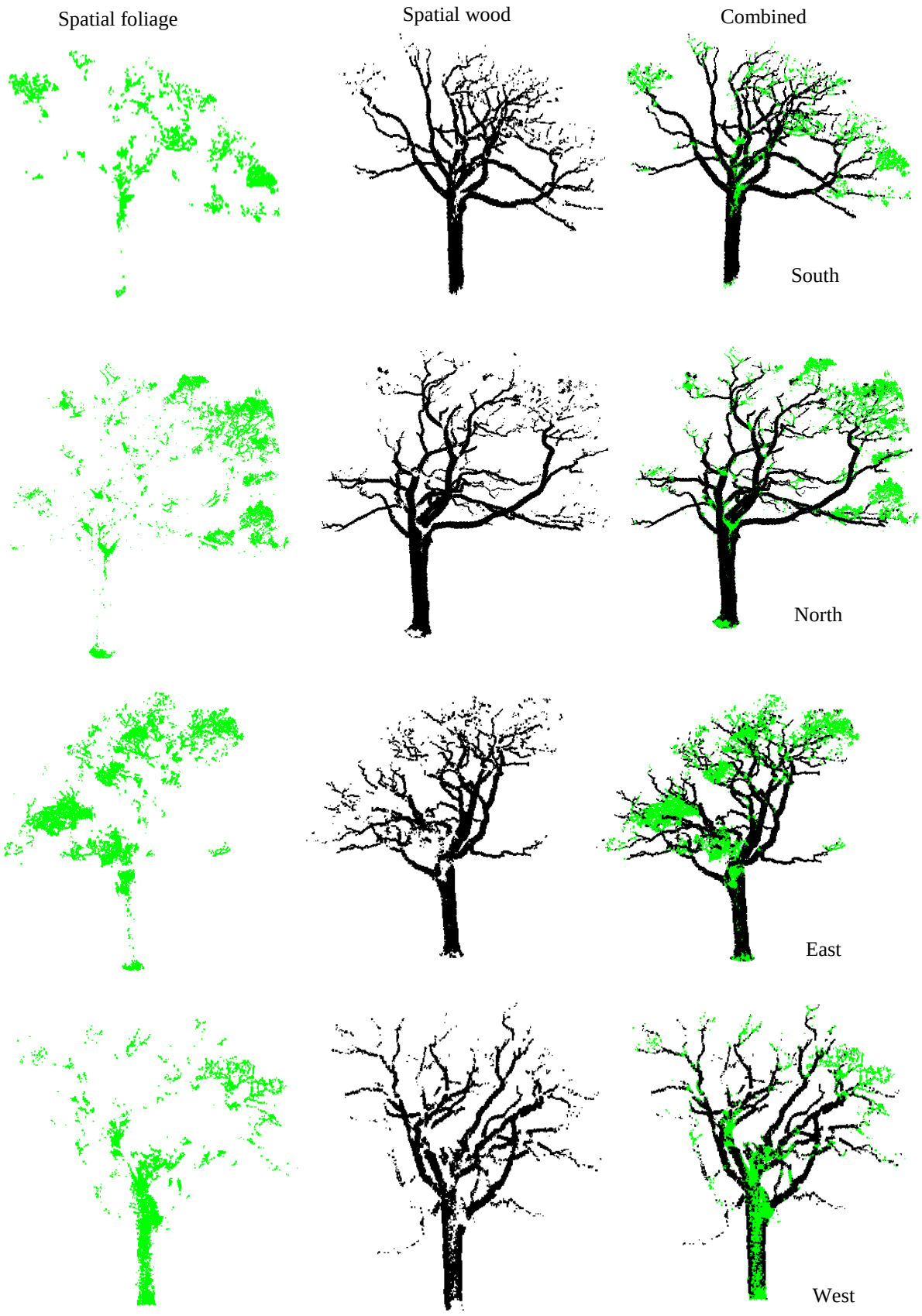

Figure 5.18: CANUPO spatial classification for the Poor tree leaf-on scan from south, north, east, and west. Green point for foliage and black for wood.

Figure 5.19: CANUPO spatial classification for the Moderate tree leaf-on scan from the south, north, east, and west. Green for foliage and black for wood.

Figure 5.20: CANUPO spatial classification for the Good tree leaf-on scan from the south, north, east, and west. Green for foliage and black for wood.

5.6 Comparing the spectral and spatial information the leaf-on scans

The spectral and spatial findings for the Poor, Moderate, and Good trees' leaf-on scans were represented as three matrices in order to compare the classifications for each tree. Each matrix contains spectral and spatial classes to represent the CANUPO classification of the three trees under study.

5.6.1 Poor tree

The classification of the Poor tree from the south was represented in CANUPO by 20690 spatial returns. The highest number of returns in the CANUPO classification was provided by the class (SWCW), with 16228 returns, comprising 78.94% of the total returns. The second highest class was represented by (SWCF), with a total percentage of 12.20%. The spectral foliage and spatial wood (SFCW) provided the lowest number of returns, at 4.22%, but the total agreement between the spectral and spatial classes was 82.28%, as detailed in Table 5.1.

Table 5.1: The agreement and disagreement between the Poor tree classes.

Four classes 20690 returns	CANUPO foliage	CANUPO wood
Spectral foliage	878 (SFCF), agreement of 4.22%	1144 (SFCW), disagreement of 5.50%
Spectral wood	2538 (SWCF), disagreement of 12.20%	16228 (SWCW), agreement of 78.06%
The total percentage of agreement between the spectral and spatial points was 82.28%		

Figure 5.21 shows the visualisation of the four classes for the Poor tree. The tree has a small number of foliage points, which were highlighted in red and represented by class SFCF. The spectral and spatial foliage were distributed across different areas of the tree canopy, as shown in the figure. The class SFCW (black) visualises part of the tree stem and a few foliage points on the tree's canopy. This happened because the class consists of spectral foliage and CANUPO wood. The SWCF class (green) comprises a few foliage points on the edges of the finer branches, while most of the classes consist of the main branches, tree stem, and some finer branches. The SWCW class (blue) dominates the tree's components. In order to map the spectral and spatial classification, all of the classes are visualised into one final figure, which shows that most of the foliage area is highlighted in green and red while the black points are not visible due to their small number.

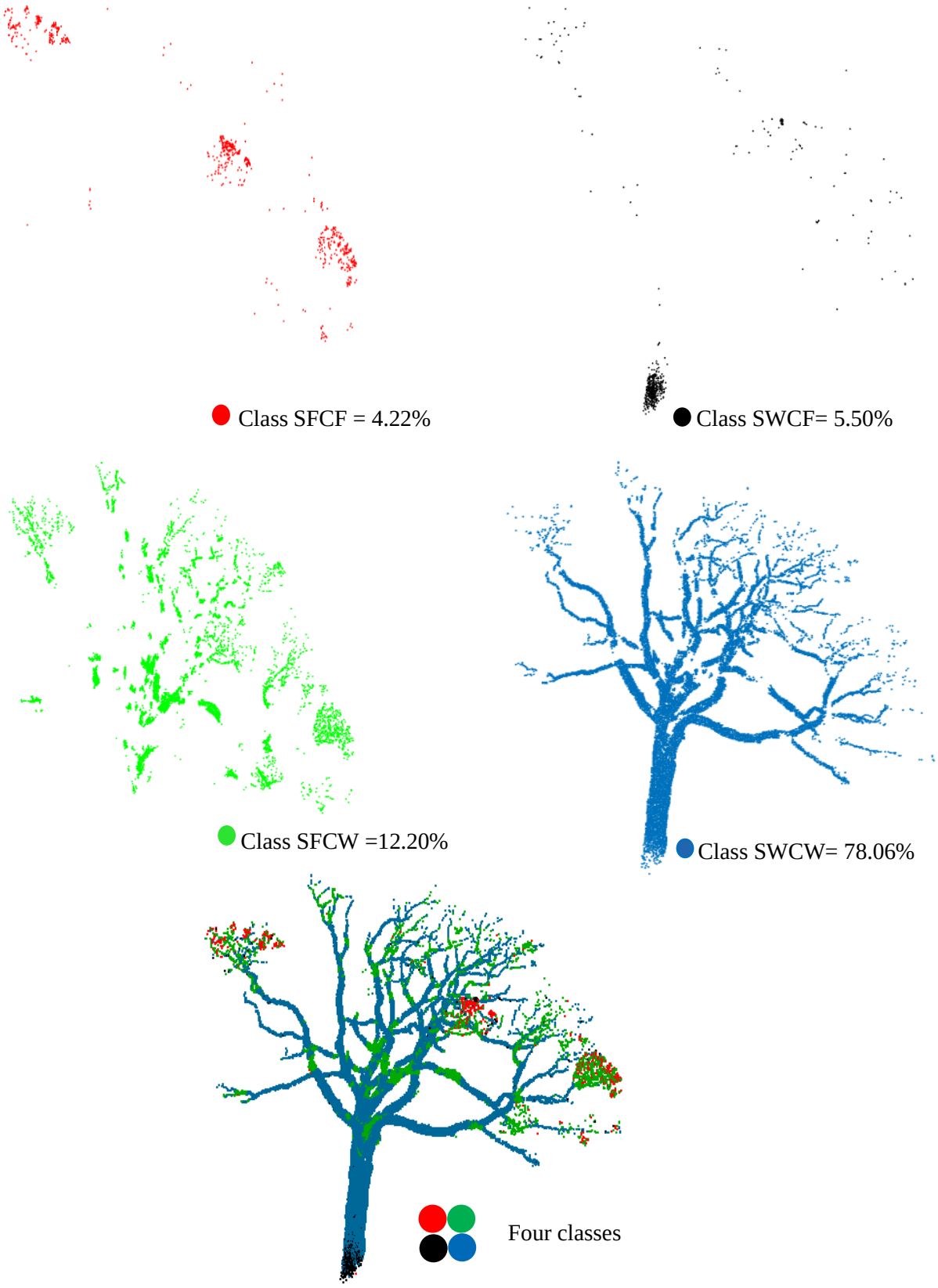

Figure 5.21: The spectral and spatial classes of the Poor tree leaf-on scan. The red points are allocated to class (SFCF), the black points to class (SFCW), the green points to class (SFCW), and the blue points to class (SWCW). The four classes are recombined into one image.

5.6.2 Moderate tree

Table 5.2 presents a summary of the matrix information extracted from the spectral and CANUPO classification for the Moderate tree. The tree sample was represented by 118916 spatial returns. A percentage of 43.63% of these returns comprised the SFCF class and consisted of 51885 returns, which was the highest number of returns compared to the other classes. The smallest number of spatial returns was the SWCF class, with a total number of 4926 returns, that comprises 4.14% of the classes. The results of the classification showed that there was a total agreement between the spectral and spatial classification of 60.35%. In addition, 40.09% of the points were considered as a disagreement, as detailed in the table.

Table 5.2: The agreement and disagreement between the Moderate tree classes.

Four classes 118916 returns	CANUPO foliage	CANUPO wood
Spectral foliage	51885 (SFCF), agreement of 43.63%	42755 (SFCW), disagreement of 35.95%
Spectral wood	4926 (SWCF), disagreement of 4.14%	19349 (SWCW), agreement of 16.72%
The total percentage of agreement between the spectral and spatial points was 60.35%		

Figure 5.22 illustrates the four classes of the spectral and spatial classification for the Moderate tree. The figure confirms that class SFCF (red) was found across most of the tree's canopy, as expected due to the presence of foliage, although a few parts of the tree's stem were coloured as foliage. Class SWCF (black) was concentrated on the tree stem and spread to cover random parts of the tree canopy. A large amount of the tree's canopy was coloured by class SFCW, with a few patches at the tree's stem. Most of the tree's wood components were attributed to class SWCW (blue).

To map the distribution of each spatial class, the figure highlights that the foliage area on the tree canopy is dominated by red and green. For the main branches, there was an overlap between the green and blue in some areas. This indicates that spatial differences in the classification occurred in these areas within the applied scales. The tree trunk showed a distribution of all colours with different quantities with a greater concentration of the blue.

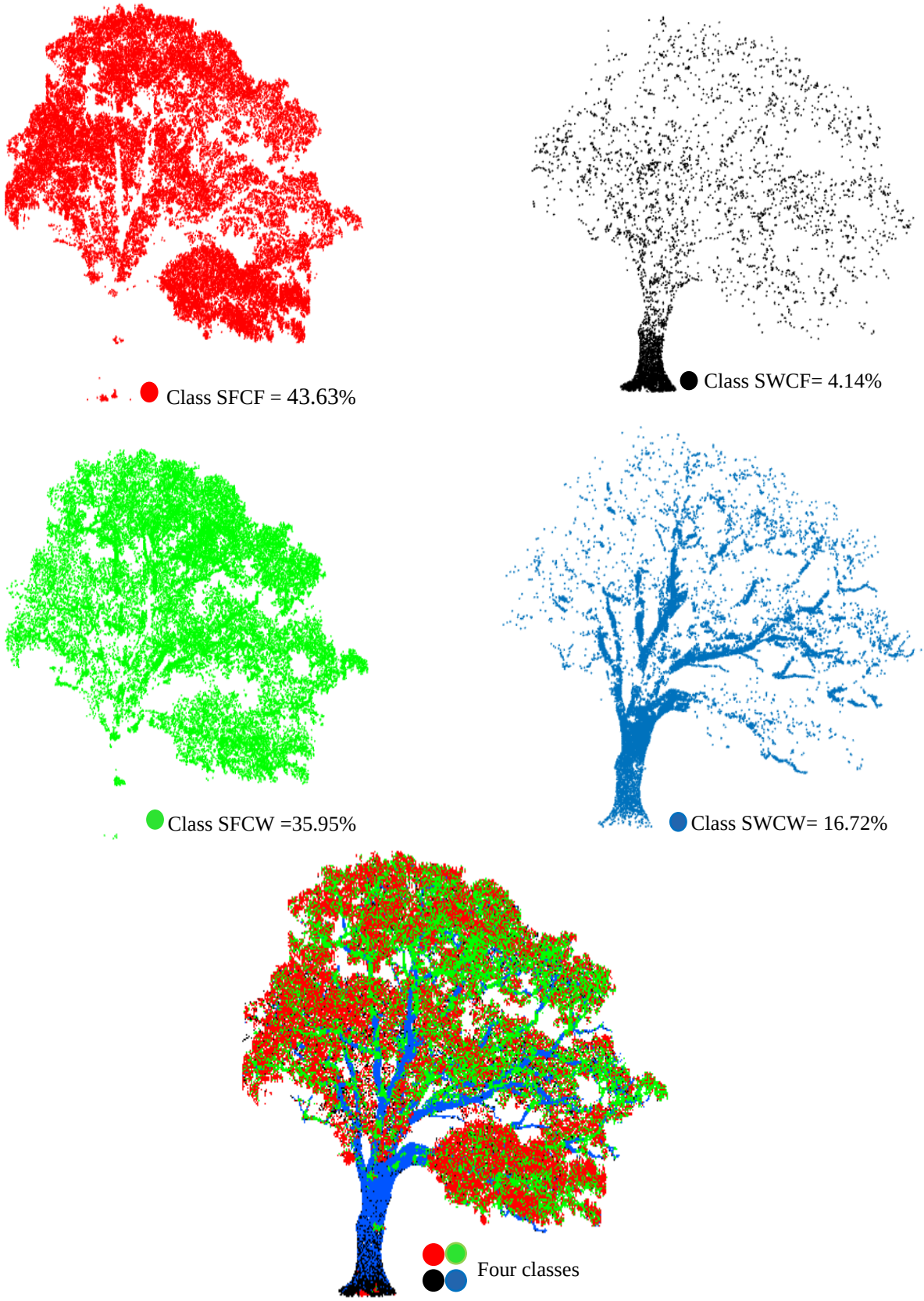

Figure 5.22: The spectral and spatial classes of the Moderate tree's leaf-on scan. The red points are allocated to class (SFCF), the black points to class (SFCW), the green points to class (SFCW), and the blue points to class (SWCW). The four classes are recombined into one image.

5.6.3 Good tree

According to Table 5.3, the Good tree's sample recorded 90766 returns in the CANUPO classifications. The spectral and spatial classifications of the Good tree suggest that class SFCF comprised 79.96% of the total points in CANUPO, which means that there was a high level of agreement between the spectral and spatial foliage. Class SFCW represented 3233 returns, which comprised 3.56% of the spectral and CANUPO classification. Class SWCF showed 16.01% with 14533 returns. The classifications also showed that the agreement between the spectral and spatial wood class was 0.46%, but the total agreement for this scan was 80.42%, and the disagreement was 19.57%.

Table 5.3: The agreement and disagreement between the Good tree classes.

Four classes 90759 returns	CANUPO foliage	CANUPO wood
Spectral foliage	72571 (SFCF), agreement of 79.96%	3233 (SFCW), disagreement of 3.56%
Spectral wood	14533 (SWCF), disagreement of 16.01%	422 (SWCW), agreement of 0.46%
The total percentage of agreement between the spectral and spatial points was 80.42 %		

The spatial points of the Good tree's sample, shown in Table 5.3, were visualised in Figure 5.23, where every class was given colour, as mentioned before. The figure showed that the class SFCF (red) dominated the other classes and covered the whole the area of the tree's canopy, with a few patches at the tree's stem. Class SWCF (black) represented on most of the stem and a large number of the main and finer branches, but there were spaces between the branches that were probably classified as foliage by the classifier. All of the returns of class SFCW (green) were concentrated on the tree's canopy, where a few random points were highlighted in blue or class SWCW. Overall, in contrast to the classification of the Poor tree, the Moderate and Good trees showed more foliage points than wood. The spectral and spatial information showed compatibility in most of the classes, as they were compared, but some leaf classes were presented as wood classes in the final merging of the output.

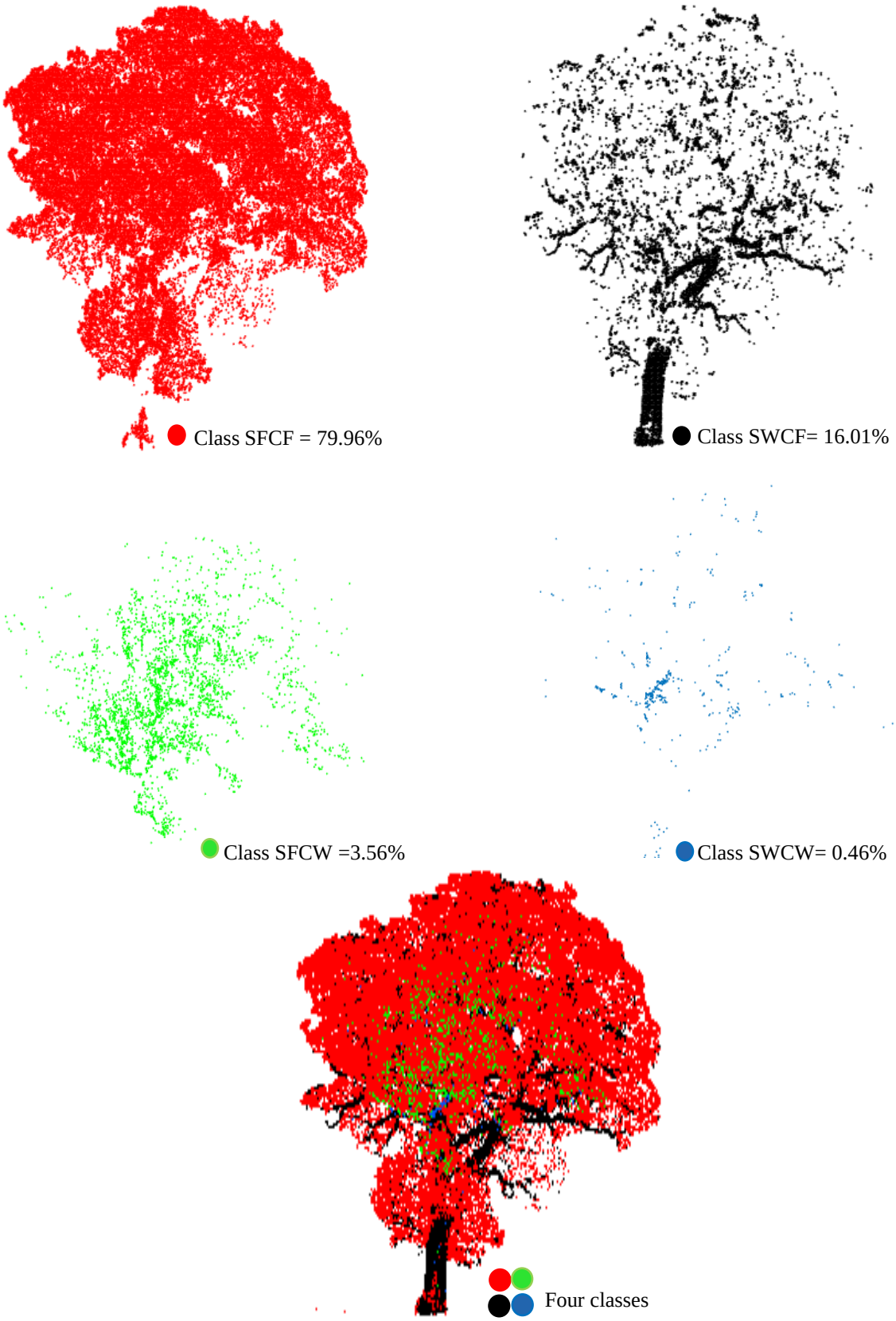

Figure 5.23: The spectral and spatial classes of the Good tree's leaf-on scan. The red points are allocated to class (SFCF), the black points to class (SFCW), the green points to class (SFCW), and the blue points to class (SWCW). The four classes are recombined into one image.

5.6.4 CANUPO confidence

As mentioned in Chapter 4, CANUPO provides confidence values that allow us to determine how certain the classification is. In order to separate the CANUPO outputs based on the confidence percentage, the data on the Poor, Moderate, and Good trees were separated into foliage or wood, based on the NDI thresholds (-0.1), where the foliage class was greater than -0.1 and the wood class was less than or equal to -0.1. This does not provide any information regarding how accurate the separation was, as the foliage class contains some wood returns and vice versa, but the confidence percentage was used here to determine the efficiency of the classifier's performance based on the chosen scales. To investigate the spatial classification of the three trees, the CANUPO confidence percentage was detailed in Table 5.4 to show how certain the classifier was for all classifications. In general, the classifier was sure about the classification of the spatial foliage and wood for most of the classes, with a confidence level of > 80%. Small values of the classification were classified with a confidence level of ≤ 80%. More details are provided in the table.

Table 5.4: Confidence regarding the spatial foliage and wood information for the Poor, Moderate and Good trees.

Tree name	CANUPO performance	Tree spatial class	
	confidence > 80%	spatial foliage	spatial wood
Poor		90.08%	73.70%
Moderate		96.29%	89.89%
Good		94.34%	88.35%
Tree name	uncertain ≤ 80%	spatial foliage	spatial wood
Poor		9.91%	26.29%
Moderate		3.70%	10.09%
Good		5.65%	11.64%

Figure 5.24 visualises the confidence percentage for the Poor tree's leaf-on scan, where the red points indicate a confidence value greater than 80% and the blue points one less than or equal to 80%. For the foliage points, the classifier was certain of 90.08% of the total points. These points were spread randomly across the Poor tree's canopy and part of the tree stem, and 9.91% of the foliage points were classified with a confidence value of ≤ 80%. For the foliage class of this tree, 73.70% of the total points were classified with a high confidence value, while only 26.29% were represented as main and finer branches, with a small amount of foliage with a confidence level of ≤ 80%. The foliage and wood points were combined on the left of the figure to map the tree points based on the confidence values.

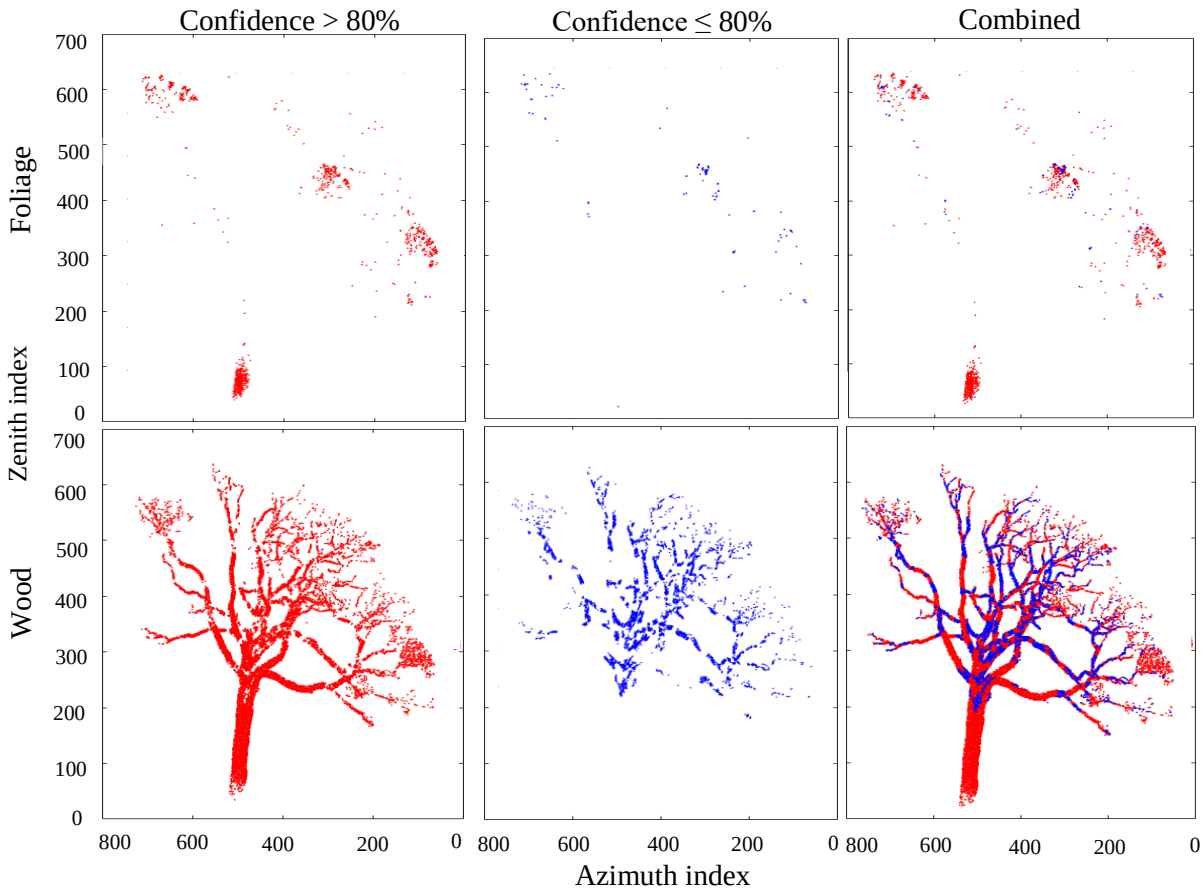

Figure 5.24: CANUPO confidence percentage for spatial foliage and wood extracted from the Poor tree points. Red indicates a confidence level of >80% and blue ≤80%.

Figure 5.25 illustrates the final percentage of CANUPO confidence for the foliage and wood points from the Moderate tree. CANUPO was certain of 96.29% of the total points of the foliage, most of which were represented on the tree canopy and the tree stem while 3.70% of the points are classified with low confidence. As mentioned earlier, the confidence values do not provide any information about how certain the classification is. In addition, the classifier was certain regarding 89.89% of the wood points and only 10.09% of these were classified with a confidence level of ≤ 80%.

Figure 5.26 shows that the spatial classifier was certain for 94.34% and uncertain for 5.65% of the total foliage points from the Good tree. For the spatial wood classification, the classifier was certain and confident for 88.35% and uncertain for 11.64%, where these points are found in the tree canopy and the stem. Overall, the classifier was more certain for the foliage class than the wood. Most of the points that showed a confidence level of ≤ 80% was found in the tree canopy for the Poor and Moderate trees.

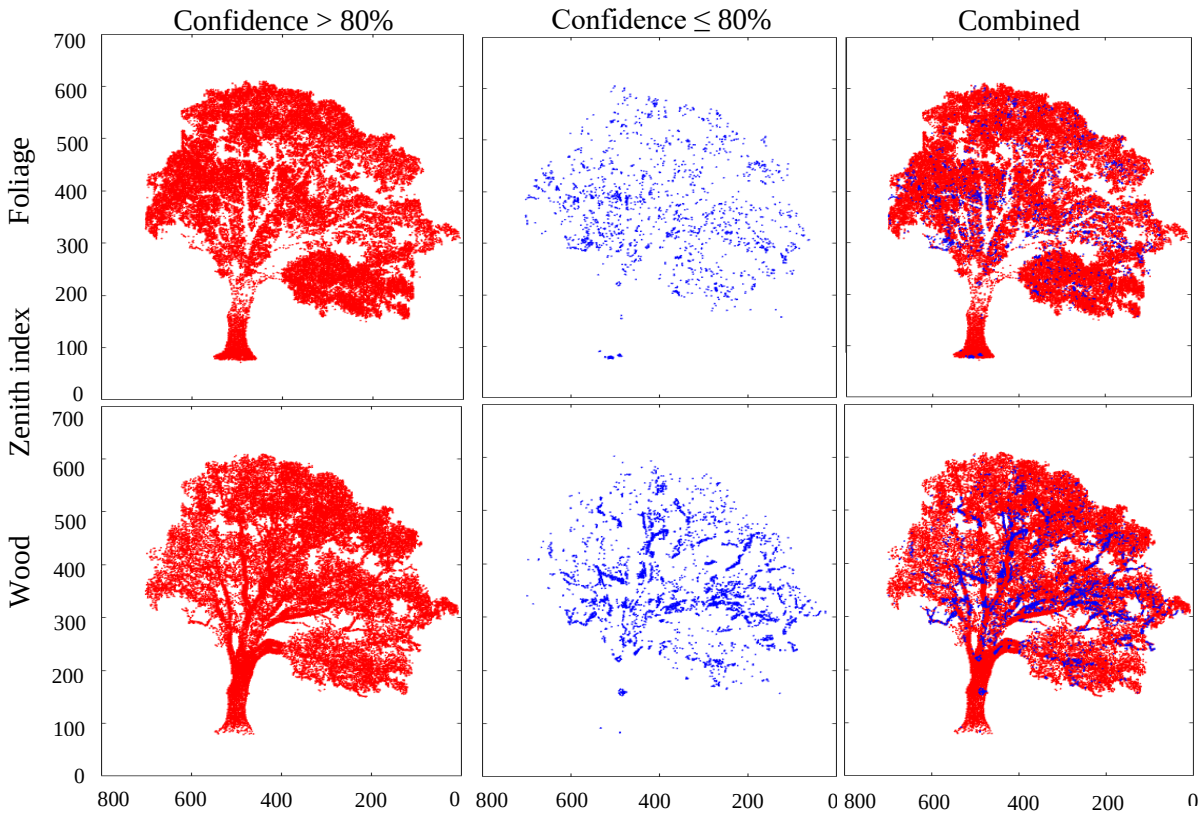

Figure 5.25: CANUPO confidence percentage for spatial foliage and wood extracted from the Moderate tree points. Red indicates a confidence level of >80 % and blue ≤80%.

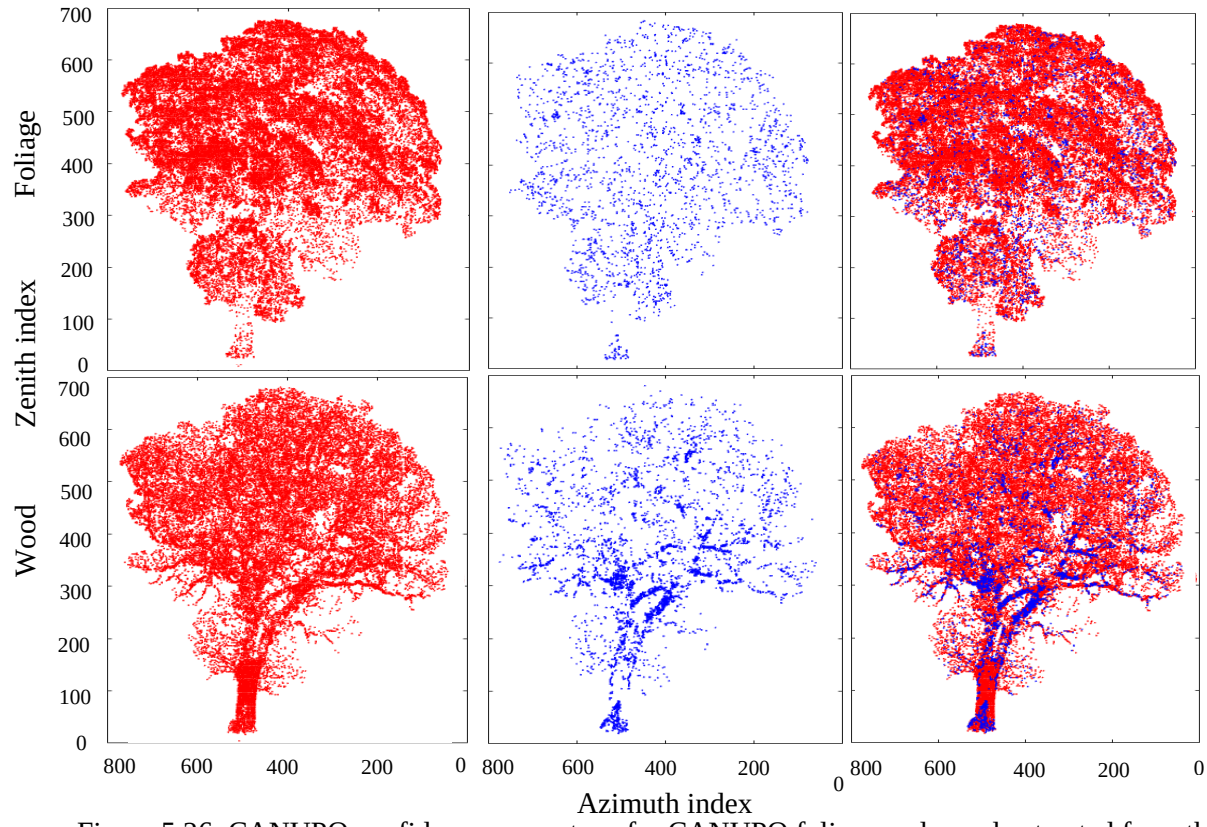

Figure 5.26: CANUPO confidence percentage for CANUPO foliage and wood extracted from the Good tree points. Red for confidence > 80% and blue for ≤ 80%.

5.6.5 Foliage and wood separation using number of returns

The number of returns for both laser wavelengths was explored to detect the single and multiple returns for foliage and wood for the three trees. This may provide more information related to foliage and wood separation. In general, Table 5.5 showed that most of the trees' returns or > 90% of the SALCA returns were produced by single returns for both laser wavelengths, as shown in the table.

Table 5.5: Percentage of the single and multiple returns for the Poor, Moderate and Good trees.

Tree name	Description			
	1063 nm		1545 nm	
	Single return	Multiple return	Single return	Multiple return
Poor tree	99.73%	0.26%	99.38%	0.61%
Moderate tree	98.76%	1.23%	97.36%	2.63%
Good tree	99.70%	0.29%	98.84%	1.15%

Figure 5.27 a-c shows the output of the separation based on the number of returns for the Poor, Moderate, and Good tree point clouds. Green indicates the single returns and red the multiple ones. For the Poor tree, 99.73% and 99.38% of all of the returns were produced by single returns for both laser wavelengths respectively. These points comprised foliage and wood returns (green), while less than 1% of the returns (red) were produced by multiple returns for both laser wavelengths. These multiple returns can be seen clearly in a very few parts of the tree stem, the foliage and the branches for the 1063 nm data and in more abundance in the areas from the 1545 nm data, as shown in Figure 5.27a. Figure 5.27b visualises the final output of the Moderate tree's components based on the number of returns. Most of the multiple returns were found in the tree canopy for both the 1063 nm and 1545 nm data. The same was found for the Good tree, where few returns were produced by multiple returns while most of the tree was produced by single returns. Compared to the Poor tree, most of the multiple returns for the Moderate and Good trees are found in the trees canopies, where the foliage was abundant. In addition, the number of multiple returns produced by the 1545nm was slightly larger than that produced by the 1063 nm data.

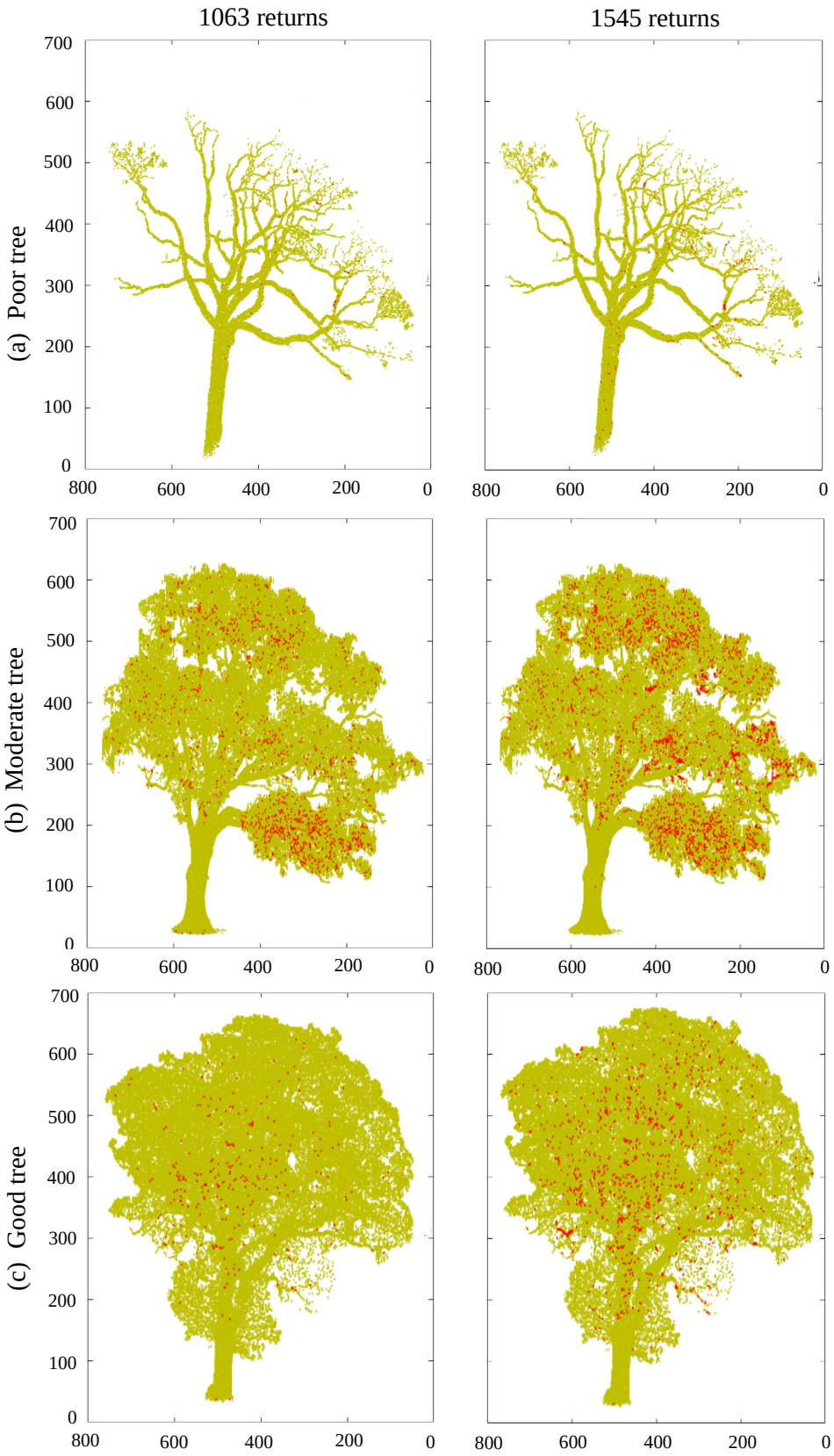

Figure 5.27: SALCA point clouds for the Poor, Moderate, and Good trees coloured by number of returns. Green refers to single returns and red to multiple

5.7 Conclusion

This chapter was designed to satisfy objective 2 of this study in order to classify single tree components in an open field environment. A series of investigations were undertaken using SALCA data. The outputs of these investigations support the hypothesis that SALCA has the potential to provide information related to tree component classification. A spectral approach was used to separate the tree components using a visual threshold on the 1063 nm, 1545 nm and NDI. A spatial approach was generated by mapping the tree points based on the geometric distribution of each point. The two approaches were applied to both conditions. In order to understand the approaches in more detail they were compared. This allowed investigating of the compatibility of both approaches.

The result of the leaf-on scan suggested that applying a threshold to AR1063 nm did not generate clear separation for all trees components due to the similar response of the 1063 nm to both foliage and wood. The classification of the AR 1545 nm data showed it was possible to distinguish the foliage from the wood points for all trees. It was expected that the NDI could produce clear separation for the components of the trees especially in terms of partial hits. However, the separation based on a -0.1 threshold was unclear and large numbers of the stem points were incorrectly classified as foliage. In terms of validation, the thresholds discussed above were applied for the leaf-off scan for the AR 1063 nm and 1545 nm, and NDI. The results showed many misclassification errors for all parameters used. The spatial analysis of the datasets provides more effective approaches related to foliage and wood separation, especially for the Moderate and Good trees for the leaf-on scan.

Misclassification errors were detected by using CANUPO for the leaf-off scan. However, the spectral and spatial information showed a total agreement of 82.28%, 60.35%, and 80.42 % for the Poor, Moderate, and Good tree respectively. The spatial classifier 80% confidence values for the classification included 90.08%, 96.29%, and 94.34% of the foliage returns and 73.70%, 89.89%, and 88.35% of the wood returns for the Poor, Moderate, and Good tree respectively. The results of this chapter indicate that the spatial classification showed more detail for the foliage points compared with the spectral classification, while the spectral classification showed more details of the wood for the leaf-on condition. In the following chapter, the spectral and spatial approaches will be discussed at the level of the full stand plot.

CHAPTER 6: POINT CLOUD CLASSIFICATION ON FULL STAND MEASUREMENTS

Summary

This chapter aims to investigate spectral and spatial approaches to foliage and wood separation using SALCA data of a full forest stand in a field environment at Alice Holt Forest, Hampshire, UK. A series of spectral and spatial analyses were performed for leaf-on and leaf-off conditions in order to distinguish the foliage points from the wood. A range of techniques was used to assess the accuracy of the classification approaches. As expected, the spectral classification for the 1545 and NDI data was more effective than the separation using the 1063 data. Most of the spatial classification had a confidence of more than 80% for the foliage and wood. The final agreement between the spectral and spatial classifiers was 55.63%, with confidence value of 95% for the foliage and 91% for the wood.

6.1 Introduction

This chapter describes the spectral and spatial classification that were performed in order to address Objective 3 of this research. The datasets were used in this chapter in order to assess the approch of the spatial and spectral classifications at the level of a full stand forest. The SALCA instrument was used to acquire leaf-on and leaf-off conditions from Alice Holt Forest, Hampshire, UK. The datasets then were processed as detailed in Section 3.4 in order to extract intensity, apparent reflectance and normalised difference index in order to use them for foliage and wood classification.

The same series of spectral and spatial classifications detailed in chapters 3 and 4 were applied to classify the TLS point clouds at the level of a full forest stand. In order to validate the classifications, the same thresholds were applied for leaf-on and leaf-off conditions for the AR of both laser wavelengths and NDI in terms of spectral classification. For the spatial classification, CANUPO classifications were performed for both scans using the same scales and CANUPO confidence for the foliage and wood was calculated. The findings of both classifications were then represented as a matrix to test the comparability of the classifications.

6.2 Field site and data description

The study location is located in the Royal Forest of Alice Holt in Hampshire (Figure 6.1). The forest is situated about 6 km south of Farnham, Surrey, UK. The Forestry Commission has owned and managed the forest since 1924, and a research station was built there in 1946. The forest is known for its timber products and recreational activities. Oak trees dominate the Alice Holt Forest, but it is planted with different species of deciduous and coniferous trees.

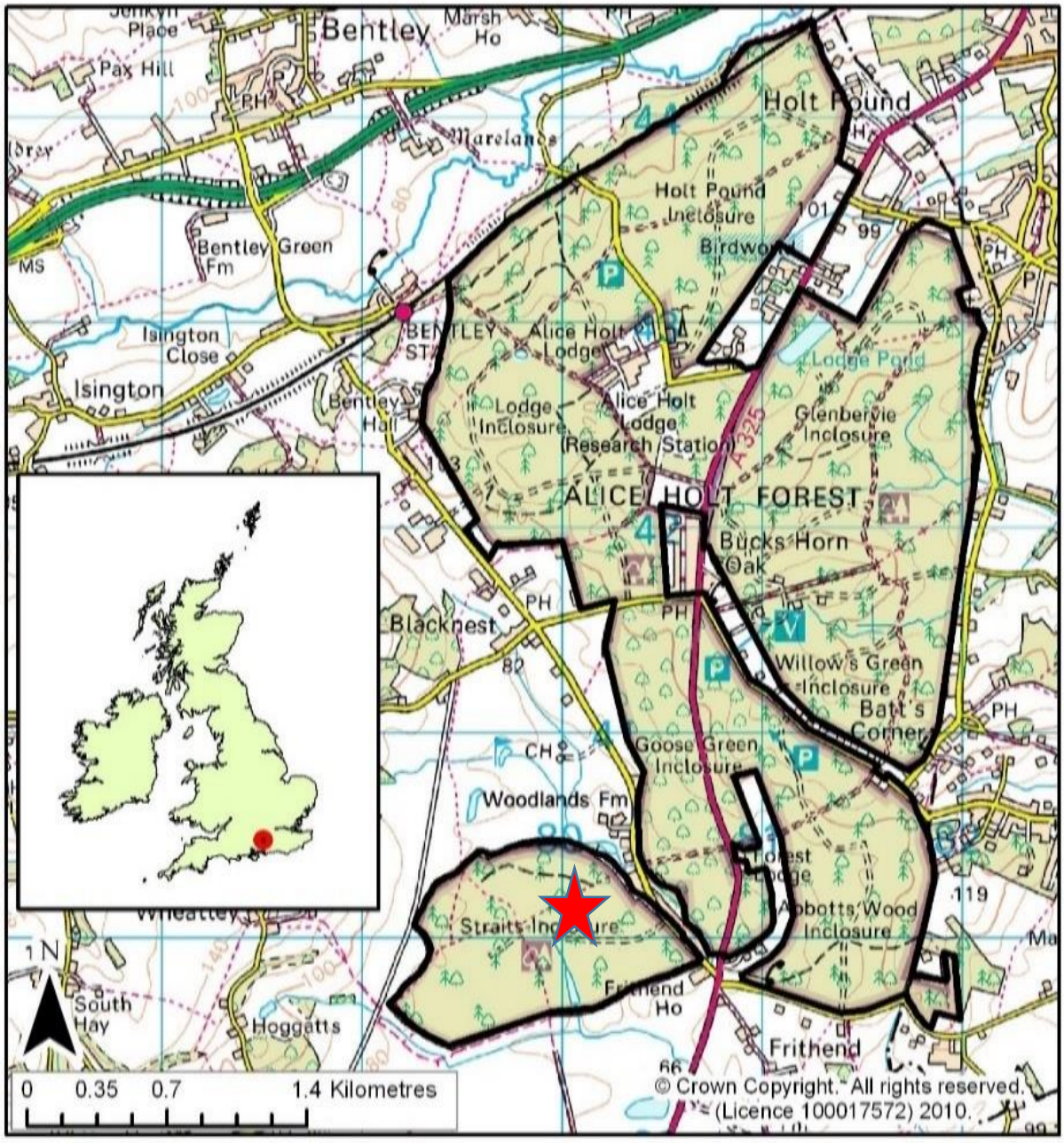

Figure 6.1: Alice Holt Forest, England. The red star refers to the plot location within the Straits Enclosure. Source: (ECN Data Centre. 2018)

The SALCA instrument was used in order to acquire point clouds for leaf-off and leaf-on conditions in March and July 2014 respectively. High-resolution scans were acquired for each condition following the SALCA protocol as described in Section 3.3. In terms of calibration, one panel was divided into six equal sub-panels with different reflectance. The sub-panels were scanned six times at multiple ranges by moving them around the scanner as the scan progressed. The data collection for the sub-panels was done during the acquisition of the leaf-off scan only since the leaf-on scan calibration was performed previously. A full description for the leaf-on and leaf-off scans is provided in Table 6.1.

Table 6.1: Description of SALCA datasets acquired at Alice Holt Forest for both conditions

No	File name	Start/End time in hours	Range in meters	Start azimuth index	Stop azimuth index	Zenith angle range 0-190°
Date 26th March 2014			Leaf-off scan + the sub-panels			
1	c_full_2_3150	10:56 - 12:49	60	0	3500	190°
Date 3rd July 2014			Leaf-on scan			
2	ah_oak_jul14_3351	9.41 - 11.36	60	0	3500	190°

6.3 Point-cloud description

This section highlights and visualises the extracted data including the intensity, AR, and NDI for Alice Holt Forest for the leaf-on and leaf-off conditions. The SALCA points from this scan were visualised using azimuth and zenith indices.

6.3.1 SALCA range

Figure 6.2 visualises the point-clouds of 1545 nm data by range for (a) the leaf-on and (b) leaf-off scans, respectively. The data were visualised using azimuth and zenith indices to represent data up to a 60 m range. The blue on the scales refers to the close-range measurements, green to data within 30 m, and red to the most distant targets. For the leaf-on scan, most of the separated clear trees are located within a range of less than 15m, except for the tree at the 980-azimuth step, which is 3 m from the scanner. A few trees were coloured red (>50m) due to their far range (Figure 6.2a). The same was found for the trees in Figure 6.2b. However, here, more trees at long distances appear due to the absence of the foliage in the leaf-off scan. The figure shows how many times the sub-panels were scanned, as they appear at six sites during the scan.

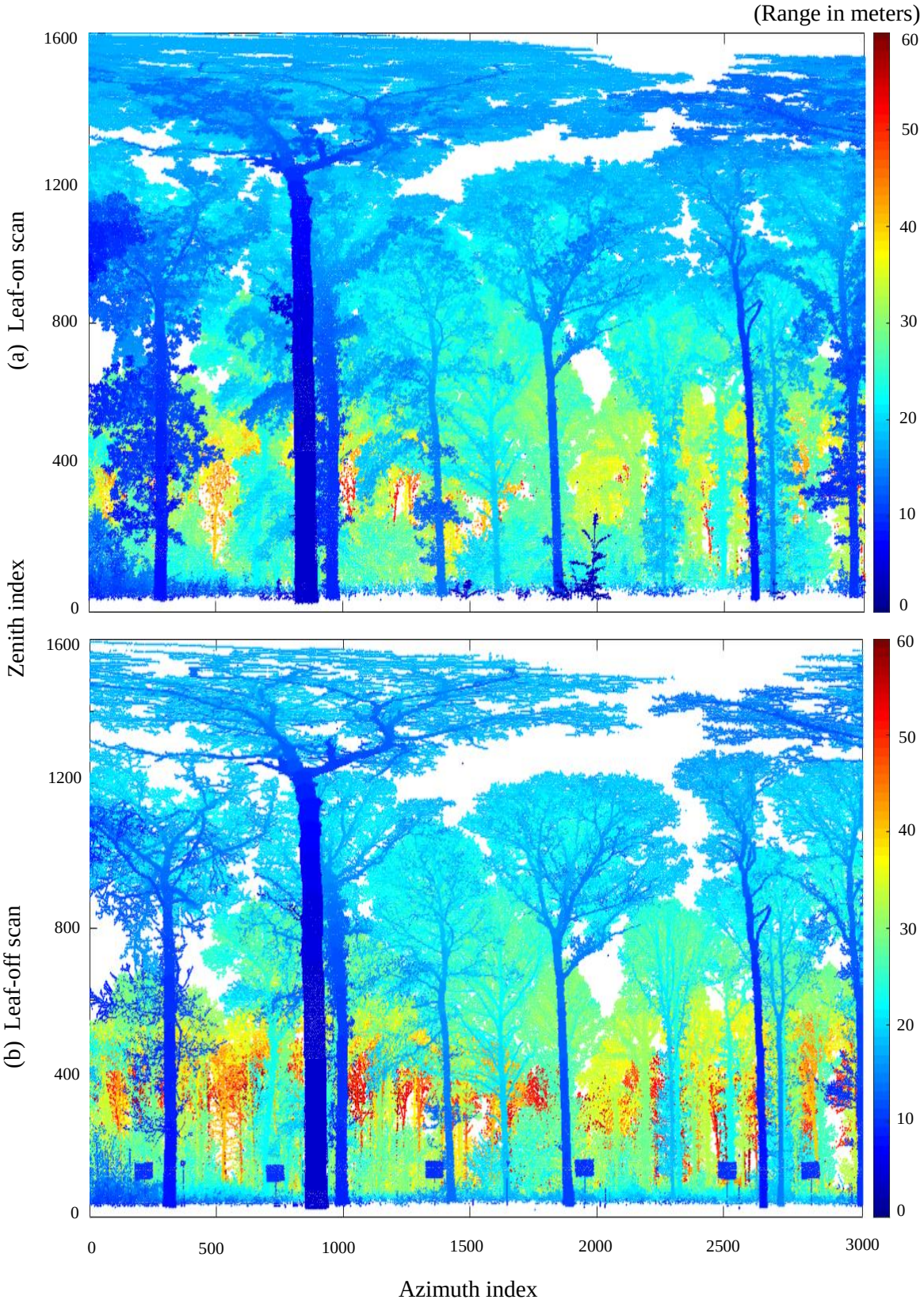

Figure 6.2: 1545 nm data for a full stand forest from Alice Holt Forest leaf-on and leaf-off scans coloured by range data.

6.3.2 Leaf-on scan

Figure 6.3 shows the visualisations of intensity, AR and NDI for the 1063 nm and 1545 nm data. For the intensity, the 1063 data show an intensity range of 0 to 350. Most of the trees show intensity values of less than 100 (blue) and values of 200 or more (yellow) are found on some parts of four trees only. In addition, the highest values (> 250) are visualised on the stem of the closest tree to the scanner and some parts of the canopies and the understorey vegetation. The 1545 data show the same range of 0 to 500. However, high values of > 250 to 500 are seen in a few trees, which are close to the scanner. A few parts of the scan are coloured with values less than 200 and greater than 100. The majority of the trees are coloured with values less than 100. For the AR 1063 data, the scan shows a normal range of reflectance (between 0-1). Values of more than 0.6 (orange-red) are found at the targets located close to the scanner, including the stem and canopies. The rest of the scan is coloured with values of less than 0.5. The same is found for the 1545 data, where the largest values (>0.6) are visualised mostly in the stems and main branches. The NDI is visualised to show a normal range of -1 to 1. It is clear from the picture that the foliage points, canopies, and the lower part were represented by >0.2 values (yellow-red). Some parts of the stems are coloured with values between 0.2 to 0.4 and this might cause errors in the classification of these areas of the scan.

6.3.3 Leaf-off scan

Figure 6.4 visualises the extracted data from the leaf-off scan. The scale colour in the figure shows that the 1545 nm data shows intensity values higher than those for the 1063 nm. The high values of both laser wavelengths are represented in the stems and part of the panels. The calibration did not work perfectly for the 1063 data, as is clear from the negative and positive values, which lie outside the normal range. Trees at a range greater than 15 m are coloured with values >1, while one close tree showed a value of < zero. In contrast, the calibration worked for the 1545 data, where most of the high values are located in parts of the stems, the main branches and parts of the panels. More high values are distributed in the trees located far from the scanner than in those close to it. The NDI visualisation shows that most of the points are coloured by values of -0.5 to 1(green-yellow-orange), including the stems, the canopy and the panels. The values outside the range (negative values of blue and dark red) are found in the closest tree stem to the scanner as randomly distributed points.

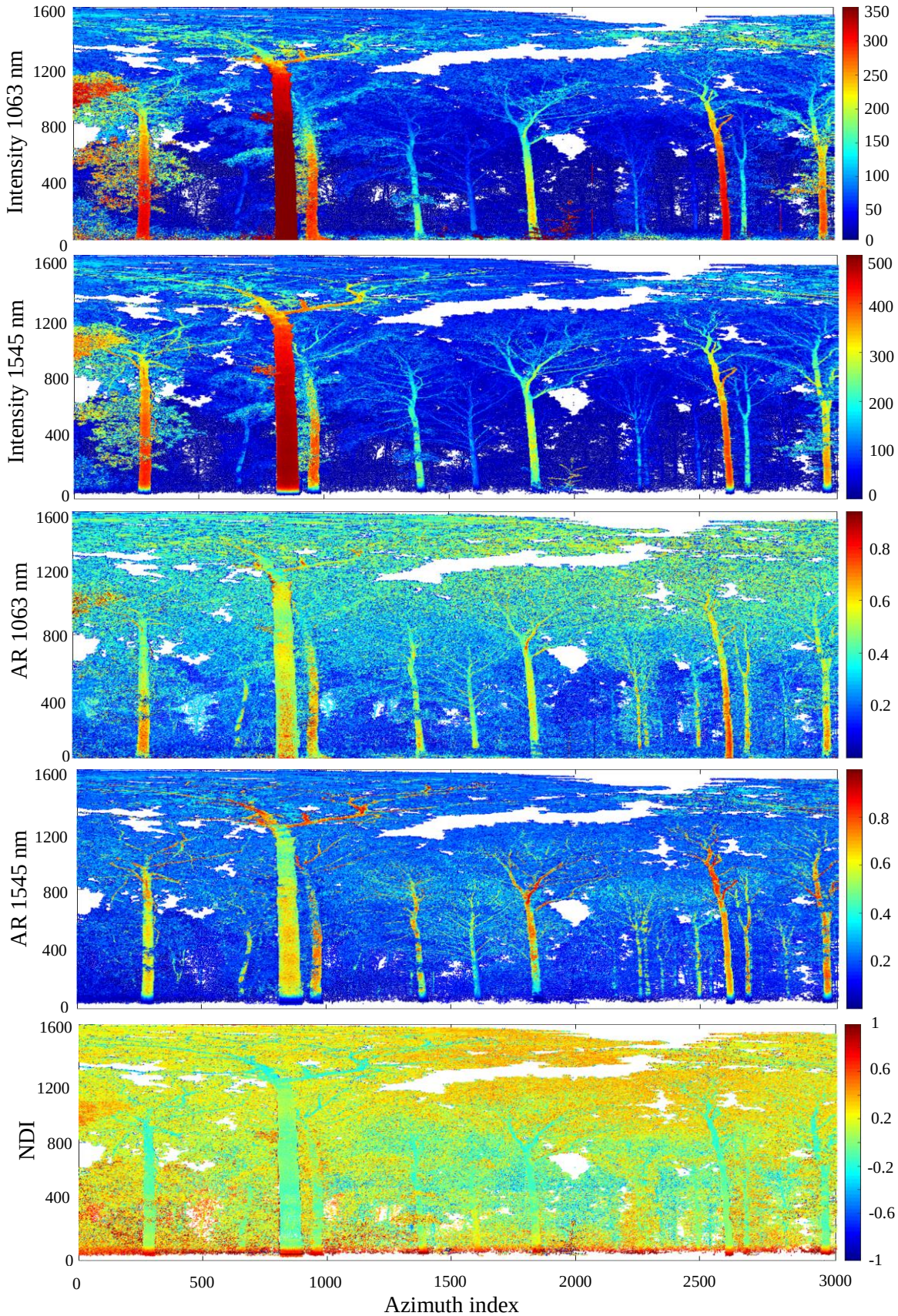

Figure 6.3: SALCA point clouds for a full stand plot from Alice Holt Forest leaf-on scan coloured by intensity, apparent reflectance for 1063 nm, 1545 nm data, and NDI respectively.

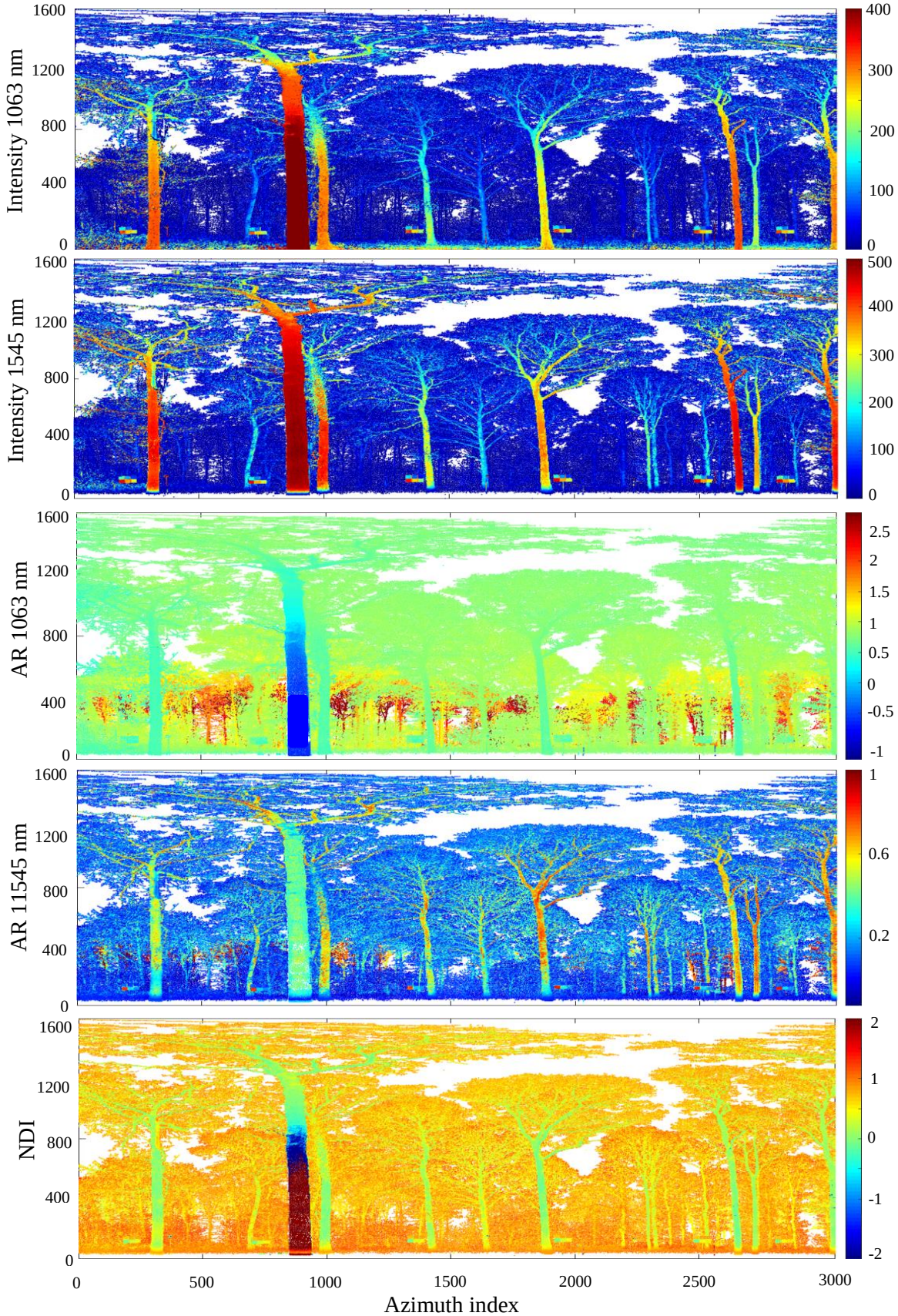

Figure 6.4: SALCA point clouds for a full stand plot from Alice Holt Forest leaf-off scan coloured by intensity, apparent reflectance for 1063 nm, 1545 nm data, and NDI respectively.

6.4 Spectral analysis of leaf-on scan

A spectral classification approach was adopted by using different thresholds on spectral information extracted from the full stand leaf-on data. Zenith and Azimuth indices were used to visualise all of the figures. The foliage points are shown in green and the wood points in red.

6.4.1 Thresholding 1063 nm apparent reflectance leaf-on scan

Figure 6.5 visualises the spectral classification produced by using a 0.2 threshold on the 1063 nm data for the leaf-on scan from Alice Holt Forest (≤0.2 = foliage, >0.2=wood). Based on the visual assessment, it is possible to distinguish the wood from the foliage points for the close stems, finer and main branches. The wood visualisation shows a successful separation at the level of the stems of the trees. However, it was not expected to obtain accurate separation at the level of the canopies, as the wood points are mixed with foliage points. The targets located far from SALCA are misclassified as foliage at a ranges greater than 15 m from the scanner, shown in the bottom of the figure.

6.4.2 Thresholding 1545 nm apparent reflectance leaf-on scan

Figure 6.6 shows the separation using a threshold of 0.3 applied at 1545 nm to classify the full stand forest components. In general, the separation was more successful for the trees that were close to the scanner; it is easy to distinguish the trees stems and most of the main branches in the canopies and even the finer branches. It is more difficult to distinguish the foliage from the wood at ranges of more than 15 meters due to the effect of the range on the spectral classifier. The understorey returns are classified as foliage and large numbers of the wood points at ranges greater than 15 meters from the scanner are misclassified as foliage.

6.4.3 Thresholding NDI leaf-on scan

Figure 6.7 displays the classification when using a 0.2 threshold at NDI. In general, the separation was successful with more errors in the foliage points in the canopies that were misclassified as wood. It seems that increasing range has a negative effect on the separation at ranges greater than 17 meters from the scanner, where the majority of the points are allocated to green.

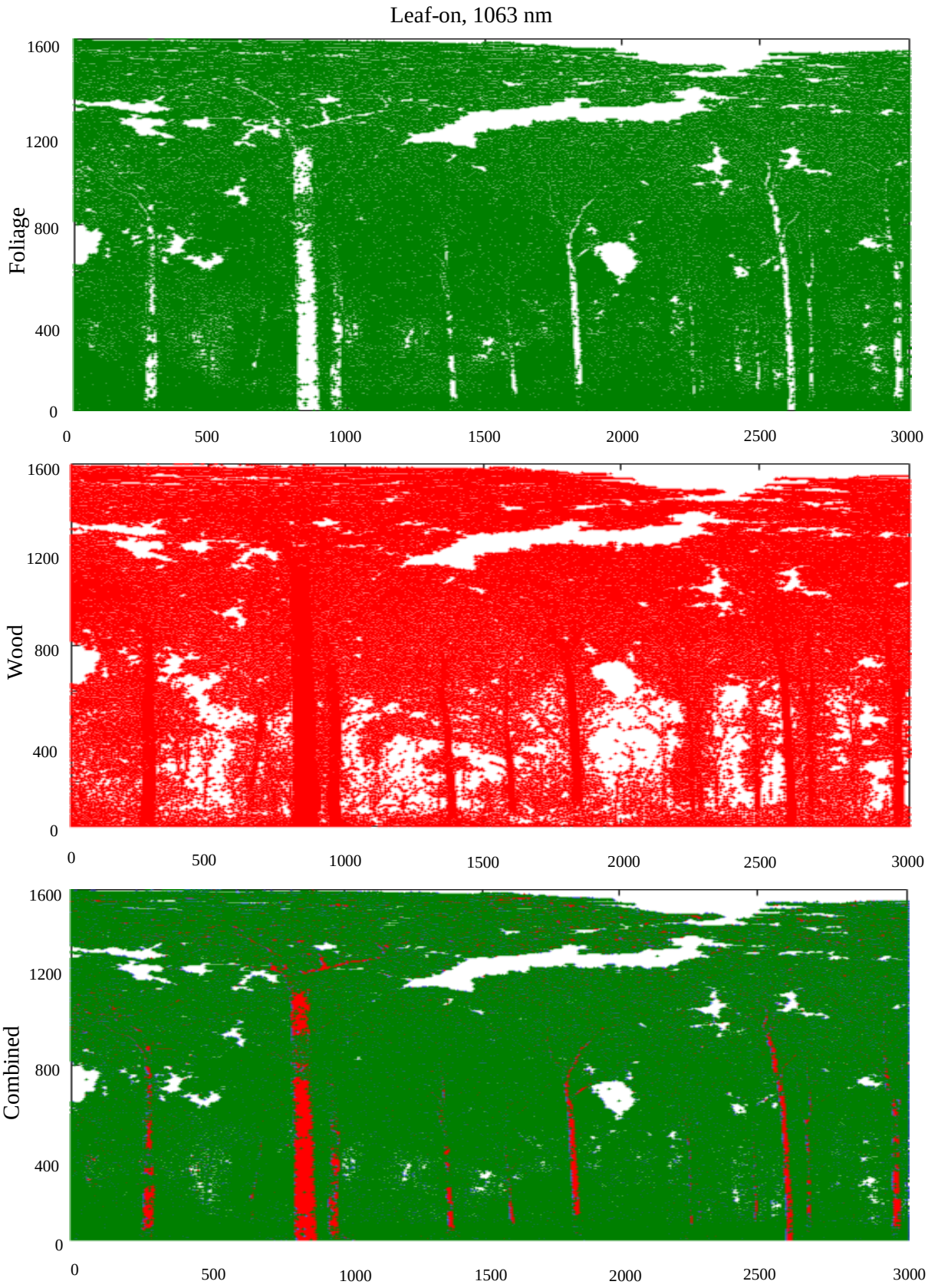

Figure 6.5: SALCA apparent reflectance for a full stand forest from Alice Holt Forest leaf-on condition classified into foliage (green) or wood (red) using 0.2 threshold for the 1063 nm.

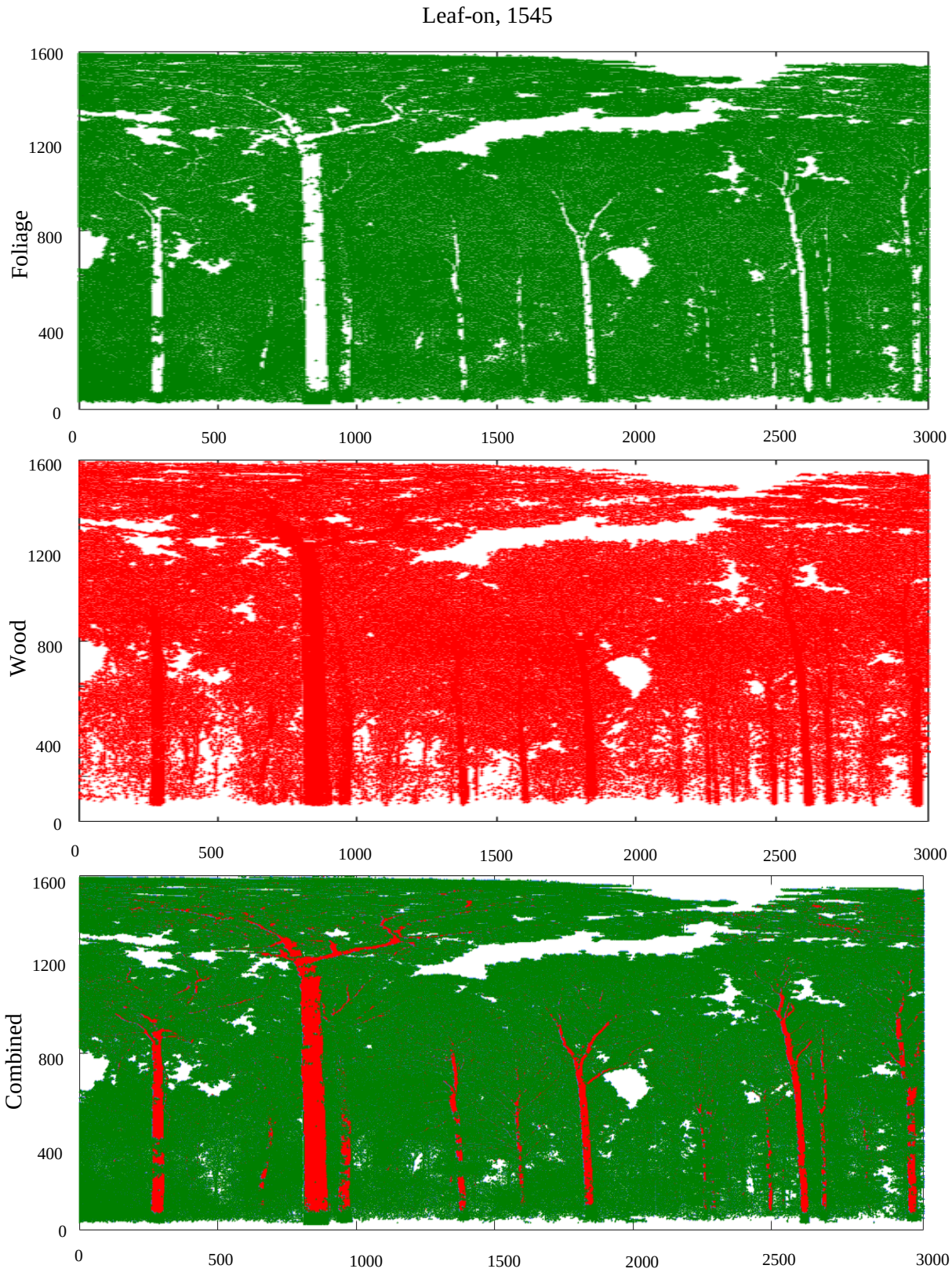

Figure 6.6: SALCA points for a full stand forest from Alice Holt Forest leaf-on condition classified into foliage (green) or wood (red) using 0.3 threshold for the 1545 nm.

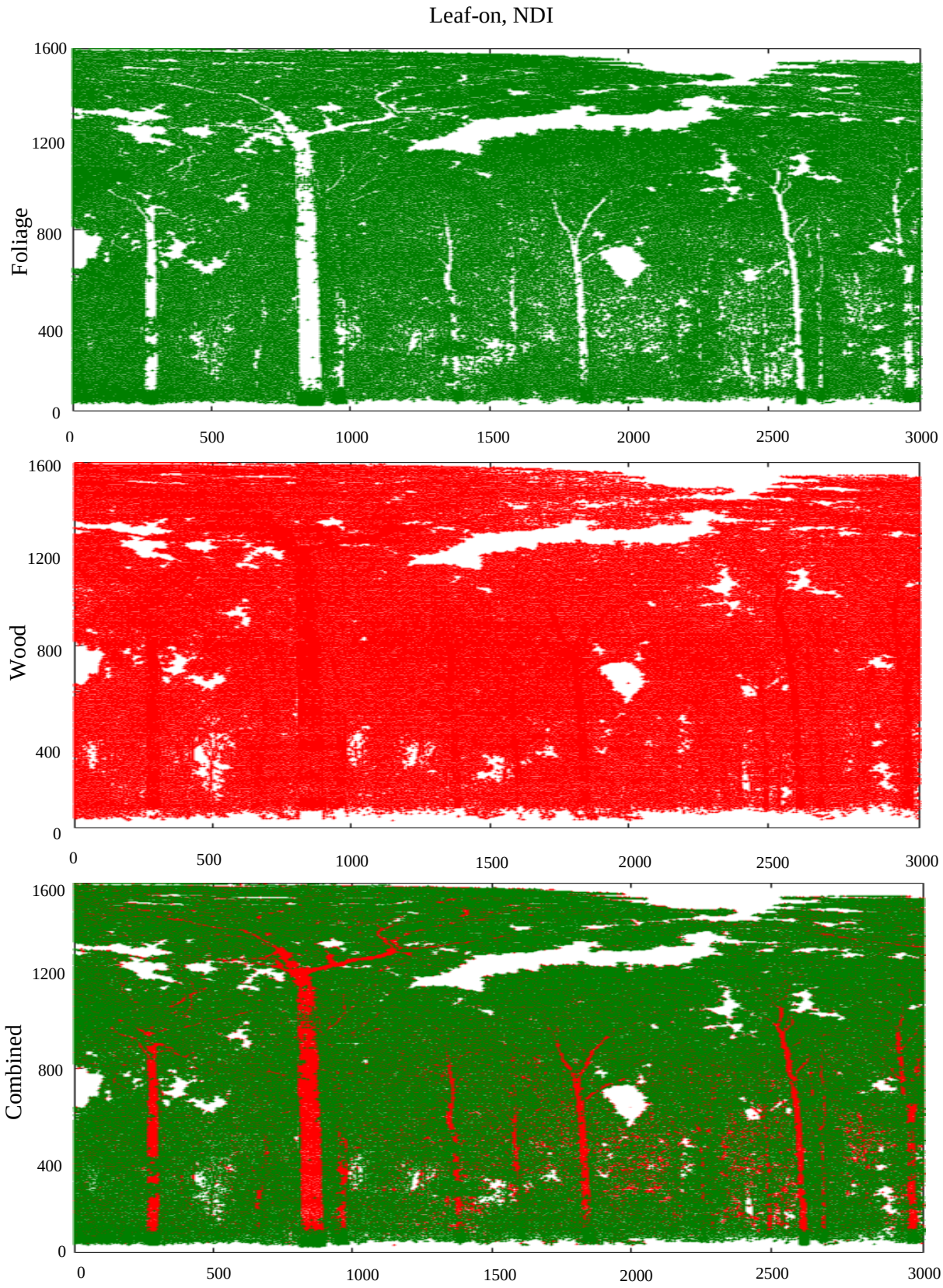

Figure 6.7: SALCA points for a full stand forest from Alice Holt Forest leaf-on condition classified into foliage (green) or wood (red) using 0.2 threshold for the NDI.

6.5 Spectral analysis of leaf-off scan

This section visualises the output for the leaf-off condition extracted from Alice Holt datasets. The same thresholds used for the leaf-on scan were applied for the leaf-off scan. The datasets are visualised using zenith and Azimuth indices. The errors points are allocated to green while validated points as wood to red.

6.5.1 Thresholding 1063 nm leaf-off scan

Figure 6.8 presents the findings of the leaf-off classification for the full stand datasets using 0.2 thresholds at the AR 1063 nm. Based on the threshold, 99% of the total returns of this scan were classified correctly as wood, including the panels, while only 1% of the scan points were not validated as foliage materials. This small percentage comprises most of the stem of the closest tree to the scanner.

6.5.2 Thresholding 1545 nm leaf-off scan

Figure 6.9 visualises the classification of the foliage or wood points using 0.3 apparent reflectance threshold on the 1545 nm. A total of 30% of the points only were validated as wood including most of the stems, part of the branches and parts of the panels, while 70% were misclassified as foliage. The misclassification occurred mostly in the canopy and the understorey level.

6.5.3 Thresholding NDI leaf-off scan

Figure 6.10 shows the classification using a 02 threshold at NDI for the leaf-off scan. The final separation shows that 86% of the total leaf-off points were incorrectly classified as foliage (green) while only 14% were validated as wood. Most of the errors were produced by the stems returns at far ranges from the scanner. The stems within a 10 m range were mostly validated as wood. It is clear that part of the stem of the closest tree to the scan (mostly at a range of less than 5 m) was misclassified as foliage. Overall, the threshold that was applied for the 1063 apparent reflectance was the most effective threshold compared to the 1545 and NDI data.

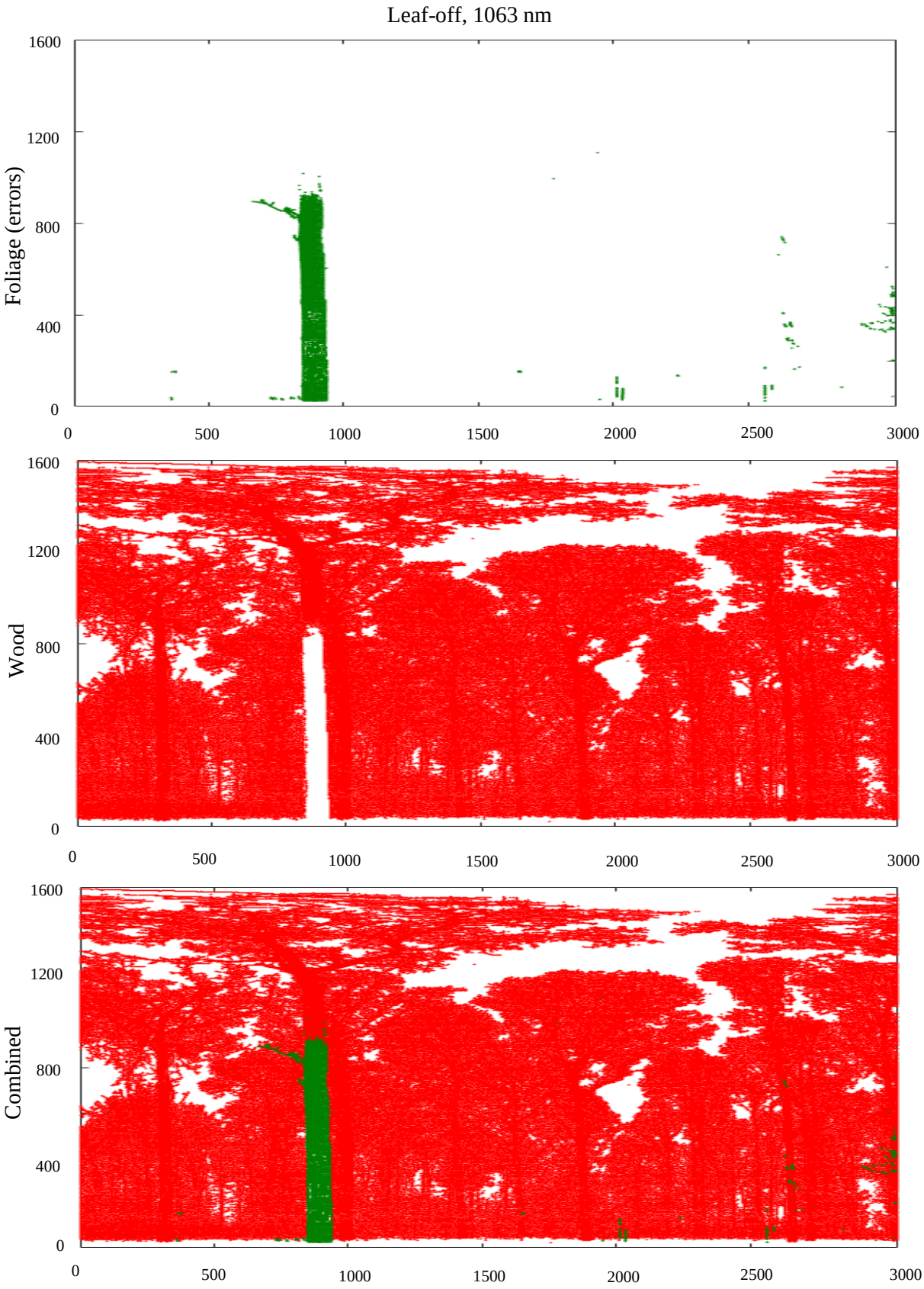

Figure 6.8: SALCA apparent reflectance for a full stand forest from Alice Holt Forest leaf-off condition classified into foliage (green) or wood (red) using 0.2 threshold on 1063 nm

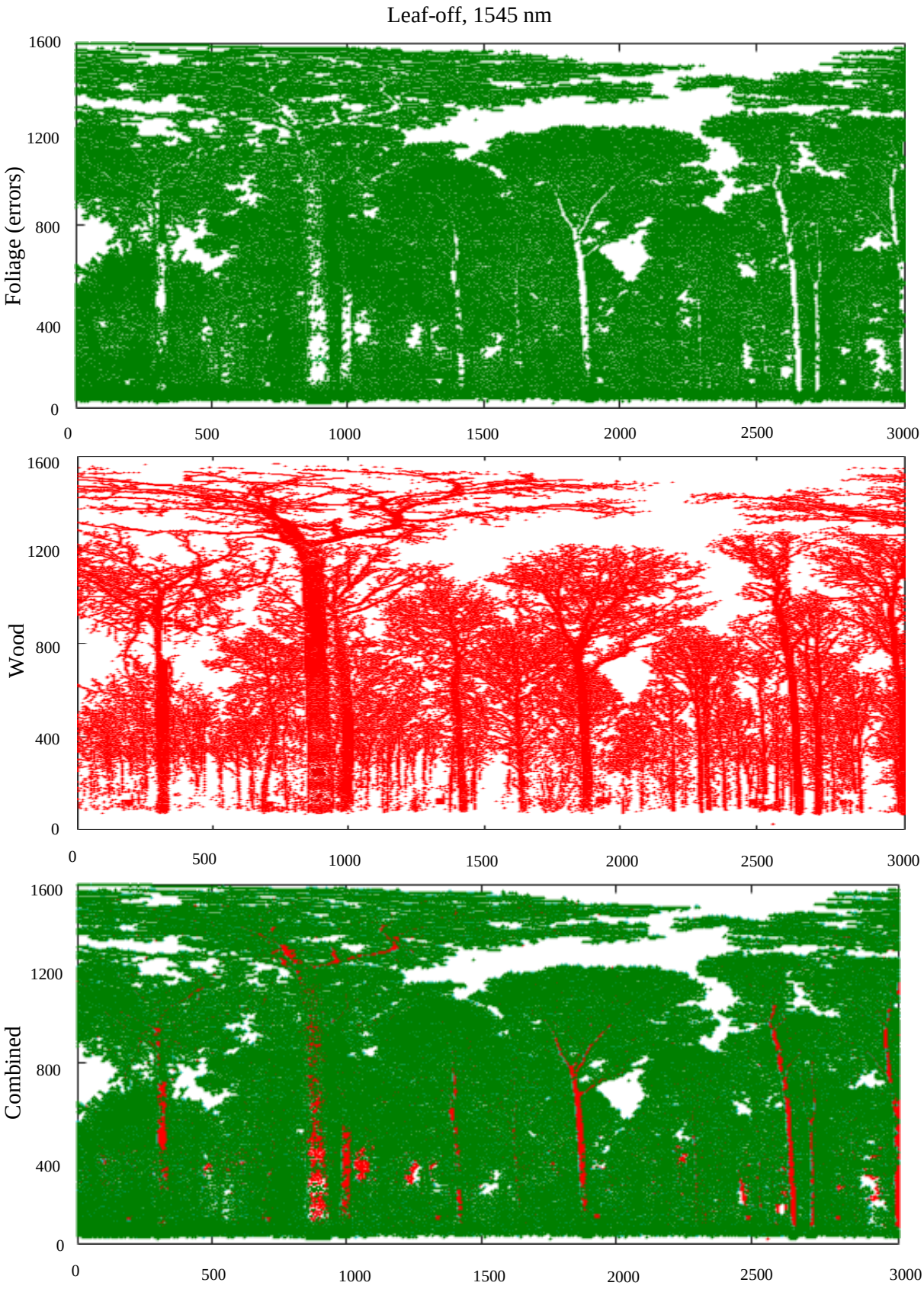

Figure 6.9: SALCA apparent reflectance for a full stand forest from Alice Holt Forest leaf-off condition classified into foliage (green) or wood (red) using 0.3 threshold on 1545 nm

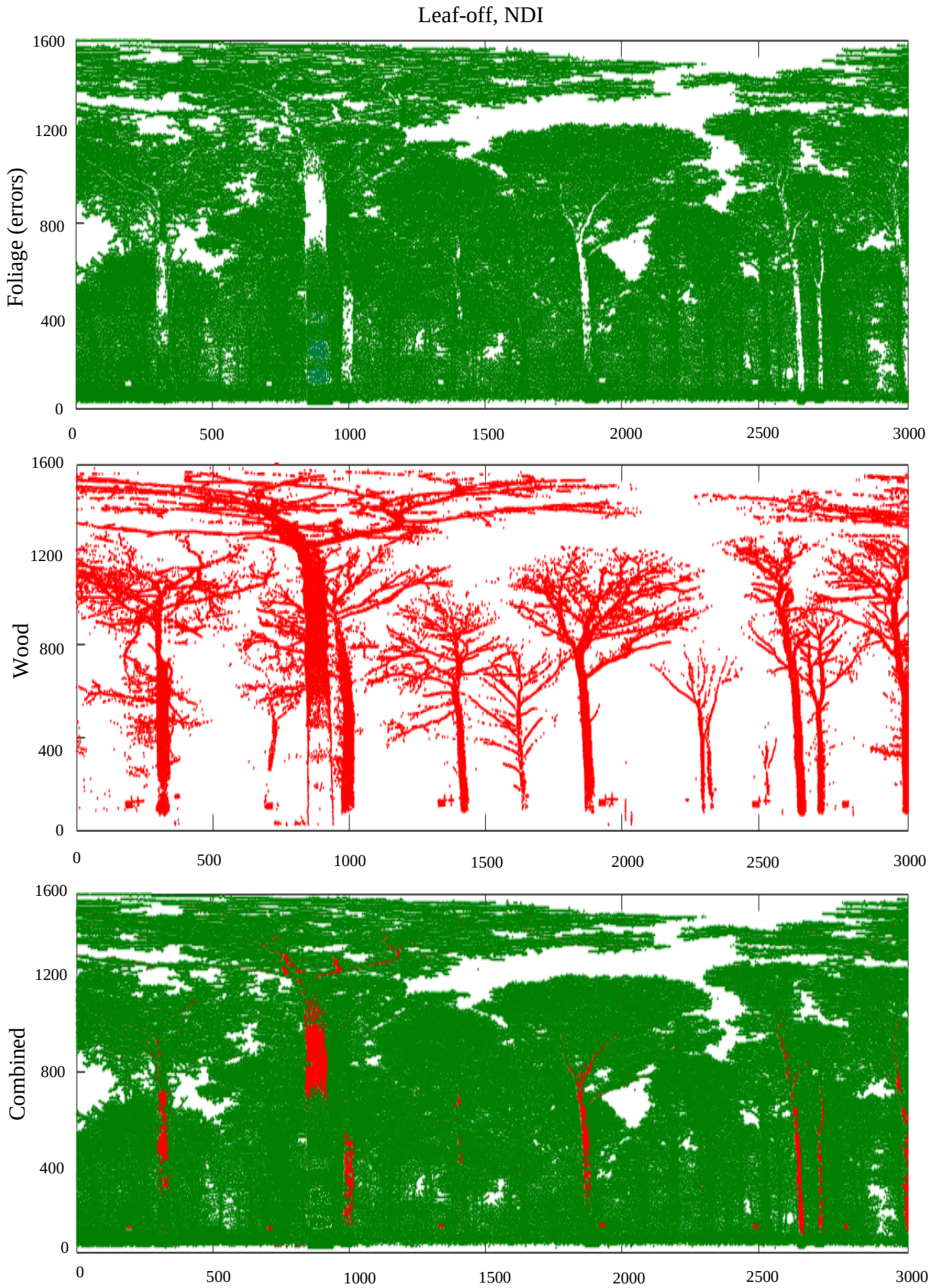

Figure 6.10: SALCA points for a full stand forest from Alice Holt Forest
leaf-off condition classified into foliage (green) or wood (red) using 0.2 threshold on NDI

6.6 Spatial analysis for full stand forest

This section illustrates an assessment of the spatial classification for the leaf-on and leaf-off data detailed in Section 6.2. Two groups of points were segmented from the foliage and the wood to train the classifier. Due to the plot size, the two groups of points were collected from different areas randomly, using Cloud Compare to segment points from different places. For instance, the wood points were collected from the stems and the branches at 5m, 15m, 25m, 40m, and 60m. These points were then combined into a single group to represent the trained wood group in CANUPO. Different scales were tested in order to gain the most accurate confidence values for the full stand forest. However, scales of 25 cm were used to train the segmented points from the full stand forest datasets due to the high confidence values they produced. The points were then classified into foliage or wood, based on their location in the scan. The spatial foliage points are allocated to green and the wood point to black.

6.6.1 Leaf-on condition

Figure 6.12 shows the final spatial classification of CANUPO for the leaf-on scan, where 85% of the spatial points for this scan were classified as foliage and only 15% as wood. Most of the classified wood points were found in the stems for the closest tree to the scanners and fewer wood points were found in the canopies. At distances greater than 15 m, there is a mixture of foliage and word that was incorrectly classified as wood, as the two classes were combined.

6.6.2 Leaf-off condition

Figure 6.13 shows the findings of the spatial classification for a leaf-off scan using the same scales and trained points that were used to classify the leaf-on scan. In general, 54% of the spatial returns for this scan were recorded as errors (foliage) in the classifications and 55% of the total returns were validated as wood, according to the applied scales. Most of the stems and parts of the panels appear to the classifier as plane shapes and, due to this, were represented as wood returns. The majority of the errors were found in the canopy and the finer and the main branches. In addition, most of the targets at a range greater than 15 m incorrectly appear to the classifier as 3D or foliage (errors).

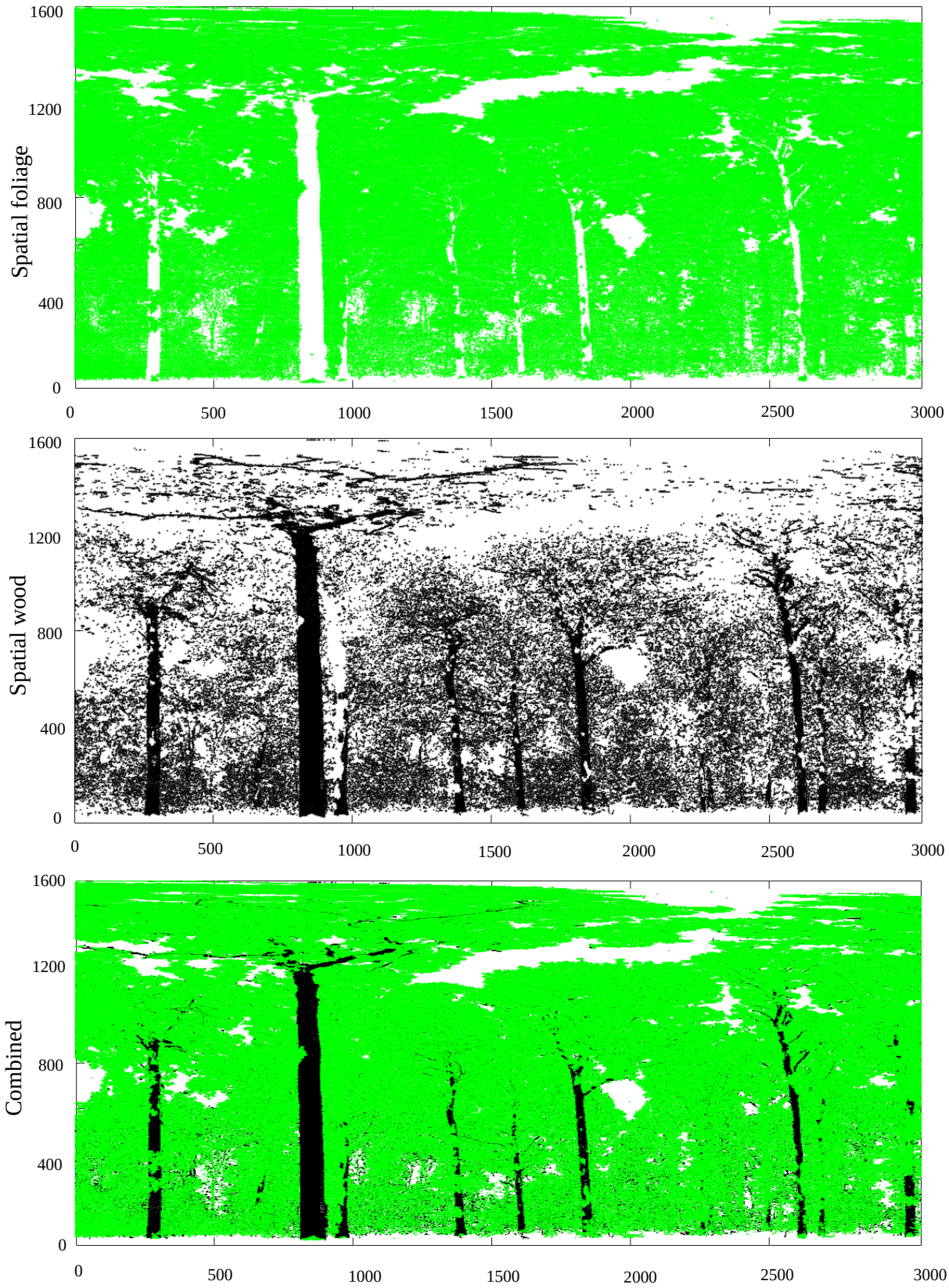

Figure 6.11: The spatial classification for the full stand plot leaf-on scan classified into foliage or wood based on their geometrical properties respectively. The green points are allocated to foliage class and black points to the wood class.

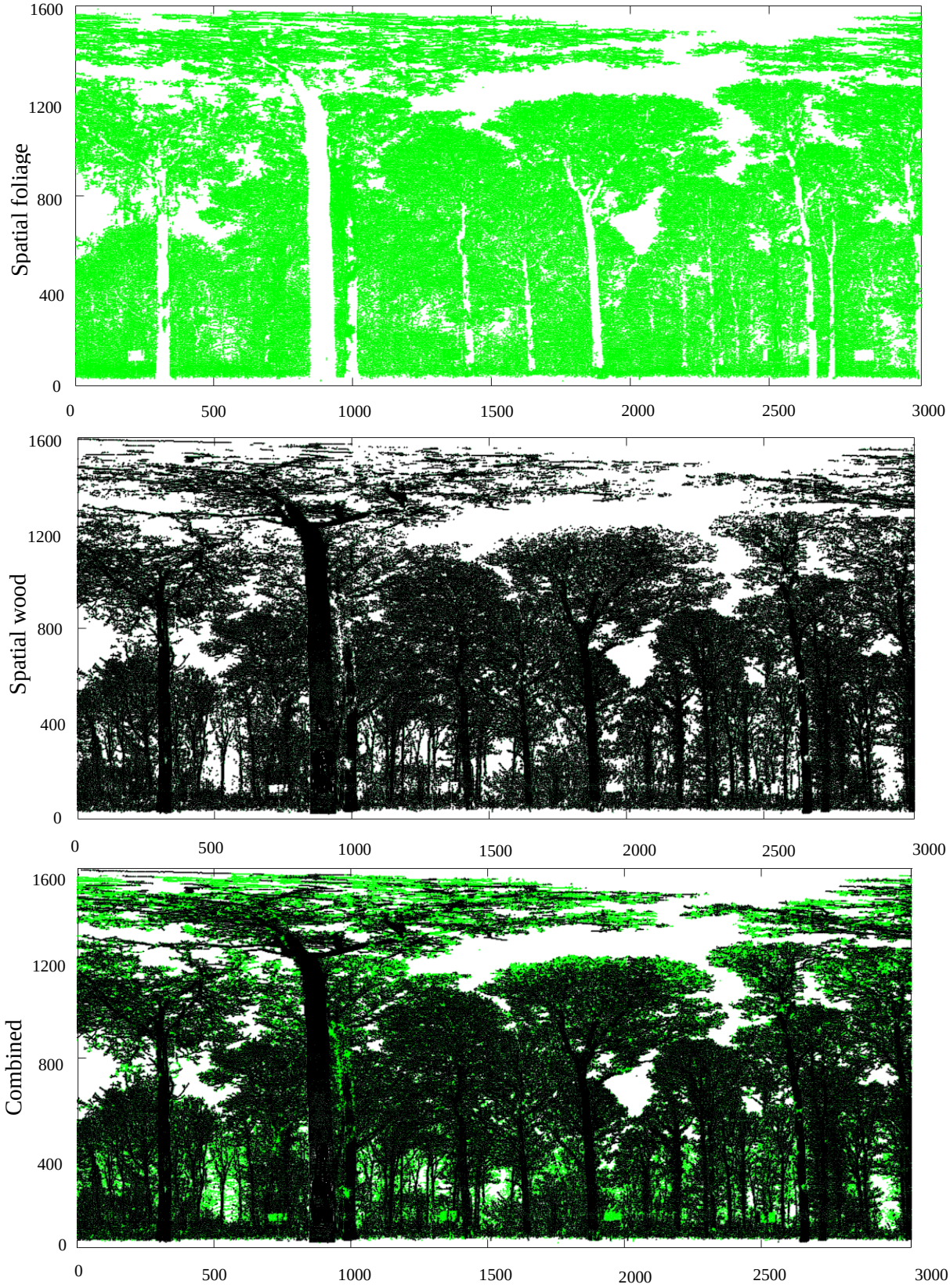

Figure 6.12: The spatial classification for the full stand plot leaf-off scan classified into foliage (errors) or wood based on their geometrical properties respectively. The green points are allocated to foliage class and black points to the wood class.

6.7 Comparing the spectral and spatial information

The spectral and spatial outputs of the full stand forest were compared together in order to investigate the compatibility between the classes. The final calculation of every class with their labelled name is detailed in Table 6.2. The final agreement between the spectral and spatial classes for the full stand forest was 55.63%. There was incompatibility in 44.37% of the total returns of CANUPO. Class SFCF recorded the highest returns, and the smallest return was for class SWCF, as detailed in the table below.

Table 6.2: The spectral and spatial classes for the full stand plot.

Four classes 3383168 returns	CANUPO foliage	CANUPO wood
Spectral foliage	1502161 (SFCF), agreement of 44.39 %	1377183 (SFCW), disagreement of 40.70 %
Spectral wood	123839 (SWCF), disagreement of 3.65 %	380498 (SWCW), agreement of 11.24%
The total percentage of agreement between the spatial and spatial points was 55.63%		

Figure 6.14 shows the visualisation for every class separately. Based on a visual assessment, class SFCF (red) was found mostly in the canopy and areas where the foliage covers parts of the stems. It is possible to distinguish some of the finer branches and most of the main branches from the foliage points at close and far distances from the scanner. Class SFCW (black) consists of spectral foliage and spatial wood, which explains the distribution of the black on the canopies and some areas on the wood class. The class SWCF (green) consists mostly of spectral and spatial foliage. However, many areas on the stems and the main branches were misclassified as wood and most of the lower parts of the tree were classified as foliage. Class SWCW (blue) covered most of the wood points. It was difficult to distinguish the finer branches from the foliage points in all classes, including the stems and canopy. The four classes were represented as one figure to map the distribution of each class. Most of the trees in the plot were coloured red (class SFCF). The stems in the figure were coloured with a mixture of all classes. However, blue dominated the stems areas for the trees located next to the scanner. In addition, parts of the stems were coloured green and these trees were situated close and far from SALCA.

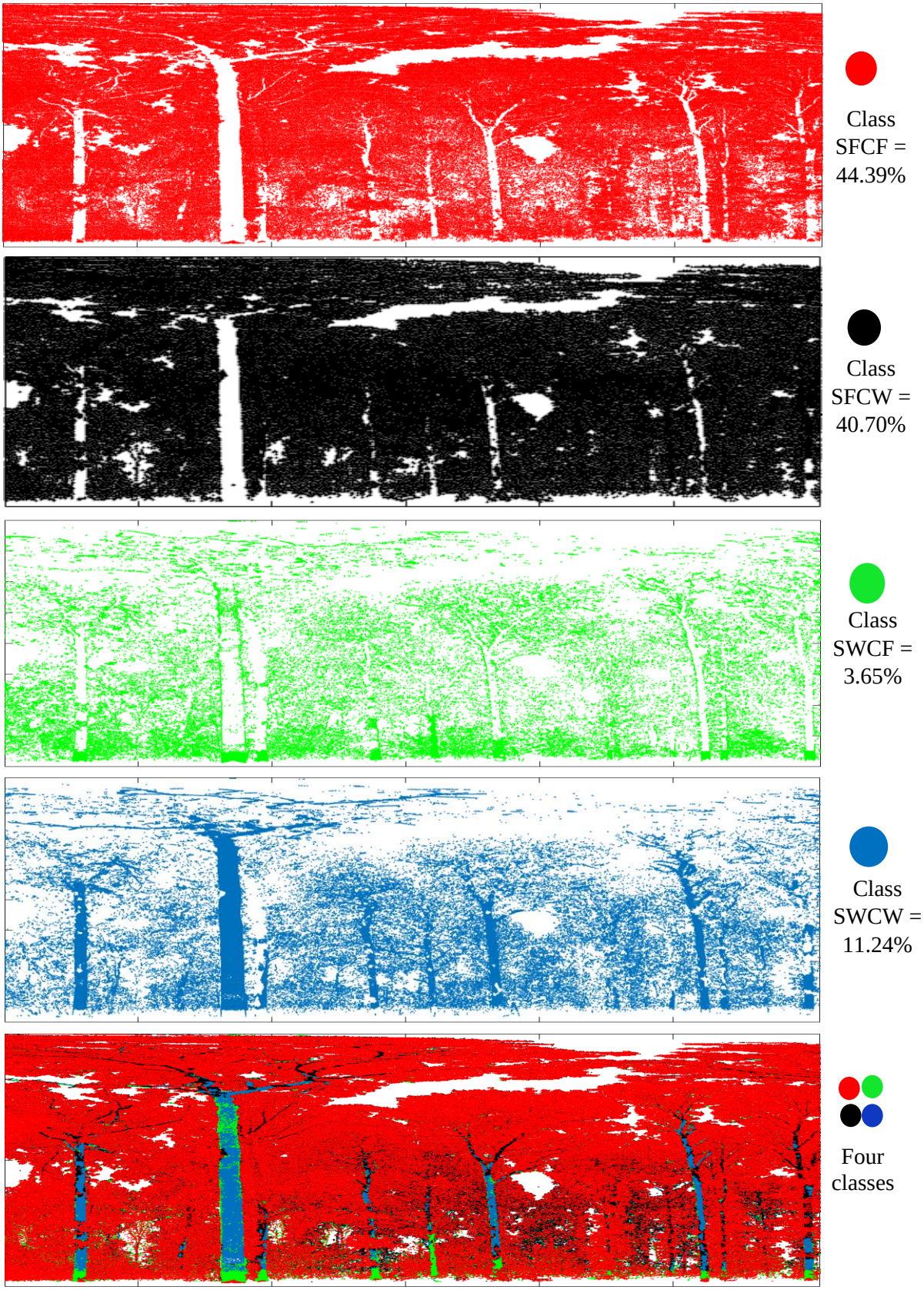

Figure 6.13: The spectral and spatial classes of the full stand plot leaf-on scan. The red points for class SFCF, black for SFCW, green for SWCF and the blue for SWCW. The classes are combined into one image.

6.7.1 CANUPO confidence

The confidence values for CANUPO outputs were obtained for the full stand leaf-on scan as detailed earlier. The values were then analysed to show how certain the foliage and wood classifications were (Table 6.3). The table showed that the spatial foliage and the wood were classified with confidence greater than 80% and the classifier was strongly certain about the final spatial classification. In addition, the classifier was less certain by 5% and 8 % for the spatial foliage and wood respectively.

Table 6.3: Confidence for the spatial foliage and wood for the full stand plot.

Name	CANUPO performance	spatial class	
	confidence	spatial foliage	spatial wood
Alice Holt plot	> 80%	95 %	91 %
Name	uncertain	spatial foliage	spatial wood
Alice Holt plot	≤ 80 %	5%	8 %

Figure 6.15 represents the confidence values for the spatial foliage, where confidence values > 80% are shown in red and ≤ 80% in blue. The spatial classifier classified 95% of the foliage points with a confidence value of greater than 80% and was less certain for 5% of the total number of spatial foliage points. Most of these small values are found in the canopy, including the finer and main branches, and a few parts of the stem at the ground level.

Figure 6.16 visualises the confidence values for the wood class, whereby 91% of the total wood points were classified with a high confidence value. These points were found mostly in the tree stems and most of the main and the fine branches, while only 8% of the points were classified with a confidence level of ≤80% and these values were found mostly in the canopy, with less presence in the stems compared to the red points.

Overall, the output of CANUPO classification for the full stand plot showed that the classifier was certain for most of the points of the foliage and wood. Most of the lower parts of the trees were classified as foliage and a large number of these points showed high confidence values (red). In addition, the range affected the classification, where targets at a far distance from the scanner showed more errors than the close targets, based on a visual assessment.

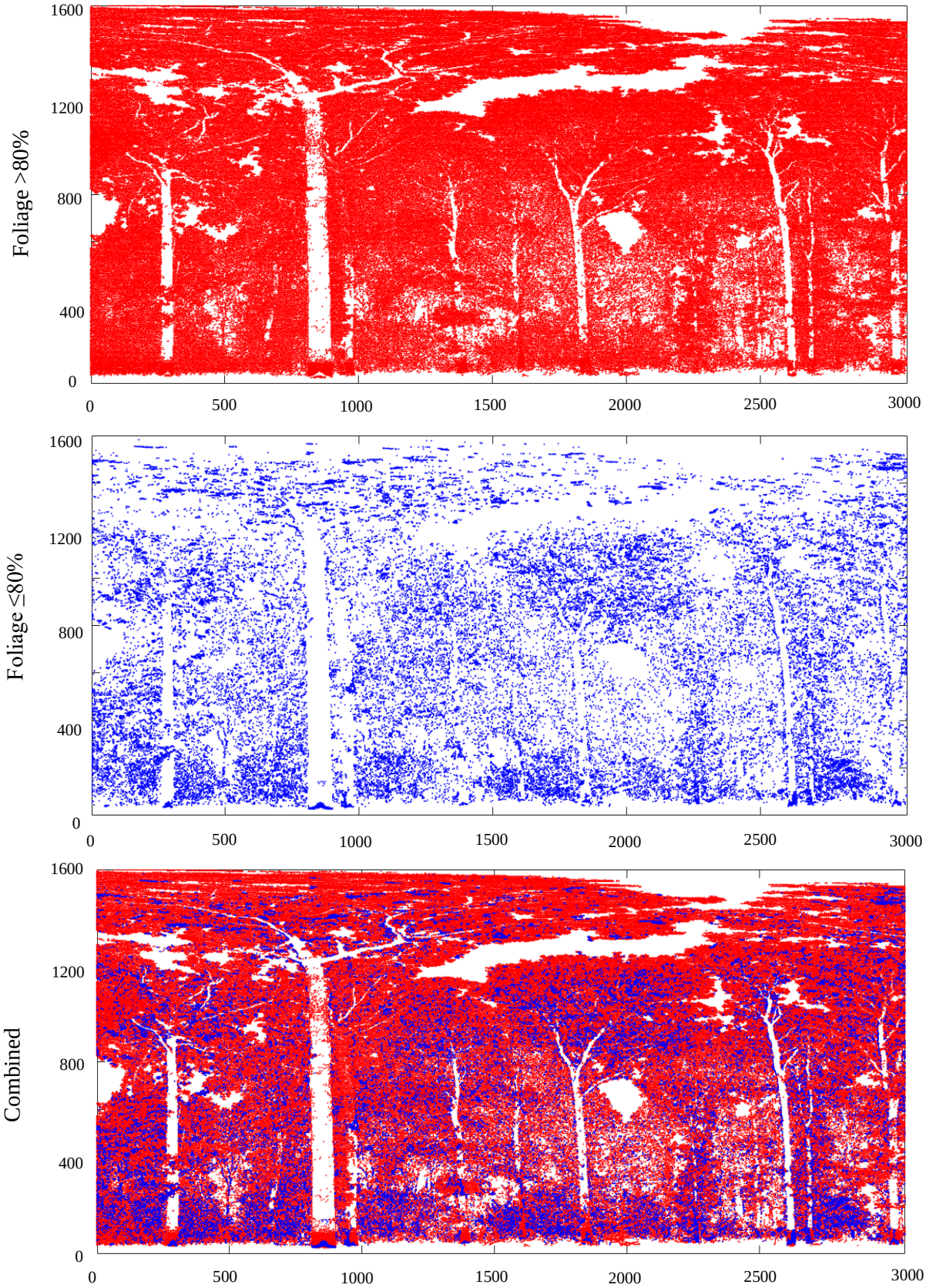

Figure 6.14: CANUPO confidence percentage for the spatial wood extracted from the full stand data. Red indicates a confidence level > 80% and blue one of ≤ 80%.

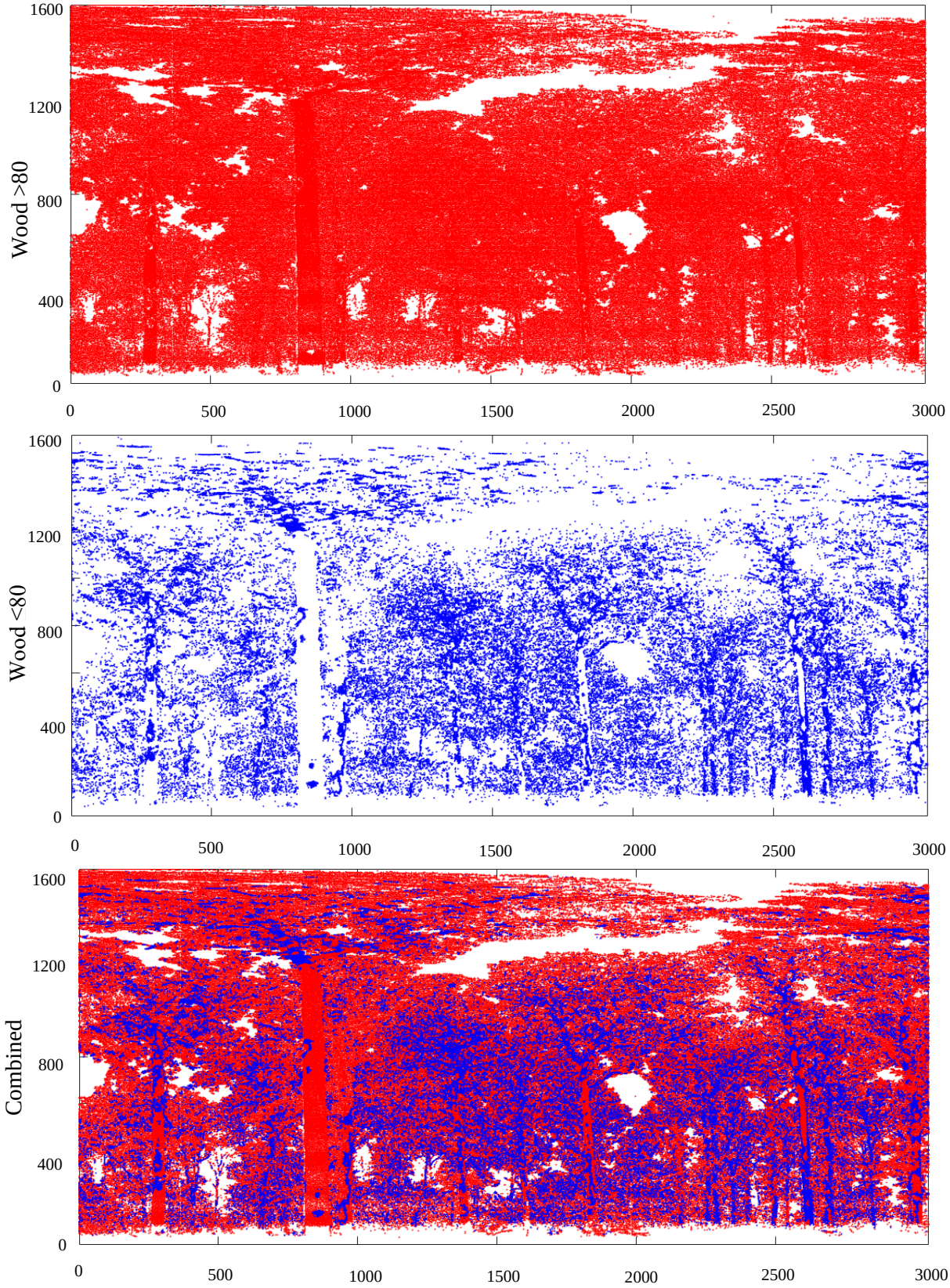

Figure 6.15: CANUPO confidence percentage for the spatial wood extracted from full stand data. Red coloured for confidence > 80% and blue for ≤ 80%.

6.8 Foliage and wood separation using number of returns

The number of returns for the 1063 nm and 1545 nm data was investigated and extracted to map the full stand plot components based on the numbers of returns per laser shot. Table 6.4 shows the percentage of single, and multiple returns for both laser wavelengths. Most of the data point were recorded as single returns for both laser wavelengths data and a small percentage of the data were recorded by two or more returns as detailed in the table.

Table 6.4: Percentage of the single and multiple returns for the full forest stand.

Plot name	Description					
	1063 nm			1545 nm		
	Single return	2 returns	3 or more	Single return	2 returns	3 or more
Alice Holt plot	91%	8%	1%	89%	10%	1%

Figure 6.17 shows the results of the full stand plot components classification, using the number of returns scanned by SALCA. Yellow refers to the single returns, red to two returns and blue to three or more returns, respectively. In general, the table above shows the convergent values produced by both of the laser wavelengths. Due to this, only the 1063 data were visualised in Figure 6.17. For the 1063 data, 91% of the total returns were allocated to green, including the stems, main branches and part of the foliage areas. At far ranges from the scanner, it can be seen that most of the targets were produced by single returns, including all of the trees components, except for a few patches that were coloured red. Eight percent of the points were coloured red and this was found in most of the canopies at short ranges and in all the components of the trees at long distances. Overall, the final outputs for the plot components separation approach produced visually plausible separation of the foliage and wood. It is likely that this approach was more effective for the wood, especially for the stems and main branches. However, a large part of the foliage returns was produced by the single returns as well.

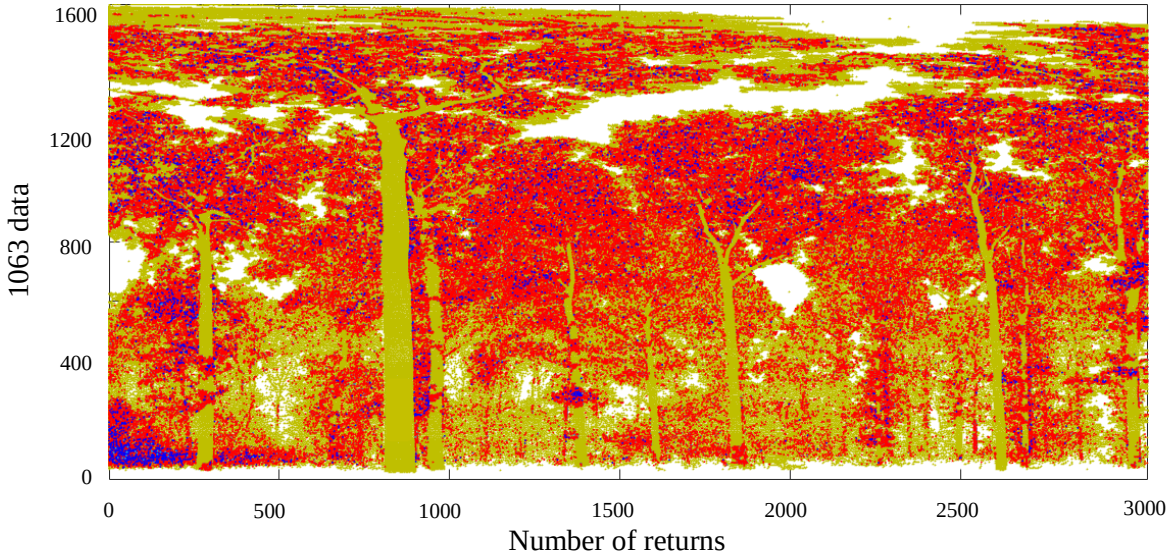

Figure 6.16: SALCA point clouds for a full stand forest from Alice Holt Forest leaf-on and scan, coloured by the number of returns for the 1063 data.

6.9 Conclusion

This chapter used high-resolution datasets to investigate the characterisation of foliage and wood at the level of a full forest stand in leaf-on and leaf-off conditions. This was done in order to satisfy Objective 3 of this research. A series of spectral and spatial analyses were applied to test the foliage and wood classification. Different thresholds were applied to the spectral variables as part of the spectral classification approach. To derive the spatial classifications, the relationship between the points was built based on their location in the scan within given scales. The trained points used as a reference to build a relationship between the TLS points were segmented from different trees at different ranges within the scan. This was done in order to assess the potential of the spatial classifier to distinguish the foliage points from wood at far ranges from the scanner.

For the spectral classification, the applied thresholds defined fairly accurately separation for the 1063 nm and 1545 nm at ranges shorter than 15 m. For the NDI data, it was possible to distinguish the foliage points from wood at ranges less than 17m from SALCA. However, the 1545 nm and NDI data showed more details of the foliage and wood separation compared to the 1063 data. In the case of a leaf-off scan, 99% of the 1063 data were validated as wood, while 70% and 86% of the 1545 nm and NDI data were classified incorrectly as foliage respectively. For the spatial classification, the final outputs showed that CANUPO provided a clear separation for the leaf-on condition. However, 85% of the spatial points were defined as

foliage since large numbers of the wood points were misclassified as foliage. For the leaf-off scan, the results showed large errors in the classification as 54% of the wood returns were defined as foliage.

The comparison between the spectral and spatial outputs showed compatibility in most of the scan classes, with a final agreement of 55.63%. The classifier confidence was high for most of the classifications as 95 % the foliage and 91% of the wood points were determined to have a confidence value of greater than 80%. The classification based on the number of returns showed that more than 85% of the full plot data were recorded by a single return for both laser wavelengths. The work in this chapter has provided a full description of the potential of SALCA to characterise the components of a full stand plot.

CHAPTER 7: DISCUSSION AND CONCLUSIONS

7.1 Introduction

Foliage and wood classification is key for a wide range of applications that use TLS to extract information on forest structure and function; for instance, quantifying above-ground biomas, foliage and wood profile measurements, and their three-dimensional distribution (Vicari et al., 2019). However, the 3D arrangement of vegetation makes TLS data analysis complex, which increases the challenges related to mapping the structure. Distinguishing wood from foliage points is therefore required in order to describe the tree structure accurately (Côté, Fournier, Luther, & van Lier, 2018). Recently, TLS has emerged as a promising technology for resolving this problem.

Previous studies have used information from single-wavelength scanners in order to classify vegetation components and the results produced were generally poor in terms of providing clear separation (Béland et al., 2014; Clawges et al., 2007). Recent advances in TLS technologies have opened up a new area of interest related to using the contrast in spectral response to foliage and wood in the NIR and SWIR wavelengths to classify the vegetation components. Recently, new dual-wavelength scanners such as SALCA have provided a wide range of new information and minimised some of the limitations of the single-wavelength lasers by using ratios of the apparent reflectance in two wavelengths (Calders et al., 2017; Danson et al., 2014).

This study set out to explore foliage/wood separation using multi-wavelength TLS datasets extracted from single trees both in the laboratory and field environment, and a full forest stand plot. A series of laboratory and field scanning experiments were conducted using the SALCA instrument for leaf-on and leaf-off conditions for the desired data. This was done in order to satisfy the main objectives detailed in Chapter 2. The work used a combination of spectral and spatial approaches to distinguish foliage points from wood points in the TLS point-clouds. The spectral approach was performed by determining the visual thresholds based on the frequency distribution of the apparent reflectance for both laser wavelengths and using a normalised difference index. This was based on a visual assessment. The spatial approach was achieved using the location of the points in the scan to generate a relationship between the points, based on their geometric properties. It was important to understand the relationship

between the two classification approaches; therefore, the outputs of both approaches were represented in matrices to investigate their compatibility.

In terms of validation, the spectral classifications were validated using the same visual thresholds for the leaf-on and leaf-off scans. For the spatial classification, the same-trained scales were used for both scan conditions. In addition, the spatial classification for the single trees was compared from the south, north, east, and west for the Poor, Moderate and Good trees, respectively. Moreover, the CANUPO confidence values were computed and visualised for all of the datasets to determine the confidence values attached to the spatial classification. The results of each activity in this research were detailed throughout Chapters 4, 5, and 6. Therefore, this chapter aims to discuss the findings and present interpretations of the key outputs in order to address the main objectives detailed in Chapter 2.

7.2 Foliage/wood classification in laboratory

The laboratory experiment was designed to address Objective 1 and investigate three hypotheses related to foliage and wood separation, detailed in Chapter 4. The objective was to test the potential of the SALCA instrument in the laboratory before using it in a more complex environment. In the laboratory, two trees were scanned at short-range with high laser case temperatures for both wavelengths. In order to derive an accurate reflectance calibration of the SALCA data, it is currently necessary to use a large number of measurements of a calibrated reflectance panel in order to train a neural network. For instance, Schofield (2016) used 868 measurements of intensity, range, reflectance, and laser case temperature, extracted from six calibrated panels to train a neural network. The data were acquired over more than 40 scans in an outdoor environment at ranges between 8m and 32 m to obtain an accurate reflectance related to the target properties. The neural network produced using the panels' data produced an accurate reflectance but only tested for outdoor data. This network was unsuitable for the short-range indoor environment due to the high temperatures that were recorded for both lasers in the laboratory. To address this issue, a new calibration was derived (equations 3.2 and 3.3) to calibrate the raw intensity, and the results showed a very accurate reflectance for both laser wavelengths compared to the panel as detailed in Section 3.6.

This work addressed the following question:

Question 1.1 Can SALCA spectral data be used to separate foliage and wood in short-range scans in the laboratory?

In general, the laboratory work in this research proved a useful background for assessing the potential of SALCA to provide initial information related to foliage/wood classification at short-ranges. In terms of extracted data, the recorded intensity of the 1545 nm for the broadleaf and needle-leaf tree of leaf-on and leaf-off scans comprised low values compared to the 1063 nm data. This may have been due to the high temperatures recorded for 1545 nm, which reached a maximum value of 35 ºC and may have caused a decrease in the recorded power of the 1545 channel. The effect of the temperature on the laser intensity was described in Ab-Rahman and Hassan (2009) and Welford and Mooradian (1982), and the results showed that there exists a strong negative linear relationship between the case laser temperature and laser power. The effect of case temperature on laser power has been noticed in the development of the SALCA instrument (Danson et al., 2014; Danson et al., 2018; Schofield, 2016).

The spectral classification for the broadleaf tree leaf-on scan produced one of the more significant findings to emerge from this chapter, as the 1063 nm data at 8m produced a clear, successful separation. The only interpretation for this is that the wood for the broad-leaf tree had a higher reflectance than the foliage, as the wood points were greater than an apparent reflectance of 0.3, whilst the foliage points were ≤ 0.3. In contrast, the 1545 nm data generated misclassification errors (unclear separation) using a 0.2 threshold. A large number of the woody points were incorrectly classified as foliage due to the similar values of AR of both components. Using the NDI produced more consistent separations (very clear) for the broad-leaf tree, as the NDI was greater than 0.2 for the wood and ≤ 0.2 for the foliage. The same thresholds were applied for the leaf-off scan, but a large number of errors were generated, with 33%, 59%, and 27% of the total points for 1063 nm, 1545 nm, and NDI respectively, not being validated as wood. This means that the calibrations were insufficiently accurate to use the same thresholds that were applied for the leaf-on scans. The leaf-off scan was performed many weeks after the leaf-on scan, so the woody materials may have lost water and had a higher reflectance compared to the leaf-on scan.

The spectral classification of the needle-leaf tree leaf-on scan generated classification errors or unclear separation using an 0.1 AR threshold on 1063 nm. A large number of the foliage points (needles) had a reflectance > 0.1 and were classified incorrectly as wood. However, a successful separation was generated using an 0.2 AR threshold for the 1545 nm data, as the woody materials showed values greater than 0.2 and the needles ≤ 0.2. Using the NDI -0.1

threshold produced errors and it was impossible to distinguish between the foliage and wood points for the needle-leaf tree. During the scanning of the leaf-on condition, the presence of dry needles was observed, especially in the lower part of the tree, which might have led to misclassification. Elsherif et al. (2018) used the NDI to generate 3D estimates of the leaf Equivalent Water Thickness (EWT) of two young needle-leaf trees in the laboratory. The extracted information was used to separate the components of the trees, based on the moisture content in the desired data. The moisture content in the wood and foliage areas was calculated manually and the final separation showed errors in the foliage as this was classified incorrectly as wood. These errors in the classification were found mostly in the lower parts of both trees due to the presence of dry needles in these areas (Figure 7.1).

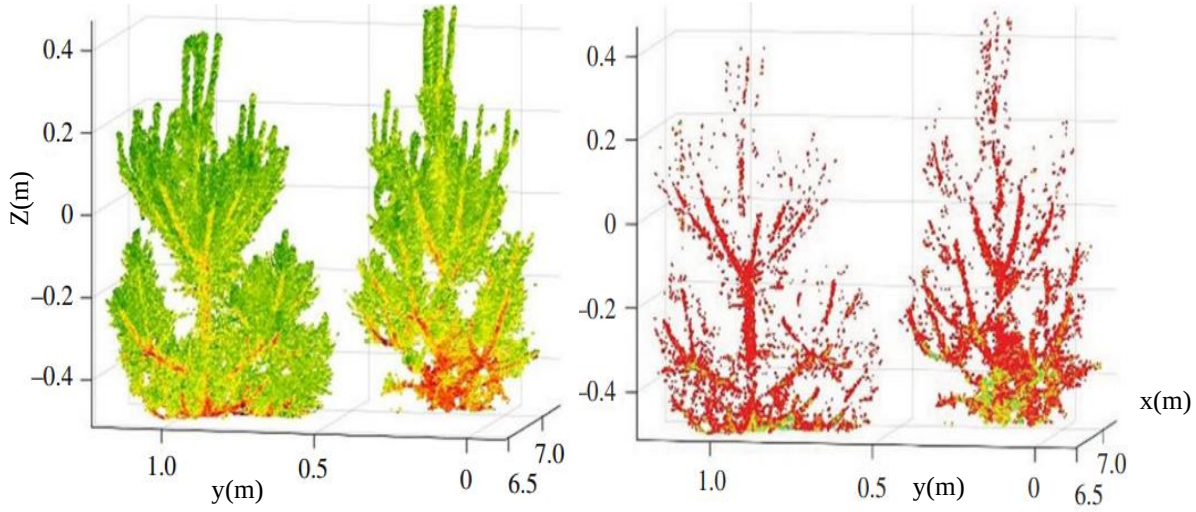

Figure 7.1: Needle-leaf tree separated into foliage (green) and wood (red) based on the moisture content. A large number of the foliage points were classified incorrectly as wood due to low amount of moisture content in the foliage materials. Source: (Elsherif, Gaulton, & Mills, 2018).

For the needle-leaf tree leaf-off scan, a large number of errors were recorded using the same thresholds that were applied for the leaf-on scan. The results showed that 25%, 77%, and 26% of the total points of this scan were classified as errors for the 1063 nm, 1545 nm, and NDI data, respectively. This means that the calibrations were again insufficiently accurate to use the same thresholds for this scan.

Overall, this research demonstrated that a simple threshold-based separation of foliage and wood points in the laboratory at short-ranges is unlikely to be accurate for the 1545 nm data for the broadleaf, 1063 nm data for the needle-leaf, and the NDI data for the needle-leaf tree.

In addition, the classification of the leaf-off and leaf-on scans showed a large number of errors in the classification, with wood points being misclassified as foliage. However, a smaller number of points were classified as foliage in the NDI data compared to the 1063 nm and 1545 nm data. The findings from this research indicate that the spectral classification using visual thresholds produces challenges related to calibration at short-ranges and the high temperatures that cause a drop in the laser power. However, the research provides an indication of the possibility of successful separation using the 1063 nm data.

Question 1.2 Can SALCA spatial data be used to separate foliage and wood in short-range scans in the laboratory?

CANUPO provides an effective method for TLS point-based classification. The classifier determines the best homogeneous distributions for the points within a given scale and location (Wu et al., 2018). Section 4.7 of this research summarised the spatial classification for the foliage and wood for the broadleaf and needle-leaf for the leaf-on and leaf-off scans, respectively. The results showed that CANUPO classified 78% of the broadleaf-tree leaf-on points as foliage, whilst only 22% of the total points were classified as woody as these points appeared as 2D or 1D to the classifier. In addition, 66% of the leaf-off scan points were recorded as errors using the 0.5 m scale. These points appeared to the classifier as 3D, based on the scales used to train the classifier. The classification of the needle-leaf tree leaf-on scan showed that 88% of the total points were classified as foliage, whilst 12% of the points were classified as wood. It is clear that the needles appeared to the classifier as 1D or 2D and that is why there were classified as wood. The classifier produced 66% errors for the leaf-of scan for the needle-leaf tree.

To conclude, this section showed that errors in the classification were generated when using a spatial approach for both trees scanned in the laboratory at short-range. The results suggested that the approach was more effective for foliage than wood, as the majority of the points were classified as the former. A large number of the wood points were allocated to foliage class for both trees in the leaf-on condition. The errors in the classification for the leaf-on and leaf-off scans might be due to the inappropriate scales used to train the points as most of the woody points appeared 3D (foliage) to the classifier. It is unlikely that this approach with small trees would provide a successful spatial separation.

Further work is needed in order to test how spatial classification is affected by the SALCA range measurements, where most of the wood materials appear as foliage or 3D. The classification might be improved by knowing the amount of the foliage points using a virtual model, as explored by Tao et al. (2015). Therefore it is easier to determine the misclassified wood points. In addition, this work was performed in an indoor environment over a relatively limited range. Futher investigations in an outdoor environment were therefore required.

Question 1.3 What is the relationship between the outputs of the two classification approaches?

Using spectral and spatial approaches to map tree components has not been yet fully explored. In this research, both approaches were used to characterise the components of small broadleaf and needle-leaf trees leaf-on scans. The outputs of both approaches were compared and showed some compatibility between them. The final results produced by the broadleaf tree leaf-on scan showed a total agreement of 67.35% between the spectral and spatial approaches; 60% of the total points were represented as spectral and spatial foliage SFCF (Figure 4.19). Part of the stem and the branches were allocated to the red points as foliage. This can be attributed to the large number of errors produced by the spatial classification, as most of the wood was incorrectly classified as foliage. Foliage points were found also in classes SFCW and SWCF, which supports that idea that most of the tree points were classified incorrectly as foliage. The CANUPO confidence was 27.73% and 9.72% for the foliage and wood classes, respectively. This was expected due to the spatial errors produced by CANUPO.

A total agreement of 73.18% was recorded for the needle-leaf tree leaf-on scan. The same was found in terms of the errors in the classification, as 70.22% were classified as spectral and spatial foliage. In addition, SFCW and SWCF contain foliage points which increases the number of misclassified points. The CANUPO confidence for this tree was 45.66% and 7.02% for the foliage and wood, respectively. Jalonen et al. (2015) and Wu et al. (2018) used CANUPO in order to separate the foliage from the wood points from single-wavelength scanners based on their geometric properties for single trees and state that the classifications were accurate. However, these results were not supported with evidence to show how certain the classifications were.

Overall, the research demonstrated the potential of SALCA to provide a wide range of information that has not been previously explored. It is possible to use this information to map

the desired data components. In addition, using two approaches to improve foliage/wood classification in the laboratory showed an agreement between the two approaches. The variation in the classes' distribution was governed mainly by the spatial classification as the points appear to the classifier as 1D, 2D, or 3D, based on the applied scales. The classification showed that CANUPO was more effective for foliage separation than wood for these scans. CANUPO's default was to train 10,000 or 20,000 core points in term of using them as a reference for the classification. This was a limitation in terms of generating accurate trained points. Future efforts are needed to expand the scales and the number of trained points to test whether that will improve the performance of the classifier. However, this approach needs to be investigated using mature trees in an outdoor environment.

7.3 Foliage and wood characterisation at the level of a single tree in an outdoor environment

This work is set out in Chapter 5 to address Objective 2 and investigate the hypotheses detailed in Section 2.6. The SALCA instrument was used to scan three isolated oak trees in an outdoor environment in order to characterise their components. The trees were scanned from different orientations in order to compare the spatial classification. A combination of spectral and spatial approaches was used for foliage/wood separation for the leaf-on scan, whilst the leaf-off scan was used to validate the spectral and spatial analysis. This work addressed three main research questions.

Question 2.1 Is it possible to separate foliage/wood at the individual tree level in an open environment using spectral information?

For the Poor tree, the spectral classification of the leaf-on scan, using a 0.1 threshold, provided an unclear separation. A large number of the main and the finer branches were incorrectly classified as foliage. This means that these points had a reflectance ≤ 0.1. This was expected, as the result supported the hypotheses that wood and foliage has a similar reflectance in the 1063 nm wavelength. The 1545 nm data for the same tree were separated into foliage and wood, using an 0.2 AR threshold. The output comprised a very clear separation, as few green points on the finer branches were separated as foliage (Figure 5.11). This successful separation was obtained due to the contrast between the reflectance of photosynthetic and nonphotosynthetic materials in tree.

Using the NDI data provided a clear separation for the Poor tree as the foliage had NDI > -0.1, whilst wood comprised ≤ -0.1. However, the lower part of the tree was incorrectly classified as foliage due to the presence of lichen. Using the same thresholds mentioned above for the leaf-off scan produced different errors; the 1063 nm data showed 2% errors in the classification whilst 98% was validated as wood. The applied threshold (0.2) for the 1545 nm data provided errors of 22%, whilst 78% of the total points were classified as wood. Using the 0.1 threshold for the NDI data produced errors of 96% of the total points, as only 4% of the points were validated as wood. The reson for this might be that the calibration was insufficiently accurate to use the same thresholds to compare the leaf-on and leaf-off scans.

The classification of the Moderate tree leaf-on scan using a 0.1 threshold for the 1063 nm data produced an unclear separation, as a large number of the foliage points were classified as wood. Using AR 1545 nm data provided a very clear separation, with a 0.2 threshold. However, the lichen on the lower part of the stem caused some errors in this area of the scan. In addition, a few partial hits caused errors at the edges on the tree stem. According to Gaulton et al. (2013) NDI is sensitive to the moisture content in the vegetation. Therefore, this allows the separation of the components accurately and limits the effect of the partial hits on the classification. However, the spectral classification of the NDI using -0.1 comprised an unclear separation, as a large number of the wood points on the stem and main branches were allocated to foliage (Figure 5.12). The only explanation for these errors is that the NDI in these areas is higher than the -0.1 threshold. Using 0.1, 0.2, and -0.1 thresholds for the 1063 nm, 1545 nm, and NDI data for the leaf-off scan generated errors of 20%, 67%, and 92% for NIR, SWIR, and NDI, respectively, for the Moderate tree.

For the Good tree leaf-on scan, the results produced using a 0.1 threshold on 1063 nm showed unclear separation. Most of the scan points showed reflectance greater than 0.1 and were incorrectly classified as wood. However, using the 1545 nm data for foliage/wood separation generated a very clear separation, with a 0.2 threshold. As expected, the wood was represented by higher values compared to the foliage points in this wavelength. The NDI points separation, using -0.1, showed clear separation, with the foliage represented by > -0.1 and the wood by ≤ -0.1. A few points on the stem were incorrectly classified as foliage due to their higher contrast. Thresholds were applied to the Good tree leaf-off scan and showed 10%, 93%, and 96% errors for the 1063 nm, 1545 nm and NDI, respectively.

In general, the NIR data showed unclear separation for all trees, whist the SWIR data provided a very clear classification for the Poor, Moderate, and the Good trees. The Poor and Good tree points produced clearer separation compared to the Moderate tree, that showed an unclear classification using NDI data. Using thresholds for the leaf-off scans showed that the calibrations were insufficiently accurate to validate the scans as wood.

Question 2.2 Is it possible to use the spatial information to improve foliage/wood classification at individual tree level?

Spatial classification for the three isolated trees was performed, using scales of 0.5 m. A group of core foliage and wood points were segmented from each tree to generate a reference that was used for foliage/wood classification. In general, the outputs of the three trees showed successful classification (figure 5.7). In terms of validation, the same scale was applied for the leaf-off scans, and also for every tree from four orientations in order to compare the classification.

For the Poor tree, the classifier provided a clear separation as most of the tree points were classified as wood. However, some areas on the lower part of the stem and canopy were incorrectly classified as foliage and the points appeared to the classifier as 3D. The leaf-off scan was computed using the 0.5 m scale and showed 18% of the total scan points as errors, as they were allocated to green points (foliage). However, 82% of the total points of the Poor tree were validated as pure wood.

The visualisation of the Poor tree from different directions (Figure 5.19) showed a variation in the foliage points (green) distribution. The scan from the west provided a high number of green points at the stem compared to the scans from the south, north, and east. To investigate these green and black points (wood) in all scans, Table 7.1 showed the percentage of every scan separately. A small variation was recorded for the scans from the south, north, and east for the foliage and the wood as well. This means that the spatial classification for these scans produced an accurate separation and all of the scans responded to the same scale. However, the scan from the west showed a higher number of foliage and fewer wood points compared to the rest of the scans. It is clear that the distribution of the points from the west appeared different to the classifier from those in the other scans.

Table 7.1: Percentage of foliage and wood classified with the spatial classifier for the Poor tree from different orientations.

Scan direction	foliage points %	wood points %
Poor tree/ south	30%	70%
Poor tree/ north	28%	72%
Poor tree/ east	29%	71%
Poor tree/ west	37%	63%

The Moderate tree's results showed a clear separation as a few of the finer branches and some patches on the stem were allocated to the green points for the leaf-on scan. However, the leaf-off scan showed errors of 38%. The calculations showed a small variation between the foliage values in all of the scans (Table 7.2). The same was found for the wood values of all scans. It was mentioned in Section 5.2 that a small hill lay close to the Moderate tree which prevented the acquisition of data from the stems and some parts of the branches from the north and east directions. However, the difference were not as large, as the scans from the south and west (full scan and no information lost) showed a small variation in the number of foliage and wood points.

Table 7.2: Percentage of spatial foliage and wood of the Moderate tree from different orientations.

Scan direction	foliage points %	wood points %
Moderate tree/ south	80%	20%
Moderate tree/ north	71%	29%
Moderate tree/ east	83%	17%
Moderate tree/ west	79%	21%

In general, the Good tree's classification produced a clear separation as it was possible to distinguish the foliage from the wood points. There were some errors in the canopy, with wood points misclassified as foliage, and these points appeared to the classifier as foliage (3D). The leaf-off scan outputs provided 44% of the wood points as errors in the classification. The classification of the Good tree showed a very small difference in the foliage percentage from different directions and the same was found for the wood (Table 7.3). This means that the applied scale was accurate for all scans that represented the Good tree.

Table 7.3: Percentage of spatial foliage and wood of the Good tree from different orientations.

Scan direction	foliage points %	wood points %
Good tree south	86%	14%
Good tree north	81%	19%
Good tree east	84%	16%
Good tree west	82%	18%

Overall, the spatial classification from different directions demonstrated that the classifier was more effective for the foliage than the wood in the case of the Moderate and Good trees only. This was concluded from the calculations detailed in Tables 7.2 and 7.3, as the percentage of the spatial wood was significantly less than that of the foliage. This can be attributed to the scale used in the classification. The smaller the scales, the more data points will be classified as foliage.

Question 2.3 Is there any relationship between the spectral and the spatial approaches at the level of a single tree?

Comparing the spectral and spatial information for the Poor, Moderate, and Good trees produced a clear background for the relationship between both approaches for every tree. The final outputs showed a total agreement of 82.28%, 60.35%, and 80.42% between the spectral and spatial classifications for the three trees, respectively.

The spectral and spatial output for the Poor tree comprised the highest value of compatibility compared to the other two trees. This can be attributed to the fact that the foliage points in the Poor tree were very few in terms of number. Therefore, the spectral and spatial classifications validated 78.06% of the total returns as spectral and spatial wood. The CANUPO confidence was 90.08% for the foliage and 73.70% for the wood. This was expected, due to the clear classification produced for this tree.

The Moderate spectral and spatial information provided a lower value of agreement compared to the Poor and Good trees. This might be attributed to class SFCW, which comprises 35.95% of the total points as disagreement mainly in the tree canopy and a few parts of the main stem. The spectral classifier treats the point-clouds point-by-point, separately. This generates a finer classification in the final output of the spatial classifier. In contrast, CANUPO uses a probabilistic technique to classify a group of points in the same location. The classifier's confidence was 96.29% for foliage and 89.89% for wood. These values do not mean that the

classification was clear and accurate, but that the classifier was certain of the classification based on the applied scale only.

The Good tree's results showed strong agreement for the foliage points, with 79.96% of the total points represented mainly in the canopy area. However, the disagreements were found in the wood returns more than in the foliage, possibly due to the errors in the spectral classification, as a group of the NDI points were incorrectly classified as foliage. These points were allocated to the wood class by the spatial classifier. The CANUPO confidence for the Good tree was 94.34% and 88.35% for the foliage and wood, respectively.

The investigation of the number of returns showed that > 90% of the points of the trees were generated by single returns. Figure 5.28 showed that single returns (yellow) mainly came from full hits on the stems, main branches, and finer branches for all trees. Whilst multiple returns were recorded mainly in the canopy areas, with very few multiple returns from the stems for the Poor, Moderate, and Good trees. Due to the density of the points in the canopy of the three trees, it was hard to separate foliage from wood as all points were single returns. Clawges et al. (2007) used the number of returns for foliage/wood separation, as mentioned earlier in previous studies. However, the experiment was designed to scan a small coniferous tree using a single-wavelength scanner and it is hard to compare the result with the outputs of this research.

To conclude, the spectral and spatial classifications for the three oak trees highlighted variation in the compatibility for all trees. The visualisations of the data (Figures 5.21, 5.22, and 5.23) showed the areas where the spectral and spatial classifiers agreed: red points represented by spectral and spatial foliage, and blue as both as the classifiers agreed to classify these areas as wood. There was generally strong agreement regarding the main stem, and the main and finer branches for the Poor tree. However, the classification for the Moderate tree showed disagreement in the canopy caused by a large number of misclassification errors in the wood points, as they were classified as foliage. The Good tree showed a smaller number of points of disagreement compared to the Moderate tree.

7.4 Foliage and wood characterisation at the level of a full stand plot

In this study, datasets from Alice Holt Forest for the leaf-on and leaf-off scans were used to extract the spectral and spatial information in order to characterise the trees within a 60 m range. The leaf-on scan was calibrated using a set of neural networks for both the 1063 and

1545 wavelengths. A group of six calibrated panels were scanned at different ranges throughout the leaf-off scan in terms of calibration. This work set out to satisfy Objective 3 in this research. Therefore, the three hypotheses mentioned in Section 2.6 were investigated. Due to the complexity of the full stand forest plot, the classifiers were not expected to provide a clear separation at far ranges from the scanner. This part of the research was essentially exploratory in nature due to the lack of previous research in terms of using both spectral and spatial information to characterise trees in a full stand forest environment.

Ferrara et al. (2018) attempted to separate the foliage and wood materials for seven broadleaf mature trees using data from a single-wavelength scanner. A density-based clustering algorithm was used to separate the components of the trees. The results showed that it was possible to reduce the errors in the classification in the canopy areas. However, the analyses were performed for each tree separately which makes it hard to compare these results with the classification of the full stand plot explored here. In addition, the components of the trees in that study were voxelised to map the points of the trees and, as mentioned earlier in the literature review, this approach has limitations as the foliage and finer branches cannot be represented accurately.

Three main questions were addressed in this part of the work:

Question 3.1 Can foliage/wood separation be done using spectral information at the level of full forest stand plot?

The visualisation in Figure 6.3 showed apparent reflectance within the normal range for the 1063 nm data for the leaf-on scan. The spectral classification for this scan was performed using a 0.2 threshold at 1063 nm. The results showed a clear separation for the targets within a 30 m range of the scanner. It was impossible to obtain a clear separation for the trees at ranges greater than 30 m, as most of the data were classified as foliage, with AR $\leq$0.2. This was generated by the range effect. Large numbers of understorey points were allocated to red (wood) and some foliage points were incorrectly classified as wood in the canopy areas. As the wood and foliage points were visualised as one 2D figure, most of the wood area was covered totally by the foliage (green) points. This means that the number of foliage points was far larger than those for wood, based on the applied threshold. Applying a 0.2 threshold for the leaf-off scan showed that 0.6% of the scan was recorded as errors, whilst 98% was

validated as wood, including the panels. This was expected, as the network did not perform well for this scan, with the AR values out of the normal range.

The 1545 nm data produced a clear separation within the 40 m range using a 0.3 threshold. More stems were separated compared to the 1063 outputs. In addition, a more accurate separation was noticed in the canopy areas, as more foliage points showed reflectance of less than 0.3. This can be attributed to the vegetation response and the contrast of the 1063 nm and 1545nm data. However, the effect of the partial hits was observed at the edges of the stems at close range to the scanner. Moreover, the lower parts of the scan were allocated to the foliage, as these points showed lower reflectance. Using the same threshold for the leaf-off scan produced errors of 62% of the total points incorrectly classified as foliage.

Using a 0.2 threshold for the NDI data provided a very clear separation, as the effect of the partial hits was eliminated. More wood materials were observed at a range greater than 25 m. This means that the NDI data were more efficient compared to the 1063 nm and 1545 nm and less affected by the range; 78% of the leaf-off points were recorded as errors using a 0.2 threshold.

Schofield (2016) applied two thresholds on a full stand plot using AR 1545 nm and NDI data. The final outputs showed that the errors produced using full stand scans were significantly greater than those produced at the single tree scale. However, foliage and wood separation at the level of a full stand using a spectral classification approach is unlikely to provide an accurate separation due to the complex architecture of forest and the large variation in the spectral and spatial properties of the materials. In addition, the effect of the partial hits on the classification is expected to introduce more errors using apparent reflectance information.

Question 3.2 Is it possible to obtain accurate spatial classification at the level of full forest stand plot?

According to Brodu & Lague (2012) vegetation has complex characteristic surface features (foliage, finer branches, main branches, and stems). This makes it difficult to train a collection of points that are segmented from one location in the scan and used to classify all of the data in the scan at different ranges. Therefore, using more points from multiple locations may have provided a clearer classification. The spatial classification was performed for the full stand plot using a combination of trained points segmented from different ranges in the scan.

The applied scales produced a clear separation for most of the stems at a range of less than 20 m. However, most of the canopy was incorrectly classified as foliage for all scans. In general, the complexity of the biological materials of the full stand plot limited the potential of the spatial classifier to provide an accurate separation. In addition, the range affected the ability of the classifier to generate a homogenous combination for the points at distances greater than 20 m. The same scale was applied for the leaf-off scan and showed errors of 54% of the total points. Most of these errors were found in the canopy area.

Question 3.3 Is there any relationship between the spectral and the spatial approaches at the level of a full stand plot?

The final calculation of the spectral and spatial classification showed a total agreement of 55.63% of the total points for the full stand plot. This can be attributed to the large number of errors in the spatial classification, mentioned earlier. This was the lowest agreement compared to those obtained from the laboratory data and the single trees in an outdoor environment. This can be attributed to the range's effect on the classification and the variations between the biological materials involved in this scan.

The classifier confidence for foliage and the wood was 95% and 91%, respectively. This may be attributed to the trained scales that were segmented from different locations in the scans, which helped in terms of finding the most homogeneous distribution of the points. In addition, the calculation of the number of returns for this scan showed that the majority of the scan was recorded as a single return, including the canopy, stems and understorey vegetation.

7.5 Opportunities for future research

Previous studies mentioned in the literature review have used single-wavelength scanners in order to distinguish foliage from wood points. However, the results showed limitations in terms of obtaining a clear separation, as detailed earlier. New dual-wavelengths scanners like SALCA have the potential to provide a robust data that can be used to understand the composition of forest communities. For the spectral classification, the quantifying of accurate measurements related to the target properties is influenced by accurate apparent reflectance calibration.

The high temperatures in the laboratory prevented accurate calibration in this research. More investigation is required regarding calibration and this work should consider scans at short-range in order to produce reflectance related to the properties of the target. In addition,

generating reliable NDI calculations depends on the calibration of intensity to AR. The results in this research highlight the limitations of the neural network method described earlier. It produced poor calibrations for some scans at short-ranges (Chapter 4). Obtaining valid calibration for leaf-on and leaf-off scans is fundamental in order to compare their measurements. Delays in scanning the leaf-off condition cause a change in the wood reflectance, as the wood material may dry out. These issues need to be investigated in a field environment, with more attention paid to the errors in the calibration.

The results of this research indicate that using the spectral data from a near-infrared laser is a valid approach for foliage/wood separation at short-ranges in the laboratory. The same was found for some of the trees that were close to the scanner at the full stand scale. Gaulton et al. (2013) stated that 1063 nm has a slight sensitivity to water content that can be used to distinguish foliage from wood points. Further research would be beneficial to investigate 1063 nm data at different ranges using different tree species in an open environment.

The classification at the level of the full forest stand showed that a large number of errors were recorded using spectral thresholds on variables, such as apparent reflectance and NDI, especially in the case of full stand plot data. Piayda et al. (2015) stated that trees of different species respond differently to laser wavelengths, as large variations in spectral properties were observed. In terms of using a full plot scale data for foliage/wood separation, the results in this research highlight that there is a large amount of spectral variability in tree species. Therefore, obtaining valid spectral reflectance information for a full forest stand environment is an important taks. Spectral reflectance of the woody material will be sensitive to tree species, and how dry or moist the trees are. In other words, using a spectral approach in a complex forest stand is insufficient to obtain a clear separation due to the large degree of variation in the spectral features. Further investigations of the spectral variability of certain tree species would be beneficial.

The spatial classifier used in this research showed a powerful approach of using the point-clouds location in order to map the scan points. However, it is unlikely to gain clear separation for a mixed species forest community due to the variation in the arrangement and size of the tree components. Using a tree species-specific classifier might improve the spatial classification. Moreover, the range affected the classification at a distances greater than 15 m in the case of the full forest stand where more errors were generated especially for the small

trees and the much of the upper conopy. Therefore, testing finer scales at ranges greater than 15 m would be beneficial in terms of distinguishing foliage from wood points.

Improving foliage and wood classification is a key goal in order to quantify forest structure. The foliage and wood classification approaches implemented in this research are used in a combination of spectral and geometrical approaches. The final output of these classifications revealed several challenges, as discussed above. Another classification approach could be added to the spectral and spatial classification in order to improve foliage/wood speration. Al Naddaf (2016) created a new version of an algorithm to extract the x, y, and z eigenvalues and compiled the algorithm with CANUPO. The new version of CANUPO is able to provide accurate values for every spatial point in the classifier; therefore, a 3D figure can be built based on the values with more certainty . Combining this new approach with the spectral approach could improve the classification of areas such as finer branches, foliage and understorey vegetation.

7.6 Conclusions

Quantifying three-dimensional information for forest structure assessment is an area of interest for ecological and scientific purposes. The absence of this information may lead to misleading results in assessing the ecological processes within a forest, which in turn could lead to poor management decisions regarding any forest environment. The complexity of the forest structure adds more challenges in term of gaining accurate measurements. However, terrestrial laser scanning technology provides an opportunity to measure forests and acquire three-dimensional models to address the crucial need for forest mapping and monitoring. One of the current unsolved issues related to quantifying forest structures using TLS is the inability to separate the photosynthetic from the non-photosynthetic biomass points. This is critical in order to obtain accurate measurements of LAI, leaf and wood profiles, and quantify ABG. In order to address this issue, a newly-developed scanner, SALCA, has been used to acquire various datasets on trees at different scales. This research has demonstrated the potential of the SALCA instrument for leaf-wood characterisation at the level of a single tree and full stand scale. The series of key findings in this research may be summarised as follows:

- The SALCA instrument has facilitated new approaches for exploring the mapping of three-dimensional foliage and wood distribution. Comparing spectral and spatial

data provided additional information that allowed the investigation of the relationship between the two approaches to classification.

- In terms of calibration, it was impossible to produce neural networks for raw intensity calibration to apparent reflectance for short-range measurements due to the high temperatures recorded during the laboratory scanning experiments.
- The spectral classification in this research showed that it is possible to separate foliage and wood successfully using 1063 nm data in the case of a small broadleaf tree. In addition, the research showed that using thresholds for the spectral classification approach at the level of a full stand scale is unlikely to be successful due to the complexity of the spectral properties at this scale, including trunks, foliage and finer branches.
- The spectral approach alone is insufficiently accurate for forest characterisation, as a large number of errors was observed related to the calibration and variation in dryness in the foliage areas.
- The spatial classification in this research showed that this approach is more effective for foliage than wood. However, errors in the classification in the finer branches and small stems showed some challenges in terms of scale.
- The spatial classification provided a powerful approach for foliage/wood separation. More investigation is required into the range effect on the classification, as foliage appears as 1D to the classifier at close range.
- Comparing the two approaches revealed new information that has not been previously explored for forest applications.

The original contributions of this work can be summarised as follows: (i) it constitutes the first attempt to map full forest stand plot data acquired using dual-wavelength laser under spectral and spatial approaches; (ii) a new range of SALCA experiments was produced by Comparing spectral and spatial data and investigating their compatibility; (iii) a range of classification tests were undertaken, that included laboratory activities, single trees in a field environment, and a full stand plot, to explore the limitations of single-wavelength scanners. Future work is needed to improve the SALCA's calibration, especially at short range, in order to produce accurate apparent reflectance related to the properties of the target. In addition, other new approaches need to be explored in order to improve foliage/wood separation.

References

Ab-Rahman, M. S., & Hassan, M. R. (2009). *Temperature-pattern dependence of initial carrier density of high-speed digitally modulated uncooled semiconductor laser diodes: Theoretical analysis*. Paper presented at the *2009* International Conference on Electrical Engineering and Informatics. IEEE. Selangor. Malaysia.

Ahlberg, S., Söderman, U., Elmqvist, M., & Persson, A. (2004). *On modelling and visualisation of high resolution virtual environments using lidar data*. In Proceedings of the 12th Int. Conf. on Geoinformatics. University of Gävle. Sweden.

Al Naddaf D. (2016). Mise en oeuvre et amélioration de méthodes de filtrage d'échos LiDAR pour la caractérisation du bois et des feuilles dans la végétation. [M2]. École Nationale Supérieure d'Ingenieurs de Caen & Centre de Recherche: UMR AMAP, Montpellier.

Andrew, M. E., & Ustin, S. L. (2008). The role of environmental context in mapping invasive plants with hyperspectral image data. *Remote Sensing of Environment, 112*(12), 4301-4317.

Ballantyne, A., Andres, R., Houghton, R., Stocker, B., Wanninkhof, R., Anderegg, W., . . . Miller, J. (2015). Audit of the global carbon budget: estimate errors and their impact on uptake uncertainty. *Biogeosciences (Online), 12*(8). 2565-2584.

Barrett, F., McRoberts, R. E., Tomppo, E., Cienciala, E., & Waser, L. T. (2016). A questionnaire-based review of the operational use of remotely sensed data by national forest inventories. *Remote Sensing of Environment, 174*, 279-289.

Barrett, E. C. (2013). Introduction to environmental remote sensing. Routledge: New York.

Bauwens, S., Bartholomeus, H., Calders, K., & Lejeune, P. (2016). Forest inventory with terrestrial LiDAR: a comparison of static and hand-held mobile laser scanning. *Forests, 7*(6), 127.

Béland, M., Baldocchi, D. D., Widlowski, J.-L., Fournier, R. A., & Verstraete, M. M. (2014). On seeing the wood from the leaves and the role of voxel size in determining leaf area distribution of forests with terrestrial LiDAR. *Agricultural and Forest Meteorology, 184*, 82-97.

Béland, M., Widlowski, J.-L., Fournier, R. A., Côté, J.-F., & Verstraete, M. M. (2011). Estimating leaf area distribution in savanna trees from terrestrial LiDAR measurements. *Agricultural and Forest Meteorology, 151*(9), 1252-1266.

Blanc, L., Maury-Lechon, G., & Pascal, J. P. (2000). Structure, floristic composition and natural regeneration in the forests of Cat Tien National Park, Vietnam: an analysis of the successional trends. *Journal of biogeography, 27*(1), 141-157.

Bravo, F., LeMay, V., Jandl, R., & von Gadow, K. (2017). *Managing forest ecosystems: the challenge of climate change.* Springer. Switzerland .

Breda, N. J. (2003). Ground-based measurements of leaf area index: a review of methods, instruments and current controversies. *Journal of Experimental Botany, 54*(392), 2403-2417.

Brodu, N., & Lague, D. (2012). 3D terrestrial lidar data classification of complex natural scenes using a multi-scale dimensionality criterion: Applications in geomorphology. *ISPRS Journal of Photogrammetry and Remote Sensing, 68*, 121-134.

Calders, K. (2015). *Terrestrial laser scanning for forest monitoring.* PhD Thesis. Wageningen University. Holland.

Calders, K., Disney, M. I., Armston, J., Burt, A., Brede, B., Origo, N., . . . Nightingale, J. (2017). Evaluation of the range accuracy and the radiometric calibration of multiple terrestrial laser scanning instruments for data interoperability. *IEEE Transactions on Geoscience and Remote Sensing, 55*(5), 2716-2724.

Calders, K., Newnham, G., Burt, A., Murphy, S., Raumonen, P., Herold, M., . . . Armston, J. (2015). Nondestructive estimates of above-ground biomass using terrestrial laser scanning. *Methods in Ecology and Evolution, 6*(2), 198-208.

Campbell, J. B., & Wynne, R. H. (2011). *Introduction to remote sensing*. Guilford: New York.

IPCC. (2018). Global Warming of 1.5 ºC: Impacts of 1.5°C of Global Warming on Natural and Human Systems. [ONLINE] Available at: https://www.ipcc.ch/site/assets/uploads/sites/2/2019/02/SR15_Chapter3_Low_Res.pdf . [A ccessed 25 December 2018].

Chen, J., John, R., Sun, G., McNulty, S., Noormets, A., Xiao, J., . . . Franklin, J. F. (2014). Carbon fluxes and storage in forests and landscapes *Forest Landscapes and Global Change* (pp. 139-166): Springer. New York.

Chen, J. M., & Black, T. (1992). Defining leaf area index for non-flat leaves. *Plant, Cell & Environment, 15*(4), 421-429.

Chen, J. M., & Cihlar, J. (1995). Quantifying the effect of canopy architecture on optical measurements of leaf area index using two gap size analysis methods. *IEEE Transactions on Geoscience and Remote Sensing, 33*(3), 777-787.

Clawges, R., Vierling, L., Calhoon, M., & Toomey, M. (2007). Use of a ground-based scanning lidar for estimation of biophysical properties of western larch (Larix occidentalis). *International Journal of Remote Sensing, 28*(19), 4331-4344.

Corona, P., Di Biase, R. M., Fattorini, L., & D'Amati, M. (2018). A Monte Carlo appraisal of tree abundance and stand basal area estimation in forest inventories based on terrestrial laser scanning. *Canadian Journal of Forest Research,49*(1),41-52.

Costanza, R., de Groot, R., Braat, L., Kubiszewski, I., Fioramonti, L., Sutton, P., . . . Grasso, M. (2017). Twenty years of ecosystem services: how far have we come and how far do we still need to go? *Ecosystem Services, 28*, 1-16.

Côté, J.-F., Fournier, R. A., Luther, J. E., & van Lier, O. R. (2018). Fine-scale three-dimensional modeling of boreal forest plots to improve forest characterization with remote sensing. *Remote Sensing of Environment, 219*, 99-114.

Cutini, A., Matteucci, G., & Mugnozza, G. S. (1998). Estimation of leaf area index with the Li-Cor LAI 2000 in deciduous forests. *Forest Ecology and Management, 105*(1-3), 55-65.

Danson, F. M., Disney, M. I., Gaulton, R., Schaaf, C., & Strahler, A. (2018). The terrestrial laser scanning revolution in forest ecology: *Interface Focus, 8*(2), 20180001.

Danson, F. M., Gaulton, R., Armitage, R. P., Disney, M., Gunawan, O., Lewis, P., . . . Ramirez, A. F. (2014). Developing a dual-wavelength full-waveform terrestrial laser scanner to characterize forest canopy structure. *Agricultural and Forest Meteorology, 198*, 7-14.

Danson, F. M., Hetherington, D., Morsdorf, F., Koetz, B., & Allgower, B. (2007). Forest canopy gap fraction from terrestrial laser scanning. *IEEE Geoscience and Remote Sensing Letters, 4*(1), 157-160.

Danson, F. M., Sasse, F., & Schofield, L. A. (2018). Spectral and spatial information from a novel dual-wavelength full-waveform terrestrial laser scanner for forest ecology. *Interface Focus, 8*(2), 20170049.

Dassot, M., Colin, A., Santenoise, P., Fournier, M., & Constant, T. (2012). Terrestrial laser scanning for measuring the solid wood volume, including branches, of adult standing trees in the forest environment. *Computers and Electronics in Agriculture, 89*, 86-93.

Disney, M., Vicari, M. B., Burt, A., Calders, K., Lewis, S., Raumonen, P., & Wilkes, P. (2018). Weighing trees with lasers: advances, challenges and opportunities. *Interface Focus, 8*(2), 20170048.

Douglas, E. S., Martel, J., Li, Z., Howe, G., Hewawasam, K., Marshall, R. A., . . . Strahler, A. (2015). Finding leaves in the forest: the dual-wavelength Echidna lidar. *IEEE Geoscience and Remote Sensing Letters, 12*(4), 776-780.

Douglas, E. S., Strahler, A., Martel, J., Cook, T., Mendillo, C., Marshall, R., . . . Li, Z. (2012). *DWEL: A dual-wavelength echidna lidar for ground-based forest scanning*. Paper presented at the Geoscience and Remote Sensing Symposium (IGARSS), 2012 IEEE International.

Drake, J. B., Knox, R. G., Dubayah, R. O., Clark, D. B., Condit, R., Blair, J. B., & Hofton, M. (2003). Above-ground biomass estimation in closed canopy neotropical forests using lidar remote sensing: Factors affecting the generality of relationships. *Global Ecology and Biogeography, 12*(2), 147-159.

Durrieu, S., Allouis, T., Fournier, R., Véga, C., & Albrech, L. (2008, September). *Spatial quantification of vegetation density from terrestrial laser scanner data for characterization of 3D forest structure at plot level*. In SilviLaser 2008: 8th international conference on LiDAR applications in forest assessment and inventory. Edinburgh, UK.

ECN Data Centre. (2010). Alice Holt Forest. [ONLINE] Available at: http://data.ecn.ac.uk/sites/ecnsites.asp?site=T09. [Accessed 29 April 2018].

Eitel, J. U., Vierling, L. A., & Long, D. S. (2010). Simultaneous measurements of plant structure and chlorophyll content in broadleaf saplings with a terrestrial laser scanner. *Remote Sensing of Environment, 114*(10), 2229-2237.

Elowitz, M. R. (2013). What is Imaging Spectroscopy (Hyperspectral Imaging). Avilabe at. https://www.markelowitz.com/Hyperspectral.html. [Accessed 15th March 2018].

Elsherif, A., Gaulton, R., & Mills, J. (2018). Estimation of vegetation water content at leaf and canopy level using dual-wavelength commercial terrestrial laser scanners. *Interface Focus, 8*(2), 20170041.

Ferrara, R., Virdis, S. G., Ventura, A., Ghisu, T., Duce, P., & Pellizzaro, G. (2018). An automated approach for wood-leaf separation from terrestrial LIDAR point clouds using the density based clustering algorithm DBSCAN. *Agricultural and Forest Meteorology*. 262, 434-444.

Fröhlich, C., & Mettenleiter, M. (2004). Terrestrial laser scanning—new perspectives in 3D surveying. *International Archives of Photogrammetry, Remote Sensing and Spatial Information Sciences, 36*(Part 8), W2.

Gamon, J., Kovalchuck, O., Wong, C., Harris, A., & Garrity, S. (2015). Monitoring seasonal and diurnal changes in photosynthetic pigments with automated PRI and NDVI sensors. *Biogeosciences, 12*(13), 4149-4159.

Garber, S. M., & Maguire, D. A. (2003). Modeling stem taper of three central Oregon species using nonlinear mixed effects models and autoregressive error structures. *Forest Ecology and Management, 179*(1-3), 507-522.

Gaulton, R., Danson, F., Pearson, G., Lewis, P., & Disney, M. (2010). *The Salford Advanced Laser Canopy Analyser (SALCA): A multispectral full waveform LiDAR for improved vegetation characterisation.* Paper presented at the Proceedings of the Remote Sensing and Photogrammetry Society Conference, Remote Sensing and the Carbon Cycle, London, UK.

Gaulton, R., Danson, F., Ramirez, F., & Gunawan, O. (2013). The potential of dual-wavelength laser scanning for estimating vegetation moisture content. *Remote Sensing of Environment, 132*, 32-39.

Goncalves-Araujo, R. (2016). *Tracing environmental variability in the changing Arctic Ocean with optical measurements of dissolved organic matter.* PhD thesis . University Bremen.

Guo, X. (2017). *Using airborne lidar to map habitat structure and connectivity across Alberta's managed forest for biodiversity conservation*. PhD thesis. University of British Columbia.

Hakala, T., Nevalainen, O., Kaasalainen, S., & Mäkipää, R. (2015). Multispectral lidar time series of pine canopy chlorophyll content. *Biogeosciences, 12*(5), 1629-1634.

Hancock, S., Armston, J., Li, Z., Gaulton, R., Lewis, P., Disney, M., . . . Anderson, K. (2015). Waveform lidar over vegetation: An evaluation of inversion methods for estimating return energy. *Remote Sensing of Environment, 164*, 208-224.

Hancock, S., Gaulton, R., & Danson, F. M. (2017). Angular Reflectance of Leaves With a Dual-Wavelength Terrestrial Lidar and Its Implications for Leaf-Bark Separation and Leaf Moisture Estimation. *IEEE Trans. Geoscience and Remote Sensing, 55*(6), 3084-3090.

Henning, J. G., & Mercker, D. C. (2009). *Conducting a simple timber inventory*. Department of Forestry, Wildlife and Fisheries, Institute of Agriculture, University of Tennessee, USA.

Hess, C., Härdtle, W., Kunz, M., Fichtner, A., & von Oheimb, G. (2018). A high-resolution approach for the spatiotemporal analysis of forest canopy space using terrestrial laser scanning data. *Ecology and Evolution*, 8(13), 6800-6811.

Hopkinson, C., Lovell, J., Chasmer, L., Jupp, D., Kljun, N., & van Gorsel, E. (2013). Integrating terrestrial and airborne lidar to calibrate a 3D canopy model of effective leaf area index. *Remote Sensing of Environment, 136*, 301-314.

Hosoi, F., & Omasa, K. (2012). Estimation of vertical plant area density profiles in a rice canopy at different growth stages by high-resolution portable scanning lidar with a lightweight mirror. *ISPRS Journal of Photogrammetry and Remote Sensing, 74*, 11-19.

Huang, W., Pohjonen, V., Johansson, S., Nashanda, M., Katigula, M., & Luukkanen, O. (2003). Species diversity, forest structure and species composition in Tanzanian tropical forests. *Forest Ecology and Management, 173*(1), 11-24.

Humphreys, D. (2014). *Forest politics: the evolution of international cooperation*. Routledge: London.

Jalonen, J., Järvelä, J., Virtanen, J.-P., Vaaja, M., Kurkela, M., & Hyyppä, H. (2015). Determining characteristic vegetation areas by terrestrial laser scanning for floodplain flow modeling. *Water*, 7(2), 420-437.

Jensen, J. R. (2009). *Remote sensing of the environment: An earth resource perspective 2/e*. Pearson Education India.

Jupp, D. L., Culvenor, D. S., Lovell, J. L., Newnham, G. J., Strahler, A. H., & Woodcock, C. E. (2009). Estimating forest LAI profiles and structural parameters using a ground-based laser called 'Echidna®. *Tree physiology, 29*(2), 171-181.

Kaasalainen, S., Kukko, A., Lindroos, T., Litkey, P., Kaartinen, H., Hyyppa, J., & Ahokas, E. (2008). Brightness measurements and calibration with airborne and terrestrial laser scanners. *IEEE Transactions on Geoscience and Remote Sensing, 46*(2), 528-534.

Keenan, R. J., Reams, G. A., Achard, F., de Freitas, J. V., Grainger, A., & Lindquist, E. (2015). Dynamics of global forest area: results from the FAO Global Forest Resources Assessment 2015. *Forest Ecology and Management, 352*, 9-20.

Kelbe, D., Romanczyk, P., van Aardt, J., & Cawse-Nicholson, K. (2013). *Reconstruction of 3D tree stem models from low-cost terrestrial laser scanner data*. Paper presented at the SPIE Laser Radar Technology and Applications XVIII. Baltimore, MD, USA.

Kirchhoefer, M., Schumacher, J., Adler, P., & Kändler, G. (2017). Considerations towards a Novel Approach for Integrating Angle-Count Sampling Data in Remote Sensing Based Forest Inventories. *Forests*, *8*(7), 239.

Koma, Z., Rutzinger, M., & Bremer, M. (2018). Automated Segmentation of Leaves From Deciduous Trees in Terrestrial Laser Scanning Point Clouds. *IEEE Geoscience and Remote Sensing Letters, 15*(9), 1456-1460.

Kurz, W. A., Apps, M., Banfield, E., & Stinson, G. (2002). Forest carbon accounting at the operational scale. *The Forestry Chronicle, 78*(5), 672-679.

Levick, S., Hessenmöller, D., and Schulze, E. D. (2016). Scaling wood volume estimates from inventory plots to landscapes with airborne LiDAR in temperate deciduous forest. *Carbon Balance and Management*, 11(1), 7.

Li, W., Guo, Q., Jakubowski, M. K., & Kelly, M. (2012). A new method for segmenting individual trees from the lidar point cloud. *Photogrammetric Engineering & Remote Sensing*, 78(1), 75-84.

Li, W., Guo, Q., Tao, S., & Su, Y. (2018). VBRT: A novel voxel-based radiative transfer model for heterogeneous three-dimensional forest scenes. *Remote Sensing of Environment, 206*, 318-335.

Li, Y., Guo, Q., Su, Y., Tao, S., Zhao, K., & Xu, G. (2017). Retrieving the gap fraction, element clumping index, and leaf area index of individual trees using single-scan data from a terrestrial laser scanner. *ISPRS Journal of Photogrammetry and Remote Sensing, 130*, 308-316.

Li, Z. (2015). *Advances in measuring forest structure by terrestrial laser scanning with the Dual Wavelength ECHIDNA® LIDAR (DWEL)*. PhD thesis. Boston University.

Li, Z., Schaefer, M., Strahler, A., Schaaf, C., & Jupp, D. (2018). On the utilization of novel spectral laser scanning for three-dimensional classification of vegetation elements. *Interface Focus*, *8*(2), 20170039.

Li, Z., Strahler, A., Schaaf, C., Jupp, D., Schaefer, M., & Olofsson, P. (2018). Seasonal change of leaf and woody area profiles in a midlatitude deciduous forest canopy from classified dual-wavelength terrestrial lidar point clouds. *Agricultural and Forest Meteorology*, *262*, 279-297.

Liang, X., Kankare, V., Hyyppä, J., Wang, Y., Kukko, A., Haggrén, H., . . . Guan, F. (2016). Terrestrial laser scanning in forest inventories. *ISPRS Journal of Photogrammetry and Remote Sensing, 115*, 63-77.

Liang, X., Kankare, V., Yu, X., Hyyppa, J., & Holopainen, M. (2014). Automated stem curve measurement using terrestrial laser scanning. *IEEE Transactions on Geoscience and Remote Sensing, 52*(3), 1739-1748.

Lillesand, T., Kiefer, R. W., & Chipman, J. (2014). *Remote sensing and image interpretation*. John Wiley & Sons: Londodn.

Lim, K., Treitz, P., Wulder, M., St-Onge, B., & Flood, M. (2003). LiDAR remote sensing of forest structure. *Progress in physical Geography, 27*(1), 88-106.

Lovell, J., Jupp, D. L., Culvenor, D., & Coops, N. (2003). Using airborne and ground-based ranging lidar to measure canopy structure in Australian forests. *Canadian Journal of Remote Sensing, 29*(5), 607-622.

Mackie, E. D., & Matthews, R. W. (2008). *Timber measurement.* Forestry Commission: Edinburgh.

Malhi, Y., Jackson, T., Bentley, L. P., Lau, A., Shenkin, A., Herold, M., . . . Disney, M. I. (2018). New perspectives on the ecology of tree structure and tree communities through terrestrial laser scanning. *Interface Focus, 8*(2), 20170052.

Mallet, C., & Bretar, F. (2009). Full-waveform topographic lidar: State-of-the-art. *ISPRS Journal of Photogrammetry and Remote Sensing, 64*(1), 1-16.

Martin, M., Newman, S., Aber, J., & Congalton, R. (1998). Determining forest species composition using high spectral resolution remote sensing data. *Remote Sensing of Environment, 65*(3), 249-254.

McIntyre, P. J., Thorne, J. H., Dolanc, C. R., Flint, A. L., Flint, L. E., Kelly, M., & Ackerly, D. D. (2015). Twentieth-century shifts in forest structure in California: Denser forests, smaller trees, and increased dominance of oaks. *Proceedings of the National Academy of Sciences, 112*(5), 1458-1463.

Milgram, J., Cheriet, M., & Sabourin, R. (2005). *Estimating accurate multi-class probabilities with support vector machines*. In Proceedings. 2005 IEEE International Joint Conference on Neural Networks, 2005. IEEE. Montreal, QC, Canada.

Morin, X., Lechowicz, M. J., Augspurger, C., O'KEEFE, J. O. H. N., Viner, D., & Chuine, I. (2009). Leaf phenology in 22 North American tree species during the 21st century. *Global Change Biology*, *15*(4), 961-975.

Moskal, L. M., & Zheng, G. (2012). Retrieving forest inventory variables with terrestrial laser scanning (TLS) in urban heterogeneous forest. *Remote Sensing*, *4*(1), 1-20.

Murphy, G. E., Acuna, M. A., & Dumbrell, I. (2010). Tree value and log product yield determination in radiata pine (Pinus radiata) plantations in Australia: comparisons of

terrestrial laser scanning with a forest inventory system and manual measurements. *Canadian Journal of Forest Research*, *40*(11), 2223-2233.

Naidoo, L., Cho, M. A., Mathieu, R., & Asner, G. (2012). Classification of savanna tree species, in the Greater Kruger National Park region, by integrating hyperspectral and LiDAR data in a Random Forest data mining environment. *ISPRS Journal of Photogrammetry and Remote Sensing*, *69*, 167-179.

Newnham, G. J., Armston, J. D., Calders, K., Disney, M. I., Lovell, J. L., Schaaf, C. B., ... & Danson, F. M. (2015). Terrestrial laser scanning for plot-scale forest measurement. *Current Forestry Reports*, *1*(4), 239-251.

Nölke, N., Fehrmann, L., I Nengah, S. J., Tiryana, T., Seidel, D., & Kleinn, C. (2015). On the geometry and allometry of big-buttressed trees-a challenge for forest monitoring: new insights from 3D-modeling with terrestrial laser scanning. *iForest-Biogeosciences and Forestry*, *8*(5), 574.

Olofsson, K., Holmgren, J., & Olsson, H. (2014). Tree stem and height measurements using terrestrial laser scanning and the RANSAC algorithm. *Remote sensing*, *6*(5), 4323-4344.

Orwig, D. A., Boucher, P., Paynter, I., Saenz, E., Li, Z., & Schaaf, C. (2018). The potential to characterize ecological data with terrestrial laser scanning in Harvard Forest, MA. *Interface focus*, *8*(2), 20170044.

Owers, C. J., Rogers, K., & Woodroffe, C. D. (2018). Terrestrial laser scanning to quantify above-ground biomass of structurally complex coastal wetland vegetation. *Estuarine, Coastal and Shelf Science*, *204*, 164-176.

Patenaude, G., Hill, R. A., Milne, R., Gaveau, D. L. A., Briggs, B. B. J., & Dawson, T. P. (2004). Quantifying forest above ground carbon content using LiDAR remote sensing. *Remote Sensing of Environment*, *93*(3), 368-380.

Pfeifer, N., & Briese, C. (2007). *Laser scanning–principles and applications*. Paper presented at the GeoSiberia 2007-International Exhibition and Scientific Congress. Novosibirsk, Russian.

Piayda, A., Dubbert, M., Werner, C., Correia, A. V., Pereira, J. S., & Cuntz, M. (2015). Influence of woody tissue and leaf clumping on vertically resolved leaf area index and angular gap probability estimates. *Forest Ecology and Management*, *340*, 103-113.

Portillo-Quintero, C., Sanchez-Azofeifa, A., & Culvenor, D. (2014). Using VEGNET in-situ monitoring LiDAR (IML) to capture dynamics of plant area index, structure and phenology in Aspen Parkland forests in Alberta, Canada. *Forests*, *5*(5), 1053-1068.

Pretzsch, H., & Kahn, M. (1995). *Modelling growth of Bavarian mixed stands in a changing environment*. In Caring for the forest: research in a changing world. Proc 20th IUFRO World Congress 6-12 Aug. Tempere, Finland , 2. 234-248.

Qu, Y., Zhu, Y., Han, W., Wang, J., & Ma, M. (2014). Crop leaf area index observations with a wireless sensor network and its potential for validating remote sensing products. *IEEE Journal of Selected Topics in Applied Earth Observations and Remote Sensing*, *7*(2), 431-444.

Rall, J. A., & Knox, R. G. (2004). *Spectral ratio biospheric lidar*. *Paper presented at the IGARSS 2004*. IEEE International Geoscience and Remote Sensing Symposium. Anchorage, AK, USA.

Raumonen, P., Kaasalainen, M., Åkerblom, M., Kaasalainen, S., Kaartinen, H., Vastaranta, M., ... & Lewis, P. (2013). Fast automatic precision tree models from terrestrial laser scanner data. *Remote Sensing*, *5*(2), 491-520.

Richards, P. W. (1952). *The tropical rain forest; an ecological study*. At The University Press; Cambridge.

Roşca, S., Suomalainen, J., Bartholomeus, H., & Herold, M. (2018). Comparing terrestrial laser scanning and unmanned aerial vehicle structure from motion to assess top of canopy structure in tropical forests. *Interface focus*, *8*(2), 20170038.

Saarinen, N., Kankare, V., Vastaranta, M., Luoma, V., Pyörälä, J., Tanhuanpää, T., ... & Yu, X. (2017). Feasibility of Terrestrial laser scanning for collecting stem volume information from single trees. *ISPRS Journal of Photogrammetry and Remote Sensing*, *123*, 140-158.

Schofield, L. A. (2016). *Quantifying structural change in UK woodland canopies with a dual-wavelength full-waveform terrestrial laser scanner*. PhD thesis. University of Salford. UK.

Schofield, L. A., Danson, F. M., Entwistle, N. S., Gaulton, R., & Hancock, S. (2016). Radiometric calibration of a dual-wavelength terrestrial laser scanner using neural networks. *Remote Sensing Letters, 7*(4), 299-308.

Shugart, H. H., Saatchi, S., & Hall, F. G. (2010). Importance of structure and its measurement in quantifying function of forest ecosystems. *Journal of Geophysical Research: Biogeosciences*, 115(G2).

Solberg, S., Brunner, A., Hanssen, K. H., Lange, H., Næsset, E., Rautiainen, M., & Stenberg, P. (2009). Mapping LAI in a Norway spruce forest using airborne laser scanning. *Remote Sensing of Environment*, *113*(11), 2317-2327.

Stovall, A. E., Vorster, A. G., Anderson, R. S., Evangelista, P. H., & Shugart, H. H. (2017). Non-destructive aboveground biomass estimation of coniferous trees using terrestrial LiDAR. *Remote Sensing of Environment, 200*, 31-42.

Strahler, A.H.; Schaaf, C.; Woodcock, C.; Jupp, D.; Culvenor, D.; Newnham, G.; Dubayah, R.; Yao, T.; Zhao, F.; Yang, X. *ECHIDNA Lidar Campaigns: Forest Canopy Imagery and Field Data, USA, 2007-2009*. Oak Ridge National Laboratory Distributed Active Archive Center: Oak Ridge, TN, USA, 2011. Available online: http://dx.doi.org/10.3334/ORNLDAAC/1045 [Accessed on 16 April 2019].

Tao, S., Guo, Q., Xu, S., Su, Y., Li, Y., & Wu, F. (2015). A geometric method for wood-leaf separation using terrestrial and simulated lidar data. *Photogrammetric Engineering & Remote Sensing*, *81*(10), 767-776.

Pachauri, R. and Meyer, L. (2015). *Climate change 2014*. Intergovernmental panel on climate change: Geneva.

Tews, J., Brose, U., Grimm, V., Tielbörger, K., Wichmann, M. C., Schwager, M., & Jeltsch, F. (2004). Animal species diversity driven by habitat heterogeneity/diversity: the importance of keystone structures. *Journal of Biogeography*, *31*(1), 79-92.

Toth, C., & Jóźków, G. (2016). Remote sensing platforms and sensors: A survey. *ISPRS Journal of Photogrammetry and Remote Sensing*, *115*, 22-36.

Trochta, J., Krůček, M., Vrška, T., & Král, K. (2017). 3D Forest: An application for descriptions of three-dimensional forest structures using terrestrial LiDAR. *PLOS One*, *12*(5), e0176871.

Ung, C. H., Bernier, P., & Guo, X. J. (2008). Canadian national biomass equations: new parameter estimates that include British Columbia data. *Canadian Journal of Forest Research*, *38*(5), 1123-1132.

Vain, A., Yu, X., Kaasalainen, S., & Hyyppa, J. (2010). Correcting airborne laser scanning intensity data for automatic gain control effect. *IEEE Geoscience and Remote Sensing Letters*, *7*(3), 511-514.

van Leeuwen, M., and Disney, M. (2018). *3.08 Vegetation Structure (LiDAR)*. London, UK: Elsevier.

Vauhkonen, J., Hakala, T., Suomalainen, J., Kaasalainen, S., Nevalainen, O., Vastaranta, M., ... & Hyyppä, J. (2013). Classification of spruce and pine trees using active hyperspectral LiDAR. *IEEE Geoscience and Remote Sensing Letters*, *10*(5), 1138-1141.

Vicari, M. B., Disney, M., Wilkes, P., Burt, A., Calders, K., & Woodgate, W. (2019). Leaf and wood classification framework for terrestrial Li DAR point clouds. *Methods in Ecology and Evolution*.

Wagner, W., Roncat, A., Melzer, T., & Ullrich, A. (2007). Waveform analysis techniques in airborne laser scanning. *International Archives of Photogrammetry and Remote Sensing*, *36*(3), 413-418.

Wagner, W., Ullrich, A., Ducic, V., Melzer, T., & Studnicka, N. (2006). Gaussian decomposition and calibration of a novel small-footprint full-waveform digitising airborne laser scanner. *ISPRS Journal of Photogrammetry and Remote Sensing*, *60*(2), 100-112.

Wallner, A., Elatawneh, A., Schneider, T., Kindu, M., Ossig, B., & Knoke, T. (2017). Remotely sensed data controlled forest inventory concept. *European Journal of Remote Sensing*, *51*(1), 75-87.

Wang, D., Hollaus, M., & Pfeifer, N. (2017). Feasibility of machine learning methods for separating wood and leaf points from terrestrial laser scanning data. *ISPRS Annals of Photogrammetry, Remote Sensing & Spatial Information Sciences,* IV-2/W4, 157-164.

Weber, R. P. (2015). *Old-growth Forests and Coniferous Forests: Ecology, Habitat and Conservation*. Nova Science Publishers: New York.

Wei, G., Shalei, S., Bo, Z., Shuo, S., Faquan, L., & Xuewu, C. (2012). Multi-wavelength canopy LiDAR for remote sensing of vegetation: Design and system performance. *ISPRS Journal of Photogrammetry and Remote Sensing, 69*, 1-9.

Welford, D., & Mooradian, A. (1982). Output power and temperature dependence of the linewidth of single-frequency cw (GaAl) As diode lasers. *Applied Physics Letters, 40*(10), 865-867.

Wu, D., Phinn, S., Johansen, K., Robson, A., Muir, J., & Searle, C. (2018). Estimating Changes in Leaf Area, Leaf Area Density, and Vertical Leaf Area Profile for Mango, Avocado, and Macadamia Tree Crowns Using Terrestrial Laser Scanning. *Remote Sensing, 10*(11), 1750.

Wulder, M. A., Coops, N. C., Hudak, A. T., Morsdorf, F., Nelson, R., Newnham, G., & Vastaranta, M. (2013). Status and prospects for LiDAR remote sensing of forested ecosystems. *Canadian Journal of Remote Sensing, 39*(sup1), S1-S5.

Yaman, A., & Yılmaz, H. M. (2017). THE EFFECT OF OBJECT SURFACE COLORS ON TERRESTRIAL LASER SCANNERS. *International Journal of Engineering and Geosciences, 2*(2), 68-74.

Yilmaz, M. T., Hunt Jr, E. R., Goins, L. D., Ustin, S. L., Vanderbilt, V. C., & Jackson, T. J. (2008). Vegetation water content during SMEX04 from ground data and Landsat 5 Thematic Mapper imagery. *Remote Sensing of Environment, 112*(2), 350-362.

Zhu, X., Skidmore, A. K., Darvishzadeh, R., Niemann, K. O., Liu, J., Shi, Y., & Wang, T. (2018). Foliar and woody materials discriminated using terrestrial LiDAR in a mixed natural forest. *International Journal of Applied Earth Observation and Geoinformation, 64*, 43-50.

Appendix I

Appendix I: SALCA intensity, AR, and NDI at 1m range for broadleaf tree-leaf-on scan

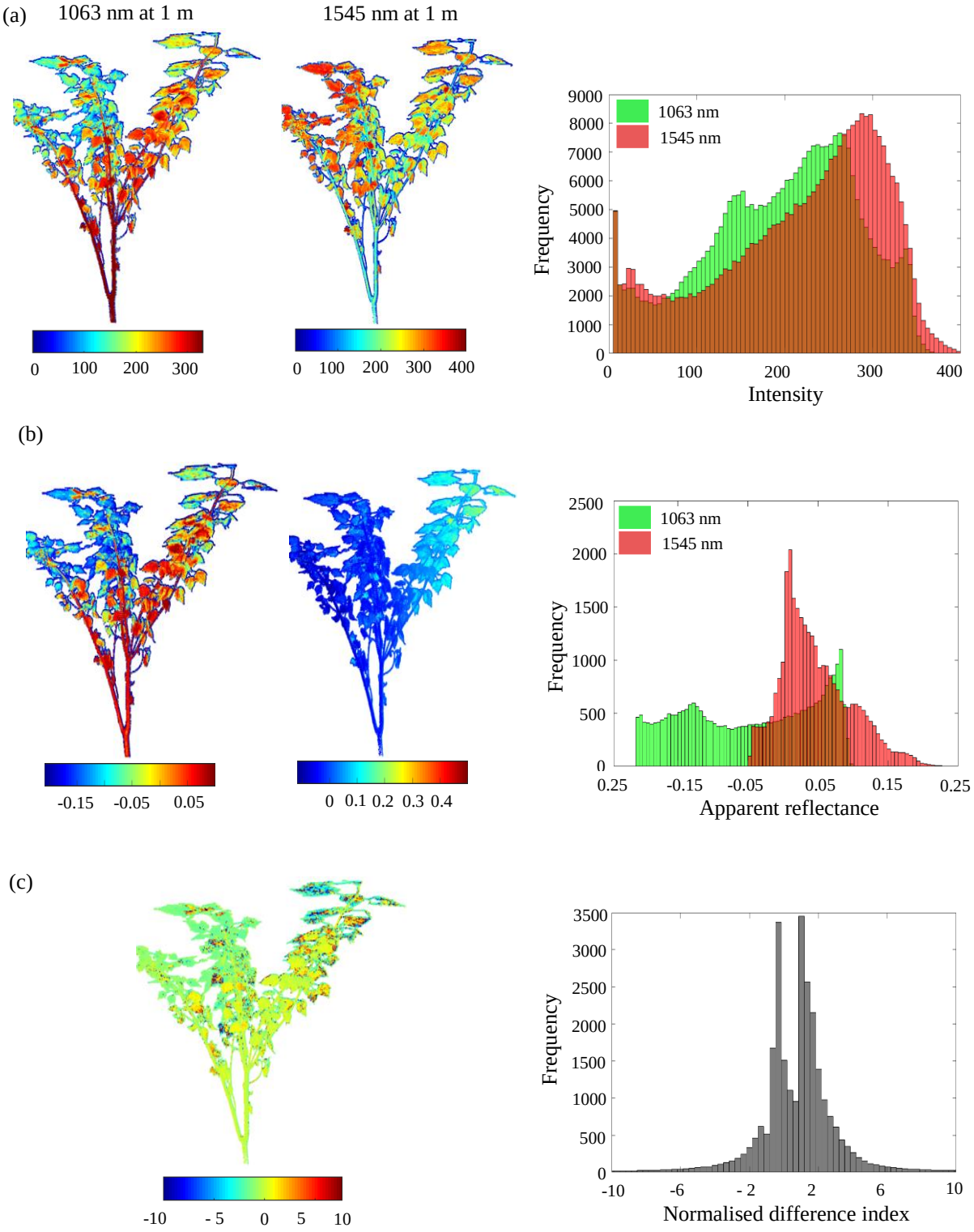

Figure A 1.1: SALCA point clouds for (a) intensity, (b) apparent reflectance, and (c) normalised difference index with their histograms for leaf-on condition respectively. Blue colour on the scales refers to minimal values, green to average values, and the high values are coloured red. Average values of panel reflectance are included for both laser wavelengths.

Appendix I: SALCA intensity, AR, and NDI at 1m range for needle-leaf tree-leaf-on scan

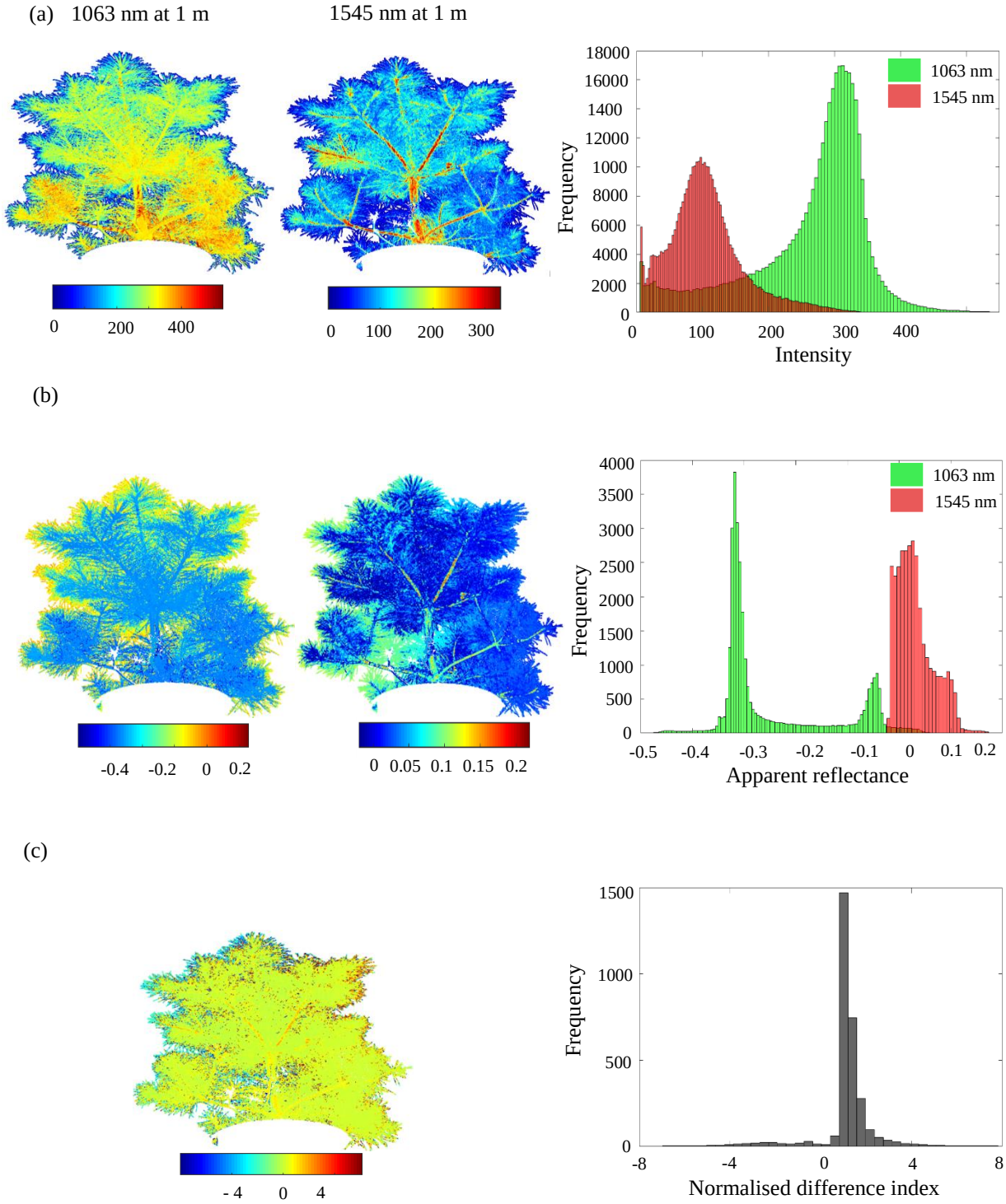

Figure A 1.2: SALCA point clouds for (a) intensity, (b) apparent reflectance, and (c) normalised difference index with their histograms for leaf-on condition respectively. Blue colour on the scales refers to minimal values, green to average values, and the high values are coloured red. Average values of panel reflectance are included for both laser wavelengths.

Appendix I: SALCA intensity, AR, and NDI at 3m range for broadleaf tree-leaf-on scan

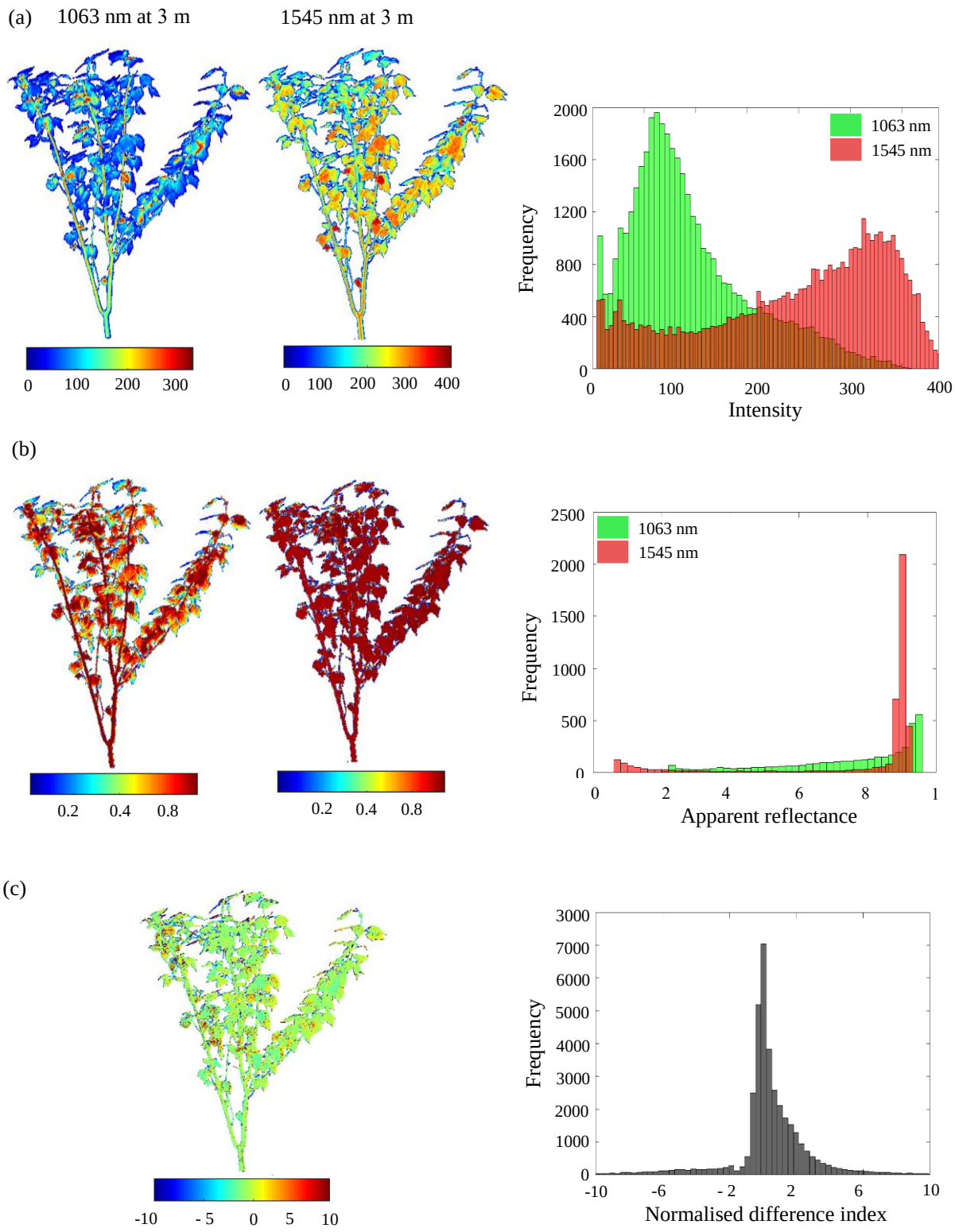

Figure A 1.3: SALCA point clouds for (a) intensity, (b) apparent reflectance, and (c) normalised difference index with their histograms for leaf-on condition respectively. Blue colour on the scales refers to minimal values, green to average values, and the high values are coloured red. Average values of panel reflectance are included for both laser wavelengths.

Appendix I: SALCA intensity, AR, and NDI at 3m range for needle-leaf tree-leaf-on scan

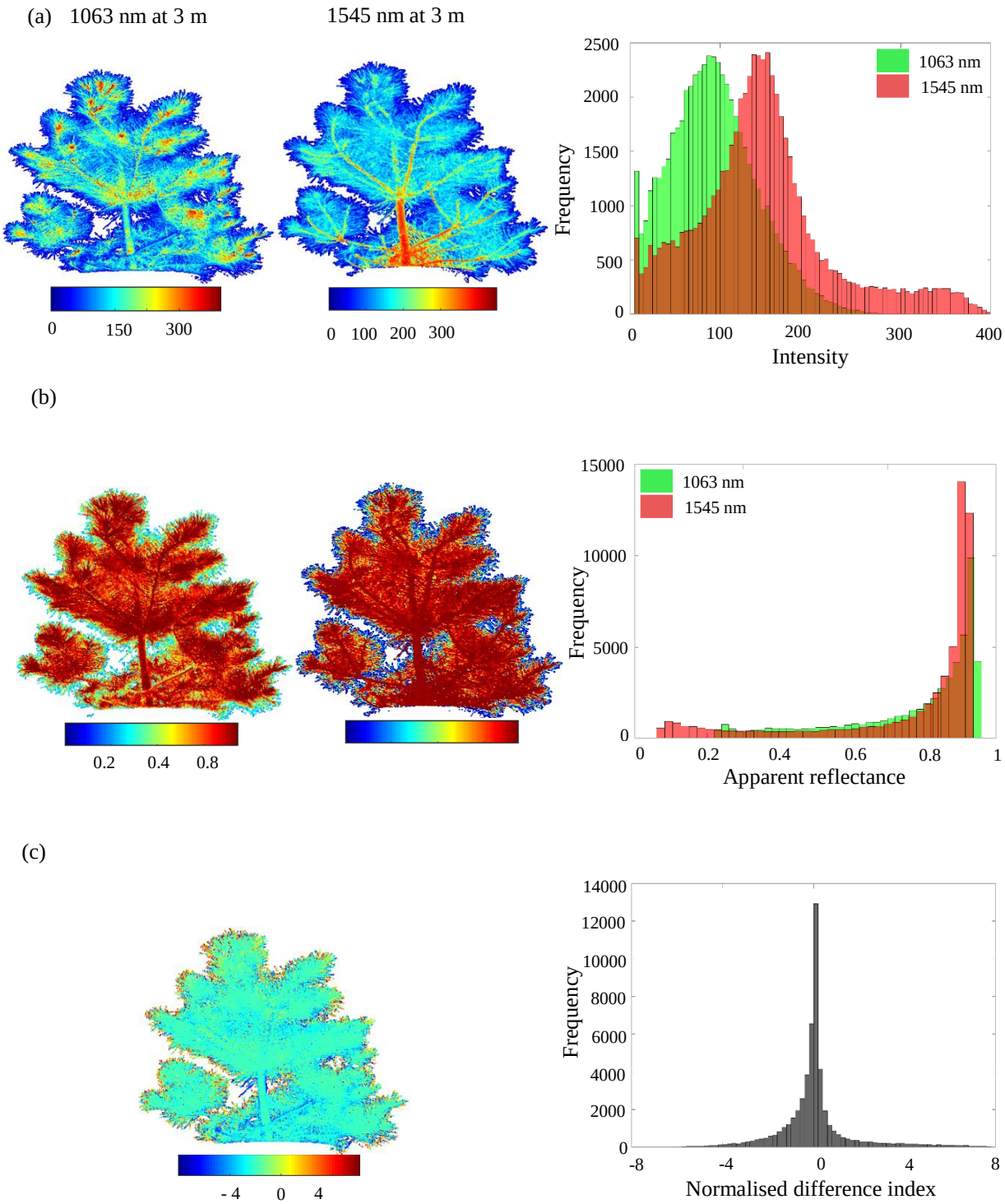

Figure A 1.4: SALCA point clouds for (a) intensity, (b) apparent reflectance, and (c) normalised difference index with their histograms for leaf-on condition respectively. Blue colour on the scales refers to minimal values, green to average values, and the high values are coloured red. Average values of panel reflectance are included for both laser wavelengths.

Appendix I: SALCA intensity, AR, and NDI at 5m range for broadleaf tree-leaf-on scan

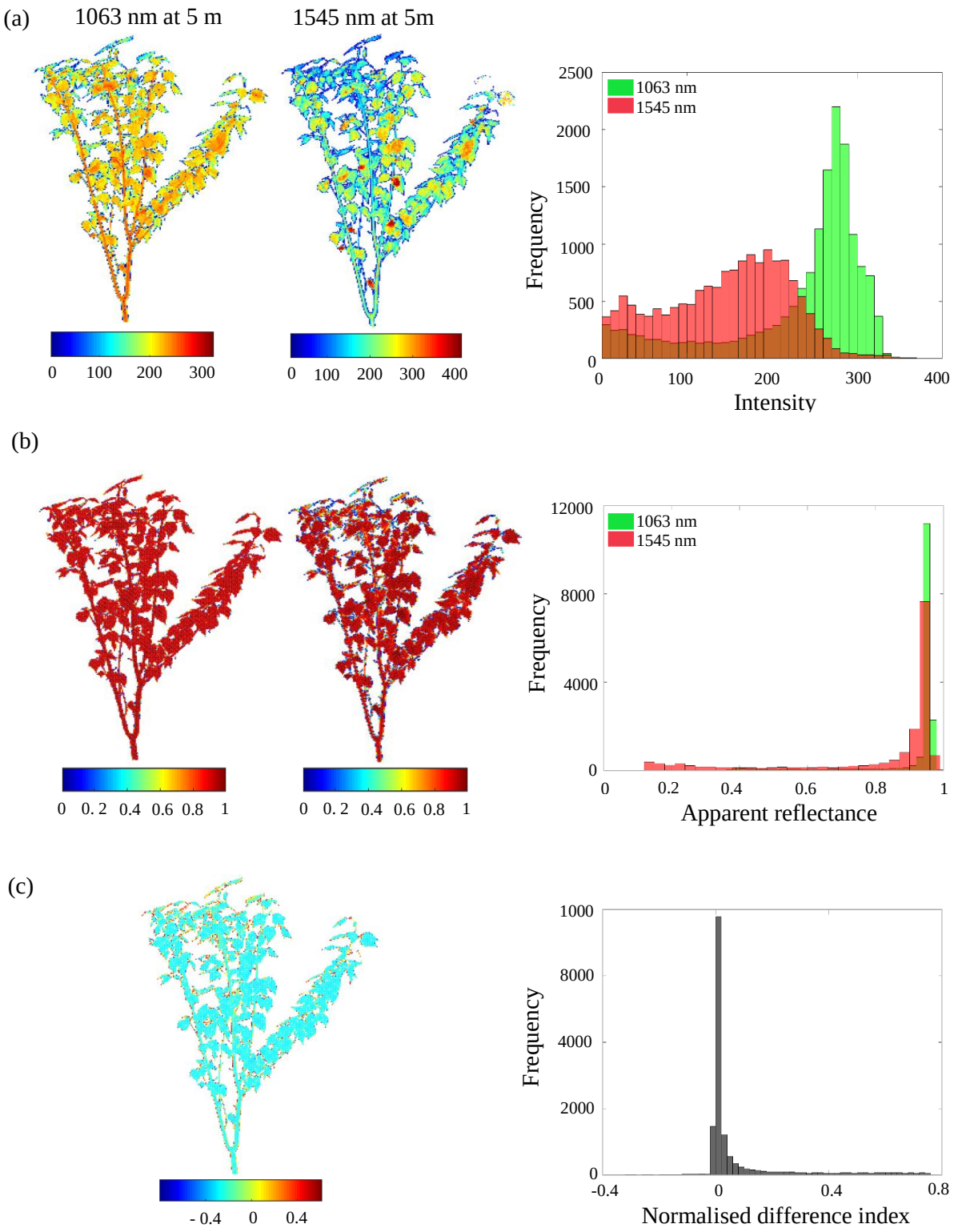

Figure A 1.5: SALCA point clouds for (a) intensity, (b) apparent reflectance, and (c) normalised difference index with their histograms for broadleaf tree leaf-on scan respectively. Blue on the scales refers to minimal values, green to average values, and the high values are coloured red.

Appendix I: SALCA intensity, AR, and NDI at 5 m range for needle-leaf leaf-on scan

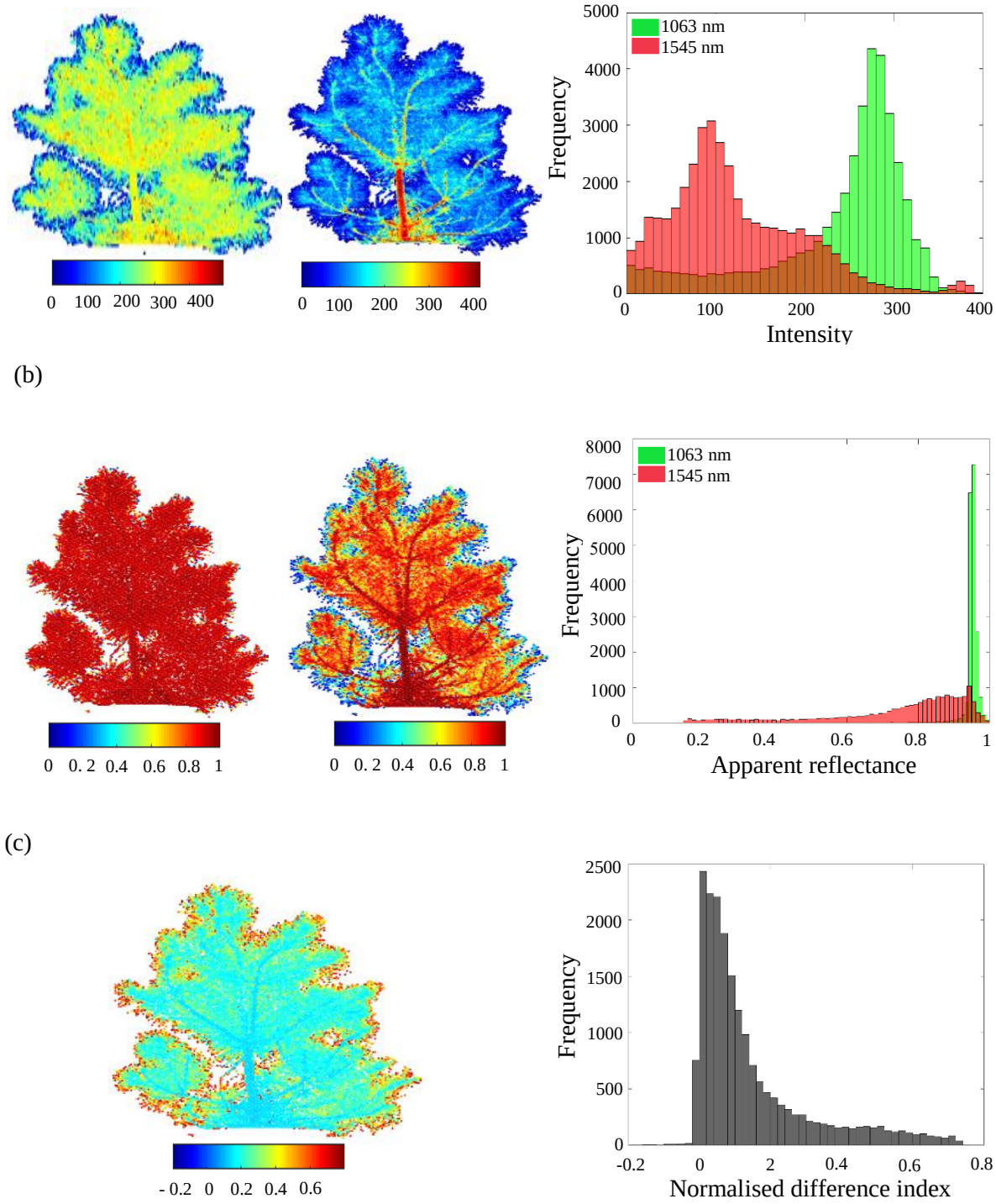

Figure A 1.6: SALCA point clouds for (a) intensity, (b) apparent reflectance, and (c) normalised difference index with their histograms for broadleaf tree leaf-on scan respectively. Blue on the scales refers to minimal values, green to average values, and the high values are coloured red. Average values of panel reflectance are included for both laser wavelengths.

Appendix II. Description of Silverdale datasets for leaf-on and leaf-off scans

Date23/07/15 Leaf-on scan			Description									
No	Tree sample name	Scan direction	Start & end time	File name	Range	Wind speed (km/h)	Start azimuth (degree)	Stop azimuth (degree)	Azimuth step angle (degree)	Azimuth steps	Shots revolution	Zenith angle (degree)
1	Good	South	11:59 -12:27	Good_s	20 m	3.6 - 4.7	0	44.98	0.06	749	3316	0-190º
2	Poor	South	12:35 -12:55	Poor_s	20 m	2.7 - 4.9	0	44.98	0.06	749	3316	0-190º
3	Good	South	13:35 -13:57	Good_s_r	20 m	-	0	44.98	0.06	749	3316	0-190º
4	Good	West	14:13 -14:35	Good_w_r	20 m	-	0	44.98	0.06	749	3316	0-190º
5	Good	North	14:52 -15:22	Good_n_r	20 m	-	0	44.98	0.06	749	3316	0-190º
6	Moderate	South	15:33 -16:52	Moderate _s	20 m	3.2 - 3.6	0	44.98	0.06	749	3316	0-190º
7	Good	East	17:10 -17:40	Good_e_r	20 m	3.6 - 6.1	0	44.98	0.06	749	3316	0-190º
8	Good	South 2	17:10 -18:00	Good_s_r_2	20 m	3.6 - 6.1	45	55.00	0.06	166	3316	0-190º
Date 13/08/2015 leaf-on scan												
9	Poor	South 2	10:50 -11:14	Poor_s2	20 m	-	70.02	113.98	0.06	732	3316	0-190º
10	Poor	West2	11:27 -11:38	Poor_w2	20 m	-	70.02	106.00	0.06	599	3316	0-190º
11	Poor	North 2	12:09-12:24	Poor_n2	20 m	-	54.00	98.02	0.06	733	3316	0-190º
12	Poor	East 2	12:48-13:06	Poor_e2	20 m	-	76.02	113.98	0.06	632	3316	0-190º
13	Moderate	South 2	13:27-13:46	Mod_s2	20 m	-	72.00	121.00	0.06	816	3316	0-190º
14	Moderate	West	14:06 -14:29	Mod_w2	20 m	-	73.98	112.00	0.06	633	3316	0-190º
15	Moderate	North 2	14:38 -15:06	Mod_n2	20 m	-	75.00	125.98	0.06	849	3316	0-190º
16	Poor	South 2	15:20 -12:37	Poor_s2	20 m	-	70.02	113.98	0.06	732	3316	0-190º
Date 11/04/2018 Leaf-off scan												
17	Poor	South	11:15 -11:40	Poor leaf-off	20 m	-	60.00	120.00	0.06	833	3200	0-190º
18	Moderate	South	12:00 -12:38	Mod leaf-off	20 m	-	60.00	140.00	0.06	1042	3200	0-190º
19	Good	South	12:50 -13:30	Good leaf-off	20 m	-	60.00	132.00	0.06	1027	3200	0-190º
20	Good	South	13:40 -14:14	Good leaf-off2	20 m	-	60.00	132.00	0.06	1027	3200	0-190º